

**An Evaluation of the Safety and Operational Impacts of a Candidate
Variable Speed Limit Control Strategy on an Urban Freeway**

by
Peter Eric Allaby

**A thesis
presented to the University of Waterloo
in fulfilment of the
thesis requirement for the degree of
Master of Applied Science
in
Civil Engineering**

Waterloo, Ontario, Canada, 2006

© Peter Eric Allaby 2006

I hereby declare that I am the sole author of this thesis. This is a true copy of the thesis, including any required final revisions, as accepted by my examiners.

I understand that my thesis may be made electronically available to the public.

ABSTRACT

Variable Speed Limit Sign (VSLS) systems enable transportation managers to dynamically change the posted speed limit in response to prevailing traffic and/or weather conditions. VSLS are thought to improve safety and reduce driver stress while improving traffic flow and travel times. Although VSLS have been implemented in a limited number of jurisdictions throughout the world, there is currently very limited documentation describing the quantitative safety and operational impacts. The impacts that have been reported are primarily from systems in Europe, and may not be directly transferable to other jurisdictions, such as North America. Furthermore, although a number of modelling studies have been performed to date that quantify the impacts of VSLS, the VSLS control strategies are often too complex or based on unrealistic assumptions and therefore cannot be directly applied for practical applications. Consequently, a need exists for an evaluation framework that quantifies the safety and traffic performance impacts of comprehensive VSLS control strategies suitable for practical applications in North America. This paper presents the results of an evaluation of a candidate VSLS system for an urban freeway in Toronto, Canada. The evaluation was conducted using a microscopic simulation model (i.e. a model that predicts individual vehicle movements) combined with a categorical crash potential model for estimating safety impacts.

The objectives of this thesis are: 1) to validate a real-time crash prediction model for a candidate section of freeway; 2) to develop a candidate VSLS control algorithm with potential for practical applications; 3) to evaluate the performance of the VSLS control strategy for a range of traffic conditions in terms of safety and travel time; and 4) to test the sensitivity of the VSLS impact results to modifications of the control algorithm.

The analysis of the VSLS impacts under varying levels of traffic congestion indicated that the candidate control strategy was able to provide large safety benefits without a significant travel time penalty, but only for a limited range of traffic conditions. The tested algorithm was found to be insufficiently robust to operate effectively over a wide range of traffic conditions. However, by modifying parameters of the control algorithm, preliminary analysis identified potential improvements in the performance of the VSLS. The modified control strategy resulted in less overall travel time penalty without an adverse impact on the safety benefits. It is anticipated that further modifications to the VSLS control strategy could

result in a VSLs that is able to operate over a wide range of traffic conditions and provide more consistent safety and travel time benefits, and it is recommended that the framework used in this study is an effective tool for optimizing the algorithm structure and parameter values.

ACKNOWLEDGEMENTS

I wish to express my sincere appreciation and gratitude to my supervisor, Dr. Bruce Hellinga, whose encouragement and enthusiasm in this research challenged me to approach my research with confidence, creativity and a sense of responsibility. The pursuance of my graduate degree was an enjoyable experience and Dr. Hellinga is surely an exemplary professor, advisor, and researcher.

I also extend my appreciation to my reviewers, Dr. Jeff Casello and Dr. Scott Walbridge for offering their time and valuable comments. I gratefully acknowledge Ms. Mara Bullock and IBI Group for their ongoing input and contribution to the development of this project. I thank Mr. David Tsui and Mr. Roger Browne at the Ministry of Transportation, Ontario for their assistance and cooperation with my data collection on the QEW. My appreciation also goes out to Scott Aitken and Julian Young of Quadstone Ltd. for their kind and helpful technical support in the use of PARAMICS software. Furthermore, I wish to thank my fellow graduate students, particularly Pedram Izadpanah and Amir Samimi for offering their knowledge in programming code, and former graduate student Chris Lee for assisting me in building upon his previous research.

My time at the University of Waterloo has been one of growth and reflection – personally as well as intellectually. I extend my heartfelt appreciation to my family and friends for their ongoing support and encouragement. Finally, special thanks to my fiancé, Nat, for her optimism, love, and understanding.

TABLE OF CONTENTS

Abstract.....	iii
Acknowledgements.....	v
Table of Contents.....	vi
List of Tables.....	viii
List of Figures.....	ix
1. INTRODUCTION.....	1
1.1 BACKGROUND	1
1.2 MOTIVATION	2
1.3 SCOPE AND OBJECTIVES	3
1.4 CONTENT OF THESIS	3
2. LITERATURE REVIEW.....	5
2.1 INTRODUCTION TO VARIABLE SPEED LIMITS.....	5
2.2 EMPIRICAL APPLICATIONS IN VSLS	6
2.2.1 <i>M25 Controlled Motorways, UK</i>	8
2.2.2 <i>A2 Motorway, The Netherlands</i>	10
2.2.3 <i>E18, Finland</i>	12
2.2.4 <i>State of Washington, USA</i>	12
2.2.5 <i>State of Michigan, USA</i>	13
2.3 MODELLING APPLICATIONS IN VSLS	15
2.3.1 <i>Macroscopic Modelling</i>	15
2.3.2 <i>Microscopic Simulation Modelling</i>	16
2.4 CHAPTER SUMMARY.....	19
3. CRASH POTENTIAL MODEL	20
3.1 SELECTION OF MODEL	20
3.2 CRASH POTENTIAL MODEL FRAMEWORK.....	20
3.2.1 <i>Crash Precursors</i>	22
3.2.2 <i>External Control Factors</i>	26
3.2.3 <i>Exposure</i>	26
3.3 CALIBRATION OF CRASH POTENTIAL MODEL	27
3.3.1 <i>Model Calibration Site</i>	29
3.3.2 <i>Crash Database</i>	29
3.3.3 <i>External Control Factors</i>	33
3.3.4 <i>Calculation of Crash Precursors</i>	36
3.3.5 <i>Categorization</i>	37
3.3.6 <i>Log-Linear Analysis</i>	44
4. DEVELOPMENT OF MICROSIMULATION MODEL	51
4.1 DESCRIPTION OF STUDY NETWORK	51
4.2 DATA COLLECTION.....	53
4.2.1 <i>Geometric Data</i>	53
4.2.2 <i>Loop Detector Data</i>	53
4.2.3 <i>Formation of O-D Trip Table</i>	54
4.2.4 <i>Existing Traffic Conditions</i>	56
4.3 CONSTRUCTION AND VALIDATION OF MICROSIMULATION MODEL	59
4.3.1 <i>Selection of Traffic Microsimulator</i>	59
4.3.2 <i>Base Model Infrastructure</i>	59

4.3.3	<i>Base Model Calibration</i>	60
4.4	CRASH PRECURSOR ADJUSTMENT FACTORS.....	63
4.5	VLSL SYSTEM DEVELOPMENT.....	67
4.5.1	<i>Dynamic Speed Control Operations within PARAMICS</i>	67
4.5.2	<i>VLSL Control Algorithm</i>	69
5.	VLSL IMPACT ANALYSIS	75
5.1	SCENARIO 1 – PEAK CONDITIONS.....	75
5.1.1	<i>VLSL Activity</i>	75
5.1.2	<i>VLSL Safety Impact</i>	80
5.1.3	<i>VLSL Travel Efficiency Impact</i>	86
5.2	SCENARIO 2 – NEAR-PEAK CONDITIONS.....	90
5.2.1	<i>VLSL Activity</i>	90
5.2.2	<i>VLSL Safety Impact</i>	91
5.2.3	<i>VLSL Travel Efficiency Impact</i>	95
5.3	SCENARIO 3 – OFF-PEAK CONDITIONS.....	98
5.3.1	<i>VLSL Activity</i>	99
5.3.2	<i>VLSL Safety Impact</i>	99
5.3.3	<i>VLSL Travel Efficiency Impact</i>	102
5.4	SUMMARY OF CHAPTER.....	103
6.	VLSL CONTROL ALGORITHM SENSITIVITY ANALYSIS	105
6.1	MODIFICATIONS OF PARAMETER VALUES.....	105
6.1.1	<i>Modification 1</i>	107
6.1.2	<i>Modification 2</i>	110
6.1.3	<i>Modification 3</i>	112
6.1.4	<i>Modification 4</i>	112
6.1.5	<i>Modification 5</i>	113
6.2	SUMMARY OF CHAPTER.....	117
7.	CONCLUSIONS AND RECOMMENDATIONS	119
7.1	CONCLUSIONS.....	119
7.1.1	<i>Validation of Crash Potential Model</i>	119
7.1.2	<i>Framework for Quantifying VLSL Impacts</i>	120
7.1.3	<i>Comparison of VLSL Impacts to those from Previous Studies</i>	122
7.2	LIMITATIONS OF STUDY.....	124
7.2.1	<i>Crash Potential Model</i>	124
7.2.2	<i>Simulation Modelling</i>	127
7.2.3	<i>Study Network</i>	130
7.3	RECOMMENDATIONS.....	130
7.3.1	<i>Crash Potential Model</i>	130
7.3.2	<i>VLSL Evaluation Framework</i>	131
8.	REFERENCES	132
	APPENDIX A	136
	APPENDIX B	137
	APPENDIX C	144
	APPENDIX D	149
	APPENDIX E	150

LIST OF TABLES

Table 2-1: Variable Speed Limit Deployments (IBI Group, 2005)	7
Table 3-1: Crash Model Control Factors	33
Table 3-2: Selected Dates for Non-Crash Data	37
Table 3-3: Categorization Cases and Corresponding Boundary Values	42
Table 3-4: Categorization from Lee (2004)	43
Table 3-5: Boundary Values for Categorization 40/40/20	44
Table 3-6: Categorization Format Example for 40/40/20	44
Table 3-7: Exposure Variables	44
Table 3-8: Categorization of statistically significant crash model	47
Table 3-9: Crash Model Parameter Estimates from Log-linear Analysis	48
Table 4-1: Loop Detector Station List	53
Table 4-2: Average peak period volumes for all mainline and ramp loop stations.	54
Table 4-3: Assumed proportions of originating volumes for internal O-D pairs	54
Table 4-4: Estimated Origin-Destination Matrix for time period 5:30 am to 10 am	56
Table 4-5: Time dependent vehicle release profiles	56
Table 4-6: Summary of adjusted crash precursor frequencies	66
Table 4-7: VSLS Control Algorithm Look-up Table	69
Table 5-1: Peak Scenario – Average VSLS Coverage	78
Table 5-2: Peak Scenario – Calculation of Relative Safety Benefit for Station 100	82
Table 5-3: Peak Scenario – Relative Safety Benefits by Station	83
Table 5-4: Peak Scenario - Summary of Average System Travel Time Impact (min/veh)	86
Table 5-5: Peak Scenario – Average Travel Time Impact for Specific O-D Pairs	87
Table 5-6: Near-Peak Scenario – Average VSLS Coverage	90
Table 5-7: Near-Peak Scenario – Relative safety benefit results	91
Table 5-8: Average Peak and Near-Peak network safety impacts after omission of Station 40	92
Table 5-9: Near-Peak Scenario – Average traffic speed (non-VSLS) and resulting VSLS safety impact	95
Table 5-10: Near-Peak Scenario – Summary of average system travel time impact (min/veh)	96
Table 5-11: Off-Peak Scenario – Relative Safety Benefit results	100
Table 5-12: Off-Peak Scenario - Proportion of Network Trigger Conditions by Station	100
Table 5-13: Off-Peak Scenario – Summary of average system travel time impact (min/veh)	103
Table 5-14: Summary of VSLS impacts	103
Table 6-1: Modifications of Parameter Values for Sensitivity Analysis	106
Table 6-2: VSLS activity resulting from parameter modifications	106
Table 6-3: Overall network safety and travel time impacts resulting from parameter modifications	107

LIST OF FIGURES

Figure 3-1: Outline of Calibration Procedure	28
Figure 3-2: Change in Flow Conditions Due to a Shockwave.....	31
Figure 3-3: Confirmation of Crash Time, t	32
Figure 3-4: Average temporal volume profile	34
Figure 3-5: Distributions of Crash Precursors from Crash and Non-Crash Data	39
Figure 3-6: Comparison of Precursor Distributions to those of Lee (2004)	40
Figure 3-7: Categorization of Precursors.....	41
Figure 3-8: Categorization Case: 20/60/20 for CVS	43
Figure 3-9: Comparison between Observed and Expected Crash Frequencies	50
Figure 4-1: QEW Burlington Study Section (©2005 Google)	52
Figure 4-2: Locations of Loop Detector Stations	52
Figure 4-3: Contour Mapping of Freeway Speeds for April 14, 2004 (2-min average speeds)	57
Figure 4-4: Volume-Occupancy Plot for Station 120 (April 14, 2005).....	58
Figure 4-5: Speed-Volume Plot for Station 120 (April 14, 2005).....	58
Figure 4-6: Individual speed profiles for Station 120 (5-min average station speeds).....	62
Figure 4-7: Average speed profile for Station 60 (averaged over 10 runs)	62
Figure 4-8: Contour mapping of simulated freeway speeds (2-min average station speeds)	63
Figure 4-9: Minimum RMS Errors for Precursor Adjustment Factors.....	65
Figure 4-10: Basic Layout of Link/Detector/VSLs Groupings.....	68
Figure 4-11: Decision Path for Determining New Posted Speed of Trigger VSLs i	70
Figure 4-12: VSLs Control Structure.....	72
Figure 4-13: Illustration of VSLs Response.....	73
Figure 4-14: Temporal Speed Profile of VSLs Response (From Simulation Output)	74
Figure 5-1: Peak Scenario – Mapping of the VSLs Displayed Speed Limits (Seed 5).....	76
Figure 5-2: Contour Mapping of Freeway Speeds without VSLs (2-min average speeds).....	77
Figure 5-3: Contour Mapping of Freeway Speeds with VSLs (2-min average speeds).....	77
Figure 5-4: Peak Scenario – Average coverage of VSLs displayed speeds by station	78
Figure 5-5: Peak Scenario – Traffic Conditions by Station for the VSLs Case.....	79
Figure 5-6: Peak Scenario – Fraction of Time during which congestion is observed (occupancy > 15%).....	80
Figure 5-7: Peak Scenario –Crash precursor distributions for VSLs and non-VSLs cases.....	84
Figure 5-8: Peak Scenario – Temporal speed profile for Station 100 (VSLs case)	85
Figure 5-9: Peak Scenario – Smoothed Average Speed Profiles for Station 100	88
Figure 5-10: Peak Scenario – Illustration of VSLs “Domino” Effect.....	89
Figure 5-11: Peak Scenario - Contour mapping of freeway speeds for non-VSLs case	89
Figure 5-12: Near-Peak Scenario – Mapping of VSLs Displayed Speed Limits.....	91
Figure 5-13: Comparison of RSB variability for the Peak and Near-Peak Scenarios	92
Figure 5-14: Near-Peak Scenario – Speed profiles for Station 100 (Run 3).....	93
Figure 5-15: Near-Peak Scenario – Speed profiles for Station 100 (Run 1).....	94
Figure 5-16: Near-Peak Scenario - Linear Correlation of VSLs safety impact to traffic congestion ..	95
Figure 5-17: Near-Peak Scenario – Variability in VSLs impact by simulation run.....	97
Figure 5-18: Near-Peak Scenario – Contour mapping of freeway speeds, Run 10 (non-VSLs).....	98
Figure 5-19: Near-Peak Scenario – Contour mapping of freeway speeds, Run 7 (non-VSLs).....	98
Figure 5-20: Off-Peak Scenario – Mapping of VSLs Displayed Speed Limits	99
Figure 5-21: Off-Peak Scenario – Distribution shift for Precursor Q, Station 100	101
Figure 5-22: Off-Peak Scenario – Distribution shift for precursor Q, Station 110.....	102
Figure 5-23: Off-Peak Scenario – Distribution shift for precursor Q, Station 120.....	102
Figure 6-1: Modification 1, Near-Peak Scenario – Average proportions of occupancy levels	108

Figure 6-2: Modification 1, Near-Peak Scenario – Average proportions of trigger conditions	109
Figure 6-3: Modification 2, Peak Scenario – Comparison of percent time congested	110
Figure 6-4: Modification 2, Near-Peak Scenario – Comparison of percent time congested	111
Figure 6-5: Modification 5, Peak Scenario – Mapping of VSLS displayed speed limits	114
Figure 6-6: Modification 5, Peak Scenario – Station Relative Safety Benefits for the Original and Modified Algorithms.....	115
Figure 6-7: Modification 5, Near-Peak Scenario – Mapping of VSLS displayed speed limits	115
Figure 6-8: Modification 5, Near Peak Scenario – Comparison of percent time congested.....	116
Figure 6-9: Modification 5, Near-Peak Scenario –Correlation of VSLS safety impact to traffic congestion	117
Figure 7-1: Precursor Level Contribution to Crash Potential	124
Figure 7-2: Precursor Q Distributions A and B	125
Figure 7-3: Q Distributions within Level 4	125

1. INTRODUCTION

1.1 Background

As urban populations escalate and travel demand continues to grow, transportation managers are faced with the increasing challenge of moving people and goods safely and efficiently within the constraints of available land access, environmental restrictions, and strained budgets. Particularly for freeways in dense urban areas with little opportunity for added road capacity, driver safety and travel time have continued to suffer as a result of mounting congestion. Previous research has found that the collision rate on a congested freeway is nearly twice that on free flowing freeways (Smulders, 1990). In recent years, the integration of technology in the form of Intelligent Transportation Systems (ITS) has been regarded as a promising solution to the effective management of freeways within the confines of existing infrastructure. Intelligent Transportation Systems are defined as the integration of advanced and emerging technologies into transportation system infrastructure to save lives, time, money, energy, and the environment (Fu et al., 2003). ITS applications provide the potential advantages of increased safety, improved travel times, long term capital savings, and reduced fuel consumption (Parviainen et al., 1997).

Variable Speed Limit Sign (VSLS) systems are a form of ITS that enables transportation managers to dynamically change the posted speed limit in response to prevailing traffic and/or weather conditions. A VSLS system consists of dynamic message signs (DMS) deployed along a roadway and connected via a communication system to a traffic management centre. The DMS are used to display a regulatory or advisory speed limit. The primary goals of a VSLS system differ between transportation agencies, but in general the systems aim to homogenize traffic flow, improve safety, and reduce driver stress. Operated and enforced properly, variable speed limits are believed to provide the benefits of improved safety, increased traffic flow, reduced travel times, and less stressful driving situations (Shi and Ziliaskopoulos, 2002).

1.2 Motivation

Worldwide, VLSL systems have been deployed in relatively few locations and with varying degrees of capability. Most systems are limited to only respond to inclement weather conditions or work zone management. Other, more sophisticated systems include measures for real-time congestion management in response to incidents or recurrent congestion. Due to the dynamic control that these ITS systems impose on traffic, estimating the direct costs and benefits in terms of performance can be difficult. Benefits have been reported from empirical studies in terms of safety with reduced collisions (UK Highways Agency, 2004; Robinson, 2000) and reduced speed variability (Rämä, 1999), and in terms of improved quality of traffic flow as perceived by the driver (van den Hoogen and Smulders, 1994). Although in general, such benefits have been recognized, most of the empirical studies to date are limited by one or more of the following:

- Lack of control of important influencing factors such as traffic volumes, degree of enforcement and compliance, etc;
- Empirical benefits reported largely in terms of qualitative evidence; and
- Transferability of results to other jurisdictions (i.e. Europe to North America).

Adding to these difficulties is the complication of evaluating the direct safety impacts of a VLSL implementation. Traditional crash prediction models which express expected crash rate as a function of static characteristics such as AADT, daily average speed, or road geometry are not appropriate. These models are developed from historical crash occurrence data to identify physical “black spots” and cannot capture the dynamic impact of VLSL application. Also, empirical “before and after” evaluations of ITS to identify changes in crash rates do not consider changes in volumes, nor do they consider temporal fluctuations in crash rates which may occur naturally regardless of an applied treatment.

In recent studies, Lee et al. (2004) and Abdel-Aty et al. (2005) have used microscopic simulation in combination with real-time crash potential models to test the impacts of VLSL response to real-time traffic safety measures. Lee et al. found that for highly congested locations, VLSL provided a reduction in crash potential of as much as 25%, but increased travel time. In contrast, Abdel-Aty et al. found that VLSL provided a large reduction in crash potential during low loading (higher speed) conditions, but had little impact for peak period

conditions Abdel-Aty et al. also found a consistent decrease in travel time for the low loading conditions using VSLS; however, the relative change in travel time from the non-VSLS case to the VSLS case was very small.

Considering these results and the limitations from empirical studies, the expected overall benefit of implementing VSLS is still unclear. Therefore, this thesis is devoted to the study of the operations of practical variable speed limit strategies and the resulting impact on traffic performance. Safety and traffic flow impacts of a candidate VSLS control strategy for an urban North American freeway section were quantified using a microscopic simulation model (PARAMICS) combined with a categorical crash potential model.

1.3 Scope and Objectives

This thesis has the following objectives:

- 1) Validate a real-time crash prediction model for a candidate section of freeway;
- 2) Develop a candidate VSLS control algorithm with potential for practical applications;
- 3) Evaluate the performance of the VSLS control strategy for a range of traffic conditions in terms of safety and travel time; and
- 4) Test the sensitivity of the VSLS impact results to modifications of the control algorithm.

1.4 Content of Thesis

This thesis is organized into seven chapters. The contents of Chapters 2 through 7 can be summarized as follows:

Chapter 2 reviews the existing VSLS deployments, macroscopic and microscopic VSLS evaluations, and the measured impacts on safety and traffic performance;

Chapter 3 explains the procedure for calibrating the real-time categorical crash prediction model used to evaluate the safety impact of the modelled VSLS system;

Chapter 4 outlines the structure of the microsimulation model, including a description of the selected study site, the development of the VSLS control algorithm and the calibration and validation of the simulation model;

Chapter 5 presents the results of the modelling analysis and discusses the details of the safety and travel time impacts of VSLS on three scenarios of traffic congestion;

Chapter 6 presents the results of a sensitivity analysis, evaluating the changes to the safety and travel time impacts upon modifications to the parameters within the VSLS control algorithm; and

Chapter 7 presents the conclusions and recommendations.

2. LITERATURE REVIEW

This chapter, consisting of four sections, reviews the past studies on VSLS applications. The first section introduces the concept of variable speed limits by outlining their advantages over static speed limits. The second and third sections review the objectives, operations and impacts of empirical and theoretical VSLS studies, respectively. The final section summarizes the limitations found in these strategies and identifies the need for further research.

2.1 Introduction to Variable Speed Limits

Conventional speed limits are set to assist drivers in choosing a safe travel speed. Regulatory static speed limits are traditionally established by law or in accordance with established engineering practices. According to the Manual on Uniform Traffic Control Devices (MUTCD, 2003) the following factors shall be taken into consideration when determining the appropriate numerical value for a static speed limit:

- 1) Road characteristics, shoulder condition, grade, alignment, and sight distance;
- 2) The 85th percentile and pace speed¹;
- 3) Roadside development and environment;
- 4) Parking practices and pedestrian activity; and
- 5) Reported crash experience for at least a 12-month period.

This practice assumes ideal road conditions and employs factors that are time invariant, and in some cases the speed limit selection may be constrained by government policy. When factors influencing vehicle speeds are time invariant, static speed limits underachieve in a rapidly changing environment (Shi and Ziliaskopoulos, 2002). For non-ideal road conditions (e.g. inclement weather or poor visibility) the posted speed limit may no longer represent a safe travel speed. For time varying traffic conditions such as the presence of turbulence or shockwaves caused by recurrent or non-current congestion, other speed limits may be appropriate to ensure safe travel and homogenous flow. Furthermore, many highways are

¹ Pace speed is defined as a 10 mph (16 km/h) range of speeds that usually takes in 70% of all drivers (FHWA, 2006).

constructed with a design speed that is considerably different than the maximum speed limit allowed under jurisdictional law. Speed limits that are perceived to be unreasonably low can lead to low speed-limit compliance rates, and high variance in vehicle speeds. This suggests that, in the absence of strict enforcement, while some drivers obey the speed limit, other drivers select their own maximum safe travel speed as a function of the quality of the highway, the level of traffic volume, the weather conditions, etc., and this speed may exceed the posted speed limit. Given the diverse composition of driver characteristics and behaviour within a traffic stream, varying reactions to changing road, weather, or traffic conditions can lead to a high variability of traffic speeds (Liu and Popoff, 1997) which can translate into potentially unsafe situations (Garber and Giradaju, 1989; Garber and Ehrhart, 2000; Taylor, 2000).

Considering the deficiencies of static speed limits, there has been a need for speed limits that adjust over time in response to prevailing environmental and traffic conditions, assist drivers in selecting a safe travel speed, and provide a more relevant and credible speed limit. Variable speed limit control can provide more realistic speed limits that in turn lead to improved driver response, higher compliance, lower speed variance, and increased safety (FHWA, 2004).

2.2 Empirical Applications in VSLS

VSLS systems are deployed as a series of electronic dynamic message signs (DMS) mounted on roadside structures or overhead gantries. Based on an industry scan, the ideal spacing of the signs has been found to be 700-800 metres (IBI Group, 2005), which is long enough for drivers to react to a speed change, but short enough to frequently update drivers of the current speed limit. To date, a limited number of VSLS systems have been successfully implemented with real-time response strategies to inclement weather, construction work-zones, and incident and congestion management. Table 2-1 summarizes most of the VSLS systems that have been deployed.

Table 2-1: Variable Speed Limit Deployments (IBI Group, 2005)

VSLs Location (Year Deployed)	Primary Reason for Implementation	Extent of Roadway Covered
<i>Deep Bay Link & Route 8</i> Hong Kong (2005)	Congestion and Incident Management	12 signs over 12 km per section
<i>A3, A5, A8, & A9 Autobahns</i> Germany (1974)	Congestion and Weather Response	Up to 30 km/motorway Signs spaced 1.5 km - 2 km
<i>M25 Controlled Motorways</i> London, UK (1995)	Congestion Response	Signs every 1 km over 20+ km
<i>A2 Motorway</i> The Netherlands (1992)	Congestion Response	40 signs over 20 km
<i>Western Ring Road</i> Melbourne, Australia (2002)	Congestion Response	37 signs/direction over 26 km
<i>Ayalon Highway</i> Israel (late 1990s)	Congestion Response	32 signs over 15 km
<i>New Jersey Turnpike</i> New Jersey, USA (1968)	Hazard Response (includes incidents, weather, congestion)	141 signs over 215 km
<i>E18</i> Finland (1994)	Weather Response	36 signs/direction over 12 km
<i>I-90</i> Washington, USA (1997)	Weather Response	13 signs over 17 km
<i>Confederation Bridge</i> New Brunswick, Canada (1997)	Weather Response	17 signs/direction over 13 km
<i>F6 Tollway</i> Sydney, Australia (1993)	Weather Response (Fog)	12 signs/direction over 11 km
<i>A16</i> The Netherlands (1991)	Weather Response (Fog)	15 signs over 12 km
<i>I-96</i> Michigan, USA (2002)	Work Zone Response	4 deployments of up to 7 signs, within 30 km

The majority of these VSLs systems use a rules-based response, accepting inputs of real-time traffic and/or environmental data. These data can either be collected and processed by an operator at a traffic management centre, or collected and fed into a central server for automatic response. Weather and road surface data can be collected via Road Weather Information Stations (RWIS) as in Finland (Rämä, 1999) or by visibility sensors, as on the A16 in the Netherlands (Hogema and van der Horst, 1994) and on the F6 in Australia (FHWA, 1995). Traffic performance data can be collected in the form of speed, volume and occupancy data via inductive loop detectors or through closed circuit television (CCTV) cameras (UK Highways Agency, 2004). The data are processed and, based on predetermined control logic, the speed limit display is updated to reflect current conditions.

Presently, limited documentation is provided on the detailed operations and performance of the existing systems. Upon review of the existing systems, only five cases were found to provide detailed information on both the VSLS control strategy and the reported VSLS impacts. These VSLS deployments are as follows:

- M25 Controlled Motorways, UK – Congestion Management;
- A2 Motorway, The Netherlands – Congestion Management;
- Finland – Weather Management;
- Washington State, US – Weather Management; and
- Michigan State, US – Work Zone Management.

2.2.1 M25 Controlled Motorways, UK

System Background and Objectives

The M25 is a highly travelled orbital motorway in London, UK, consisting of dual 4-lane carriageways, one running in a clockwise direction and the other in an anticlockwise direction. In 1995 the UK Highways Agency introduced Controlled Motorways, an intelligent freeway management system on the M25 motorway. The freeway management system includes mandatory variable speed limit signs placed between Junctions 11 and 15 at one kilometer intervals and mounted on overhead gantries. The primary objective of the system is congestion management, by harmonizing speeds and reducing the severity of shockwaves to delay the onset of flow breakdown and to aid flow recovery (UK Highways Agency, 2004). Secondary objectives included a calmer driving experience and reduced fuel consumption.

System Control Strategy

The motorway is instrumented with dual loop detectors spaced every 500 m that provide speed, volume and occupancy data. The posted speed limits are based on a measure of directional traffic volumes. When station volumes reach 1650 vehicles per hour per lane (vphpl), the speed limits reduce from a default of 70 mph to 60 mph. When the volumes reach 2050 vphpl, the speed limit is further reduced to 50 mph. The overall VSLS system is equipped for automatic response, but can be overridden by police officers.

System Impacts

Evaluating the impacts of the original system was difficult since traffic data were unavailable prior to 1995. However, upon planning for an expansion in 2002, traffic data were collected from 2000 onwards so a before-and-after evaluation could be formed around the expanded sections. A comprehensive impact analysis of the new VSLS was performed. The results of the impact analysis were presented in a business case for Controlled Motorways (UK Highways Agency, 2004) and are described below.

- **Safety** – Introduction of the Controlled Motorways resulted in an estimated 10% decrease in injury collisions. Collision data were compiled from 13 years prior to the VSLS expansion in 2002 and compared with collision activity following the new VSLS deployment. Also, collision data from nearby M25 sections without VSLS were collected to allow comparisons against trends.
- **Travel Times** – The anticlockwise carriageway experienced a reduction in travel time during weekdays, whereas the clockwise carriageway experienced an increase in travel time. This difference is suspected to be caused by the different levels of congestion between the two carriageways. The clockwise carriageway experiences significantly less congestion than the anticlockwise carriageway, particularly during the morning peak period. However, assuming volume levels are still large enough to induce a speed limit reduction, the speed restrictions will slow traffic down and cause delays. Travel times were also found to increase in the off-peak periods, not due to speed limit reductions, but due to the stricter enforcement measures which have resulted in compliance. Considering the varying impacts to travel times, the overall net impact is considered to be neutral.
- **Journey Time Reliability** – It was reported that the Controlled Motorways has contributed to more reliable journey times during the peak periods. These more predictable journey times are thought to offset increases in travel time; however, no data were provided to quantitatively substantiate this claim.

- **Flow Breakdown** – On the anticlockwise carriageway, the amount of time flow breakdown (speeds less than 25 mph) occurred was reduced by 9% and start-stop driving conditions were reduced by 6%. However a slight increase in flow breakdown occurred on the clockwise carriageway.
- **Lane Utilization** – The anticlockwise carriageway experienced an increase in lane utilization of 1% to 2% on lanes 1 and 2 and a similar reduction in lane utilization on lanes 3 and 4. This results in an overall more evenly distributed flow.
- **Headways** – Headways have been observed to be more uniformly distributed with fewer headways below 0.8 seconds and fewer headways above 1.5 seconds.

Other impacts include increased compliance, reduced emissions and noise, and reduced driver stress. Overall, the net benefit is unclear. It seems that the most positive benefits arise from congested periods on the anticlockwise carriageway. This raises concerns for the applicability of the current VSLS system for certain sections of road and certain periods of the day that experience lower levels of congestion.

The conclusion of the business case echoes this concern stating that the economic benefits (reduced collisions and emissions) of the VSLS expansion do not outweigh the economic costs of installation and increase in journey times. It is recommended that for the selection of further deployments, the presence of congestion is vital for economically favourable impacts.

2.2.2 A2 Motorway, The Netherlands

System Background and Objectives

Van den Hoogen and Smulders (1994) studied the impacts of a variable speed limit system on a 20 km segment of the A2 motorway in The Netherlands between the cities of Utrecht and Amsterdam. The VSLS system was implemented in 1992 with the objective of managing the congested morning and evening peak periods resulting from commuters travelling to and from Amsterdam on the 3-lane motorway. Mainline volumes during the peak period were as high as 2200 vphpl, and some single lane entrance ramp volumes as high as 1600 veh/h.

Motivation for the project stemmed from observed inefficiencies in lane utilization, speed differentials between lanes, and frequent lane changing, all contributing to dangerous instabilities within the traffic stream (Smulders, 1992).

System Control Strategy

A control strategy was developed to homogenize traffic flow by encouraging more uniform lane usage and less speed differential between lanes. Based on 1-minute averages of speed and volume data collected at dual loop detector stations every 500 m, the displayed speed limit could be reduced to 90 km/h or 70 km/h from the standard limit of 120 km/h. Speed limits were only implemented when station volumes approached capacity. The decision to post 90 km/h or 70 km/h speed limits was based on the average station speed. The objective of the system was not to reduce average speeds, but to reduce speed differences within and between lanes.

System Impacts

Data were collected for a seven month period in 1992 following the VSLS implementation and compared with data collected for the same period in 1991 when VSLS were not deployed. Note that one limitation of the study was a rise in traffic demand between 1991 and 1992, so the analysis had to be carried out on grouped levels of observed volumes (i.e. 5600-6000, 6000-6400 veh/h over 3 lanes). The analyses of the VSLS deployment measured a reduction in speed in all lanes, reduced speed differential between lanes, a reduction in the number and severity of shockwaves (particularly in the presence of high volumes), and a lower percentage of headways smaller than 1 second. Occupancies were found to have increased in all lanes, but such that the highest increase was experienced by the outer, less occupied, lane. From a qualitative perspective, drivers found the VSLS had created a “more quiet traffic situation.” The VSLS deployment did not, however, provide any quantitative evidence of a positive impact on capacity and throughput.

Van den Hoogen and Smulders conclude that the evidence of homogenized flow supports the use of VSLS as suitable tool for addressing road sections with turbulent traffic flow and unsafe driving behaviour. They also conclude that while VSLS can be useful for mitigating the impacts of traffic upstream of a bottleneck, due to the lack of evidence

supporting any benefit to throughput, a VSL system is not a suitable tool for solving congestion at a bottleneck itself.

2.2.3 E18, Finland

System Background and Objectives

A study in Finland (Rämä, 1999) evaluated the effectiveness of variable speed limits in response to poor weather and road surface conditions. The objective of the system was to influence driver behaviour and improve road safety through lower speed limits during inclement weather conditions. A 14 km section of the E18 in southern Finland was selected as the test site and equipped with 36 VSL.

System Control Strategy

Based on data received on 5-min intervals from road weather stations, variable speed limits were programmed to display either 100 km/h or 80 km/h during the winter and either 120 km/h or 100 km/h during the summer. Speed is reduced in the presence of snow or heavy rain or when thresholds of visibility and wind speed are breached. The system can operate autonomously, and when conditions worsen, the signs are updated immediately; however to prevent frequent fluctuations in the displayed speed limit, there is an adjustable time delay that postpones changes when conditions improve (Pilli-Sihvola, 1996).

System Impacts

Traffic data collected from sites equipped with VSL were compared with data from sites not equipped with VSL. Over a one year deployment period, Rämä found that the VSL deployment resulted in a statistically significant decrease in average speed as well as a decrease in speed variability. She also found a slight decrease in the proportion of short headways (less than 1.5 seconds) during the VSL deployment.

2.2.4 State of Washington, USA

System Background and Objectives

Ulfarsson et al. (2005) studied the effects of variable speed limits on mean speed and speed deviation from a deployment on the Interstate-90 in Washington State, USA. The objective of

this system was to address the significant variations in speed due to the combined effects of vehicle mix, inclement weather, and challenging road geometrics. Thirteen speed signs were deployed over 17 km for the winter months spanning 1997 and 1998.

System Control Strategy

Based on environmental data such as precipitation and visibility, and pavement conditions such as ice/snow accumulations or amount of standing water, speed limits were reduced from 105 km/h (65 mph) to as low as 56 km/h (35 mph) in 16 km/h (10 mph) decrements.

System Impacts

Ulfarsson et al. evaluated the VSLs impacts considering the interdependent relationship between mean speed and speed deviation. They found that for conditions of high speeds and lower speed deviations, the VSLs reduced the mean speed but increased speed deviation. On the other hand, for conditions resulting in low speeds and high speed deviation, the VSLs reduced both mean speed and speed deviation. From these results, Ulfarsson et al. recommended that VSLs provides the most benefit when used only during certain adverse conditions by harmonizing the speeds of drivers who would otherwise respond differently to the prevailing conditions.

2.2.5 State of Michigan, USA

System Background and Objectives

The U.S. Department of Transportation Federal Highway Administration evaluated the impacts of a VSLs deployment throughout an 18 mile work zone on Interstate-96 in Michigan, USA, during the summer of 2002 (FHWA, 2004).

System Control Strategy

The system collected traffic statistics (i.e. average speed, 85th percentile speed, etc.) at given locations and displayed speed limits based on predetermined logic. At spacing ranging from a few hundred metres to over a kilometre, each VSLs was programmed to display the estimated 85th percentile speed from the next downstream location, but the displayed speed could not exceed 60 mph throughout the work zone. Prior to VSLs deployment the maximum speed limit throughout the work zone was a static 50 mph.

System Impacts

By collecting traffic performance data before and during the VSLS deployment, the study evaluated the impacts of VSLS on speed limit compliance, speed limit credibility, safety, and travel time. The study found that the effectiveness of VSLS on traffic performance within the work zone was relatively minor. Speed variance and 85th percentile speeds experienced no measurable impact; travel time savings were small and unlikely to be perceptible by the driver; and, although the VSLS deployment did not appear to further contribute to crash situations, it was unclear whether any positive safety benefit resulted. The only significant result was an increase to average speeds. Also, evidence of a decreased percentage of high speed drivers (> 70 mph) suggests increased compliance with VSLS. The authors felt the lack of VSLS effectiveness was due to limited disaggregated data and traffic speeds being more affected by geometry and merging traffic than by the posted speed limits. Nevertheless, the authors concluded that by responding to changes in congestion and geometry, a VSLS system can present far more credible information to drivers than traditional static speed limits.

These case studies demonstrate the objectives, control strategies and general impacts of existing VSLS deployments. Despite varying applications (i.e. congestion, weather, or work zone management), the systems share common objectives of smoothing traffic flow and adjusting vehicle speeds to prevailing conditions. The control strategies range from being more basic, as in rules based weather response, to more complex algorithms for congestion management. For these, VSLS typically activate upon some measure of congestion, and display the speed limit best matching the current traffic speed. The impacts are also somewhat consistent, expressing improvements in reduced speeds, smoothed traffic flow through reduced speed variation, and a calmer driving experience – all of which may account for measured reductions in crash frequency and/or severity. Also consistent is the lack of positive impact on throughputs and travel time. Although it is useful to have impacts reported from empirical deployments, these studies lack in achieving the following:

- Developing an understanding of the interaction between traffic flow changes and VSLS activity;

- Proposing evidence of relationships between VSLs activity and resulting safety improvements; and/or
- Studying the impacts on performance of varying the parameters within the VSLs control strategies.

These limitations are in part due to the risk and effort involved in deploying live systems. Field operational tests can be very expensive, time consuming, limited in flexibility, and difficult to implement. In addition, before and after studies are difficult to control and can be hindered by confounding effects (Ben-Akiva, 2003). For instance, potential confounding effects include temporal changes in collision risk (Hirst et al. 2005), changes in traffic demands prior to and after VSLs deployment (van den Hoogen and Smulders, 1994) and effects of enforcement policies (e.g. advisory vs. mandatory enforcement) undertaken during speed limit changes (TRB, 1998, Lee et al., 2004). To overcome these limitations, the impacts of variable speed limit have been examined through macroscopic and microscopic traffic simulation modelling studies.

2.3 Modelling Applications in VSLs

Macroscopic traffic models employ an analytical approach to representing vehicle behaviour by describing traffic as a continuous flow obeying global rules (Bourrel and Lesort, 2003); whereas microscopic models are based on the interaction of individual vehicle behaviour. Macroscopic models can use mathematical relationships to help understand the relationship between speed limit changes and traffic flow, therefore offering an advantage over microscopic models which require assumptions about individual driver behaviour (Lee et al., 2004).

2.3.1 Macroscopic Modelling

Previous research in the macroscopic modelling of variable speed control has taken two approaches – the first with emphasis on homogenizing traffic flow, and the second on preventing breakdown by controlling traffic flow (Hegyi et al. 2005). For example, Smulders (1990) applied and evaluated homogenizing control on a simplistic macroscopic traffic model (consisting of stochastic differential equations for density and mean speed) over one section

of freeway. The result was an increase in the stability of traffic flow measured by a reduction in small headways on the “fast” lane, and by an increase in the mean time to congestion. Although the control strategy of homogenization could not prevent the onset of congestion, it was successful in postponing congestion, particularly for volumes 10% to 15% below capacity. Alessandri et al. (1997) developed a macroscopic model to apply a variable speed signaling (VSL) strategy to optimize cost functions of throughput, density, and mean time. They found that speed signaling was capable of avoiding congestion and improving flow, but had little impact on mean travel time.

Since the homogenization approach can only prolong the time to flow breakdown and not suppress or resolve existing shockwaves (Hegyi et al., 2005) research has been performed to demonstrate how optimizing variable speed limits can, in fact, control flow and prevent traffic breakdown (Breton et al., 2002; Hegyi et al., 2003). Breton et al. used model predictive control to optimize a continuous speed control signal every time step. They found that by reducing speed limits and thereby temporarily reducing the flow upstream of locations of expected congestion, a downstream traveling low-density wave is created which meets the high-density shockwave, leading to the eventual dissipation of the congestion before it can propagate upstream. Hegyi et al. (2005) extended this research by addressing several limitations important to the practical applicability of the work. For example, discrete values of speed limits were included to replace continuous values, and a safety constraint was included that limited the magnitude of speed limit drops vehicles could encounter. Results from a simulated network showed that even with the inclusion of such constraints, variable speed limits were successful in eliminating shockwaves and reducing the time spent on the network by 17.3%.

2.3.2 Microscopic Simulation Modelling

Although macroscopic models have successfully described the theoretical impact of variable speed limit logic on traffic flow, the inexplicit description of individual vehicle variables and interactions may hinder the realistic impact of the speed control on traffic flow patterns (Beh-Akiva, 2003). Furthermore, to date, macroscopic studies fail to include a safety evaluation of variable speed limits regarding the temporal changes in crash potential. To overcome these limitations, microscopic simulation can be combined with crash potential models to evaluate

the impacts of VSLs on safety and network performance. For example, Torday and Bierlaire (2001) evaluated variable speed limits for a section of a 4-lane roadway in Lausanne, Switzerland using the microscopic simulator, MITSIM. They tested the impacts of imposing reduced speed limit from the default of 120 km/h by 5 km/h decrements upstream of a heavily congested location. They concluded that the variable speed limits provide little benefit to system performance, particularly for speed limits below 100 km/h which had a negative impact on throughput. However, the study results indicated that lowering speed limits positively impacts safety by lowering speeds and reducing the severity of a rear-end collision should it occur. Yadlapati and Park (2004) used the microscopic simulator VISSIM to study the safety and mobility impacts of VSL control strategies at work zones in Virginia. They tested several different VSL control logics, incorporating average speeds, volume, and a minimum safety distance equation as a surrogate measure for safety. They found that the impact of the control strategies varied with driver compliance and traffic demand level (i.e. oversaturated vs. undersaturated), but that variable speed limits could be effective for improving both safety and mobility.

Lee et al. (2004) extended upon previous VSL strategies and evaluations by including a real-time crash prediction model. Calibrated from existing crash data, their crash model calculates a real-time measure of crash potential based on loop detector data (e.g. 20-second speed, volume, and occupancy data). By combining this crash model with the microscopic simulator, PARAMICS, they evaluated a variable speed control strategy based on changes in crash potential during congested conditions on a hypothetical 1-mile freeway section. The results indicated that by temporarily reducing speed limits during risky traffic conditions, variable speed limits can reduce average total crash potential by approximately 25%, with the greatest benefit at locations of high traffic turbulence (e.g. merging locations). However, Lee et al. found that variable speed limit control that produced positive safety benefits was associated with an increase in system travel time.

Recently, in a similar approach, Abdel-Aty et al. (2005) used PARAMICS to simulate a variable speed limit deployment on a section of the Interstate-4 near Orlando, Florida. The study focused on improving safety at a location of high collision frequency for both high-loading (congested) and low-loading (less congested) conditions. As in Lee et al. (2004), the

variable speed limit control was based on real-time measures of crash potential, but with a broader application. Twenty miles were simulated with VSLS control rather than just 1 mile and speed limits were allowed to both increase and decrease simultaneously at upstream and downstream locations, respectively. Abdel-Aty et al. found that variable speed limits were able to significantly reduce crash likelihood at the location of interest during low-loading conditions. They also found that travel time was slightly improved under the VSLS strategy. However, although a safety benefit was recognized in the area being targeted, negative safety impacts were identified upstream and downstream of the active VSLS control. This phenomenon of crash risk migration raises the concern that particular VSLS strategies can contribute to a crash situation that they are meant to solve (Abdel-Aty et al., 2006). Abdel-Aty et al. recommend that implementing advance warnings of speed changes may mitigate this problem. Also of interest was the lack of effectiveness of VSLS during high-loading conditions. Abdel-Aty et al. found that the use of VSLS yielded little benefit to safety and network performance during periods of higher congestion. Although the results indicate the positive potential of VSLS during off-peak periods, they contradict the findings from previous research (empirical and theoretical) that promote the effectiveness of VSLS during periods of high congestion (UK Highways Agency, 2004; Lee et al., 2004; Hegyi et al., 2005). In lieu of VSLS, Abdel-Aty et al. recommend that alternative ITS strategies such as ramp metering and lane changing restrictions should be investigated for periods of high congestion.

Modelling applications of VSLS allow a cost-effective and risk free analysis of complex VSLS control algorithms to gain a better understanding of their impacts on traffic performance. In addition, microscopic simulation studies on variable speed limits reveal the potential benefits regarding improved safety under various control strategies. However, these studies are limited by one or more of the following:

1. Evaluation of VSLS is made on hypothetical road sections;
2. Transferability of control strategies to practical applications. Control strategies based on theoretical measures of crash potential may not be readily accepted by transportation authorities, nor are they likely to adopt complex optimization strategies;

3. Lack of consideration of secondary impacts (crash migration) as identified by Abdely-Aty et al. (2006).

Furthermore, the discussion above indicates that the VSLS control strategies employed in the modelling studies to date have primarily focused on either safety objectives or travel time objectives, but rarely both. Macroscopic studies have focused on speed control as a means to improve traffic throughput and dampen the amplification of shockwaves, whereas microscopic studies have primarily evaluated VSLS as a tool for crash reduction. Therefore, a need exists for a VSLS evaluation framework with the objective of capturing both safety and traffic performance impacts to identify a VSLS control strategy suitable for practical deployment.

2.4 Chapter Summary

This chapter explored the objectives, operations and impacts of variable speed limits applied both in real deployments and in theoretical deployments. Limitations were identified for each type of application. Empirical applications have practical objectives and employ tangible and clearly understood control strategies, but the reporting of impacts is limited. On the other hand, modelling applications have taken an in depth approach to understanding the impacts of changing speed limits on traffic flow or crash potential, but the studies are limited in analyzing multiple objectives and the control strategies are often too complex or based on unrealistic assumptions and therefore cannot be directly applied for practical applications.

Considering these limitations, a disconnect exists between a practical VSLS control strategy and a broad evaluation framework. Therefore, there is a need for further research that evaluates the safety and traffic performance impacts of comprehensive VSLS control strategies suitable for practical applications. The following chapters outline such an evaluation procedure, using a microscopic simulation model combined with a categorical crash potential model.

3. CRASH POTENTIAL MODEL

3.1 Selection of Model

The term crash potential can be defined as the number of crashes expected to occur for a roadway segment under given traffic, environmental and roadway conditions. Many traditional crash prediction models measure crash potential based on static variables such as Annual Average Daily Traffic (AADT) and do not consider the short term variations in traffic flow (Lee et al., 2002). Evaluating the safety impact of a dynamic ITS deployment such as variable speed limits requires a crash prediction model that can measure changes to crash potential as traffic conditions vary with time. Recent research has found that freeway traffic flow characteristics can be employed to predict the likelihood of a crash occurrence (Abdel-Aty et al., 2004; Golob and Recker, 2004; Lee et al., 2003; Oh et al., 2001). The studies explore varying approaches to developing models that can predict changes to crash potential in real-time.

The work of Lee et al. (2003) was deemed appropriate in this study because a) the model was developed using data from a freeway section in Toronto, Canada, and b) the authors applied their real-time crash potential model in evaluating the impacts of a short VSL deployment on a hypothetical, simulated freeway. The following sections describe the original model framework and the process undertaken to calibrate and validate the model parameters for the application to a different freeway segment.

3.2 Crash Potential Model Framework

The crash potential model developed by Lee et al. (2003) calculates crash frequency as a function of traffic conditions called crash precursors, external control factors and exposure. A log-linear model was chosen for the development of the crash potential model since it allows the investigation of the relationships between the input variables for different levels of crash frequency. Also, it can incorporate a value of exposure that is associated with each traffic condition and external control factors. The log-linear function developed by Lee et al. to

calculate crash potential is shown in Equation 3-1. The inputs to the log-linear model are described in the following sections.

$$\text{Crash Potential} = \frac{F}{EXP^\beta} = \exp(\theta + \lambda_{CVS(i)} + \lambda_{Q(j)} + \lambda_{COVV(k)} + \lambda_{R(l)} + \lambda_{P(m)}) \quad (3-1)$$

where,

- F : expected number of crashes;
- EXP : exposure (veh-km);
- β : parameter for exposure;
- θ : constant;
- $\lambda_{CVS(i)}$: effect of the i^{th} level of crash precursor variable CVS ;
- $\lambda_{Q(j)}$: effect of the j^{th} level of crash precursor variable Q ;
- $\lambda_{COVV(k)}$: effect of the k^{th} level of crash precursor variable $COVV$;
- $\lambda_{R(l)}$: effect of the l^{th} level of road geometry (control factor);
- $\lambda_{P(m)}$: effect of the m^{th} level of time of day (control factor).

In the above functional specification, exposure must be converted to logarithmic form before estimating the parameter for exposure, β . To circumvent the conversion of exposure values, Lee (2004) rewrote Equation 3-1 as follows:

$$\ln(F) = \theta + \lambda_{CVS(i)} + \lambda_{Q(j)} + \lambda_{COVV(k)} + \lambda_{R(l)} + \lambda_{P(m)} + \beta' EXP$$

$$\ln(F) - \beta' \frac{EXP}{\ln(EXP)} \cdot \ln(EXP) = \theta + \lambda_{CVS(i)} + \lambda_{Q(j)} + \lambda_{COVV(k)} + \lambda_{R(l)} + \lambda_{P(m)}$$

$$\ln \left(\frac{F}{EXP^{\beta' \frac{EXP}{\ln(EXP)}}} \right) = \theta + \lambda_{CVS(i)} + \lambda_{Q(j)} + \lambda_{COVV(k)} + \lambda_{R(l)} + \lambda_{P(m)}$$

$$\frac{F}{EXP^{\beta' \frac{EXP}{\ln(EXP)}}} = \exp(\theta + \lambda_{CVS(i)} + \lambda_{Q(j)} + \lambda_{COVV(k)} + \lambda_{R(l)} + \lambda_{P(m)}) \quad (3-2)$$

Lee (2004) claimed the last line of Equation 3-2 demonstrated that the parameter for exposure is not constant as in traditional crash prediction models; rather, in this real-time crash potential model, exposure values vary as the traffic conditions represented by crash precursor values constantly change.

3.2.1 Crash Precursors

The measures of traffic conditions, termed crash precursors, represent the traffic flow conditions prior to a crash occurrence. More turbulent levels of crash precursors correspond to a higher likelihood of an impending crash situation. Lee et al. (2003) explored a number of traffic flow characteristics believed to be related to crash occurrence, including:

- temporal variation of speed at a fixed location;
- longitudinal variation in speed along road sections;
- variation in speed across lanes;
- lane changing behaviour; and
- traffic density.

Three of these characteristics were found to be the most statistically powerful in predicting crash occurrence: 1) temporal variation of speed at a fixed location; 2) longitudinal variation in speed; and 3) lane changing behaviour.

The temporal variation of speed at a fixed location represents the stability of speeds between vehicles in a traffic stream. Low variation of speed is an indication of smooth traffic flow in which vehicles are travelling at nearly constant speeds over time. An increase in this speed variation indicates more variability in the speed choice among drivers. This in turn requires drivers to adjust speeds more frequently, leading to the deterioration of flow stability and a higher risk of driver error and an impending crash situation. The temporal variation of speed is measured by the coefficient of variation of speed (precursor *CVS*), calculated at the nearest detector station upstream of a crash location. *CVS* is a measure of dispersion which normalizes the standard deviation (Lee, 2004; May 1990). It is expressed by Lee et al. (2002) through Equation 3-3.

$$\begin{aligned}
CVS &= \frac{1}{n} \sum_{i=1}^n \frac{(\sigma_s)_i}{\bar{s}_i} \\
&= \frac{1}{n} \sum_{i=1}^n \left(\sqrt{\frac{\frac{\Delta t}{t_p} \sum_{t=t^*-\Delta t}^{t^*} (s_i(t))^2 - \left(\sum_{t=t^*-\Delta t}^{t^*} s_i(t) \right)^2}{\frac{\Delta t}{t_p} \left(\frac{\Delta t}{t_p} - 1 \right)}} \right) / \left(\frac{\sum_{t=t^*-\Delta t}^{t^*} s_i(t)}{\left(\frac{\Delta t}{t_p} \right)} \right) \quad (3-3)
\end{aligned}$$

where,

n : total number of lanes.

$(\sigma_s)_i$: standard deviation of speed on lane i computed over period Δt ;

\bar{s}_i : average speed on lane i computed over period Δt (km/hour);

Δt : observation time slice duration (seconds);

t_p : time interval of observation of speed (seconds);

t^* : time of crash occurrence;

$s_i(t)$: speed on lane i at time t upstream of a location (km/hour);

The spatial (longitudinal) variation of speed along road sections measures the difference in average travel speeds between two consecutive loop detector stations. A small spatial variation indicates constant speeds and a traffic state of little acceleration. However, a large spatial variation in speed indicates traffic will experience an abrupt change in travel speed, requiring either sudden acceleration or deceleration. A state of sudden deceleration is most likely to cause crashes and often occurs as a traffic queue is formed during recurrent or non-recurrent congestion. Spatial variation of speed, represented by the precursor Q is expressed through Equation 3-4.

$$Q = \bar{s}_1 - \bar{s}_2$$

$$= \frac{t_p}{\Delta t} \sum_{t=t^*-\Delta t}^{t^*} \left(\frac{\sum_{i=1}^{n_1} s_{1i}(t)v_{1i}(t)}{\sum_{i=1}^{n_1} v_{1i}(t)} \right) - \frac{t_p}{\Delta t} \sum_{t=t^*-\Delta t}^{t^*} \left(\frac{\sum_{i=1}^{n_2} s_{2i}(t)v_{2i}(t)}{\sum_{i=1}^{n_1} v_{2i}(t)} \right) \quad (\text{Equation 3-4})$$

where,

- Q : average speed difference between upstream and downstream locations (km/hour);
- \bar{s}_1, \bar{s}_2 : average speeds computed over period of Δt upstream and downstream of a location, respectively (km/hour);
- $s_{1i}(t)$: speed on lane i at time t upstream of a location (km/hour);
- $s_{2i}(t)$: speed on lane i at time t downstream of a location (km/hour);
- $v_{1i}(t)$: volume on lane i at time t upstream of a location (km/hour);
- $v_{2i}(t)$: volume on lane i at time t downstream of a location (km/hour);
- n_1, n_2 : numbers of lanes upstream and downstream of a location, respectively.

This expression has been modified slightly from the work of Lee et al. (2003). Equation 3-4 calculates average station speed by means of a volume weighted average speed, whereas Lee et al. (2003) expressed station average speed simply as the sum of individual average lane speeds divided by the number of lanes. A volume-weighted average is considered to be a more representative value of average speed across lanes. Also, Lee et al. expressed Q as the absolute difference between upstream and downstream station speeds. Equation 3-4 maintains the directional difference between the station speeds. A negative difference is associated with a state of acceleration whereas a positive difference is associated with a state of deceleration. In an extension of his earlier work, Lee (2004) found that a deceleration state contributed more to crash risk than a state of acceleration. Therefore, the directional differences were preserved.

The third traffic characteristic, lane changing behaviour, is estimated by the average covariance of volume difference between upstream and downstream locations across adjacent

lanes (precursor *COVV*). The covariance of volume captures the correlation of traffic volume changes between two lanes (i.e. traffic moving from lane 1 to lane 2 creates a volume reduction on lane 1 and subsequently a volume increase on lane 2). Thus, *COVV* is a surrogate measure of lane changing activity. High levels of *COVV* indicate frequent lane changing and thus more turbulence within the traffic stream, which increases the likelihood of a crash occurrence. Lee (2004) expresses *COVV* through Equation 3-5.

$$COVV = \frac{1}{n-1} \sum_{i=1}^{n-1} |cov(\mathbf{V}_i, \mathbf{V}_{i+1})|$$

$$= \frac{1}{n-1} \sum_{i=1}^{n-1} \sum_{t=t^*-\Delta t}^{t^*} [(\Delta v_i(t) - \Delta \bar{v}_i)(\Delta v_{i+1}(t) - \Delta \bar{v}_{i+1})] \quad (\text{Equation 3-5})$$

where,

$\Delta v_i(t)$: volume difference between upstream and downstream locations on lane i at time t ;

$\Delta \bar{v}_i$: average volume difference on lane i over period Δt ;

\mathbf{V}_i : vector of $\Delta v_i(t)$ over period Δt (i.e. $\mathbf{V}_i = \{\Delta v_i(t_0), \Delta v_i(t_0+1), \dots, \Delta v_i(t_0+\Delta t)\}$).

* Lane i and lane $i+1$ are adjacent lanes.

The three crash precursors, *CVS*, *Q*, and *COVV* can be post-processed or calculated in real-time using traffic flow measures such as volume, speed, and occupancy, which are easily extracted from dual loop detector data. The period over which the precursors values are calculated is called an observation time slice, Δt . The selection of Δt involves identifying the time over which the impact of crash precursors on crash occurrence is maximized. For example: is the impact of *CVS* most significant when it is computed over periods of 2-minutes, 5-minutes, or 10-minutes prior to a crash? To establish the best observation time slice for each precursor, Lee et al. applied a method to determine the maximum difference in precursor values between crash and non-crash cases. For a number of time intervals, they measured the difference in the frequency distribution of the precursor values between crash and non-crash data. They found that the frequency differences in *CVS*, *Q*, and *COVV*, were maximized at Δt

= 8 minutes, 2 minutes, and 2 minutes, respectively. These observation time slice durations were carried forward for use in this study.

3.2.2 External Control Factors

External control factors include road geometry, time of day and environmental conditions. These factors alone can affect driver behaviour, so it was necessary to include them in the crash potential model to identify the isolated effects of the crash precursors. Road geometry refers to the lane configuration of a freeway segment with regard to entrances and exits, rather than horizontal or vertical alignment. Lee et al. found that freeway segments with merging or diverging traffic contribute more to crash potential than straight freeway segments with no changes in lane configuration. Time of day refers to peak and off-peak periods. Typically, traffic volumes and congestion are higher during peak periods and drivers, particularly commuters, may react more aggressively to maintain their schedules. These factors are likely to increase the likelihood of a crash occurrence during the peak periods. Lastly, environmental conditions include such factors as local weather, road surface quality, and lighting. Due to the limited amount of available environmental data, the effect of these factors can be difficult to capture. The most disaggregated data available is one-hour weather data collected at nearby weather stations. Lee et al. found that weather was not a strong explanatory variable (at least from the data that was readily available) and omitted it from their final crash model.

3.2.3 Exposure

Exposure is a crucial component for the calibration of the log-linear parameters employed in the crash model as it forms a relationship between the frequency of traffic and environmental events and the associated crash frequency. For example, consider two traffic scenarios. The first scenario arises 20% of the time and experiences 20% of all crashes. The second scenario also experiences 20% of all crashes, but arises only 5% of the time. Although the crash frequencies are identical, the crash rate (crash frequency divided by level of exposure) is clearly higher for the second scenario.

Exposure is expressed in the crash model as the number of vehicle-kilometres corresponding with the exposure to each combination of traffic characteristics and external

control factors. In other words, the average vehicle-kilometres present over a road section are multiplied by occurrence of the probability of a certain time of day (peak or off-peak) at a certain type of road geometry (merge/diverge or straight) under a certain range of crash precursor values. The expression for exposure is shown in Equation 3-6.

$$EXP = p(CVS) \cdot p(Q) \cdot p(COVV) \cdot p(P) \cdot p(G) \cdot V \cdot L \cdot T \quad (\text{Equation 3-6})$$

where,

- EXP : exposure (veh-km);
- $p(CVS), p(Q), p(COVV)$: probabilities that precursors (i.e. CVS, Q and $COVV$) calculated from normal daily traffic will fall within the range of values from a specified category;
- $p(P)$: proportion of normal daily traffic volume associated with the peak and off-peak periods;
- $p(G)$: proportion of road section associated with merging/diverging and straight geometry;
- V : average annual daily traffic of the road section (veh/day);
- L : length of roadway section (km);
- T : observation time period (days).

Since the crash potential model is log-linear, the crash precursors are categorized. The probabilities corresponding with each precursor in the expression for exposure depend on the selection of categories. A category spanning a larger range of crash precursor values results in a higher probability for exposure than a category spanning a small range of values.

3.3 Calibration of Crash Potential Model

Lee et al. (2003) developed their crash potential model using traffic data and crash records from the Gardiner Expressway in Toronto, Canada. However, since the model had not been

applied elsewhere, the transferability of the parameter values to other freeway sections was unknown. Therefore, prior to application in this study, the crash potential model needed to be recalibrated using traffic data and crash records from the freeway section proposed for this study. The same procedure for calibration outlined by Lee et al. (2003) was applied and required the tasks provided in Figure 3.1. Each stage of the calibration process is explained further in the following sections.

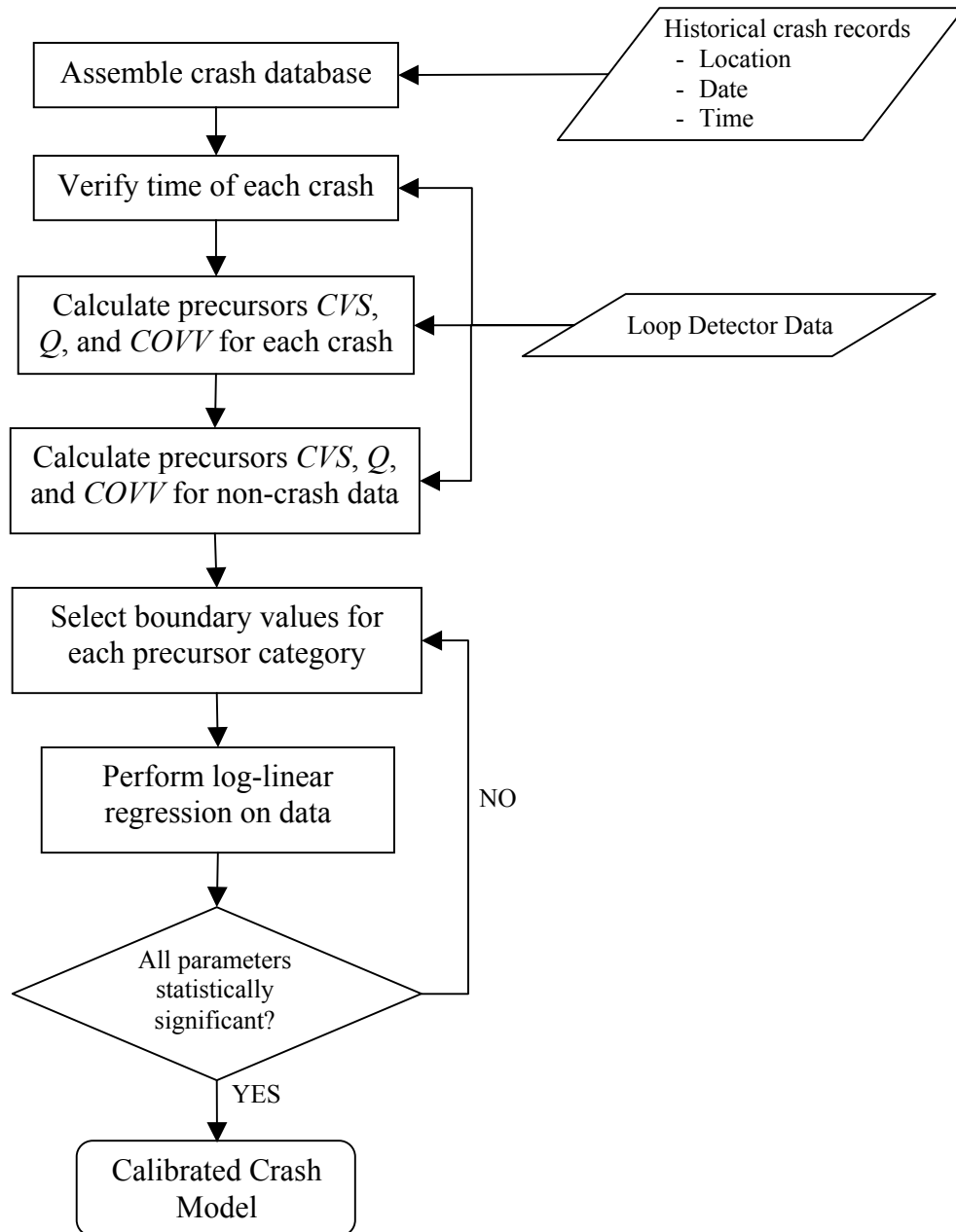


Figure 3-1: Outline of Calibration Procedure

3.3.1 Model Calibration Site

A segment of the Queen Elizabeth Way (QEW) in Mississauga, Ontario was chosen to calibrate the crash potential model for this study. The QEW is a multilane freeway located in southwestern Ontario, Canada. The freeway begins near the Canadian/American border at Fort Eerie and, following the coastline of Lake Ontario, passes through several urban centres such as Niagara Falls, St. Catharines, Hamilton, Burlington, Mississauga, and finally into Toronto. The QEW near Toronto services a large volume of commuter traffic in the morning and evening peak periods, resulting in heavy congestion and a high frequency of crashes.

The segment used for calibration was a 13 km section between Royal Windsor Drive and HWY 427 (schematic of section provided in Appendix A) including both directions of travel. This freeway segment features a posted speed limit of 100 km/hr, has 3 to 4 mainline lanes, and experiences a directional AADT of about 70 000 vehicles. The section is instrumented with dual loop detector stations in each mainline lane spaced at approximately 600 m. The study segment contains 26 loop detector stations in each travel direction. Every 20 seconds, speed, volume, and occupancy are recorded for all mainline stations.

3.3.2 Crash Database

The first step in calibrating the crash potential model was to assemble a database of crash records, including the reported date, time and location of each crash. This information was obtained through Freeway Traffic Management System (FTMS) incident logs provided by the Ministry of Transportation of Ontario (MTO). Crash records were compiled for the period of January 1998 through February 2003. The FTMS incident logs provided several pieces of information on every incident detected on the highway. Of most importance to this study were:

- Date and time incident was reported;
- Identity of upstream loop detector station; and
- Type of incident (e.g. accidents, breakdowns, etc.).

Using the information provided, the FTMS incident logs were filtered to form a crash database with records appropriate for the crash model calibration. The logs were first filtered to remove any incidents not reported as a crash. Next, loop detector data was obtained for the upstream and downstream location of each crash, for a thirty minute time period before and after the reported time of the crash. Since detector data are required to calculate crash precursors, any crashes that occurred at times or locations for which complete detector data were unavailable were removed from the database. Lastly, the remaining crash logs were filtered to include only those records for which the precise time of the crash could be verified. This was necessary since the calculation of crash precursors requires an accurate record of the time of the crash, t . The crash times reported in the FTMS incident logs lack reliability since they are generally either recorded by an operator after the crash has occurred or obtained from a police report.

3.3.2.1 Confirmation of Crash Time, t

The actual time of crash, t , can be accurately estimated by examining changes in traffic flow conditions surrounding a crash occurrence. When a crash occurs, it may block one or more lanes causing a reduction in the roadway capacity. An increase in traffic density upstream of the crash location ensues, while downstream, the density decreases. The density increase will move upstream as a queue forms. How quickly this increasing density moves upstream and the magnitude of the congestion within the queue may depend on the severity of the capacity reduction and the volume present at the time of the crash. In more severe cases, a new flow condition is created which can be clearly distinguished from normal conditions. The discontinuity between normal flow conditions and the new flow condition is called a shockwave. As the shock wave passes over a location, the traffic conditions transition from one flow condition to another (Figure 3-2).

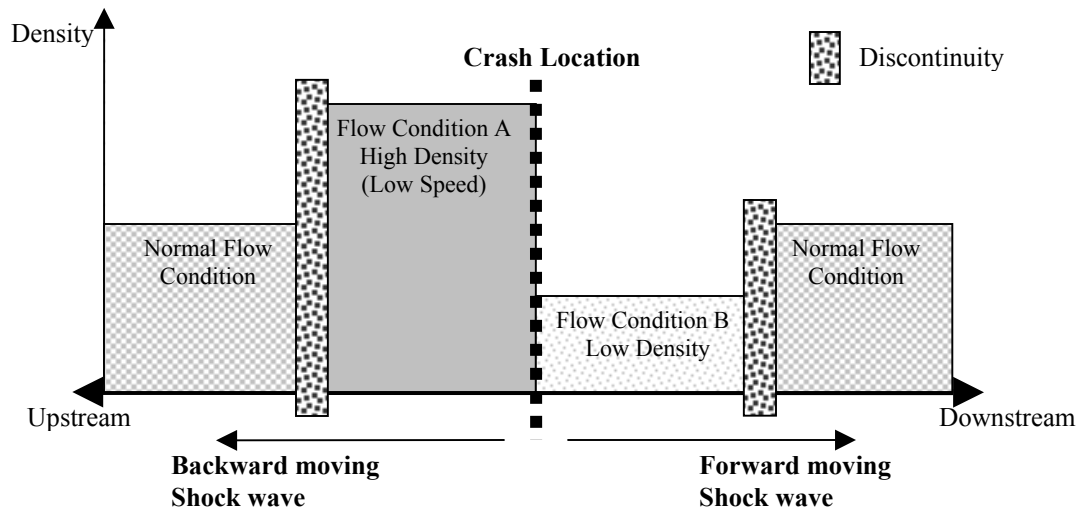


Figure 3-2: Change in Flow Conditions Due to a Shockwave

The time of this transition can be identified at a specific detector location by examining the temporal speed data recorded by that detector. When the backward moving shockwave passes over the nearest detector upstream of the crash location, an abrupt transition (decrease) in speed can be observed (Figure 3-3). Note that in Figure 3-3, the reported time of the crash was 14:29:00, whereas the time at which the shockwave passed over the upstream detector was 14:27:00. Also note that the speeds at the downstream detector remained high, indicating the shockwave was a result of the crash. The crash actually occurs slightly earlier than the time at which the shockwave passes over the nearest upstream detector, but this method provides a more accurate estimate of the time of crash, t , than the reported time.

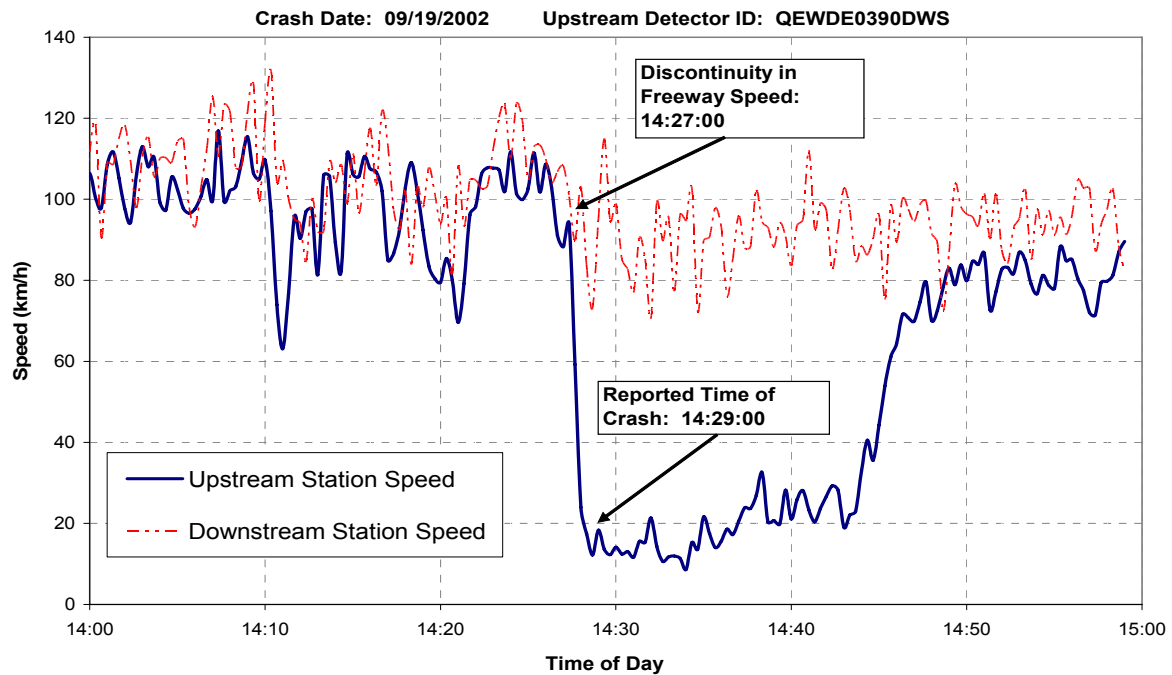


Figure 3-3: Confirmation of Crash Time, t

Confirming the actual time of each crash required a visual inspection of the temporal speed profiles at the upstream and downstream detector stations of the crash. The crash time could only be confirmed for those crashes that resulted in a clear reduction in freeway speed, similar to that shown in Figure 3-3. All other crashes could not be carried forward for the calibration. Crashes that did not result in this clear speed reduction may be explained by the following:

- The crash occurred off the roadway causing no lane blockage;
- The crash was minor and vehicles were cleared quickly from the roadway; or
- The flow condition at the time of the crash was already in a high density, low speed state.

The last explanation was readily observed in the crash data. This is not surprising considering evidence that this flow condition experiences a higher number of crashes (Golob and Recker, 2004) due to the presence of turbulence and frequent start/stop activity. Still,

since a clear time of crash cannot be identified these types of crashes could not be included in the calibration process.

Once the filtering of the crash records was complete, a crash database was formed from the remaining crash records. A total of 299 crashes were included to be carried forward for the remainder of the calibration process.

3.3.3 External Control Factors

For each of the crashes in the crash database the control factor conditions associated with each crash were examined and tabulated. Each control factor had two possible conditions as shown in Table 3-1.

Table 3-1: Crash Model Control Factors

Control Factor		
Time of Day	Geometric Configuration	Weather
<i>Off-Peak</i>	<i>Straight</i>	<i>Clear</i>
<i>Peak</i>	<i>Merging or Diverging</i>	<i>Precipitation</i>

3.3.3.1 Time of Day

Traffic conditions can vary widely by time of day, in reaction to periodic fluctuations in traffic volume. This is especially true for roadways with high volumes of commuters. Often, two distinct peaks in volume occur – one in the morning and one in the evening. A period which exhibits relatively higher volumes than other periods is termed a peak period. Before the crashes can be sorted by time of day, peak and off-peak periods need to be established. To examine the distribution of hourly traffic volume on the QEW, loop detector data were obtained for two non-incident weekdays from each of the months of January 2000, April 2001, July 2001 and September 2002. Figure 3-4 shows the temporal volume profiles for each month (average of two sample days) including the overall average. The distributions of hourly volume for each sample were practically identical. Not surprisingly, their distributions follow the trend for commuter traffic and exhibit two distinct peaks. The figure shows the peak periods occur from 06:00 to 10:00 and from 16:00 to 19:00. The traffic flow occurring within these two periods comprises 44% of the total daily traffic volume, while, with respect to time, those seven hours only comprises 29% of the day.

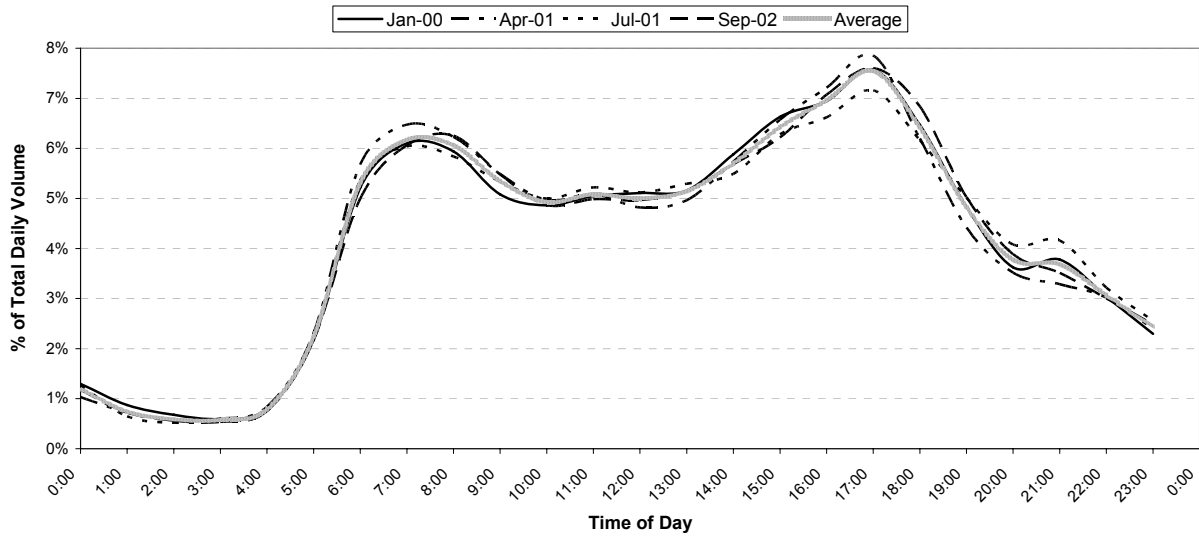


Figure 3-4: Average temporal volume profile

Based on the confirmed crash times, the crashes in the crash database were classified as either occurring during the peak or off-peak periods. Of the 299 crashes, 69% occurred during the peak intervals whereas 31% occurred during off-peak periods. The proportion of crashes occurring during the peak is considerably higher than the proportion of traffic volume occurring during the peak (i.e. 44%). This suggests that time of day has some impact on the level of crash risk.

3.3.3.2 Geometric Configuration

The control factor for geometry refers to the lane configuration on a section of the roadway. Typically a change in lane configuration is due to either a) a merging lane; b) a diverging lane; c) addition of a lane; or d) a lane reduction. These changes in lane configuration often result in disruptions within the traffic flow as many drivers attempt lane changes. This is particularly true for merge, diverge, or lane reduction sections where drivers have a limited distance of roadway over which to complete a maneuver. It is suspected that driver urgency and aggressiveness increases within these sections and this could have an adverse impact on safety.

To include the impacts of lane geometry within the calibration of the crash potential model, crashes needed to be classified by the type of road section within which crashes occurred. The physical layout of the study freeway section was examined and each loop detector was categorized as being located immediately upstream of either a “straight” segment

or a “merge/diverge” segment. The merge and diverge designations were combined into one rather than treated separately. It is suspected that merge and diverge section each exhibit unique characteristics; however, the objective of the combined designation was to minimize the number of categories carried forward in the calibration of the model and simply capture the effect of sections with high traffic weaving activity. Of the 49 loop station segments (including both directions of travel), 51% were classified as preceding straight segments whereas 49% were classified as preceding merge/diverge segments. Since the spacing of the loop detectors is fairly consistent, these percentages represent a reasonable approximation of the proportion of the entire study section belonging to either straight or merge/diverge configurations.

All crashes in the database were classified as straight or merge/diverge based on the crash location (nearest upstream loop station) reported for each crash. Of the 299 crashes, 35% occurred within a straight segment while 65% occurred within a merge/diverge segment. The proportion of crashes occurring within a merge/diverge segments (65%) is substantially larger than the level of exposure to these segments (49%). Therefore, road segments containing merging and diverging configurations are associated with a higher crash potential, supporting the inclusion of road geometry as an explanatory variable within the crash model.

3.3.3.3 *Weather*

Lee (2004) omitted weather from the crash model because he found it was not a strong explanatory variable for predicting crash potential. The current study aimed to revisit the investigation of weather and its impact on crash occurrence; however, due to a number of limitations, it was unclear how the direct impacts of weather could be appropriately included in the model. These limitations are as follows:

1. Exposure – The levels of exposure associated with time of day and geometric configuration are easily formulated because of their static nature. However, because weather is unpredictable and irregular, it is difficult to predetermine a level of exposure for different weather conditions.
2. Crash Database – The crash database was filtered to only include crashes that could be used to compute crash precursors. Of the 299 crashes, only 13%

occurred during a condition of precipitation; but this may not reflect the total number of crashes during inclement weather over 5-year collection period. As a result, the 299 crashes used in this analysis may not offer an accurate cross section of crashes under varying weather conditions.

3. Accuracy of weather data – Historical weather data can be extracted from Environment Canada’s website. Although free and easily accessible, the data are only available in an hourly form from central weather stations. This creates difficulty in assigning an accurate, localized road condition prior to a crash occurrence.

Prior to including weather as an explanatory variable in the crash potential model, these limitations would need to be addressed and overcome. Although it was considered outside the scope of this study, it is recommended that these limitations be investigated since weather may be a valuable addition to the model.

3.3.4 Calculation of Crash Precursors

3.3.4.1 Cleaning of Loop Detector Data

Loop data were compiled for the nearest upstream and downstream locations relative to each crash location. Since loop data occasionally contain erroneous or inconsistent values (due to communication errors or irregular readings), all loop data were “cleaned” prior to being used in the precursor calculations. This process removed outliers and improved consistency by applying a number of simple conditional rules. Values that were found to be true under these rules were set to null. Setting the erroneous values to null provided an alternative to deleting an entire section of data, since crash precursors could still be calculated from the surrounding set of good data. The rules used to clean the data were as follows:

- Speed data reported to be greater than 140 km/h or less than 10 km/h were set to null. The intent of this rule was to omit outliers from the data. Upon an initial examination of the data, values outside of these limits were reported on individual lanes but were not found to be consistent with the adjacent lane data. These limits were chosen as reasonable boundaries for identifying outliers while maintaining representative data.

- Speed data which had no corresponding volume data and vice versa were set to null. This established consistency between the categories of reported data. If a speed was reported on a particular lane, but no vehicle volume was detected on that lane, an error existed in the data. Similarly, a volume count with no corresponding speed indicated an error.

For each of the 299 crashes, crash precursors *CVS*, *Q*, and *COVV* were computed using the cleaned loop detector data. The complete list of crashes including crash information and crash precursor values are shown in Appendix B.

3.3.5 Categorization

Since the log-linear model required crash precursors to be categorized, the boundary values for the categories needed to be determined. The goal in selecting boundary values was to identify a disparity between the levels of precursors which exist prior to a crash and those which exist during non-crash conditions. The best category boundaries to select are the ones which can best predict this disparity. From a database of crash precursors calculated from normal (non-crash) conditions, boundary values were calculated for many cases of categorization as described in the following sections.

3.3.5.1 Crash Precursors for Non-Crash Data

Non-crash data were compiled from twelve days throughout the years 2000 to 2002. Days were selected on the condition that they were weekdays and that no incidents were reported to have occurred². The selected dates for compiling non-crash data are shown in Table 3-2.

Table 3-2: Selected Dates for Non-Crash Data

2000	2001	2002
January 6	January 17	June 12
April 4	February 14	August 15
	March 15	October 8
	May 10	November 25
	September 19	
	December 12	

² Using hourly data from Environment Canada, weather conditions were investigated and included in the selection of non-crash days, but upon examination of the crash precursor distributions from both clear and precipitation conditions, no discernable difference could be identified.

Loop detector data were extracted for the entire 24-hour period of each of the days, and from all loop stations. These data were cleaned using the previously mentioned methodology. Crash precursors were then calculated on intervals equal to their respective observation time slices. The distributions of the crash precursors *CVS*, *Q*, and *COVV* calculated from both the crash and non-crash data are shown in Figure 3-5. For each crash precursor, the shape of the distributions for crash and non-crash data are somewhat similar. However, for *CVS* and *Q*, the proportions of high precursor values were higher when preceding crash occurrences than during non-crash situations. This supports the theory that more turbulent levels of crash are likely to be observed prior to a crash occurrence. On that other hand, for *COVV* the most noticeable disparity between distributions occurred for lower to moderate values.

It is interesting to note that the distributions presented in this report do not resemble the striking disparities evident in the work of Lee (2004). Lee compared distributions of crash precursors calculated from crash data³ to precursors calculated from two days of non-crash loop detector data. In his plots, the crash precursors for non-crash data are noticeably concentrated at low values, while the precursors for crash data occur at higher frequencies at higher values. To investigate the potential reasons for the difference in results, the crash precursor values from this research were compared to those from Lee (2004). It was found that the distributions for the crash precursors were extremely similar, indicating a consistency in the turbulence present prior to a crash between different road sections. However, for all three crash precursors, a significant difference was observed between the distributions of the precursors for the non-crash data. Figure 3-6 provides the plot for *COVV* to demonstrate this difference.

³ Lee (2004) compiled crash data from the Gardiner Expressway in Toronto between 1998 and 1999.

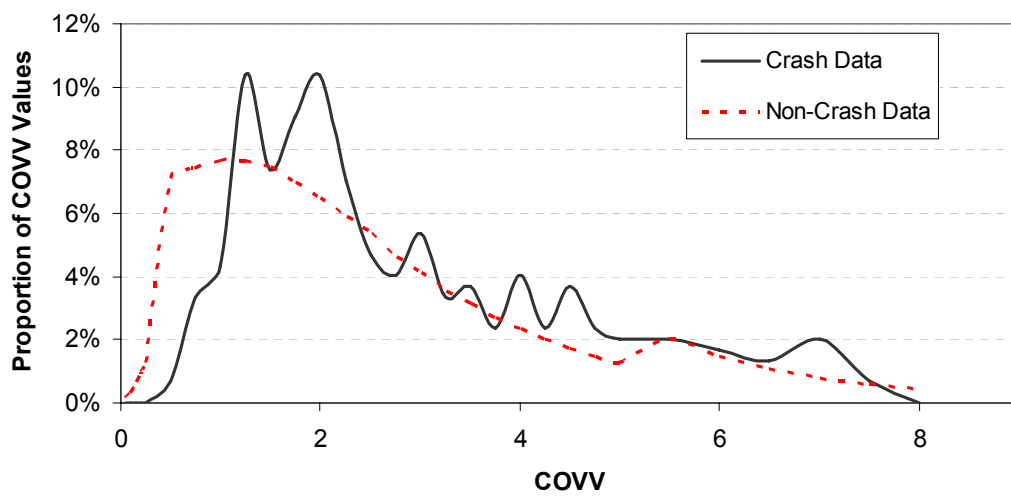
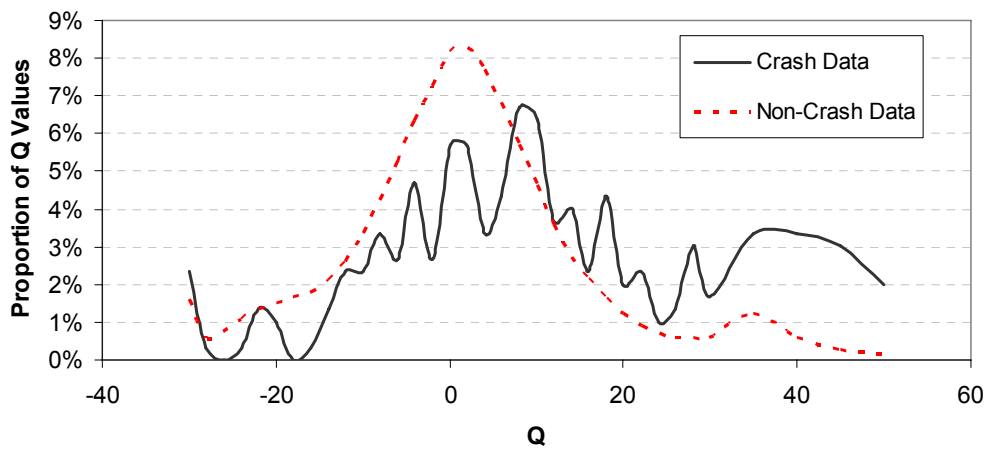
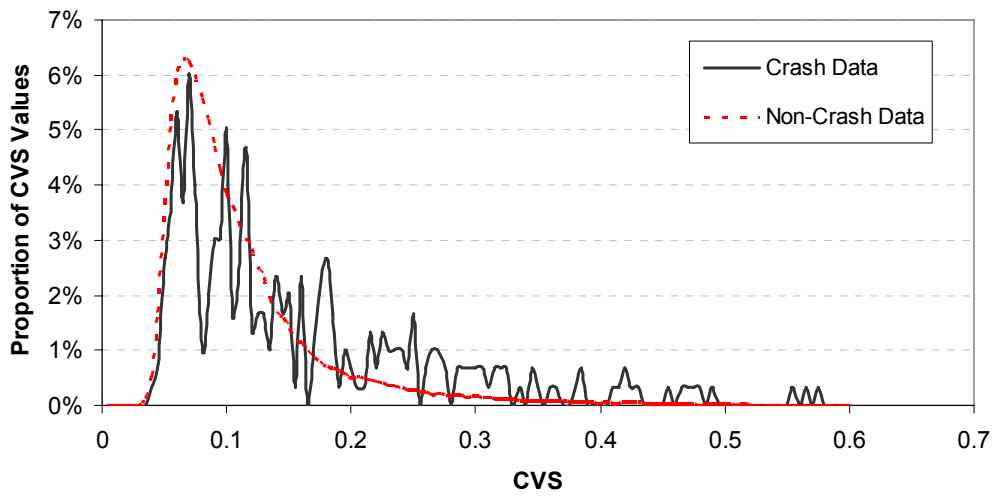


Figure 3-5: Distributions of Crash Precursors from Crash and Non-Crash Data

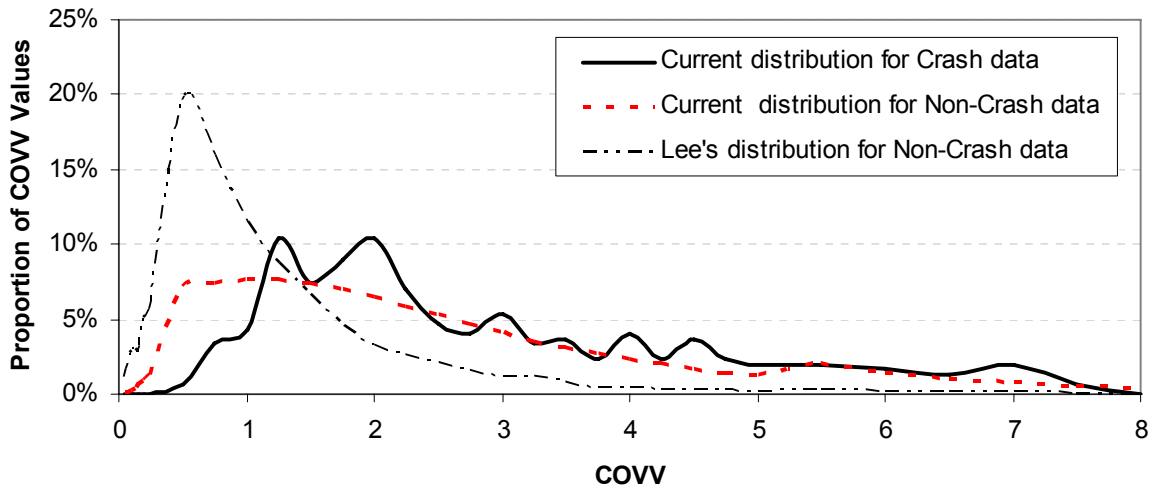


Figure 3-6: Comparison of Precursor Distributions to those of Lee (2004)

It is evident from this comparison that under non crash conditions, crash precursors from Lee (2004) occurred more frequently at lower values than the precursors from this study. This can be interpreted as follows:

- The higher proportions of low value crash precursor indicate that traffic flow on the Gardiner Expressway is less turbulent than on the study segment of the QEW in Mississauga;
- Turbulent conditions on the Gardiner Expressway often lead to a crash condition whereas many “near-misses” occur on the QEW in Mississauga; and/or
- Two days of non-crash traffic data from the Gardiner Expressway during July may not provide a sufficient representation of average non-crash conditions. Twelve days of data (from QEW Mississauga) from all periods of the year is more likely to provide average conditions.

It is interesting to note that Lee’s precursor values for non-crash conditions from Lee (2004) would favour a good model fit due to the higher disparity from crash conditions. In contrast, similarity of the crash and non-crash distributions in this work and the possibility of frequent near misses do not present as strong of an opportunity for predicting crash conditions. Therefore, the transferability of this model to other road sections with varying traffic behaviour requires special and careful attention.

3.3.5.2 Selection of Boundary Values

The procedure for selecting candidate boundary values was similar to that described in Lee (2004). Categorization can vary by both the number of categories selected, and the proportions assigned to each category. For example, if three categories are selected for *CVS*, then all values will be categorized as either “Low”, “Intermediate”, or “High” (Figure 3-7).



Figure 3-7: Categorization of Precursors

Because it is difficult to objectively determine the appropriate number of categories and the correct boundary from the crash precursor distributions, many different cases of categorization were prepared for calibration. In this study, only categorizations consisting of 2, 3, or 4 levels were considered. The number of cells in a cross-tabulation of categorical variables (contingency table) of a log-linear model should be less than the number of samples used to calibrate the model. The number of cells in the contingency table equals the total number of cross-classifications resulting from both precursor categorization and the number of control factors. The size of the contingency table can be calculated by multiplying the following:

- 2 categories for time of day (Peak and Off-Peak);
- 2 categories for road geometry (Straight and Merge/Diverge);
- x categories for *CVS*;
- y categories for Q; and
- z categories for *COVV*.

If each precursor categorization consists of 4 categories, the number of cells in the contingency table equals 256 (2 x 2 x 4 x 4 x 4). Therefore, because it is desirable to maintain

a contingency table smaller than the dataset of 299 crashes, categorizations consisting of more than 4 categories were not considered.

Table 3-3 shows the cases of categorization tested in the calibration of the log-linear model and the boundary values calculated from the database crash precursors for normal (non-crash) conditions.

Table 3-3: Categorization Cases and Corresponding Boundary Values

No. of Categories	Assumed Proportions *	CVS (No Unit)			Q (km/hr)			COVV (No Unit)		
		B ₁ **	B ₂ **	B ₃ **	B ₁	B ₂	B ₃	B ₁	B ₂	B ₃
2 Categories	50/50	0.089	-	-	0.1	-	-	1.85	-	-
	60/40	0.101	-	-	2.5	-	-	2.25	-	-
	70/30	0.117	-	-	5.3	-	-	2.75	-	-
	80/20	0.139	-	-	8.8	-	-	3.44	-	-
3 Categories	20/60/20	0.062	0.139	-	-9.2	8.8	-	0.83	3.44	-
	20/50/30	0.062	0.117	-	-9.2	5.3	-	0.83	2.75	-
	30/50/20	0.070	0.139	-	-5.3	8.8	-	1.16	3.44	-
	33/33/33	0.073	0.111	-	-4.3	4.3	-	1.26	2.57	-
	40/40/20	0.079	0.139	-	-2.4	8.8	-	1.49	3.44	-
	40/30/30	0.079	0.117	-	-2.4	5.3	-	1.49	2.75	-
	50/30/20	0.089	0.139	-	0.1	8.8	-	1.85	3.44	-
	50/20/30	0.089	0.117	-	0.1	5.3	-	1.85	2.75	-
60/20/20	0.101	0.139	-	2.5	8.8	-	2.25	3.44	-	
4 Categories	40/20/20/20	0.079	0.101	0.139	-2.4	2.5	8.8	1.49	2.25	3.44
	30/30/20/20	0.070	0.101	0.139	-5.3	2.5	8.8	1.16	2.25	3.44
	30/20/30/20	0.070	0.089	0.139	-5.3	0.1	8.8	1.16	1.85	3.44
	25/25/25/25	0.066	0.089	0.188	-7.0	0.1	6.9	1.00	1.85	3.06
	20/20/40/20	0.062	0.079	0.139	-9.2	-1.8	8.8	0.83	1.49	3.44
	20/30/30/20	0.062	0.089	0.139	-9.2	0.1	8.8	0.83	1.85	3.44
	20/40/20/20	0.062	0.101	0.139	-9.2	2.5	8.8	0.83	2.25	3.44

*The first number represents the percentage of the lowest level, the second number the percentage of the second lowest level, etc.

**B₁ denotes the boundary value between the lowest and second lowest level for given crash precursor, B₂ the boundary value between the second lowest crash precursor and the third lowest, etc.

The proportion designations in Table 3-3 (i.e. 20/60/20) represent the proportion of crash precursors belonging to each category when the precursors are ordered from smallest to largest. For example, the 3 category case of 20/60/20 for CVS indicates that the lowest 20% of crash precursor values belong to the “low” level, the next 60% of precursors belong to the “intermediate” level, and the final highest 20% belong to the “high” level. In this case, the boundary value between the low and intermediate level is 0.062 and the boundary value between the intermediate level and high level is 0.168 (Figure 3-8).

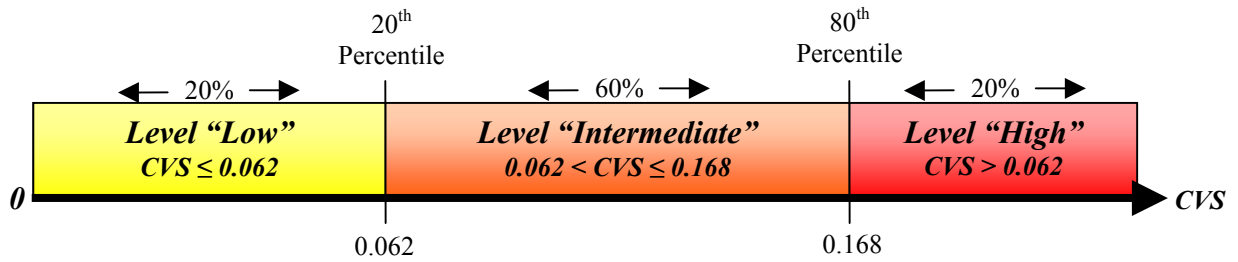


Figure 3-8: Categorization Case: 20/60/20 for CVS

The same cases of categorization were used in this study as in Lee (2004) to investigate similarities or differences between the boundary values from the two studies. Table 3-3 presents the boundary values from this study, whereas Table 3-4 presents the boundary values found in Lee (2004).

Table 3-4: Categorization from Lee (2004)

No. of Categories	Assumed Proportions	CVS (No Unit)			Q (km/hr)			COVV (No Unit)		
		B1	B2	B3	B1	B2	B3	B1	B2	B3
2 Categories	50/50	0.056	-	-	2.7	-	-	0.80	-	-
	60/40	0.060	-	-	3.5	-	-	1.00	-	-
	70/30	0.065	-	-	4.7	-	-	1.25	-	-
	80/20	0.074	-	-	8.3	-	-	1.63	-	-
3 Categories	20/60/20	0.046	0.074	-	1.1	8.3	-	0.39	1.63	-
	20/50/30	0.046	0.064	-	1.1	4.7	-	0.39	1.25	-
	30/50/20	0.048	0.074	-	1.6	8.3	-	0.51	1.63	-
	33/33/33	0.049	0.063	-	1.7	4.2	-	0.58	1.16	-
	40/40/20	0.052	0.074	-	2.1	8.2	-	0.67	1.63	-
	40/30/30	0.052	0.064	-	2.1	4.7	-	0.67	1.25	-
	50/30/20	0.056	0.074	-	2.7	8.3	-	0.81	1.63	-
	50/20/30	0.056	0.064	-	2.7	4.7	-	0.81	1.25	-
4 Categories	60/20/20	0.060	0.074	-	3.5	8.3	-	1.00	1.63	-
	40/20/20/20	0.052	0.060	0.074	2.1	3.5	8.3	0.67	1.00	1.63
	30/30/20/20	0.048	0.060	0.074	1.6	3.5	8.3	0.51	1.00	1.63
	30/20/30/20	0.048	0.056	0.074	1.6	2.7	8.3	0.51	0.81	1.63
	25/25/25/25	0.047	0.056	0.068	1.3	2.7	5.9	0.46	0.81	1.45
	20/20/40/20	0.046	0.052	0.074	1.1	2.1	8.3	0.39	0.67	1.63
	20/30/30/20	0.046	0.056	0.074	1.1	2.7	8.3	0.39	0.81	1.63
20/40/20/20	0.046	0.060	0.074	1.1	3.5	8.3	0.39	1.00	1.63	

As shown in Table 3-3 and Table 3-4, the boundary values for CVS and COVV from this study are consistently higher than those found in Lee (2004). Note that the values for Q cannot be directly compared because Lee expressed Q as an absolute value⁴. However, the

⁴ Lee (2004) later reevaluated Q preserving its signed value, however the boundary values were not documented.

differences for *CVS* and *COVV* provide further evidence to that presented previously in this section that crash precursors values from data representing normal conditions for the Gardiner Expressway are noticeably lower than those for the QEW in Mississauga.

3.3.6 Log-Linear Analysis

Prior to performing the calibration analysis, the crash data were categorized into an acceptable format for each case of categorization. For every crash record, the crash precursors and control factors were each assigned a categorical reference. Table 3-6 provides examples of the assignment of category values for the categorization case of 40/40/20.

Table 3-5: Boundary Values for Categorization 40/40/20

	B ₁	B ₂
<i>CVS</i>	0.079	0.139
<i>Q</i>	-2.4	8.8
<i>COVV</i>	1.49	3.44

Table 3-6: Categorization Format Example for 40/40/20

Crash Precursors and Control Factors					Categorization				
<i>COVV</i>	<i>Q</i>	<i>CVS</i>	Time of Day	Geometry*	Precursor**			Time of Day***	
					<i>COVV</i>	<i>Q</i>	<i>CVS</i>	Day***	Geometry****
0.83	-6.6	0.180	Peak	M/D	1	1	3	1	1
4.32	11.0	0.080	Off-Peak	M/D	3	3	2	0	1
1.40	15.8	0.144	Off-Peak	S	1	3	3	0	0

*M/D represents Merge/Diverge sections, S represents Straight sections

** Crash precursors are categorized as 1 for lowest level, 2 for second lowest level and so on.

*** Time of Day is categorized as 1 for “Peak”, 0 for “Off-Peak”

****Road geometry is categorized as 1 for Merge/Diverge, 0 for Straight.

Calculating values of exposure was also necessary at this stage as exposure was included as a continuous covariate in the log-linear analysis. Table 3-7 presents the information required for the calculation of exposure.

Table 3-7: Exposure Variables

Variable	Value
AADT	140,000
Proportion of Merge/Diverge road sections	49%
Proportion of Straight road sections	51%
# of Road Sections (loop stations)	52
Length per Road Section	0.6
Proportion of Vehicles exposed to Peak Conditions	44%
Proportion of Vehicles exposed to Off-Peak Conditions	56%
# of Weekdays throughout evaluation period	1349
Proportion of exposure to each precursor condition	Depends on categorization

Using Equation 3-4, a value of exposure was calculated for each crash. An example calculation is presented below for a 40/40/20 categorization, during the peak period, on a straight road section, with precursor levels of $CVS = \text{“Low”}$; $Q = \text{“High”}$; and $COVV = \text{“High”}$.

$$\begin{aligned}
 EXP(x_0, t) &= p(CVS(x_0, t)) \cdot p(Q(x_0, t)) \cdot p(COVV(x_0, t)) \cdot p(P) \cdot p(G) \cdot V \cdot L \cdot T \\
 &= 0.40 \times 0.20 \times 0.20 \times 0.44 \times 0.51 \times (140,000 \times 52 \times 0.6) \frac{\text{veh-km}}{\text{day}} \times 1349 \frac{\text{weekdays}}{62\text{-months}} \\
 &= 20.32 \times 10^6 \text{ veh-km over 62 months}
 \end{aligned}$$

Note that although exposure is a continuous rather than a categorical variable, due to the limited options of input values, there is a finite set of potential exposure values for each categorization case.

After all data were formatted with categorically references and values of exposure were calculated, log-linear analysis was performed using SPSS Version 13.0 (SPSS Inc., 2004) to calibrate the crash potential model. This procedure analyzes the frequency of samples in each cell of the contingency table to yield maximum likelihood estimates of the expected frequency of crashes under each possible condition. The analysis used an iterative fitting process until the difference between the current and previous estimates converged to 0.001. Because crashes are considered to be random events, the crash frequency was assumed to follow a Poisson distribution in the fitting process.

The log-linear analysis was performed on many cases of categorization. The performance of each categorization case was measured in terms of 1) overall model fit; 2) the statistical significance of individual coefficients; and 3) the consistency of coefficients with the order of levels of precursors (i.e. it is expected that “high” levels of precursors contribute more to crash potential than “low” level precursors). The categorization that produced that best model fit was carried forward for the remainder of this study.

The overall model fit was measured by a log-likelihood ratio χ^2 test. This test measures the differences between the observed crash frequencies and expected crash frequencies for any combination of crash precursor categories and control factors. A low χ^2

and a high p-value (greater than $1 - \alpha$) indicate that the distribution of the expected crash frequencies is not significantly different from the distribution of the observed crash frequencies – or in other words, the model fits well.

Lee's (2004) calibration effort tested models of 2, 3 and 4 categories. He found that models with 3 categories produced the best results, with many models that were statistically significant in terms of both model fit and for individual coefficients. Lee was able to select from this set of candidate models, the one with the lowest χ^2 value, or, the one with the strongest fit.

In the current study, many models were tested using Lee's categorizations of 2, 3 and 4 category models; however, no model could be calibrated to produce a statistically significant model fit. The lack of success compared to Lee can likely be explained by the distributions of crash precursors calculated from normal conditions. Because Lee's boundary values for normal conditions were lower, the opportunity for calibrating successful model fits was likely higher. In search of a statistically significant model fit, two primary deviations from Lee's methodology were investigated:

1. First, crash precursors calculated from normal conditions were sorted by their corresponding conditions of time of day and roadway geometry. With 2 categories for each control factor, this produced 4 (2x2) datasets of precursor values for each of *CVS*, *Q*, and *COVV*. Boundary values were determined for each set of conditions and crash precursors from the crash data were categorized based on their corresponding conditions. The idea behind this stemmed from evidence that the distributions of crash precursor were different for each set of conditions (e.g. the distribution for peak, merge/diverge conditions contained a higher proportion of high precursor values than the distribution for off-peak, straight conditions). In other words, a crash precursor value considered to be high during the off-peak period on a straight road section might only be an intermediate value when compared to values for the peak period on a merge/diverge road section. It was found that this method of categorization was much more complex than the original method, and did not

produce results that showed any indication of a statistically significant model fit.

2. The second deviation from Lee's (2004) model was less complex than the first, but aimed to add more flexibility to the categorization process. In the work of Lee (2004), for each case of categorization, the same categorical breakdown (e.g. 40/40/20) applied to *CVS*, *Q*, and *COVV*; however, because the distributions of each precursor differ, there is no evidence to suggest that it is appropriate to apply the same categorical breakdown or even the same number of categories to each precursor. Therefore, many cases were tested using different combinations of individual categorizations for precursors. These tests produced much better results, including a number of candidate models that passed the tests for statistical significance.

It was found that the models that produced at least some degree of statistically significant results all consisted of 4 categories for *CVS*, 4 categories for *Q* and 3 categories for *COVV*. For most of these models, not all parameter estimates were found to be significant. The only model that produced both overall statistically significant results and statistically significant parameter estimates at a 95% level of confidence consisted categorical breakdowns shown in Table 3-8.

Table 3-8: Categorization of statistically significant crash model

Crash Precursor	Categorization	Boundary Values		
		B ₁	B ₂	B ₃
<i>CVS</i>	20/30/30/20	0.062	0.089	0.139
<i>Q</i>	20/30/30/20	-9.19	0.09	8.77
<i>COVV</i>	40/40/20	1.49	3.44	--

The log-linear analysis of this model resulted in a p-value close to 1.0 and a chi-squared likelihood ratio of 112.18 with degrees of freedom of 180. The parameter estimates for this model and the individual values for statistical fit are shown in Table 3-9.

Table 3-9: Crash Model Parameter Estimates from Log-linear Analysis

Parameter	Category Level	Estimate	Z-Value
Constant (θ)	N/A	1.518	9.783
λ_{covv}	[1] Low	-1.300	-5.315
	[2] Intermediate	-0.884	-3.696
	[3] High	0	.
λ_{cvs}	[1] Low	-0.914	-5.165
	[2] Intermediate A	-1.735	-8.105
	[3] Intermediate B	-1.496	-7.317
	[4] High	0	.
λ_Q	[1] High Acceleration	-0.875	-4.887
	[2] Moderate Acc.	-1.738	-8.122
	[3] Mod Deceleration	-1.508	-7.443
	[4] High Deceleration	0	.
λ_R (for Geometry)	Straight	-0.530	-4.397
	Merge Diverge	0	.
λ_P (for Time)	Off-Peak	-1.254	-8.156
	Peak	0	.
β (for Exposure)	N/A	0.084	7.218

The constant term in the model provides the crash frequency ($=e^\theta$) for base case factors (parameters with estimates equal to 0) for given values of exposure. Parameters for which estimates are negative indicate a declining contribution to crash potential, whereas positive estimates indicate an increasing contribution to crash potential. The results in this table agree with Lee's (2004) results and indicate that:

- High level precursors contribute more to crash potential than low level precursors;
- Road geometry of merging and diverging sections contribute more to crash potential than straight sections;
- Peak period conditions contribute more to crash potential than off-peak period conditions; and
- Crash frequency increases as exposure increases (as more vehicles travel through the section).

Note that for Q, a state of high deceleration (level 4) contributes most to crash potential; however, the first level contributes more to crash potential than the second and third levels. This indicates that a state of high acceleration is more likely to precede a crash than

conditions of moderate acceleration or moderate deceleration. Also note that the first level of *CVS* contributes more to crash potential than the moderate levels (2 and 3). Examination of the contingency table revealed a high number of zero valued cells for *CVS* of levels 1 and 2. Therefore, crashes containing low levels of *CVS* were difficult to predict, explaining the unexpected parameter estimates.

To illustrate the calculation of crash potential, consider the following two examples (refer to Table 3-8 for boundary values of given categorizations):

Example 1:

CVS = 0.045 (Level 1); *Q* = - 1 km/h (Level 2); *COVV* = 1.3 (Level 1); Peak period; Merge/Diverge geometry

Exposure = 30.5×10^6 veh-km

$$F(x_0, t) = \exp(\theta + \lambda_{CVS=1} + \lambda_{Q=2} + \lambda_{COVV=1} + \lambda_{R=0} + \lambda_{P=0} + \beta' \times EXP(x_0, t))$$

$$F(x_0, t) = \exp(1.518 - 0.914 - 1.738 - 1.3 + 0 + 0 + 0.084 \times 30.5)$$

$F(x_0, t) = 1.14$ crashes

$$CP(x_0, t) = F(x_0, t) / EXP(x_0, t)^\beta$$

$$CP(x_0, t) = 1.14 / 30.5^{0.084 \frac{30.5}{\ln 30.5}}$$

$CP(x_0, t) = 0.088$ crashes/ 10^6 veh-km over 62 months

Example 2:

CVS = 1.6 (Level 4); *Q* = 15 km/h (Level 4); *COVV* = 3.8 (Level 3); Peak period; Merge/Diverge geometry

Exposure = 10.2×10^6 veh-km

$$F(x_0, t) = \exp(1.518 + 0 + 0 + 0 + 0 + 0 + 0.084 \times 10.2)$$

$F(x_0, t) = 10.7$ crashes

$CP(x_0, t) = 4.54$ crashes/ 10^6 veh-km over 62 months

Note that the crash frequency and crash potential increase significantly with higher levels of crash precursors even though the control factors remain the same and exposure decreases. Figure 3-9 shows the comparison between the observed and expected crash frequencies. The complete contingency table of observed and estimated crash frequency is provided in Appendix C. It is evident from Figure 3-9 that crash frequency increases for high levels of precursors, for peak conditions, and for merge/diverge road geometry. The expected frequencies of crashes calculated from the calibrated crash potential model closely agree with the observed frequencies for each category.

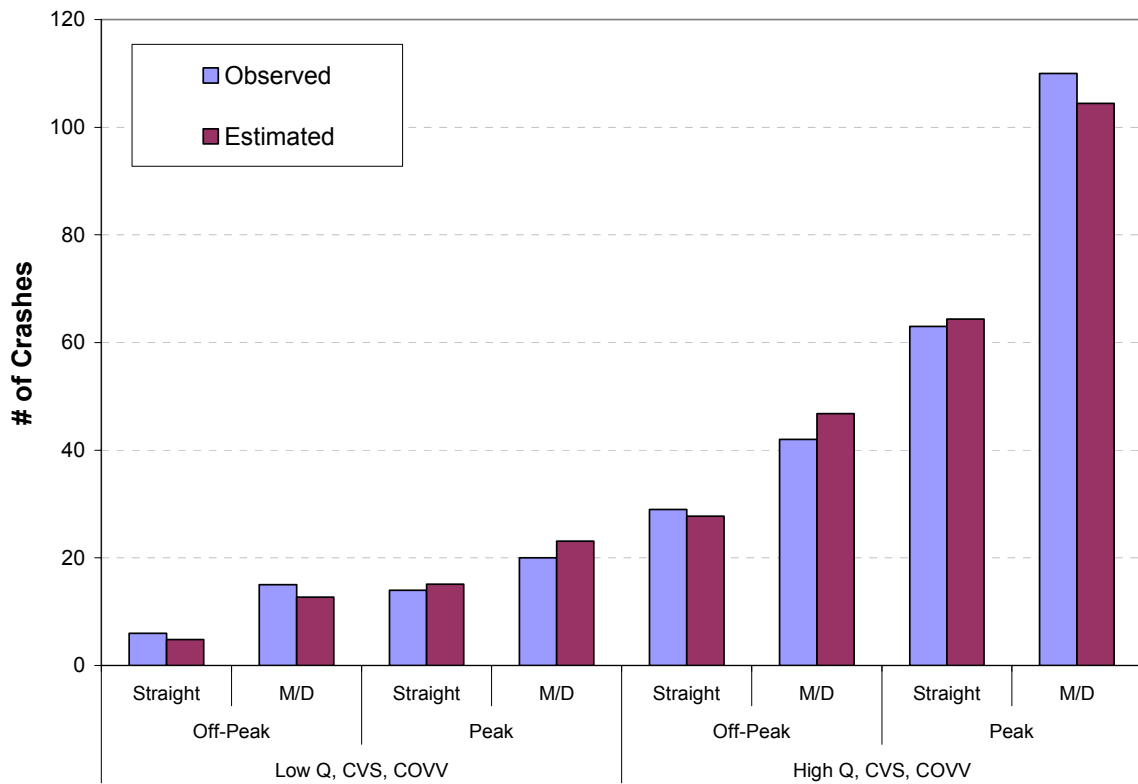


Figure 3-9: Comparison between Observed and Expected Crash Frequencies

Because of the statistically significant results and the close agreement between the observed and expected crash frequencies, the crash model described above was considered to be successfully calibrated. This model was carried forward and applied in quantifying the safety impacts of candidate variable speed limit strategies on a modelled section of the QEW, as described in the following chapters.

4. DEVELOPMENT OF MICROSIMULATION MODEL

This chapter describes the steps taken to develop the microsimulation model used to quantify the safety and travel time impacts of a Variable Speed Limit Sign (VSL) system application. The first section describes the study network selected for modelling the application of a VSL, the data collection procedure and the existing traffic conditions. The second section describes the physical structure of the model and the approach for calibration and model validation. The third section describes the process of adjusting the crash precursors calculated from the modelled conditions to better match those calculated from the field. Finally, the fourth section introduces the initial candidate VSL control algorithm and how it was integrated with the microsimulation model.

4.1 Description of Study Network

An 8 km section of the eastbound Queen Elizabeth Way (QEW) was selected to be modelled in PARAMICS. This section was recommended by the Ministry of Transportation of Ontario (MTO) as a candidate freeway segment for the application of variable speed limits due to the turbulent and congested nature of traffic during the peak periods. Although further upstream than the segment used to calibrate the crash potential model, it was assumed that, because this segment services similar traffic, the traffic characteristics would not be dissimilar and therefore the calibrated crash potential model could be transferable.

This segment, termed “QEW Burlington”, begins upstream of the Guelph Line interchange and extends to a point downstream of the Burloak Drive interchange. The study segment features a posted speed limit of 100 km/h, has 3 mainline lanes, and contains four interchanges (Figure 4-1). The section is instrumented with dual loop detector stations in each mainline lane spaced at approximately 600m and single loop stations on entrance and exit ramps (Figure 4-2). Every 20-seconds, speed, volume, and occupancy are recorded for all mainline stations while only volume is recorded for ramp stations.

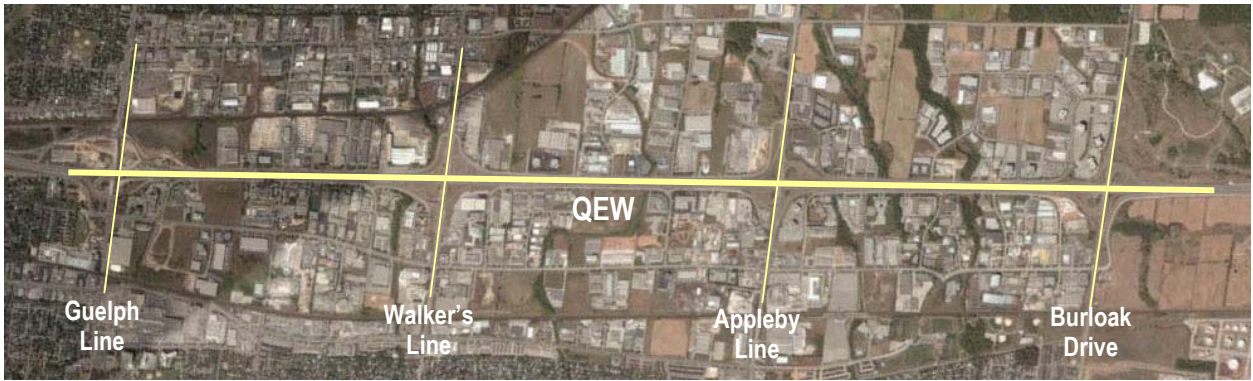


Figure 4-1: QEW Burlington Study Section (©2005 Google)

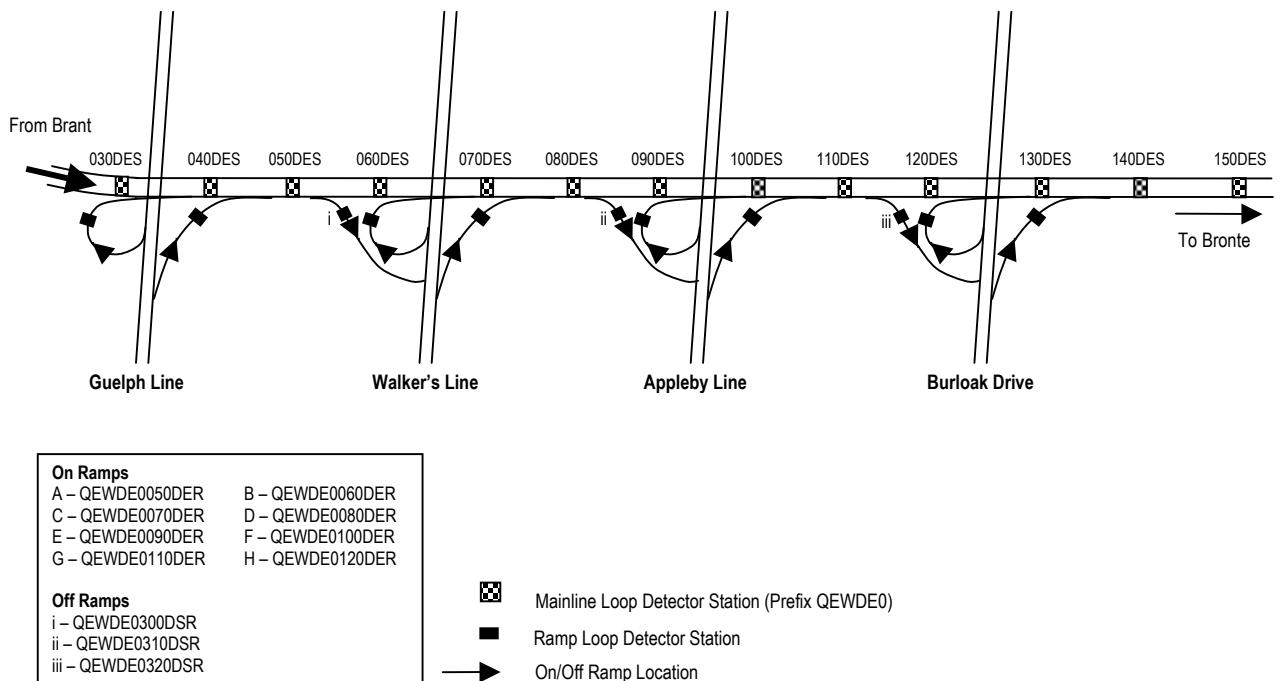


Figure 4-2: Locations of Loop Detector Stations

This section of the QEW services very high volumes of commuter traffic traveling to and from the Toronto area. To capture the eastbound peak volume, the morning peak period was chosen for modelling. All traffic volume data were obtained from archived loop detector data. The procedure for collecting the necessary data for building the simulation model is explained in the following section.

4.2 Data Collection

4.2.1 Geometric Data

Satellite imagery of the freeway section (©2005 Google) was obtained and used as the main geometric reference for the model. In addition, the MTO provided as-built CAD drawings of the section and a separate CAD schematic with the location and name of each loop detector station. These three sources of information provided all the physical knowledge of the study section required for modelling.

4.2.2 Loop Detector Data

Access to traffic data from loop detector data logs was provided by the MTO. Fifteen days of 5-minute averaged loop data (speed, volume, and occupancy) were extracted. The days were chosen from November 2004 and April 2005 under the conditions that a) the day was a weekday but not a Friday; b) no incidents were recorded during that day; and c) complete detector data were available for that day (i.e. no large blocks of missing data). Further examination of the data for the fifteen days revealed that only ten of the days exhibited congested conditions causing a prolonged shockwave. Since this study aimed to model a VSLs response to recurrent congestion, the five days which showed only minor reductions in freeway speed were removed from the calibration data set. For four of the remaining 10 days, 20-second averaged loop data were extracted. These data were to be used for more detailed analysis, including the calculation of observed crash precursors and observation of detailed traffic behaviour. The loop detectors included for the data collection are shown in Table 4-1.

Table 4-1. Loop Detector Station List

Mainline QEW	On-Ramps	Off-Ramps
QEWDE0030DES	QEWDE0050DER	QEWDE0300DSR
QEWDE0040DES	QEWDE0060DER	QEWDE0310DSR
QEWDE0050DES	QEWDE0070DER	QEWDE0320DSR
QEWDE0060DES	QEWDE0080DER	
QEWDE0070DES	QEWDE0090DER	
QEWDE0080DES	QEWDE0100DER	
QEWDE0090DES	QEWDE0100DER	
QEWDE0100DES	QEWDE0120DER	
QEWDE0110DES		
QEWDE0120DES		
QEWDE0130DES		
QEWDE0140DES		
QEWDE0150DES		

4.2.3 Formation of O-D Trip Table

A time dependent Origin-Destination (O-D) trip table needed to be derived for the peak period for coding the traffic volumes into the simulation model. First, the average traffic volume for each loop station was calculated from the observed volumes between 5:30 am and 10:00 am over the 10 days sampled (Table 4-2).

Table 4-2. Average peak period volumes for all mainline and ramp loop stations.

Mainline		On Ramps		Off Ramps	
Station	Average Volume	Station	Average Volume	Station	Average Volume
030des	23280	050der	250	300dsr	3510
040des	23620	060der	670	310dsr	3740
050des	24760	070der	1090	320dsr	1290
060des	20930	080der	910		
070des	22000	090der	690		
080des	22910	100der	1520		
090des	19030	110der	2110		
100des	19470	120der	2280		
110des	14490				
120des	19890				
130des	22140				
140des	24410				
150des	24430				

The O-D trip table was estimated by constraining the sums of the O-D pairs by the volumes entering and exiting the study area and through the following logical assumptions:

- Vehicles entering at the mainline would not exit the mainline at the next downstream interchange. This assumption was based on the commuting behaviour of the traffic stream and the presence of adjacent arterials that provide alternative access between interchanges.

Of the vehicles entering the mainline, the majority would remain on the mainline, with only small proportions exiting at downstream interchanges within the study segment. Because the trip patterns of vehicles were unknown, the proportions of vehicles exiting at each interchange were selected subjectively but with some basis on the relative size of on-ramp and off-ramp volumes.

- Table 4-3 provides these assumed proportions.

Table 4-3: Assumed proportions of originating volumes for internal O-D pairs

	Destination	Total

		Walker's Line (300dsr)	Appleby Line (310dsr)	Burloak Drive (320dsr)	Mainline Downstream (150des)	Originating Volume
Origin	Guelph Line	0	0.15	0.1	0.75	920
	Walker's Line	--	0	0.05	0.95	2020
	Appleby Line	--	--	0	1.00	2210
	Burloak Dr.	--	--	--	1.00	4390
Total Destination Volumes		3510	3740	1300	24440	9540

Although these proportions were selected subjectively, considering the constraints of entering and exiting volumes and the limited number of interchanges within the study segment, the resulting O-D estimates were assumed to be reasonable. Then, for each interchange the O-D pair originating at the upstream mainline (Station 30) was calculated as the difference between the sum of the internal O-D pairs (as in Table 4-4) and the total destination volume. The final O-D matrix is shown in Table 4-4, with volumes rounded to the nearest ten.

To best reflect reality, traffic volumes for each O-D pair were assigned a time dependent "vehicle release profile" to define the rate at which vehicles would be released into the simulated network. The loop detector data from the field were examined on a more disaggregated basis and for each O-D pair, a proportion of its total volume was assigned to every half-hour period. Table 4-5 describes each release profile type by the proportion of volume released over each half-hour period. The release profile associated with each O-D pair is indicated in parentheses in Table 4-4.

Table 4-4: Estimated Origin-Destination Matrix for time period 5:30 am to 10 am

		Destination				Total Originating Volume
		Walker's Line (295dsr)	Appleby Line (300dsr)	Burloak Drive (310dsr)	Mainline Downstream (320dsr)	
Origin	Mainline Upstream (30des)	3510 (4)*	3600 (4)	1100 (4)	15240 (5)	23450
	Guelph Line N (50der)	--	60 (1)	40 (1)	300 (1)	400
	Guelph Line S (60der)	--	80 (1)	50 (1)	390 (1)	520
	Walker's Line N (70der)	--	--	60 (1)	1040 (1)	1100
	Walker's Line S (80der)	--	--	50 (1)	870 (1)	920
	Appleby Line N (90der)	--	--	--	690 (3)	690
	Appleby Line S (100der)	--	--	--	1520 (1)	1520
	Burloak Dr. N (110der)	--	--	--	2110 (2)	2110
	Burloak Dr. S (120der)	--	--	--	2280 (2)	2280
Total Destination Volumes		3510	3740	1300	24440	32990

*Values in parentheses indicate the corresponding vehicle release profile. Refer to Table 4-5.

Table 4-5: Time dependent vehicle release profiles

	5:30-6:00	6:00-6:30	6:30-7:00	7:00-7:30	7:30-8:00	8:00-8:30	8:30-9:00	9:00-9:30	9:30-10:00	Total
Profile 1	9%	10%	10%	12%	11%	12%	13%	12%	12%	100%
Profile 2	4%	9%	11%	14%	19%	16%	12%	8%	6%	100%
Profile 3	7%	7%	7%	10%	12%	13%	13%	16%	15%	100%
Profile 4	6%	7%	13%	12%	14%	15%	14%	10%	8%	100%
Profile 5	13%	14%	12%	12%	10%	10%	10%	11%	10%	100%

For the analysis of “off-peak” and “near-peak” conditions, rather than estimating new matrices from observed volumes, reduction factors were applied to the cells of the current matrix to reflect less congested periods. The purpose of modelling a “near-peak” condition was to capture mounting congestion that was significant but not as severe as peak congestion. Reduction factors of 0.75 and 0.93⁵ were applied to the peak matrix for respective off-peak and near-peak analyses. This was considered a suitable alternative to deriving non-peak traffic conditions.

4.2.4 Existing Traffic Conditions

During the morning peak hour, the Burlington section of the QEW experiences a significant amount of traffic congestion. As can be seen from the speed contours in Figure 4-3, congestion begins to build as early as 6 am, beginning at the downstream end of the section and propagating upstream over time. The cause of this downstream congestion is suspected to

⁵ The reduction factor of 0.93 was chosen after running a number of test simulations. At approximately 93% of the peak volume a noticeable breakdown in traffic performance was found to occur.

be the high volume of vehicles entering the already crowded mainline from the Burloak Drive on-ramps. It is important to note that the volume of traffic entering the downstream end of the mainline is much higher than the volume entering from the upstream interchanges. Thus, most congestion in the network results from recurring shockwaves originating at this downstream bottleneck.

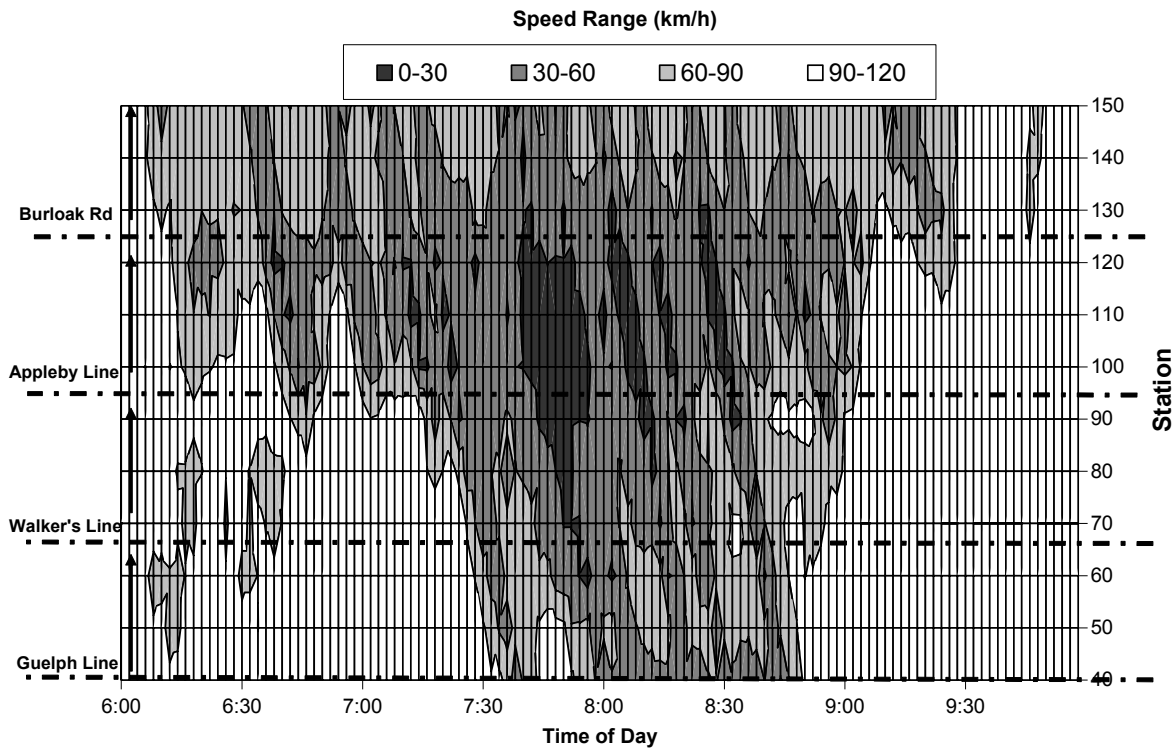


Figure 4-3: Contour Mapping of Freeway Speeds for April 14, 2004 (2-min average speeds)

To provide a more detailed snapshot of the existing traffic conditions for a typical morning peak period, Figure 4-4 and Figure 4-5 show volume-occupancy and speed-volume relationships, respectively, for Station 120 located just upstream of Burloak Drive. Figure 4-4 indicates that performance begins to deteriorate at occupancies greater than 15%, while Figure 4-5 exhibits the “un-congested” and “congested” speed regimes and indicates the capacity of the freeway is approximately 2250 vphpl.

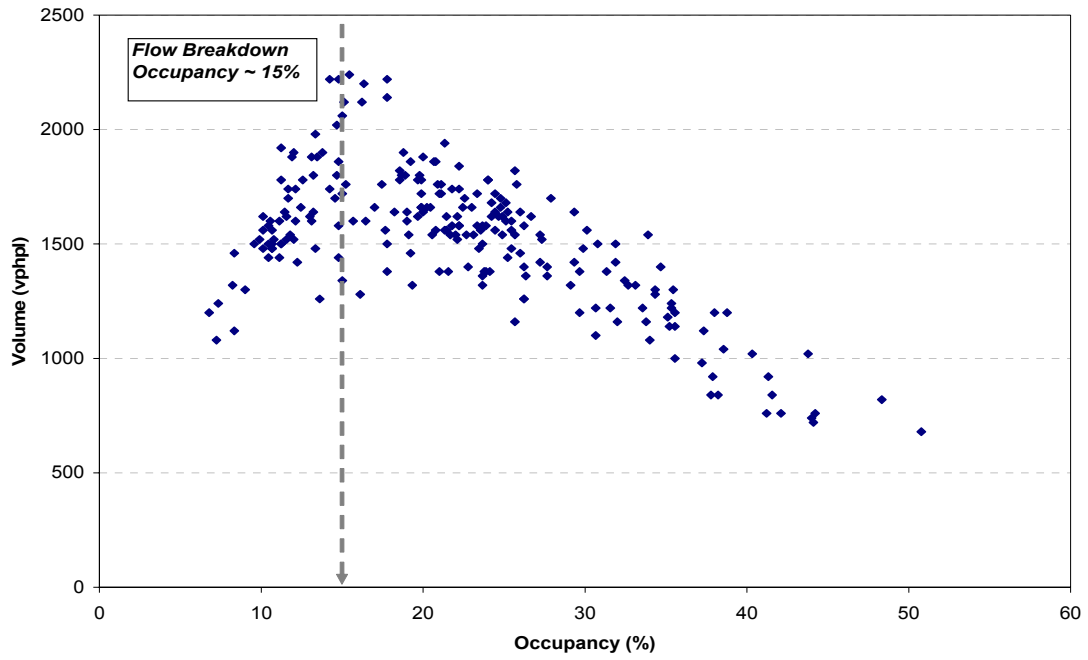


Figure 4-4: Volume-Occupancy Plot for Station 120 (April 14, 2005)

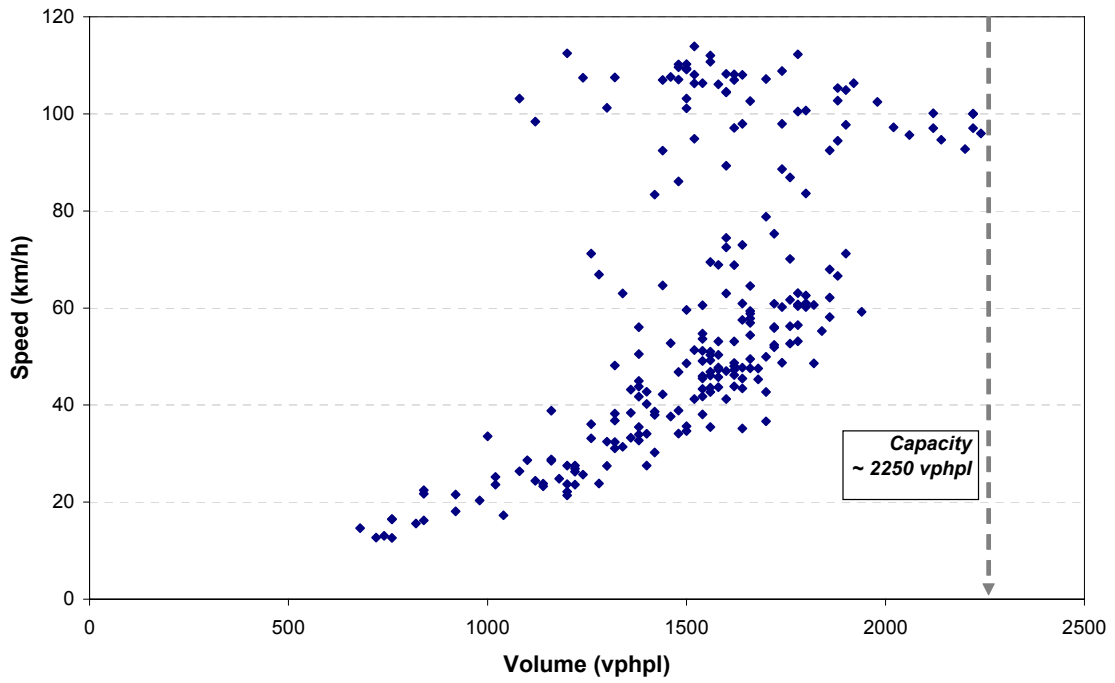


Figure 4-5: Speed-Volume Plot for Station 120 (April 14, 2005)

4.3 Construction and Validation of Microsimulation Model

4.3.1 Selection of Traffic Microsimulator

The microsimulation program PARAMICS (Quadstone Ltd, 2004) was selected to perform the modelling work. PARAMICS was chosen primarily because it allows the user to implement custom control logic through an Application Programming Interface (API). Through the API, data from the model can be read and processed and standard code can be overwritten to perform custom applications in real time. In terms of integrating variable speed limits, instantaneous traffic data can be read from the model and the posted speed limits changed according to the algorithm. All traffic data and VSL activity can be logged for post-processing.

The following sections describe the physical development and calibration procedure required to establish the validated “base case model” for all further analyses. When discussing simulation, the following terms are used:

- *Seed Value* – An integer value allocated to an individual simulation trial. Each seed generates random numbers for every vehicle which work with the simulation logic to govern their behaviour.
- *Simulation Run* – An individual simulation trial performed for the modelling time period. Generally, each simulation run corresponds to a seed value. For any analysis, several simulation runs are performed to generate variability in unique results, similar to the day to day variability observed in reality.

4.3.2 Base Model Infrastructure

The first stage of the modelling process was to build a base network similar in physical features to the actual freeway segment. The infrastructure included the 3-lane mainline freeway, off-ramps, on-ramps and loop detectors. All roadways were coded over a satellite image, providing accurate alignment. The mainline was created as a series of links, with a loop detector placed on each link. The boundaries between the links corresponded to the planned spacing of the VSL because within PARAMICS, speed control is set for each link

and cannot be varied spatially within a link. The loop detectors were placed at approximately the same locations as those in the field, given the same names, and were programmed to report 20-second speed, volume and occupancy data like those in the field. A VSLS was situated next to each detector and would communicate with that detector; but of course for the base model, the VSLS were not activated. Images of the simulated network are provided in Appendix B.

4.3.3 Base Model Calibration

Once constructed, the simulation model was calibrated using real traffic to ensure that it appropriately replicated existing traffic conditions and behaviour. Since the study was primarily a speed control study, it was decided that the network would be calibrated on the basis of temporal 5-minute averaged station speed profiles produced from both observed and simulated data. For the observed data, speed profiles were plotted for each station using speed data averaged over ten days between 6 am and 10 am. Similar station profiles were plotted from the average of ten simulation runs between 6 am and 10 am following an initial 30-minute warm-up period. The goal of the calibration procedure was to validate the model by satisfying three criteria:

1. For a single simulation run, the simulated speed profile for each station should follow a similar trend to the corresponding observed field data for a single day;
2. Erratic behaviour in the simulation performance should be minimized (amplified start-stop conditions, frequent mini-shockwaves, etc.); and
3. The speed profile averaged over 10 simulation runs should fall within the 95% confidence limits of +/- 2 standard deviations of the observed average speed profile.

One of the difficulties of calibration is the sensitivity of the simulation software to its many adjustable parameters. The most influential parameters are those controlling driver behaviour, such as mean target headway, driver reaction time, driver aggressiveness, and driver awareness (surrogate measure of familiarity with roadway). These simulation parameters were adjusted until the speed profiles adequately matched the observed profiles.

The parameter values that produced the best results were 1.2 seconds for mean target headway and 1.1 second for driver reaction time (compared to default values of 1.0 seconds each). The mean target headway was increased from the default to promote the smooth, prolonged shockwave evident from observed data. Driver aggressiveness was not changed from the default level, but driver awareness was increased to reflect the familiarity of commuters. Calibration parameters found in other PARAMICS calibration research (Gardes et. al, 2002 and Lee et. al, 2001) were also tested, but these values produced model results that were not representative of the observed traffic conditions.

Examples of the resultant speed profile are shown below. Figure 4-6 represents speeds from an individual day and individual simulation run for Station 120, located at the downstream end of the segment. The simulation profile follows a smooth trend that closely agrees with that observed in the field. Figure 4-7 represents speeds from data averaged over 10 days (runs) at Station 60, at the upstream end of the network. The simulated profile follows the same trend as the observed profile and, overall, falls with +/- 2 standard deviations of the observed data. Profiles for the other stations can be found in Appendix B. Although the simulated speed profiles deviate from the actual profiles for some stations, the speed drop occurs at approximately the same time and degree for the simulation as for the observed data.

On the basis of these results, the simulation model was considered to be validated, and was established as the base “non-VSLS” model. Figure 4-8 represents the mapping of the freeway speed for a single simulation run of the base model. Comparing this to the observed speed mapping from Figure 4-3, both maps show that congestion begins to build shortly after 6 am, propagating to the upstream end of the network section by 7:30 am.

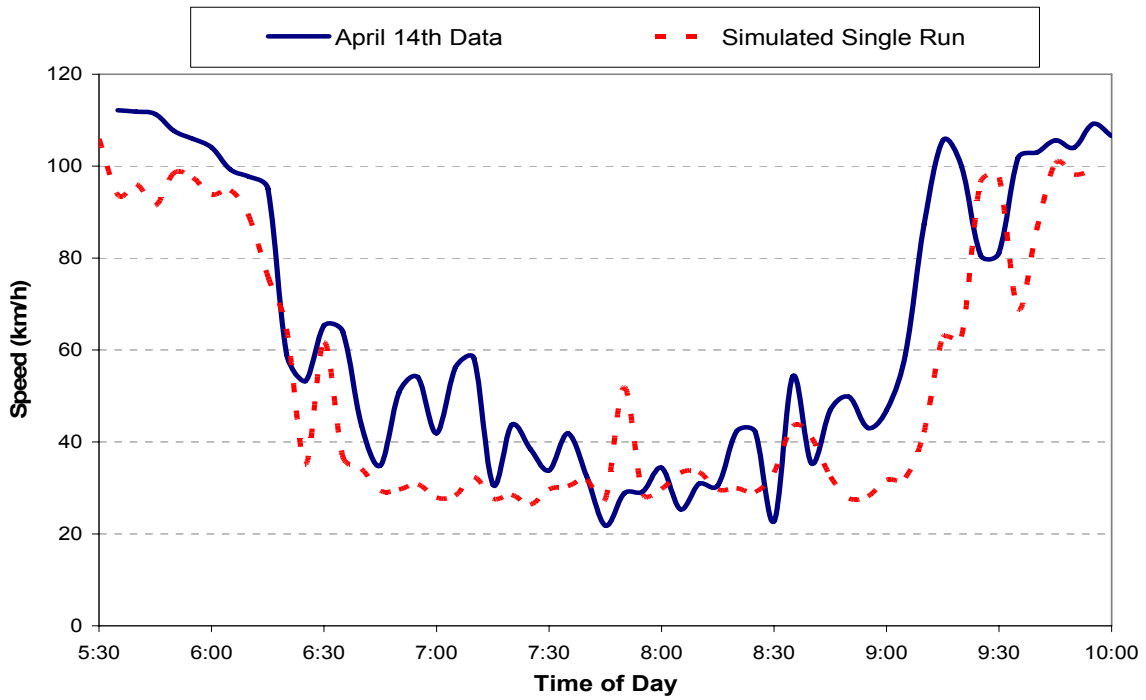


Figure 4-6: Individual speed profiles for Station 120 (5-min average station speeds)

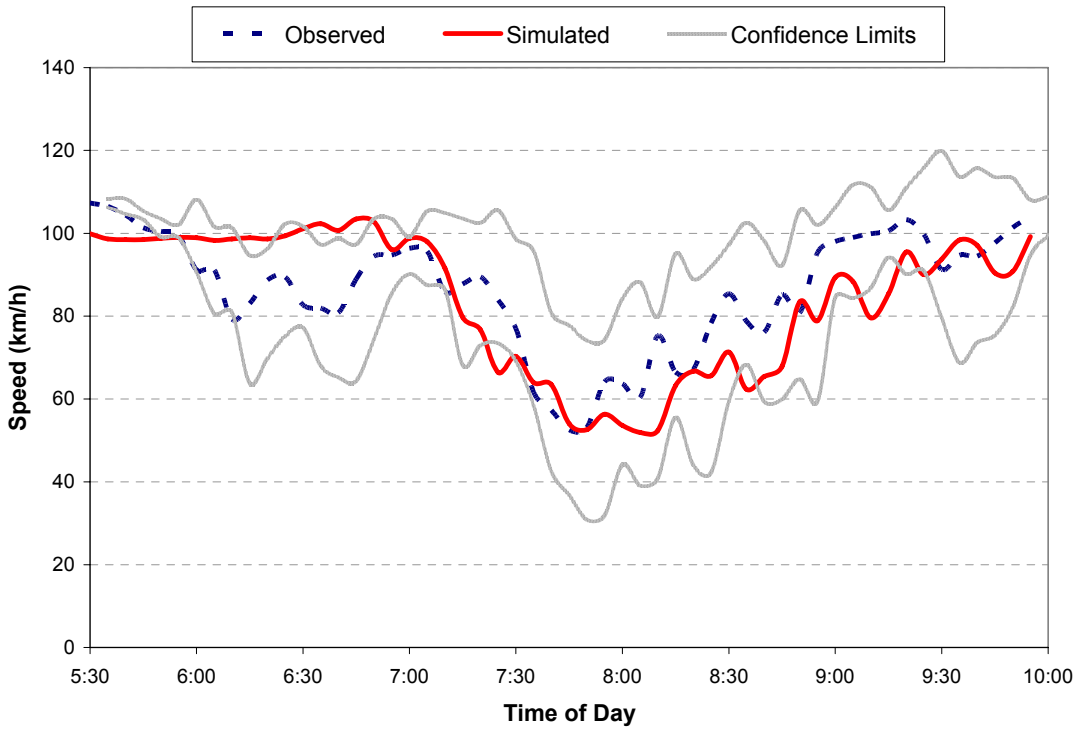


Figure 4-7: Average speed profile for Station 60 (averaged over 10 runs)

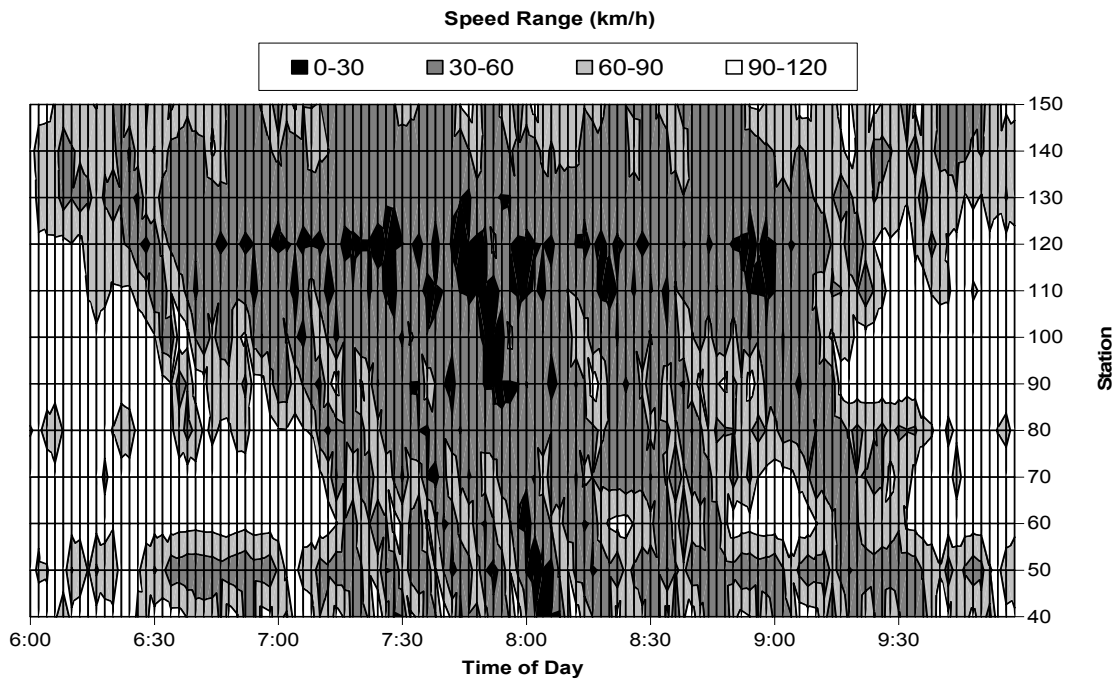


Figure 4-8: Contour mapping of simulated freeway speeds (2-min average station speeds)

4.4 Crash Precursor Adjustment Factors

The distributions of crash precursors impact the categorization of precursors and thus the crash potential calculated through the log-linear crash model. To limit the difference between the crash potential computed for simulated conditions and for observed conditions, adjustment factors were determined for the simulated crash precursors so that their distributions would most closely match those associated with field conditions.

Following the establishment of the base simulation model, crash precursors were calculated continually over the 4-hour simulation period for ten simulation runs. The precursors were separated by their associated geometry (straight or merge/diverge) and into their respective crash precursor categories. Similarly, crash precursors were calculated and categorized for the morning peak periods of four non-incident days from the QEW Burlington section between 2004 and 2005⁶. Using the boundary values from the calibrated crash potential model, the frequencies of precursors in each category were calculated. Also, precursors were separated by road geometry to allow for the individual comparison of

⁶ Note that this set of crash precursors is different than those used in the calibration of the crash potential model.

precursors from straight sections and then those from merge/diverge sections. To quantify the similarity between the distributions of observed and simulated precursors, a similar methodology to that of Lee (2004) was applied by calculating the root-mean square (RMS) error as follows:

$$\varepsilon_{CVS} = \sqrt{\frac{\sum_{i=1}^N (f_{CVS(i)} - f'_{CVS(i)})^2}{N-1}} \quad (\text{Equation 4-1})$$

$$\varepsilon_Q = \sqrt{\frac{\sum_{j=1}^N (f_{Q(j)} - f'_{Q(j)})^2}{N-1}}$$

$$\varepsilon_{COVV} = \sqrt{\frac{\sum_{k=1}^N (f_{COVV(k)} - f'_{COVV(k)})^2}{N-1}}$$

where,

$\varepsilon_{CVS}, \varepsilon_Q, \varepsilon_{COVV}$: RMS errors in distributions of *CVS*, *Q*, and *COVV*, respectively;

$f_{CVS(i)}, f_{Q(j)}, f_{COVV(k)}$: observed frequency of *CVS*, *Q*, and *COVV* for corresponding levels *i*, *j*, and *k*, respectively (average frequency over 4 observed peak periods) ;

$f'_{CVS(i)}, f'_{Q(j)}, f'_{COVV(k)}$: estimated frequency of *CVS*, *Q*, and *COVV* for corresponding levels *i*, *j*, and *k*, respectively; (average frequency of 10 simulation runs) ;

N : number of levels (categories).

The goal of this process was to identify the adjustment factors that, when applied to each simulated precursor value, would shift the distributions such that the difference (RMS error) with the observed distributions would be minimized. A range of adjustment factors was chosen arbitrarily for each of *CVS*, *Q*, and *COVV*. After the initial calculations, the range of factors was refined to identify the factor associated with the minimum RMS error (Figure 4-9).

For merging/diverging road sections, the best adjustment factors were found to be 0.39 for *CVS*, 0.2 for *Q* and 0.73 for *COVV*. For straight road sections, the best adjustment factors were found to be 0.48 for *CVS*, -7 for *Q*, and 0.75 for *COVV*. It is important to note that the adjustment factors for precursor *Q* are additive factors, whereas factors for *CVS* and *COVV* are multiplicative. Because *Q* spans a positive and negative range of values, a multiplicative factor could not be applied since it was unable to shift values of one sign to the other across categories (e.g. positive values in categories 3 or 4 could not be transformed to negative values in categories 1 or 2). Therefore additive adjustment factors had to be applied to *Q* values.

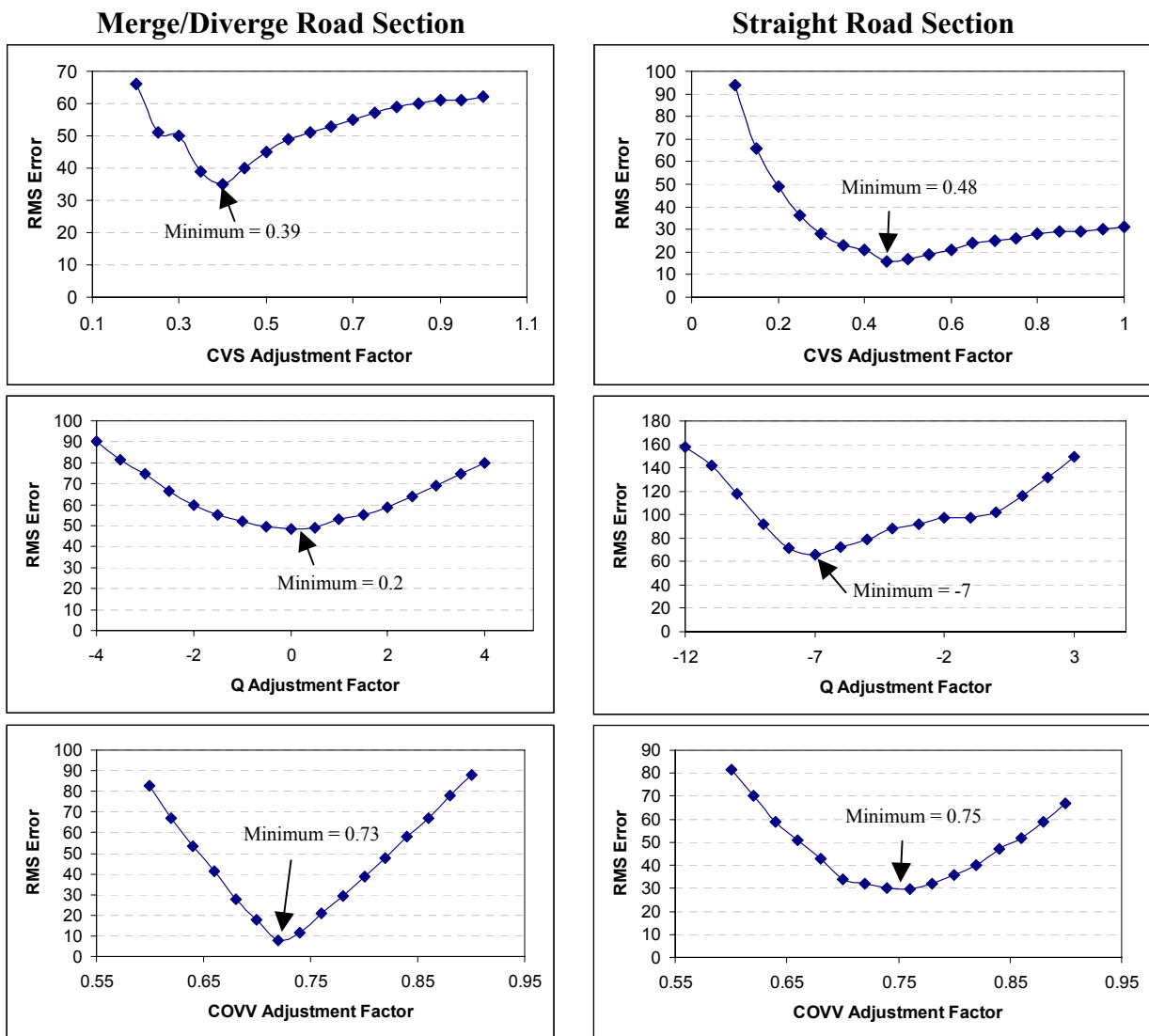


Figure 4-9: Minimum RMS Errors for Precursor Adjustment Factors

Table 4-6 presents the results from this calibration process, including the observed precursor frequencies, unadjusted precursors frequencies (from simulation), the adjustment factors, the adjusted precursor frequencies, and the associated minimum RMS error.

Table 4-6: Summary of adjusted crash precursor frequencies

Crash Precursor			Observed Frequency*	Unadjusted Frequency**	Adjustment Factor	Adjusted Frequency	RMS Error
Merge/Diverge	CVS	Low	28	9	0.39	26	7.2
		Int 1	21	5		12	
		Int 2	15	9		41	
		High	56	157		101	
	Q	Low	193	166	0.2	165	47.6
		Int 1	111	132		131	
		Int 2	47	138		139	
		High	129	163		166	
	COVV	Low	184	78	0.73	164	34.7
		Int	245	288		315	
		High	51	234		121	
	Straight	CVS	Low	26	11	0.48	26
Int 1			43	11	8		
Int 2			28	5	23		
High			84	93	64		
Q		Low	130	125	-7	220	65.6
		Int 1	161	159		157	
		Int 2	128	103		37	
		High	180	94		66	
COVV		Low	166	113	0.75	185	16.2
		Int	320	227		221	
		High	114	141		75	

The values of the adjustment factors for *CVS* and *COVV* indicate that the simulated conditions are more turbulent than the observed conditions. For *CVS*, the adjustment factors are quite low, suggesting a significantly higher amount of speed variation within lanes in the simulation than is observed in the field data. The *COVV* values, also less than 1, indicate the presence of higher lane changing activity in the simulation than in the field. The values for *Q*, which are added, rather than multiplied, are small enough to suggest a relatively low deviation from field calculations. Note that the adjustment factor of 0.2 does not mean the distribution is a perfect match, but that no other factor provides a better match.

At this point the crash precursors from the simulated conditions were considered to appropriately represent those from the actual freeway.

4.5 VSL System Development

The development of the VSL system and the integration of the system with the simulation network were accomplished via the following five tasks:

1. Code the necessary infrastructure into the simulation network and acquire a knowledge of how the dynamic speed control would operate within the simulation;
2. Confirm an appropriate candidate VSL control algorithm;
3. Compose and debug the API code communicating the control algorithm to the simulation;
4. Run the VSL system and identify any corrections to control algorithm/code; and
5. Confirm proper sign coordination and overall VSL system performance.

4.5.1 Dynamic Speed Control Operations within PARAMICS

Within PARAMICS, speed limits are controlled on a per link basis. A link speed limit is the starting point of a compliance algorithm for assigning the operating speed to each individual vehicle. Overall, the “mean” driver behaviour is set at default to exceed the speed limit by a small amount and then a driver’s aggression factor⁷ is used to calculate its individual target speed. Drivers who are more aggressive (assigned a larger driver aggressiveness factor value) will tend to exceed the speed limit, while drivers who are less aggressive will not. Of course, the speed at which a vehicle actually travels may not be the speed at which it wishes to travel. Other factors such as vehicle type characteristics, car following, and hazards will influence a vehicle’s speed. For speed limit changes, vehicles see their target speed on the next downstream link and adapt their speed accordingly in a smooth manner.

⁷ The driver aggression factor is assigned to each vehicle as a value between 1 and 8. The probability of an each value assignment is based on a user defined distribution – this study used the default Normal distribution.

The speed sign displays, or VSLS, were placed throughout network, each next to a loop detector (images of the simulated network showing VSLS and loop detector placement are provided in Appendix D). Thirteen VSLS were coded, spaced at about 500 – 600 m. Since speed limits are assigned by link, the mainline was coded as a series of links corresponding to each detector-VSLS pair. The VSLS actually do not play a functional role within the simulation other than providing a graphic of the current displayed speed for the link; but to be as realistic as possible, the network was designed to place a VSLS at the upstream end of each link so drivers would respond to the link speed limit as they pass the sign. Each link/detector/VLS set can act as its own entity – the detector gathers information about traffic conditions, the appropriate “condition based” speed is assigned to the link, and the VSLS displays the current speed limit for the benefit of the user/observer. Figure 4-10 illustrates this layout. Based on traffic data received every 20-seconds from loop detector A, a control algorithm determines the appropriate speed limit to be displayed at VSLS A. This displayed speed limit governs until the end of Link A, at which point a new displayed speed limit at VSLS B is determined by traffic data from loop detector B.

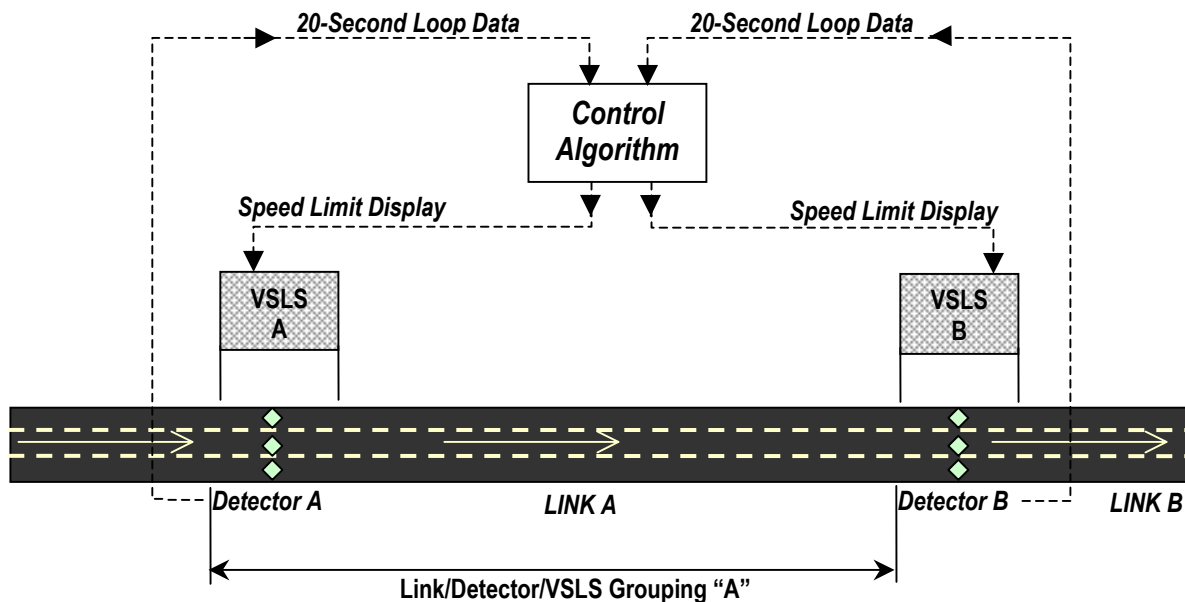


Figure 4-10: Basic Layout of Link/Detector/VLS Groupings

4.5.2 VSLS Control Algorithm

The VSLS control algorithm, governing the operations of the speed signs, was developed by IBI Group. The control algorithm not only determines the displayed speed of a single VSLS based on its local traffic conditions, but also the resultant displayed speed of adjacent speed signs within a given upstream distance. Two control algorithms were developed, one for recurrent congestion and one for non-recurrent (incident) congestion.

The VSLS control algorithm was designed to determine an appropriate displayed speed limit on the basis of volume, occupancy and speed data received every 20-seconds. The core of the algorithm is a traffic condition look-up table (Table 4-7). From any combination of volume and occupancy data, either one of three conditions will be satisfied. Within the satisfied condition, the posted speed is determined by the average station speed represented by sub-conditions a, b, or c. As shown in the table, traffic conditions 2b, 2c, 3b, and 3c result in a speed limit reduction. For this study, only decrements of 20 km/h and 40 km/h were included. Based on the look-up table, Figure 4-11 provides the decision process for determining the appropriate speed limit displayed for a trigger VSLS.

Table 4-7: VSLS Control Algorithm Look-up Table

Condition	Volume (veh/hr/lane)	Average Occupancy	Sub Condition	Average Station Speed (km/h)	Posted VSL (km/h)
1	< 1600*	< 15 %	--	Any	100
2	< 1600	> 15 %	a	> 80	100
	< 1600	> 15 %	b	> 60 and < 80	80
	< 1600	> 15 %	c	< 60	60
3	> 1600	Any	a	> 80	100
	> 1600	Any	b	> 60 and < 80	80
	>1600	Any	c	< 60	60

*A volume of 1600 vphpl was selected as it represents a freeway level of service C (HCM, 2000).

**An occupancy threshold of 15% was selected as it represents the approximate level of traffic flow breakdown (as confirmed in Figure 4-4).

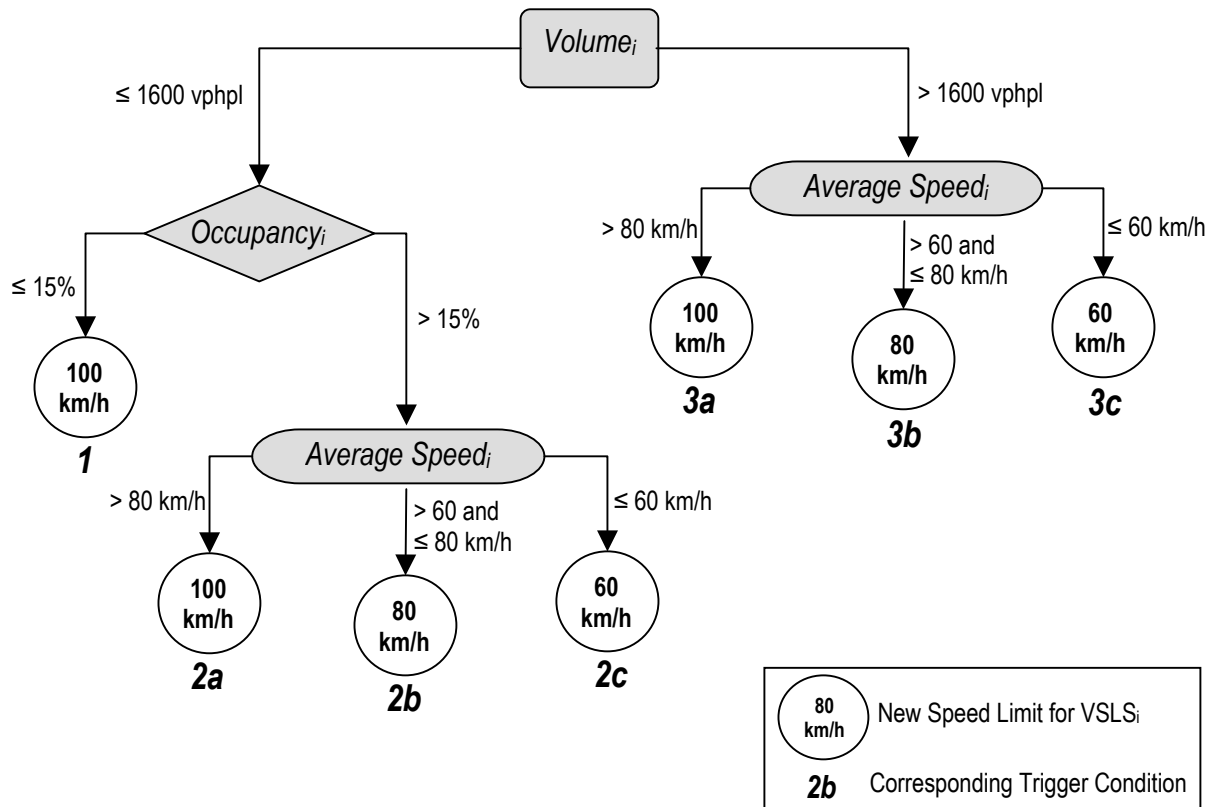


Figure 4-11: Decision Path for Determining New Posted Speed of Trigger VSLs i

Once a speed is determined for the current, or trigger VSLs, the speeds displayed for its upstream speed signs are determined based on a response zone, a transition zone, and a temporal countdown as described below:

- *Response Zone* – Includes the two nearest upstream speed signs. These will display the same speed limit as the trigger VSL;
- *Transition Zone* – If VSLs are decremented by 40 km/h, the 3rd upstream sign (1 upstream of response zone) will display 80 km/h to provide a gradual transition for drivers required to slow from 100 km/h; and
- *Temporal Countdown* – If the VSLs are decremented by 40 km/h, signs will display 80 km/h for 10 seconds prior to displaying 60 km/h.

Since the VSLs system has a definitive beginning and end, it was confined to prohibit the VSLs past a particular upstream point to act as a trigger. This would ensure a smooth

transition for vehicles entering the VSLS active zone. Based on the distance required for response and transition zones, only speed signs between Station 70 and Station 140 inclusively, could act as a trigger to initiate a drop in posted speed, while VSLS upstream of Station 70 (i.e. Stations 60, 50, & 40) could only respond as part of the response or transition zones. To fix boundaries to the system, the most upstream and downstream speed signs (i.e. Stations 30 and 150 respectively) were prohibited from reducing their posted speed from 100 km/h.

Upon primary testing of the preliminary algorithm, it was frequently observed that multiple “trigger” signs fell within close proximity of one another. As a result, new response and transition zones would attempt to override existing ones causing fluctuations and inconsistencies between consecutive signs. For example, if VSLS “A” is triggered and then one cycle later, VSLS “B” is triggered downstream, the response zone for VSLS “B” would override VSLS “A”. To mitigate this, a set of “communication rules” was established in addition to the original algorithm to check the current posted speed of neighboring VSLS prior to setting their new posted speeds (Figure 4-12). This coordinated all speed control rules enabling the thirteen speed signs to operate in harmony.

A final control algorithm was coded into the API using C++ programming software. Figure 4-12 illustrates the control structure of the final algorithm for traffic conditions 2 and 3 from the look-up table. Figure 4-13 illustrates the VSLS response to traffic conditions 3c for a one-minute period.

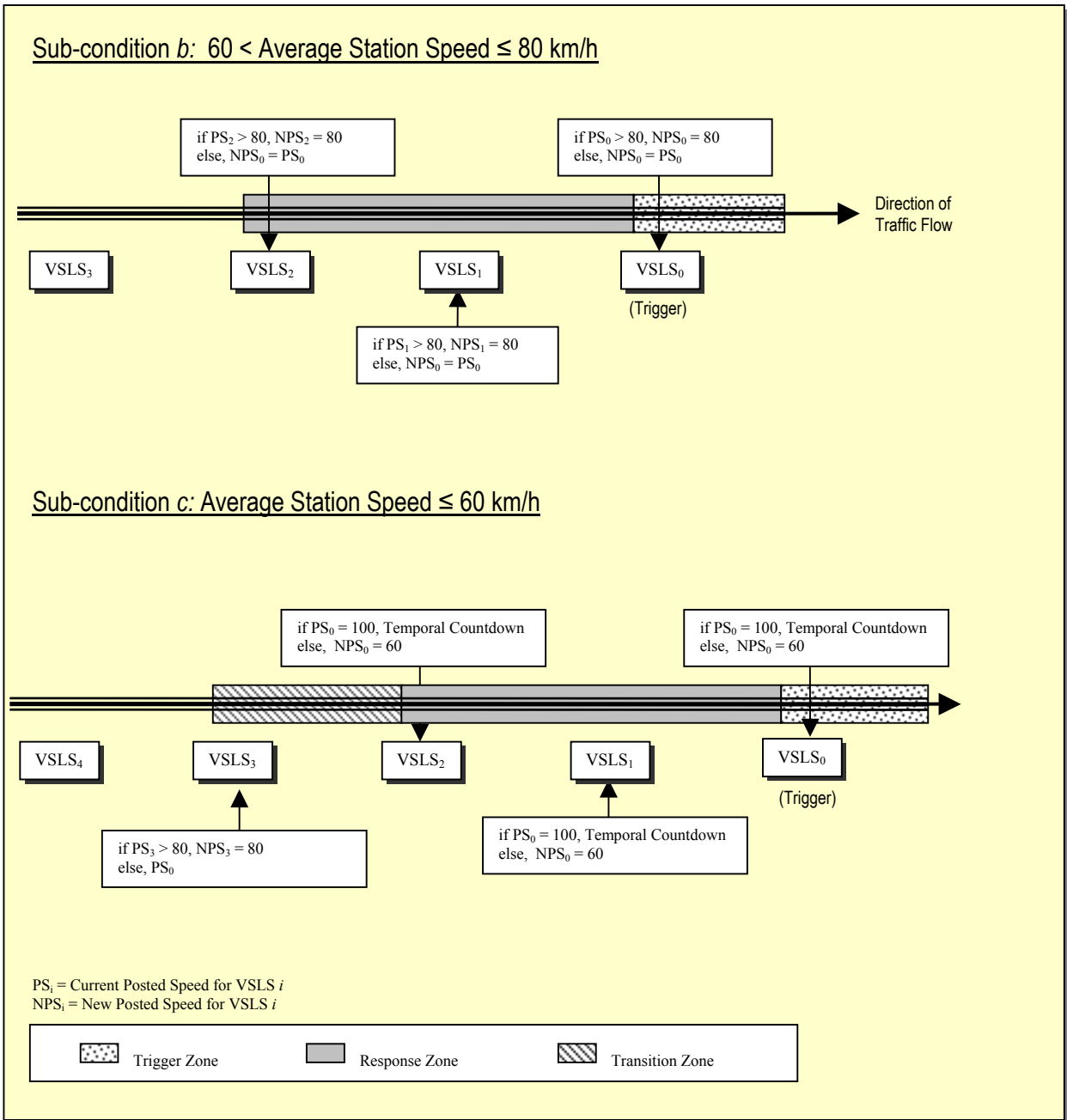


Figure 4-12: VLSL Control Structure

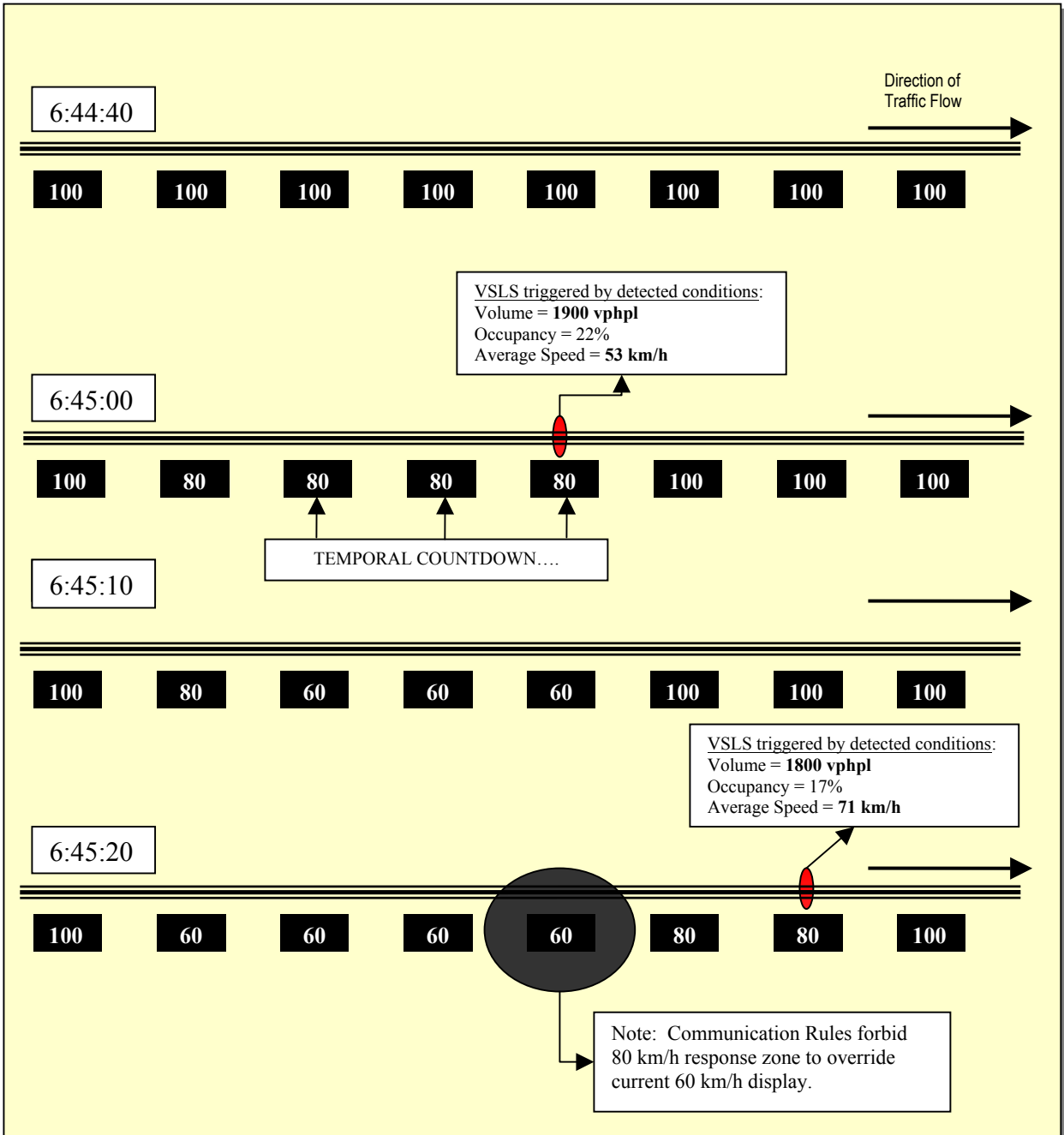


Figure 4-13: Illustration of VLS Response

Once a reduction in posted speed has occurred, it cannot be incremented until traffic flow has improved. IBI Group specified that posted speed could be increased following three consecutive cycles (1 minute) of detected station occupancy less than or equal to 15%. The value of 15% was chosen since the traffic plots indicate it is approximately the threshold of flow breakdown. VLS are not required to be incremented in the same sequence as they were

decremented and can be incremented individually; however a VSLS cannot display a speed more than 20 km/h higher than the displayed speed of its next downstream VSLS.

Once developed, the VSLS control algorithm was programmed into the PARAMICS API using C++ programming code (content of code is provided in Appendix E). Figure 4-14 shows an example of a resulting speed profile after the application of the final candidate control algorithm. Note the response of the VSLS speed decrements to detected freeway speeds and their subsequent recovery.

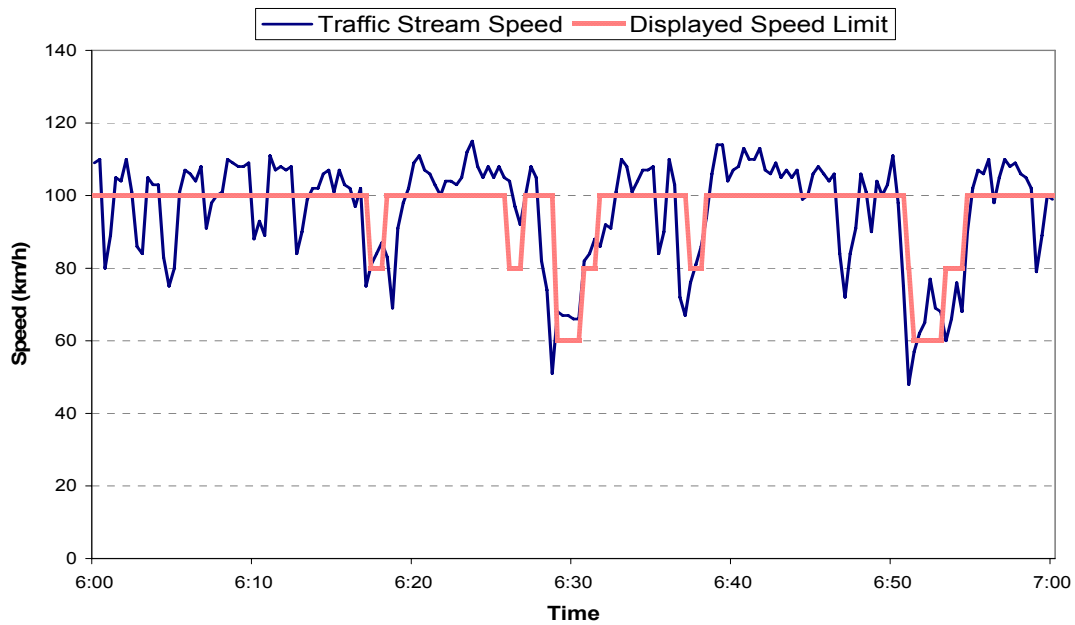


Figure 4-14: Temporal Speed Profile of VSLS Response (From Simulation Output)

5. VSLS IMPACT ANALYSIS

Using the microsimulation model, three traffic scenarios were modelled with and without the implementation of the variable speed limit control strategy:

- Scenario 1 – Peak Conditions (base model);
- Scenario 2 – “Near Peak” Conditions (93% of peak volume); and
- Scenario 3 – “Off-Peak” Conditions (75% of peak volume)

This chapter presents the results of the VSLS impact analysis performed on the three scenarios in terms of VSLS activity, the safety impact measured through the application of the crash potential model, and the travel time impact measured from simulation output. Although evaluation results are presented for all scenarios, the detailed VSLS impact investigation for recurrent congestion is focused primarily on Scenario 1, since it was the only scenario directly calibrated to field conditions. Given the project scope, the other scenarios were not calibrated but their purpose was to investigate and understand the varying reaction of the VSLS system, rather than to replicate real traffic conditions.

The evaluation of the VSLS performance is based on the entire simulation period, excluding the initial 30 minute warm-up period. The impact analysis focuses on the safety impact, in terms of crash potential and reduction in speed variability, and the travel efficiency impact in terms of average system travel time per vehicle and O-D pair trip times. The goal of these sections is to not only report the results, but to interpret the results and identify the relationship between the response of the VSLS and its impact on safety and travel time.

5.1 Scenario 1 – Peak Conditions

5.1.1 VSLS Activity

The peak scenario resulted in a very high amount of VSLS activity. Responding to high volume and congestion very early in the simulation, nearly every speed sign was forced to reduce its displayed speed to 60 km/h, which then held throughout most of the remaining simulation period. Figure 5-1, which shows the displayed speed of all VSLS for a single simulation run, illustrates this behaviour. The figure is divided into individual shaded cells each depicting the displayed speed limit on a VSLS during a time interval. A time interval of

1-minute was selected to limit the number of intervals in the figure. Consequently, each cell depicts the most frequently displayed speed limit. The results in Figure 5-1 show that during the heavily congested morning peak period, the VSLS control strategy results in a speed limit of 60 km/h at all stations for the vast majority of the simulated 4-hour period. Figure 5-2 and Figure 5-3 display the travel speeds for a simulation without and with VSLS control, respectively. The speed mapping under VSLS control indicates that travel speeds were oftentimes lower than without VSLS. The VSLS coverage for each station averaged over five simulation runs is summarized in Figure 5-4. VSLS coverage is expressed as the number of 20-second intervals a particular speed limit was displayed out of the total available 20-second intervals for the 4-hour period ($3 \times 60 \times 4 = 720$). The average coverage across all stations is shown in Table 5-1.

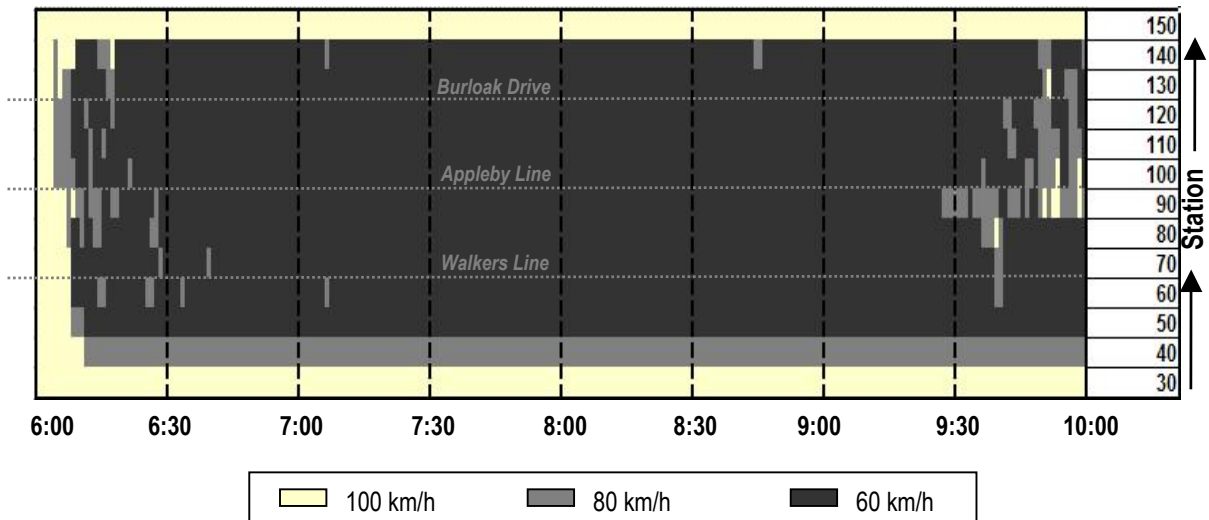


Figure 5-1: Peak Scenario – Mapping of the VSLS Displayed Speed Limits (Seed 5)

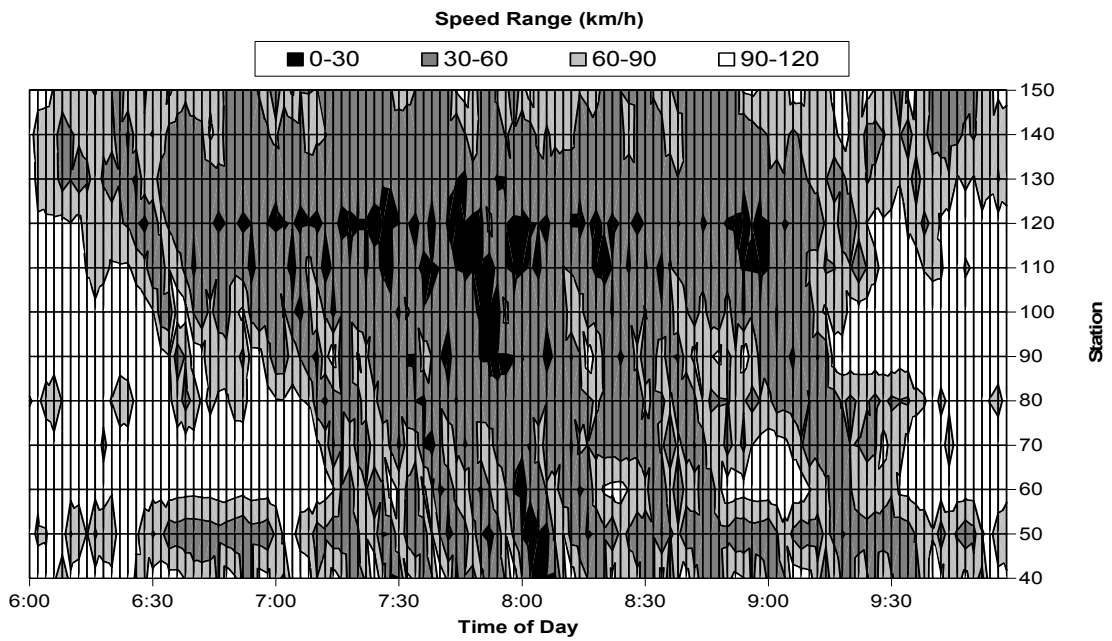


Figure 5-2: Contour Mapping of Freeway Speeds without VLS (2-min average speeds)

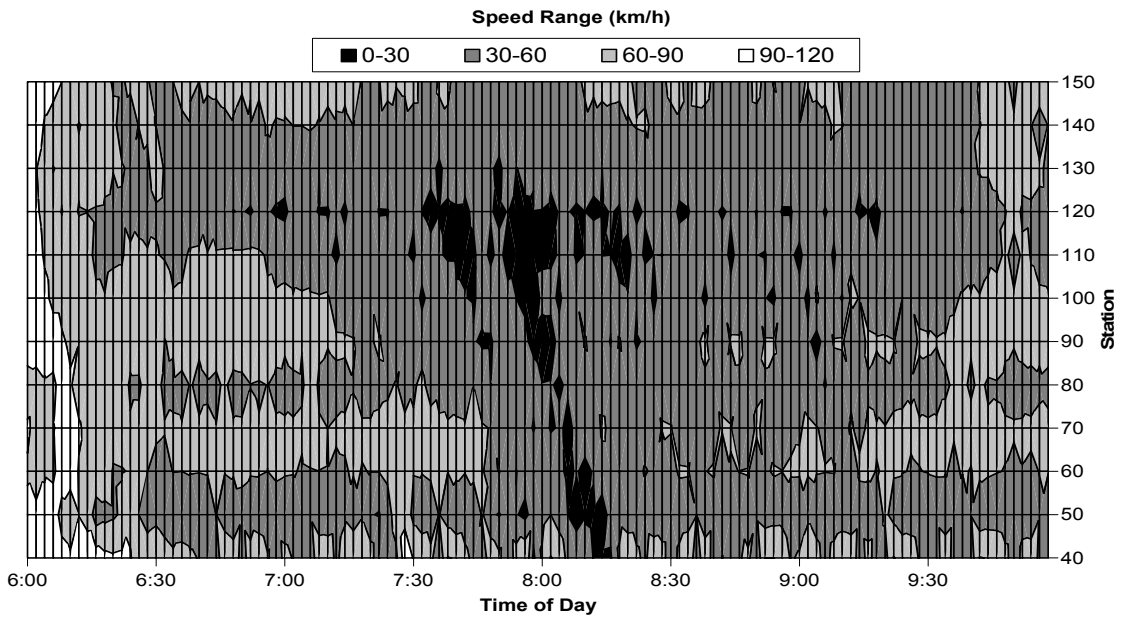


Figure 5-3: Contour Mapping of Freeway Speeds with VLS (2-min average speeds)

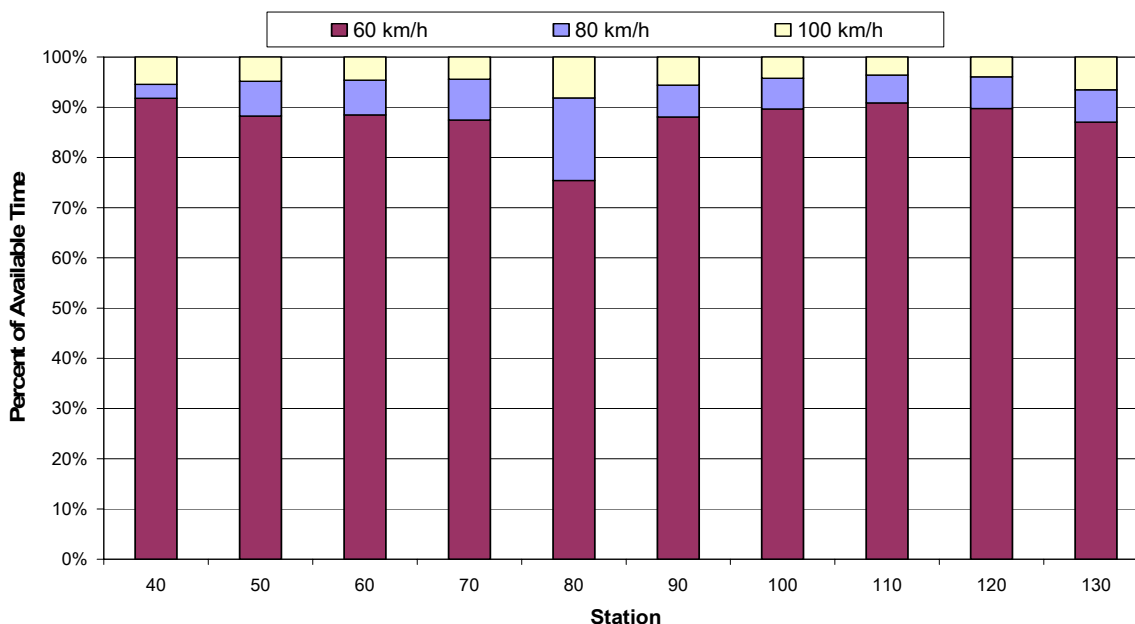


Figure 5-4: Peak Scenario – Average coverage of VLS displayed speeds by station

Table 5-1: Peak Scenario – Average VLS Coverage

Displayed Speed Limit	Fraction of Time Speed Limit is Displayed
100 km/h	5%
80 km/h	7%
60 km/h	88%

In addition to logging the activity of the VLS, the traffic conditions for each interval and station were also recorded to understand the influence of the traffic conditions on the control algorithm. Figure 5-5 displays the proportional breakdown of conditions experienced at each station. Recall from the control algorithm that the four conditions which prompt a speed limit reduction are:

- Condition 2b → [volume < 1600 vphpl; occupancy > 15%; 60 < average speed < 80];
- Condition 2c → [volume < 1600 vphpl; occupancy > 15%; average speed ≤ 60];
- Condition 3b → [volume > 1600 vphpl; any occupancy; 60 < average speed < 80]; and
- Condition 3c → [volume > 1600 vphpl; any occupancy; average speed ≤ 60].

For the peak scenario, Condition 2c was observed the most frequently, followed by Condition 3c. These conditions were responsible for triggering 60 km/h displays and together

represent, on average, 61% of the network conditions. Notice that this is less than the 88% of average 60 km/h coverage (Table 5-1). This is likely due to speed limits that are reduced due to response and transition zone requirements even though conditions at the local detector do not warrant a speed reduction.

This type of output is also useful for evaluating station performance. For example, Stations 110 and 120 experience frequent conditions of high occupancy and low volume (Condition 2c) indicating high congestion and low throughput. On the other hand, Stations 90 and 100 seem to experience somewhat less congestion as evidenced by the lower proportions of Condition 2c.

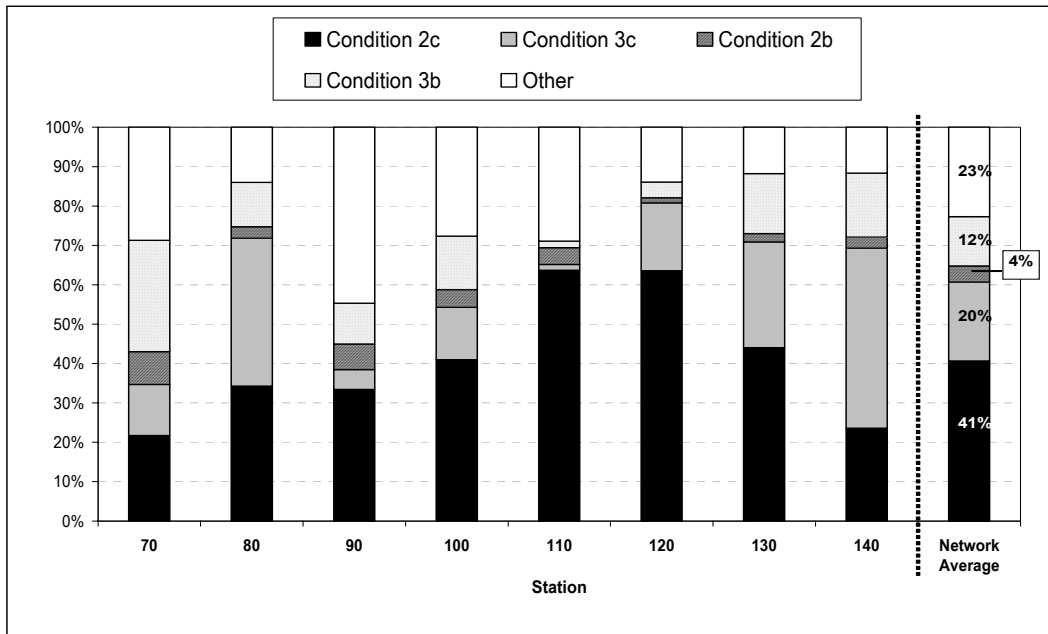


Figure 5-5: Peak Scenario – Traffic Conditions by Station for the VSL Case

For the most congested areas, an important question to ask is whether or not the speed limit reductions contribute to congestion. To answer this question, occupancy data from each station were examined for both the non-VSL and VSL cases. The proportion of the simulated period during which occupancy was greater than 15% was calculated for each case to measure any changes in congestion. Figure 5-6 shows, for each station, the percent time during which congestion was observed for the non-VSL and VSL cases. On average for the network, the VSL case experienced only a 1% increase in percent time congested. Interestingly, stations downstream of, and including Station 90 all experienced a slight

decrease in frequency of congestion after the implementation of VSLS. However, stations upstream of Station 90 all experienced an increase in frequency of congestion – as large as 25% for Station 60. These results indicate that the downstream half of the modeled network may benefit more from the VSLS system in terms of reduced congestion than the upstream half. Note that results only take into account the breach of an occupancy threshold to identify the point at which flow breakdown occurs and not the severity of the flow breakdown. Nevertheless, little evidence suggests that, on average, the VSLS system contributes to the amount of time the network experiences congestion.

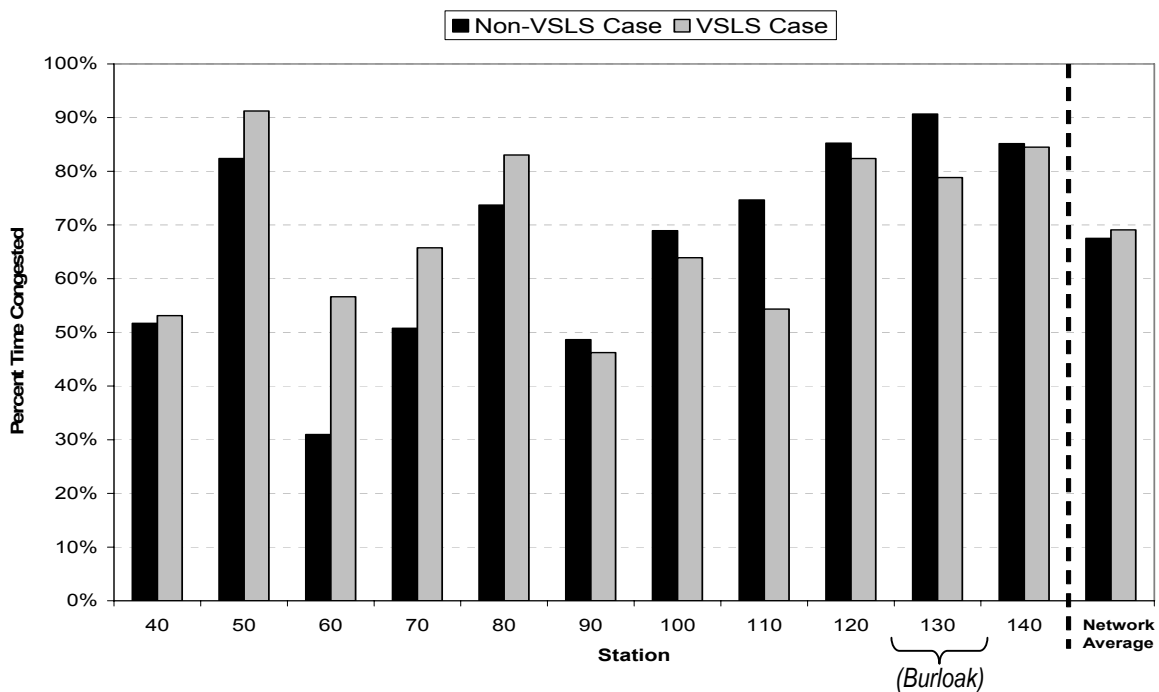


Figure 5-6: Peak Scenario – Percentage of Time during which congestion is observed (occupancy > 15%)

5.1.2 VSLS Safety Impact

The safety impact was measured by the relative change in crash potential between the non-VSLS and VSLS cases. For each simulation run, a value of crash potential (CP) was calculated at 20 second intervals for each station from the corresponding crash precursors. Ten simulation runs were performed for the non-VSLS case and ten for the VSLS case. The same set of ten seed values was used for the VSLS and non-VSLS runs. For each case, an average value of station crash potential (SCP) was obtained for each station over the simulation period for every run using Equation 5-1.

$$SCP_{ik} = \frac{1}{n} \sum_{j=1}^n CP_{ijk} \quad (5-1)$$

where,

SCP_{ik} : Station Crash Potential for Station i from simulation run k (crashes/million veh-km);

CP_{ijk} : Crash Potential for Station i at 20-second interval j in simulation run k (crashes/million veh-km);

n : Number of 20-second intervals in period (720 for 4-hour period)

Since the non-VSLS and VSLS cases differed only by the introduction of the VSLS system, the SCP values could be paired by simulation run. A paired 2-tailed student t-test was used to test for the significance of the change in SCP (or VSLS impact) at the 95% level of confidence. If the difference was found to be significant, the relative safety benefit (RSB) was calculated using Equation 5-2.

$$RSB_i = \left(\frac{ASCP_i(non-VSLS) - ASCP_i(VSLS)}{ASCP_i(non-VSLS)} \right) \times 100 \quad (5-2)$$

where,

RSB_i : Relative Safety Benefit at Station i (%); and

$ASCP_i$: Average Station Crash Potential (average of SCP over 10 simulation runs) at Station i (crashes/million veh-km). Refer to Equation 5-3.

$$ASCP_i = \frac{1}{10} \sum_{k=1}^{10} SCP_{ik} \quad (5-3)$$

Table 5-2 provides an example of the calculation process for Station 100. Table 5-3 summarizes the resulting significance tests and relative safety benefits for each station.

Table 5-2: Peak Scenario – Calculation of Relative Safety Benefit for Station 100

	SCP _{100,k} (non-VSLS)	SCP _{100,k} (VSLS)	SCP _{100,k} Difference	Test for Significance of SCP ₁₀₀ Difference
Run 1, Seed 5	1.168	0.991	0.177	<i>Confidence Level: 95%</i> <i>Degrees of Freedom = 9</i> <i>Table value: 2.262</i> <i>t-test statistic: 5.22</i> <i>(Calculated from data)</i> <i> t-stat > t-table ,</i> <i>Therefore: SIGNIFICANT</i>
Run 2, Seed 10	0.972	0.914	0.058	
Run 3, Seed 15	0.962	0.887	0.075	
Run 4, Seed 20	1.257	0.833	0.425	
Run 5, Seed 25	1.136	0.686	0.450	
Run 6, Seed 30	1.305	0.854	0.451	
Run 7, Seed 35	1.316	0.810	0.506	
Run 8, Seed 40	1.210	0.837	0.373	
Run 9, Seed 45	1.213	0.866	0.346	
Run 10, Seed 50	0.967	0.890	0.077	
For 10 Runs	ASCP ₁₀₀ (non-VSLS)	ASCP ₁₀₀ (VSLS)		
	1.151	0.857		
	RSB₁₀₀ = 26%			

For the paired t-test, the t-test statistic was calculated from Equation 5-4.

$$\bar{D} = \frac{m_D - d_0}{S_D / \sqrt{n}} \quad (5-4)$$

where

- \bar{D} : test statistic;
- m_D : mean of difference between paired population samples;
- d_0 : hypothesized difference between populations (equal to 0);
- S_D : standard deviation of difference between paired population samples;
- n : sample size.

The t-statistic in the above example for Station 100 would be calculated as follows:

$$\bar{D} = \frac{2.94 - 0}{2.78 / \sqrt{10}}$$

$$\bar{D} = 5.22$$

Table 5-3: Peak Scenario – Relative Safety Benefits by Station

Station	ACP		Change	RSB	Impact	Significant at 95%?
	Non-VSLS	VSLS				
40	1.401	1.428	-0.027	-2%	NEGATIVE	NO
50	0.716	0.398	0.318	44%	POSITIVE	YES
60	0.466	0.257	0.209	45%	POSITIVE	YES
70	0.963	0.582	0.381	40%	POSITIVE	YES
80	0.747	0.429	0.318	43%	POSITIVE	YES
90	0.656	0.416	0.240	37%	POSITIVE	YES
100	1.151	0.857	0.294	26%	POSITIVE	YES
110	1.023	0.651	0.371	36%	POSITIVE	YES
120	0.386	0.275	0.111	29%	POSITIVE	YES
130	0.808	0.344	0.464	57%	POSITIVE	YES
140	0.196	0.109	0.087	44%	POSITIVE	YES
Network Average	0.774	0.522	0.251	32%	POSITIVE	YES

The results of the crash potential impact analysis show that all stations but one experienced a significant reduction in crash potential. For the network, the average relative safety benefit across all stations was a 32% decrease in crash potential. Of the significant results, Station 130 benefits the most (in terms of relative and absolute impact) from the VSLS with a crash potential reduction of 57%, while Station 100 experiences the smallest significant relative benefit of 26% and Station 140 the smallest significant absolute benefit. Station 40 showed no clear change in crash potential, as its results were not significant.

It is instructive to understand what causes these safety benefits. The crash precursor values for each station were compiled to investigate the change in their distributions from the non-VSLS case to the VSLS case. Since the crash precursor levels correspond to the degree of turbulence in the traffic stream, a crash potential reduction would be associated with a shift in the frequency of precursor values from a high category (i.e. Levels 3 and/or 4) to a lower category. The distributions for Station 130 (Figure 5-7) best exhibit the expected shift in distributions for a crash potential reduction. For each precursor, the frequency of “high level” values is reduced for the VSLS case, indicating less severe turbulence in the traffic stream. In contrast, the distributions for Station 40 show little deviation, reflecting the lack of significant safety benefits.

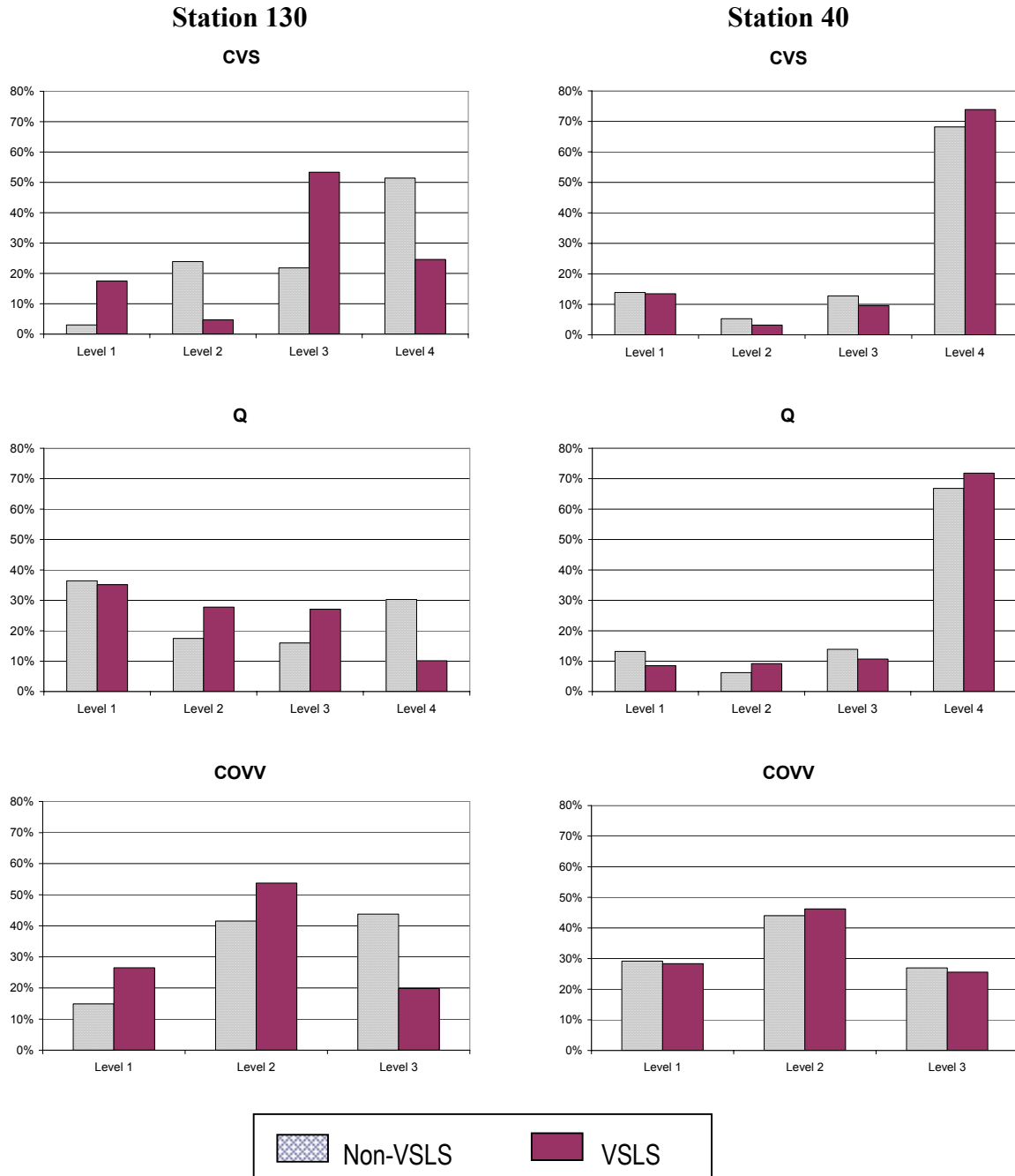


Figure 5-7: Peak Scenario – Crash precursor distributions for VSLS and non-VSLS cases

The shifts in precursor distributions illustrated in Figure 5-7 can be interpreted in terms of traffic stream behaviour. The deployment of a VSLS system during peak conditions appears to reduce severe in-lane speed variation, severe speed differential between upstream and downstream locations, and severe lane changing activity. However, for the peak conditions, it is difficult to fully understand the direct interaction between dynamic VSLS

activity and the resulting precursor shifts, since for the majority of the 4-hour simulation period, the VSLS continuously displays a static 60 km/h speed limit.

What can be understood is that the reduced speed limit appears to reduce severe momentary speed fluctuations within the traffic stream. Examination of the non-VSLS data reveals that these speed fluctuations tend to occur when the mean freeway speed is low, but gaps in the traffic stream allow drivers to accelerate for short distances. Within the simulation model, the introduction of VSLS dampens these fluctuations (with default driver compliance to speed limits). Figure 5-8 shows the VSLS displayed speed limit superimposed onto non-VSLS and VSLS temporal freeway speed profiles for Station 100.

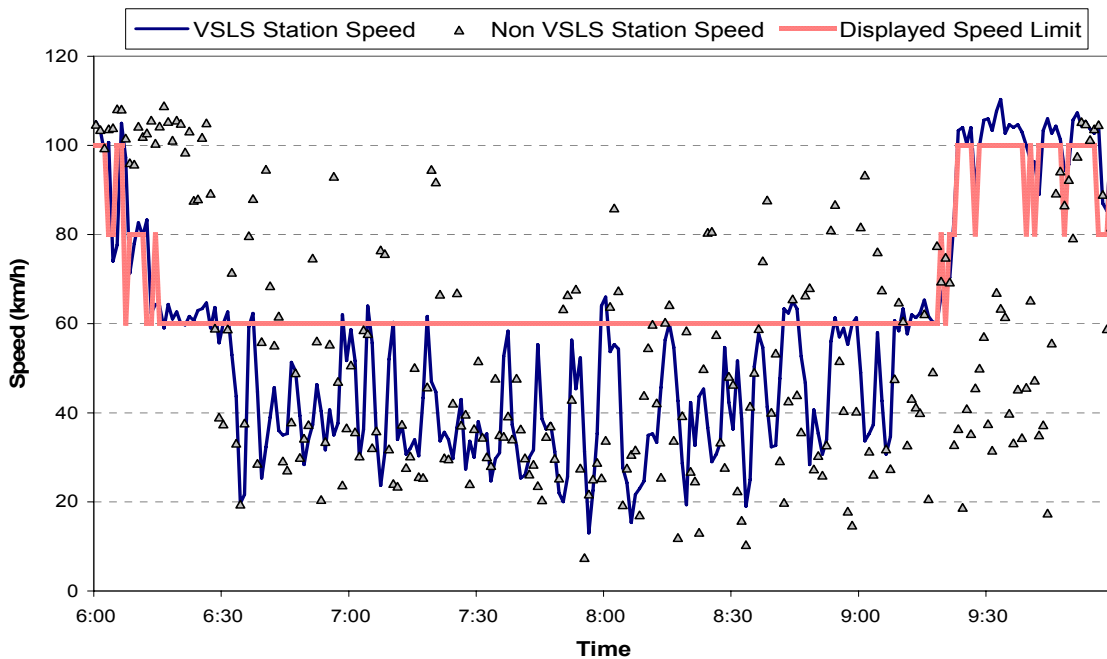


Figure 5-8: Peak Scenario – Temporal speed profile for Station 100 (VSLS case)

From about 6:30 am until 9:30 am, the mean freeway speed is controlled by congestion in both the non-VSLS and VSLS cases, but the VSLS reduces short term speed increases between recurring shockwaves. This may cause delays for some drivers, but has an overall safety benefit. Previous research has indicated that a reduction in speed variability within a traffic stream decreases the likelihood of a crash (Garber, N.J., and Gadiraju, R., 1989). From the speed profiles, it appears that for the VSLS case less variability exists. To provide quantitative evidence, a moving 5-min standard deviation was calculated for the non-

VLS and VLS freeway speeds corresponding to Figure 5-8. For the simulation period, the 85th percentile of standard deviation decreased from 25 km/h to 17 km/h after VLS implementation. A similar trend is evident for all other stations. The reduction in speed variability is also supported by the observed change in the *CVS* distribution toward lower level categories (as *CVS* is an alternative measure for speed variability).

5.1.3 VLS Travel Efficiency Impact

The most desirable results from the VLS impact analysis would be a safety benefit in terms of reduced crash potential, and a travel efficiency benefit in terms of reduced or unaffected travel time.

Similarly to the crash potential analysis, travel time data was collected for each of 10 simulation runs and paired by the non-VLS and VLS cases. PARAMICS provides travel time data in terms of overall network travel time (i.e. an aggregate of the times all vehicles spend in the network) and disaggregated travel times for specified O-D trips. The number of vehicles serviced by the network is known, so the overall network travel time can be converted to an average network travel time per vehicle. Since the largest proportion of vehicles in the network are originating from the mainline and destined to remain on the mainline, the overall network travel time is biased towards those vehicle trips. These vehicles also pass through all VLS controlled stations and are therefore more likely to be impacted by VLS. To investigate the range of travel time impact by trip length, the disaggregated travel times for individual O-D trips were also examined. The change in average network travel time per vehicle from the non-VLS case to VLS case was tested for significance using a paired 2-tailed student t-test. Table 5-4 shows the resulting network travel times for each simulation run.

Table 5-4: Peak Scenario - Summary of Average System Travel Time Impact (min/veh)

	Simulation Run										Average
	1	2	3	4	5	6	7	8	9	10	
Non-VLS Case	14.1	13.3	14.0	11.7	14.2	13.6	12.4	12.8	14.7	11.3	13.2
VLS Case	15.5	13.3	15.3	14.2	12.9	15.0	14.7	14.6	15.9	14.7	14.6
Change (min)	+1.4	0	+1.3	+2.5	-1.3	+1.4	+2.3	+1.8	+1.2	+3.4	+1.4
% Increase	+10%	0%	+10%	+21%	-9%	+10%	+18%	+14%	+9%	+30%	+11%

Overall, the change in average network travel time per vehicle was found to be significant at the 95% confidence level, but as a negative impact. From the average of 10 simulation runs, the travel time per vehicle increased by 1.4 minutes (~80 seconds) after the introduction of the VSLS system. This represents an 11% increase to travel time. Note, however, that this travel time analysis did not consider the delay reductions that would be realized through improvements to safety. In the long run, improving safety should result in a reduction of severe collisions. This translates to fewer occurrences of non-recurrent congestion and thus fewer periods of very high delay. Drivers may be more tolerant of marginal increases to their regular commutes, if it meant fewer very long commutes.

It is interesting that when the travel times are investigated on an O-D specific basis, only trips of longer distance appear to be negatively impacted. The trip specific travel time results in Table 5-5 indicate that vehicles originating near the downstream end half of the network (Appleby Line and Burloak Drive, near Station 100 and Station 130, respectively) experience little impact from the VSLS. Yet, vehicle trips that are entirely on the mainline are delayed by VSLS. From a travel time perspective for the peak conditions, VSLS does not seem to favor drivers originating near the upstream end of the VSLS active zone.

Table 5-5: Peak Scenario – Average Travel Time Impact for Specific O-D Pairs

Origin Specific Travel Time/Vehicle		Average Travel Times (min/veh)		Change (sec)	Relative TT Impact		Significant at 95%?
Origin	Nearest Detector	Non-VSLS	VSLS				
Upstream Mainline	Station 30	20.9	23.2	138	-11%	INCREASE	YES
Appleby Line N	Station 70	11.7	11.5	-12	2%	DECREASE	NO
Burloak Drive	Station 130	3.7	3.7	0	0	None	N/A
Network Travel Time/Vehicle		13.2	14.6	84	-11%	INCREASE	YES

The negative travel time impact contradicts some claims that VSLS systems enhance system throughput and improve travel times. The primary explanation for this could be that the peak conditions modelled are very congested and that under the current control strategy, the VSLS are forced to display 60 km/h for most of the simulation period and most of the network. Under these conditions, the VSLS do not have the opportunity to provide a dynamic, reactive system and therefore likely cannot optimize traffic throughput.

Figure 5-9 shows the station speed profiles for Station 100 smoothed by a 5-minute moving average. For the majority of the simulated period, the speed profiles exhibit similar trends, falling below the VLSL displayed speed. This suggests the limiting factor for freeway speeds is congestion and the current VLSL algorithm does little to mitigate this. Note also that for this particular station, although speeds were reduced earlier in the simulation with VLSL, they increased sooner near the end of the simulation than without VLSL.

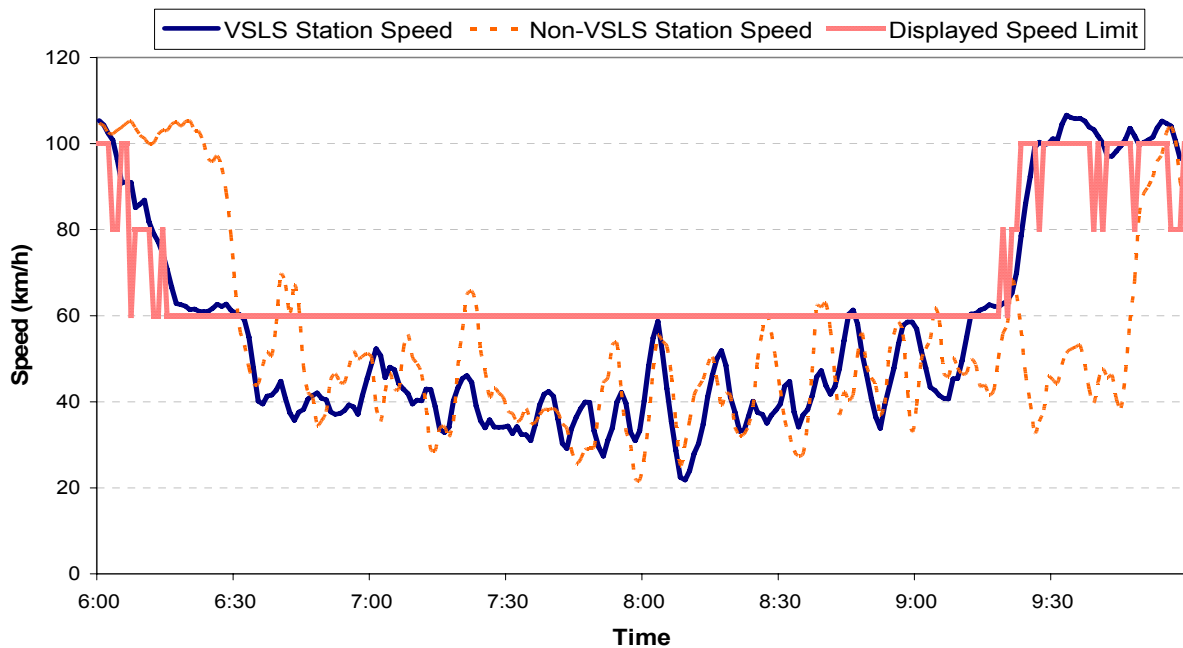


Figure 5-9: Peak Scenario – Smoothed Average Speed Profiles for Station 100

A second explanation for the negative travel time impacts is that when VLSL are decremented at the downstream end of the network, a response zone displaying 80 km/h or 60 km/h is initiated. Then, with reduced speeds, VLSL within this response zone are apt to become new triggers and initiate a new upstream response zone. The result is a domino effect of speed limit decrements cascading upstream over the network (Figure 5-10). Upstream zones display reduced speed limits, although congestion in the non-VLSL case does not exist (Figure 5-11). From the speed mapping it is clear that vehicles in the VLSL case, particularly in the upstream portion, are forced to reduce their speeds significantly earlier than without VLSL, causing the increase in travel times.

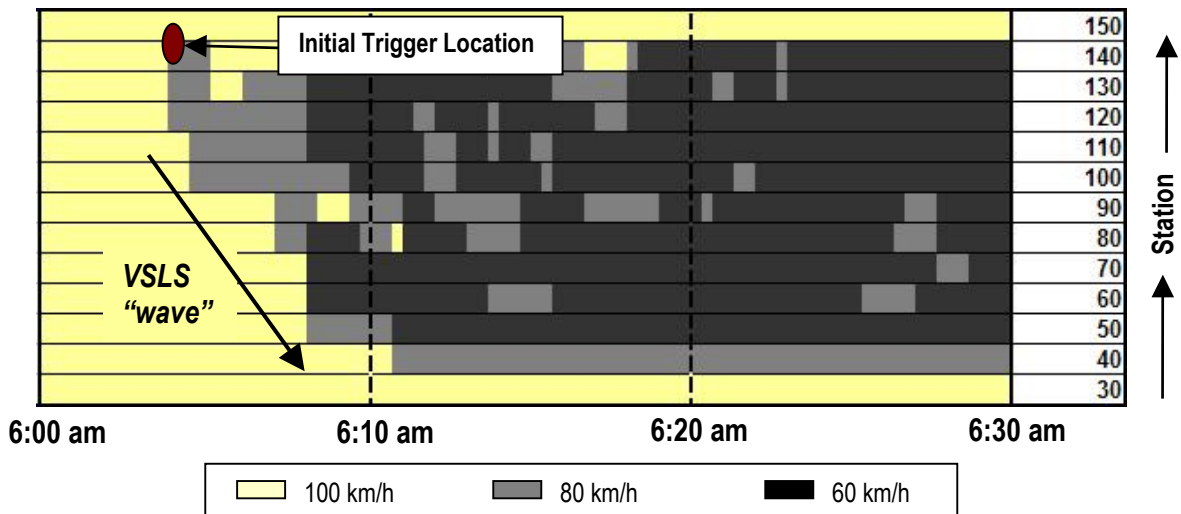


Figure 5-10: Peak Scenario – Illustration of VSLs “Domino” Effect

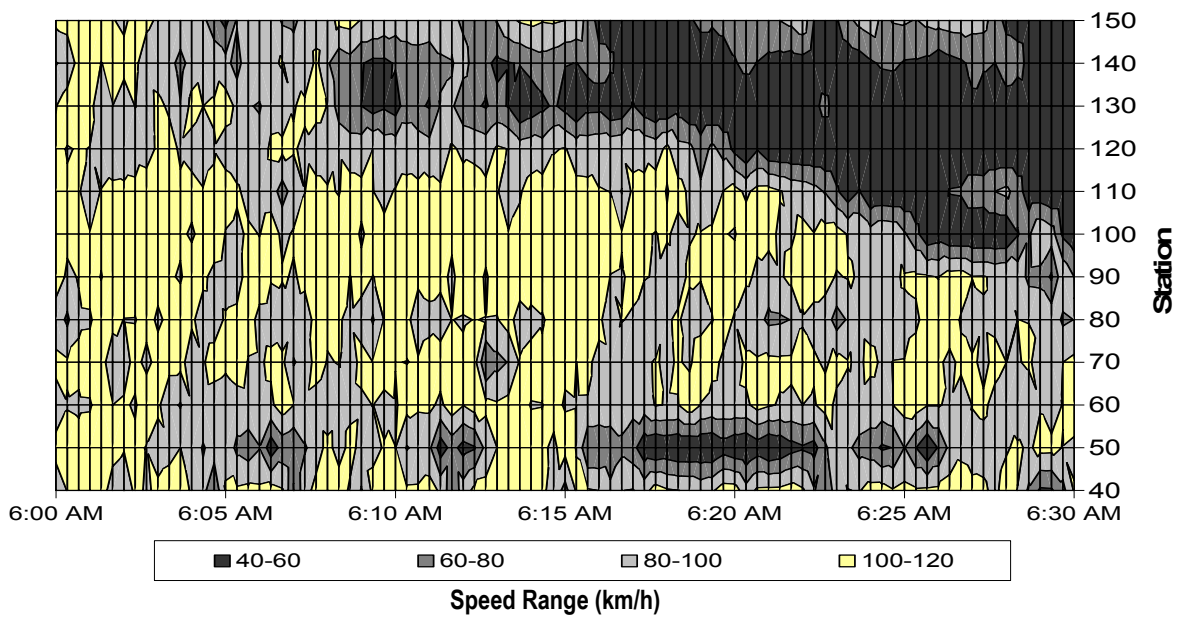


Figure 5-11: Peak Scenario - Contour mapping of freeway speeds for non-VSLs case

A third reason for increased travel time may be that under the current strategy, VSLs react to data collected over individual 20-second intervals. As a result, there are times that a

VSLs react to an isolated “pocket” of brief congestion causing speed limit reductions that may be otherwise unnecessary. Instead of this pocket clearing up quickly on its own (without VSLs), speed limits are displayed at 80 km/h or even 60 km/h. Sometimes the VSLs can recover as quickly, but many times it cannot.

5.2 Scenario 2 – Near-Peak Conditions

Near-Peak conditions were modelled to investigate the performance of VSLs during less severe congestion than the peak period. Through preliminary simulation runs, different degrees of reduction in the peak volume were tested to find which volume would result in a noticeable breakdown in freeway speed but still exhibit a recovery prior to the period end. A threshold was found at about 93% of peak volume. Any volume less than this did not exhibit a very noticeable speed drop. The same method of impact analysis was applied to the near-peak conditions as peak conditions. The results are summarized below, in less detail than peak conditions, but points of particular interest are highlighted.

5.2.1 VSL Activity

For the near-peak scenario the VSLs were able to respond with more dynamic response to traffic conditions. The 60 km/h posted speed was still the most dominant in terms of coverage, but the VSL system was able to recover more frequently. Table 5-6 shows the proportional breakdown of average coverage for the near-peak scenario. Figure 5-12 provides the VSL mapping for a single simulation run.

Table 5-6: Near-Peak Scenario – Average VSL Coverage

Displayed Speed Limit	Fraction of Time Speed Limit is Displayed
100 km/h	15%
80 km/h	17%
60 km/h	68%

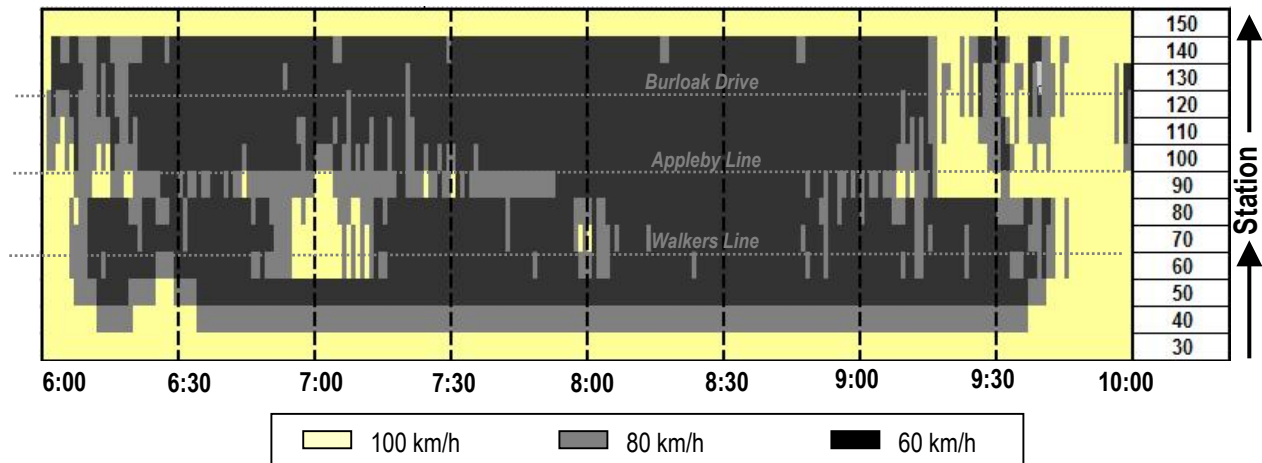


Figure 5-12: Near-Peak Scenario – Mapping of VLSL Displayed Speed Limits

5.2.2 VLSL Safety Impact

The results from the safety impact analysis for near-peak conditions show that an overall positive safety benefit was achieved by the introduction of the VLSL system (Table 5-7).

Table 5-7: Near-Peak Scenario – Relative safety benefit results

Station	Average CP		Change	RSB	Impact	Significant at 95%?
	Non-VLSL	VLSL				
40	0.681	1.192	0.511	-75%	NEGATIVE	YES
50	0.375	0.272	-0.103	27%	POSITIVE	YES
60	0.144	0.083	-0.062	43%	POSITIVE	YES
70	0.512	0.383	-0.129	25%	POSITIVE	YES
80	0.263	0.210	-0.053	20%	POSITIVE	NO
90	0.266	0.219	-0.047	18%	POSITIVE	NO
100	0.646	0.535	-0.111	17%	POSITIVE	NO
110	0.600	0.421	-0.178	30%	POSITIVE	YES
120	0.317	0.237	-0.080	25%	POSITIVE	YES
130	0.496	0.307	-0.189	38%	POSITIVE	YES
140	0.203	0.109	-0.094	46%	POSITIVE	YES
Network Average	0.409	0.361	-0.049	12%	POSITIVE	YES

Of the stations with significant results, all but one experienced a positive relative benefit of similar magnitude to the results from the peak scenario. The station experiencing the highest relative safety benefit is Station 140, while Station 40 experienced the lone negative impact. Examination of the safety impact results revealed that the non-VLSL and VLSL crash potential estimates at Station 40 fell consistently higher than the other stations, of a magnitude that skewed the overall results. These outlying high crash potential values seem

to indicate irregular traffic behaviour occurring at the upstream end of the simulated network. It is suspected that Station 40's positioning near the mainline release zone is the cause for this irregularity. At this location vehicles are released onto a link with a 100 km/h speed limit only to be caught in nearby congestion. Because of the unreliability of the traffic representation at Station 40, its results were omitted from the remainder of this analysis. The resulting average network safety impacts for the peak and near-peak scenarios are shown in Table 5-8.

Table 5-8: Average Peak and Near-Peak network safety impacts after omission of Station 40

Scenario	Average CP		Change	RSB	Impact	Significant at 95%?
	Non-VSLs	VSLs				
Peak	0.711	0.432	-0.279	39%	POSITIVE	YES
Near Peak	0.382	0.278	-0.105	27%	POSITIVE	YES

Although the overall average network safety benefit for the near-peak scenario is 27%, the results exhibit much more variability across simulation runs than for peak conditions. Considering each simulation run on its own, the overall average network RSB varies from -4% to 47%, compared to a range of 22% to 42% for peak conditions (Figure 5-13).

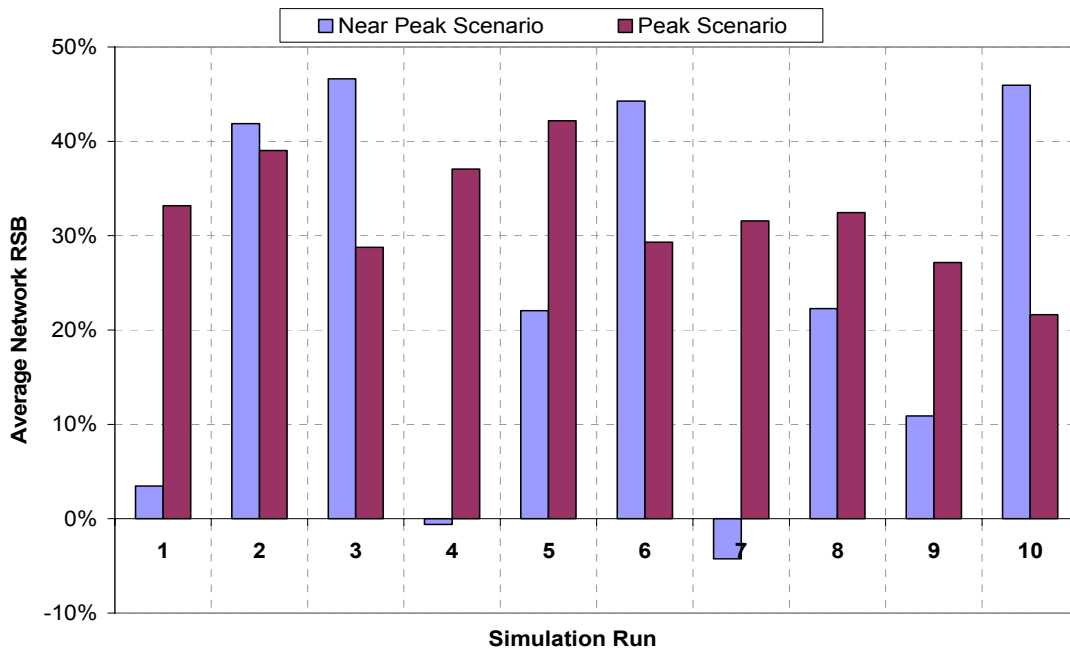


Figure 5-13: Comparison of RSB variability for the Peak and Near-Peak Scenarios

Much of the network variability stems from Stations 80, 90 and 100. For the near peak scenario, the occurrence of flow breakdown was less consistent between simulation runs so the VSLs response varied greatly. For example, comparing the speed profiles at Station 100 for two simulation runs, it is clear why such variability exists in the safety impact. Figure 5-14 represents the speed profiles for Run 3 from which a positive individual safety benefit of 54% was found for Station 100. The VSLs provides frequent dynamic response, resulting in smoother flows than the non-VSLs case and higher average speeds. In contrast, the speed profiles for Run 1 are shown in Figure 5-15. For the most part, the non-VSLs case exhibits a high and consistent freeway speed, while the VSLs case exhibits low speeds with evidence of cyclical congestion. For this run, the individual station safety impact was found to be an undesirable -25%. Clearly, under the current control algorithm, the safety impact of the VSLs system is dependent on the random variability of day-to-day traffic congestion.

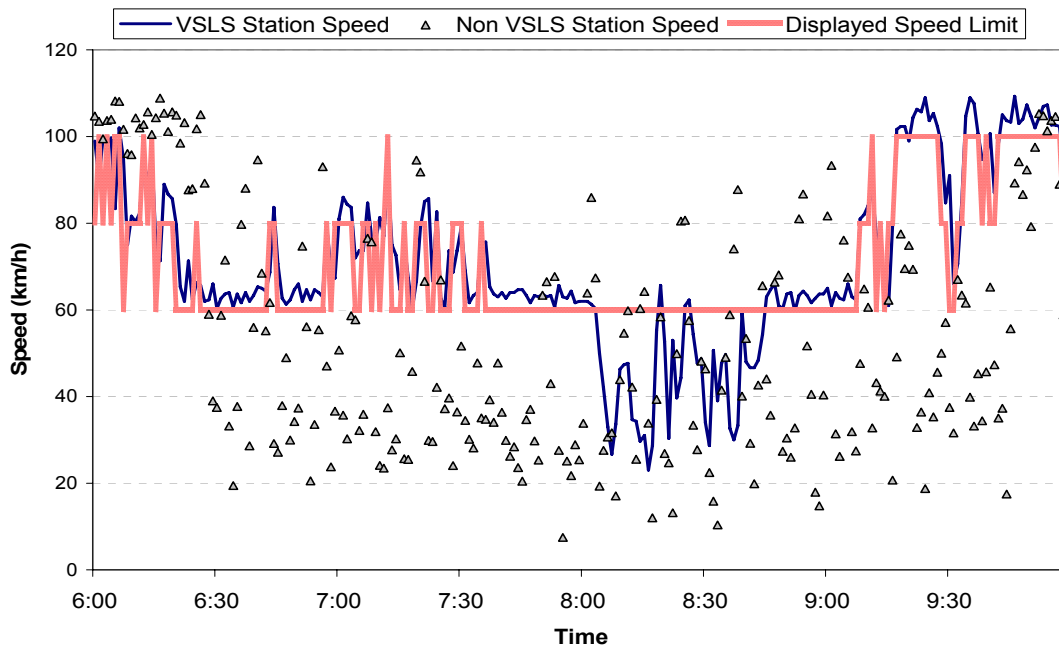


Figure 5-14: Near-Peak Scenario – Speed profiles for Station 100 (Run 3)

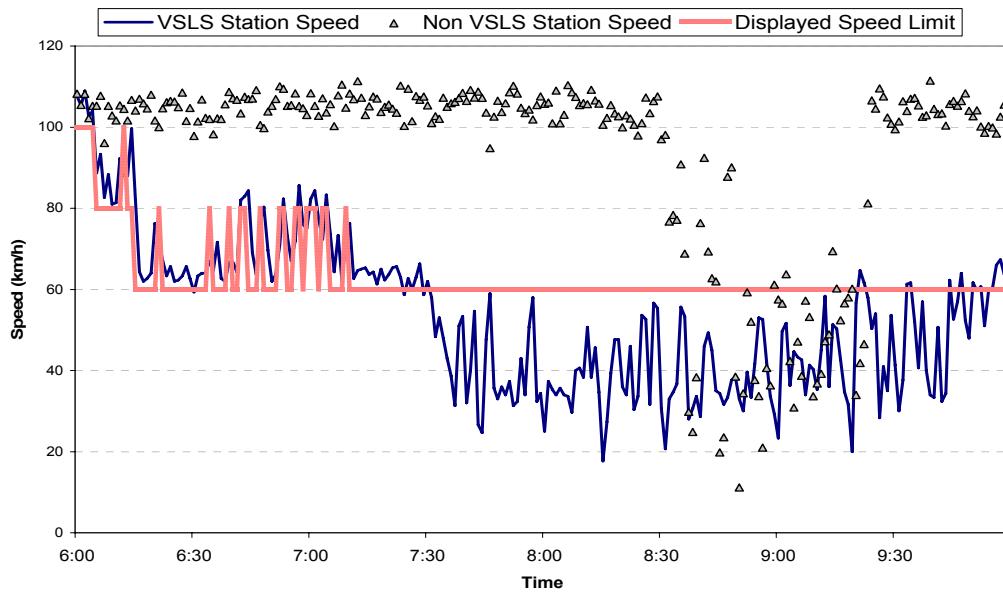


Figure 5-15: Near-Peak Scenario – Speed profiles for Station 100 (Run 1)

The results in Figure 5-15 raise concern regarding the efficiency of the VLSL operation. It is evident that the VLSL control is causing much more congestion than would otherwise be experienced. In the non-VLSL case, no conditions exist which satisfy the criteria to reduce the speed limit until well into the simulated period (~8:30 am). In the VLSL case, the reduced speed limit occurs as part of the response zone to a triggered VLSL at Station 130 early in the simulated period. Since the congestion at Station 130 in the non-VLSL case is not sufficient to result in a rapidly building shockwave, the congestion does not spill back to Station 100 until much later. This indicates that the resulting safety benefits and efficiency of a VLSL system may depend on the number of VLSL programmed to respond to varying degrees of congestion.

The varying safety impact between simulation runs was investigated further to find evidence of a relationship between the degree of congestion present on the network and the resulting VLSL response and safety impact. To represent the level of congestion existing in each non-VLSL simulation run, the average network traffic speed was calculated from the simulation output. A linear regression was then performed on the average speeds present in each simulation run without VLSL and the corresponding safety impacts with VLSL (Table 5-9). A relatively large proportion of the variance exhibited by the data is explained by the linear model as indicated by an R^2 value of 0.78. The regression equation, constant, and slope

are all significant at the 95% level of confidence. This provides strong evidence that the safety impact of this VSLS control algorithm is highly dependent on the level of congestion present in the network. As shown in Figure 5-16, simulation runs experiencing less congestion in the non-VSLS case are associated with a diminishing safety benefit upon VSLS implementation.

Table 5-9: Near-Peak Scenario – Average traffic speed (non-VSLS) and resulting VSLS safety impact

	Simulation Run									
	1	2	3	4	5	6	7	8	9	10
Average Network Speed without VSLS (km/h)	67	60	53	78	72	61	76	70	74	48
Network RSB (with VSLS)	3%	42%	47%	-1%	22%	44%	-4%	22%	11%	46%

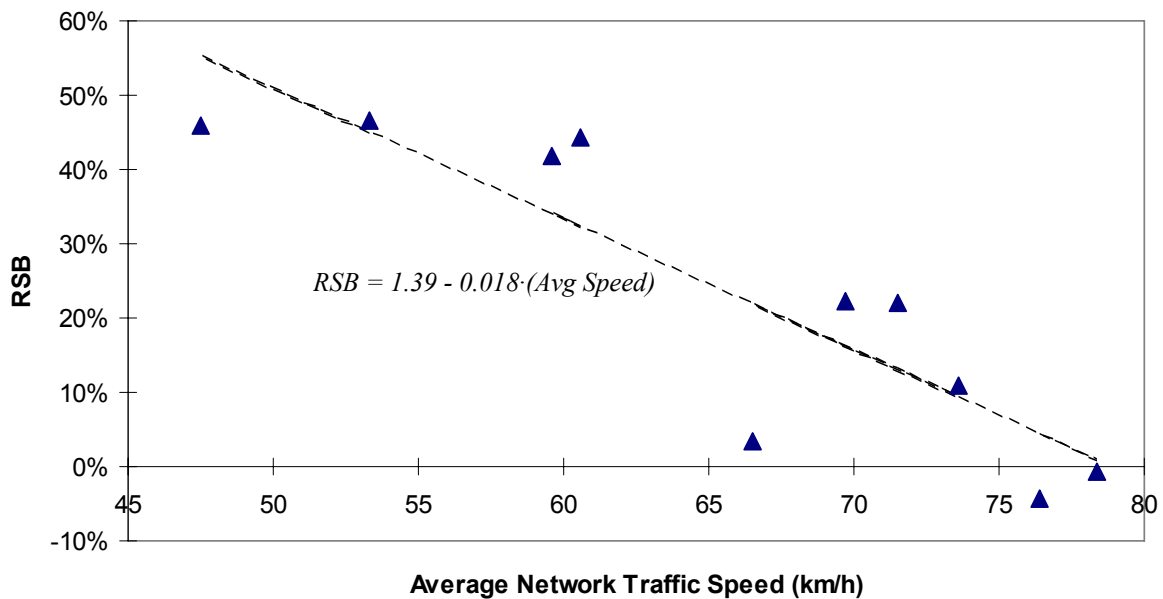


Figure 5-16: Near-Peak Scenario - Linear Correlation of VSLS safety impact to traffic congestion

5.2.3 VSLS Travel Efficiency Impact

The level of volume in the near-peak scenario is high enough to create congestion that triggers VSLS, but not enough to always create a severe shockwave that penetrates the entire network. Figure 5-15 indicates that for at least one simulation run, freeways speeds were substantially lower in the VSLS case than without VSLS. Just as the safety impact results showed considered variability, so do the results for travel times (Table 5-10). From the paired t-test the results are significant at the 95% level of confidence. The overall outcome is an increase

to the average network travel time from 6.1 min/veh to 7.6 min/veh, a relative increase of 23%.

Table 5-10: Near-Peak Scenario – Summary of average system travel time impact (min/veh)

	Simulation Run										Average
	1	2	3	4	5	6	7	8	9	10	
Non-VSLS	5.9	6.6	7.4	5.0	5.5	6.5	5.1	5.7	5.3	8.3	6.1
VSLS	9.0	7.1	7.6	7.5	6.4	7.1	7.9	8.1	7.1	7.9	7.6
Change (min)	+3.1	+0.5	+0.1	+2.5	+0.9	+0.6	+2.8	+2.4	+1.8	-0.4	+1.5
% Change	+52%	+8%	+2%	+49%	+17%	+9%	+54%	+43%	+34%	-5%	+23%

It is suspected that most of this delay occurs on the upstream portion of the network where the speed limit is reduced even though no evidence of significant congestion exists. These results are somewhat troubling as they imply that the use of VSLS (at least with the specified control algorithm) can create sustained congestion when no sustained congestion would have occurred if VSLS had not been implemented. An investigation of the data revealed the cause of these results. Early in the simulation, congestion occurs sporadically in very short time periods. In the absence of VSLS control, this congestion clears very quickly. However, when VSLS is implemented, the control algorithm responds to the detected congestion and reduces the speed limit. Due to response zone requirements, the reduced speed limit cascades upstream.

One positive result from the travel time analysis is that the standard deviation among VSLS average travel times is lower than non-VSLS times. It is reduced from 63 seconds to 42 seconds, meaning that though the VSLS travel times are higher, they are more predictable.

It is interesting to note that Runs 3 and 10, which experienced the smallest increase in travel time, experienced the highest positive network safety benefits (Figure 5-17). On the other hand, Runs 4 and 7, which experienced poor travel time results, experienced the most negative safety impact. Looking at the freeway speed mapping for the non-VSLS cases of Run 10 (Figure 5-18) and Run 7 (Figure 5-19) provides some insight on the respective positive and negative VSLS impacts. First, Run 10 clearly experiences more congestion than Run 7. As a result, the non-VSLS freeway speeds would naturally be forced down by congestion, reducing the travel time impact of VSLS decrements. Secondly, although mostly uncongested, Run 7 does exhibit frequent pockets of minimal congestion. These pockets

would trigger VSLS decrements causing undue turbulence and delay for drivers. Thirdly, the shockwave extent in Run 7 only reaches upstream as far as Station 100, but a VSLS at this point could trigger a response zone as far back as Station 70. This is likely the most prominent cause of negative travel time impact. This evidence, compounded by the peak scenario investigation, suggests that the specified VSLS control algorithm provides more positive safety and travel time impacts for heavily congested periods than moderately congested periods.

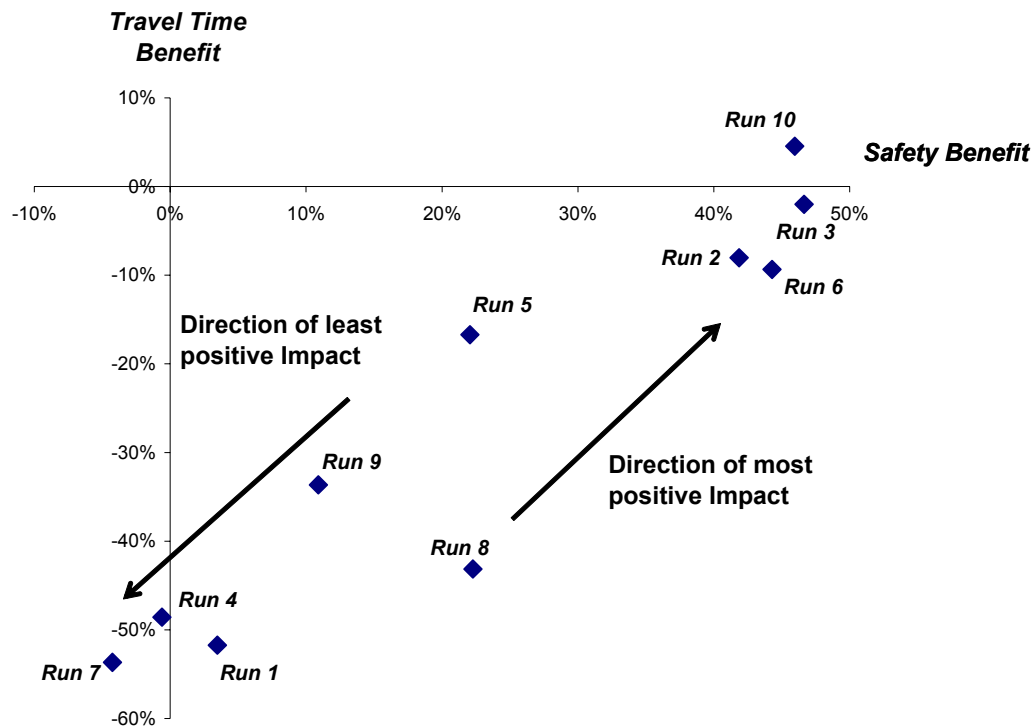


Figure 5-17: Near-Peak Scenario – Variability in VSLS impact by simulation run

For the near-peak scenario, the traffic conditions vary from run-to-run, as do the resulting VSLS impact for both safety and travel efficiency. If this result holds true for the field application of a full-time VSLS system, the day-to-day variation in traffic conditions and corresponding VSLS performance would be undesirable. These results suggest that the specified VSLS control algorithm may not be sufficiently robust to appropriately respond to a wide range of traffic conditions.

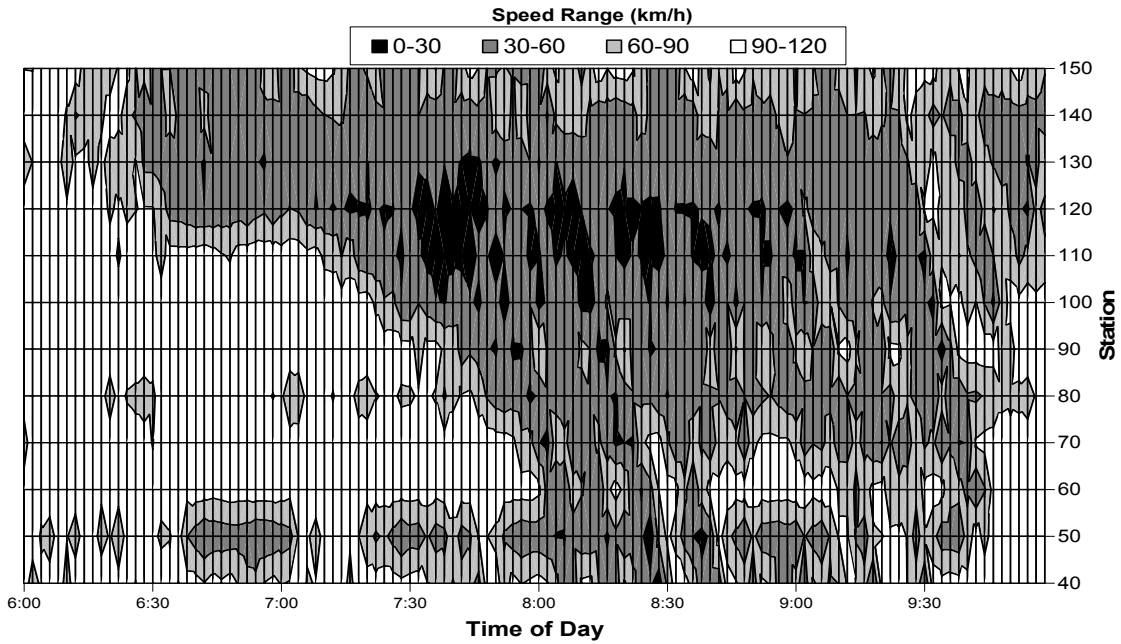


Figure 5-18: Near-Peak Scenario – Contour mapping of freeway speeds, Run 10 (non-VSLS)

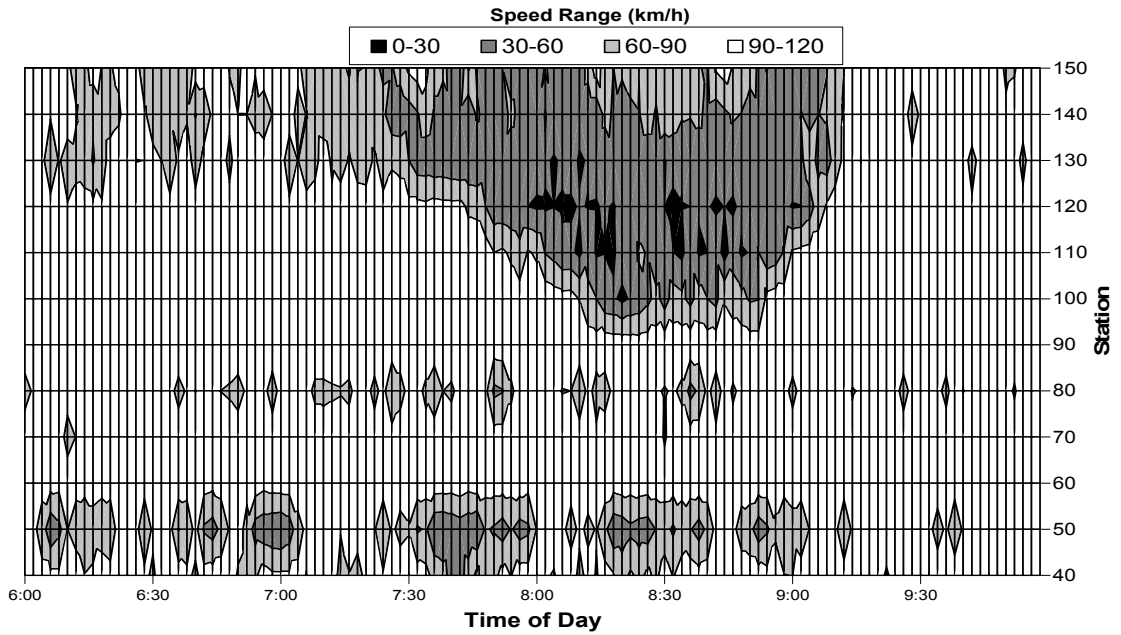


Figure 5-19: Near-Peak Scenario – Contour mapping of freeway speeds, Run 7 (non-VSLS)

5.3 Scenario 3 – Off-Peak Conditions

The off-peak scenario was modelled by reducing the peak volumes to 75% of their original value. The modelled network exhibits mainly free flow speed interrupted by temporary speed reductions. Since a real-life VSL system would be completely autonomous and constantly

online, it is important to measure its impact on traffic conditions even for “low-response” periods. The safety and travel efficiency impacts were measured by the same method outlined for the previous scenarios, and the results are presented below.

5.3.1 VSLs Activity

Upon the introduction of the VSLs system, the resulting VSLs activity was very low. For 80 km/h and 60 km/h displayed speeds, average coverage for the entire network only amounted to 6% and 2% respectively. Since shockwaves did not build during this scenario, the VSLs responded mainly to isolated events featuring momentary drops in freeway speed. Figure 5-20 provides the VSLs mapping for a single simulation run.

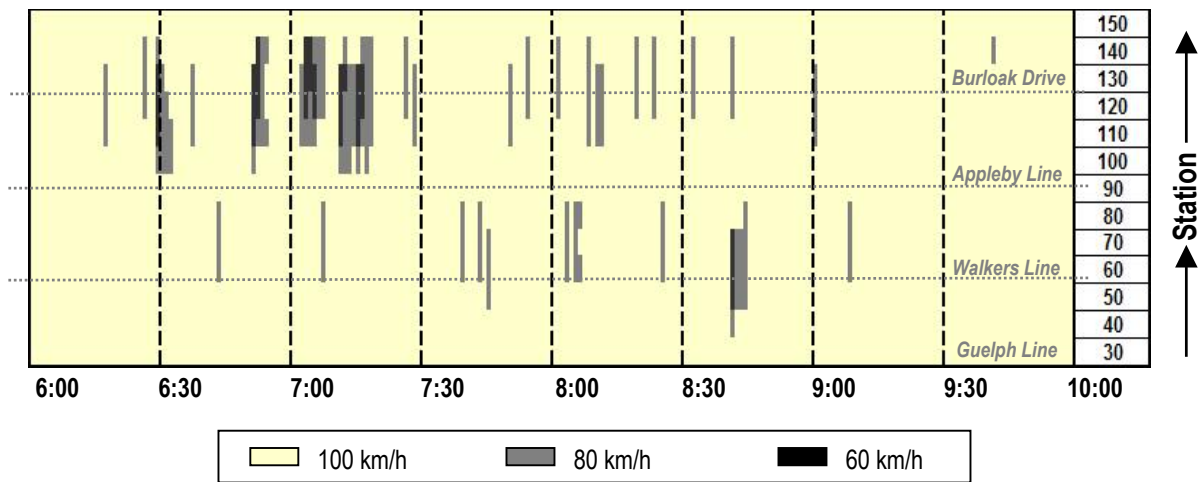


Figure 5-20: Off-Peak Scenario – Mapping of VSLs Displayed Speed Limits

5.3.2 VSLs Safety Impact

The results from the safety impact analysis for off-peak conditions show that an overall negative relative safety benefit (-5%) resulted from the introduction of the VSLs system. For this scenario only half of the stations experienced significant safety results (Table 5-11). Of these stations only Station 120 and 130 experienced a positive safety benefit, while Stations 50, 100, and 110 were negatively impacted. Although these values of relative impact appear somewhat high, note that the original crash potential values are only a small fraction of the crash potential values for the previous scenarios. So, the relative impacts represent only minor changes in absolute crash potential.

Table 5-11: Off-Peak Scenario – Relative Safety Benefit results

Station	Average CP		Change	RSB	Impact	Significant at 95%?
	Non-VSLS	VSLS				
50	0.158	0.171	-0.013	-8%	NEGATIVE	YES
60	0.103	0.100	0.003	3%	POSITIVE	NO
70	0.241	0.244	-0.003	-1%	NEGATIVE	NO
80	0.164	0.166	-0.002	-1%	NEGATIVE	NO
90	0.074	0.076	-0.002	-3%	NEGATIVE	NO
100	0.128	0.191	-0.063	-49%	NEGATIVE	YES
110	0.164	0.204	-0.040	-24%	NEGATIVE	YES
120	0.122	0.105	0.017	14%	POSITIVE	YES
130	0.233	0.204	0.029	13%	POSITIVE	YES
140	0.103	0.105	-0.002	-2%	NEGATIVE	NO
Average	0.149	0.157	-0.008	-5%	NEGATIVE	YES

The safety impact results show very different impacts experienced within the downstream end of the network. After viewing the VSLS activity log, there appears to be a relationship between the location of the VSLS decrements and the spatial variation in safety impacts. On average, conditions for a VSLS decrement were satisfied during 75 time intervals. Of these, 85% occurred between Station 120, 130 and 140, while none occurred between Station 100 and 110. Table 5-12 indicates that the VSLS trigger was almost always located at Station 130 or 140, meaning Stations 100 and 110 were almost always at the upstream end of the response zone (also evident in the VSLS mapping, Figure 5-20). Note as well that for 14% of the time period, the other location of negative impact, Station 50, would have been at the upstream end of the response zone for Station 80.

Table 5-12: Off-Peak Scenario - Proportion of Network Trigger Conditions by Station

Station	% of Total Network Trigger Conditions
70	1%
80	14%
90	0%
100	0%
110	0%
120	6%
130	37%
140	42%

The majority of the crash potential impact was due to changes in the precursor, Q . Recall that Q measures the difference in 20-second average speed between stations. A

difference < -9 km/h is considered Level 1 and is associated with vehicles accelerating as they move downstream. Level 2 is a difference between -9 km/h and 0 . Level 3 is a difference between 0 and $+9$ km/h and Level 4 is a difference $> +9$ km/h. Levels 3 and 4 are associated with conditions for which vehicles must decelerate as they travel downstream. The majority of the safety impacts for this scenario arise due to changes in the value of Q between levels 3 and 4. Figure 5-21, Figure 5-22, and Figure 5-23 show the changes in the Q distribution at different stations for Simulation Run 2. Stations 100 and 110 each experience a significant increase in Level 4, or “high-level”, Q (implying an increase in crash risk), while Station 120 experiences a decrease (implying a decrease in crash risk). These results suggest that a VSL speed reduction in a response zone may provide the most benefit for the location triggering the response but the least benefit to the locations immediately upstream of trigger station.

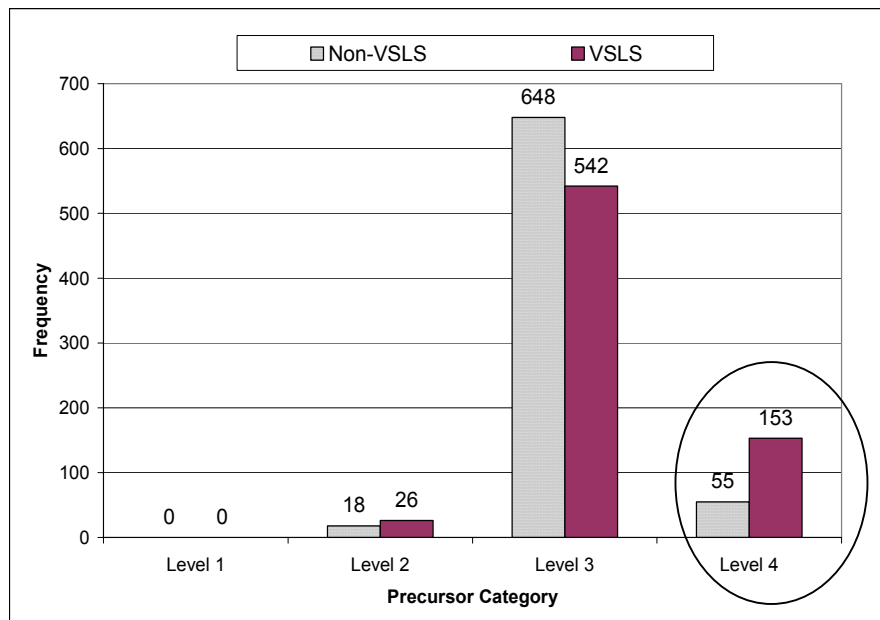


Figure 5-21: Off-Peak Scenario – Distribution shift for Precursor Q, Station 100

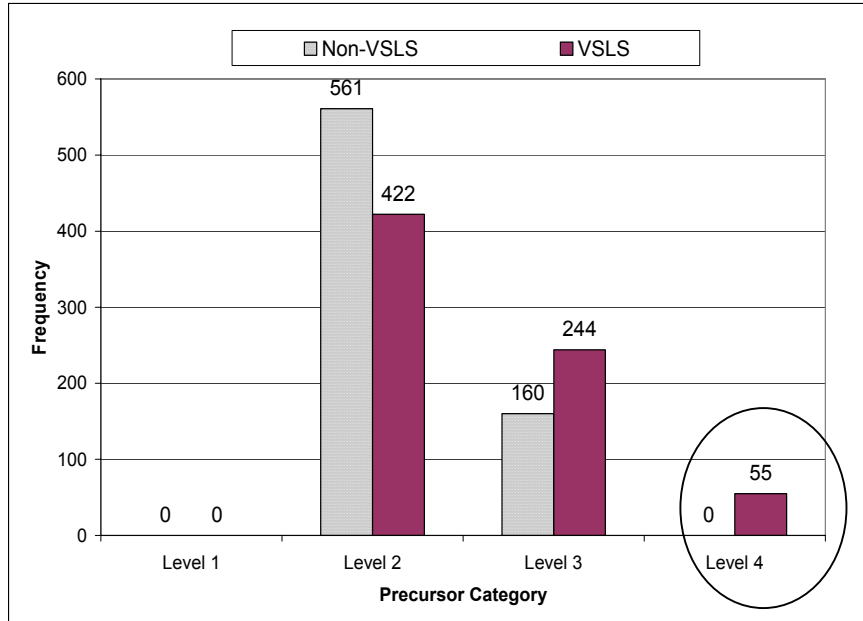


Figure 5-22: Off-Peak Scenario – Distribution shift for precursor Q, Station 110

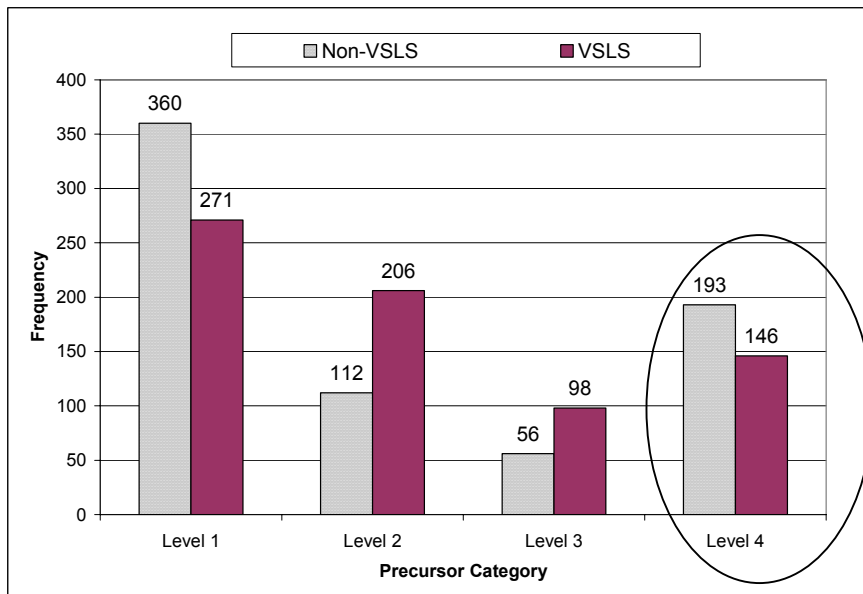


Figure 5-23: Off-Peak Scenario – Distribution shift for precursor Q, Station 120

5.3.3 VLS Travel Efficiency Impact

For the off-peak conditions, travel efficiency experiences very little impact. Although an increase in travel time was found for the VLS case to be significant at the 95% level, the average network travel time impact (Table 5-13) was only 3 second/vehicle (1.25%). If this level of impact can be considered negligible, the VLS system had no impact on travel times during the off-peak scenario.

Table 5-13: Off-Peak Scenario – Summary of average system travel time impact (min/veh)

	Simulation Run										Average
	1	2	3	4	5	6	7	8	9	10	
Non-VSLS	3.97	4.00	4.00	3.98	3.98	3.98	3.97	4.00	3.98	3.98	3.985
VSLS	4.03	4.04	4.04	4.01	4.03	4.05	4.02	4.07	4.07	4.02	4.040
Change	<i>0.06</i>	<i>0.04</i>	<i>0.05</i>	<i>0.03</i>	<i>0.05</i>	<i>0.07</i>	<i>0.05</i>	<i>0.07</i>	<i>0.08</i>	<i>0.04</i>	0.055
% Increase	1%	1%	1%	1%	1%	2%	1%	2%	2%	1%	1%

5.4 Summary of Chapter

The VSLS impact analyses were performed on three traffic scenarios of varying levels of congestion – peak, near-peak, and off-peak. VSLS impacts were quantified in terms of the relative changes in safety (crash potential) and vehicle travel times before and after the implementation of the VSLS control strategy. The most desirable outcomes for the VSLS impact would be a large positive relative safety benefit associated with a decrease in travel time. Table 5-14 summarizes the overall average safety and travel time impacts for each scenario, including the average percent time each speed limit was displayed during the simulation period.

Table 5-14: Summary of VSLS impacts

Impact measure		Scenario		
		Peak	Near-Peak	Off-Peak
% Time Speed limit was displayed	100 km/h	5	15	92
	80 km/h	7	17	6
	60 km/h	88	68	2
Relative Safety Benefit		+39%	+27%	-5%
Change in Travel Time		+11% (1.4 min)	+23% (1.5 min)	+1.3% (0.05 min)

The most desirable results (both positive safety and positive travel time impacts) were usually observed for moderately congested scenarios during which the VSLS response exhibited frequent speed limit decrements and frequency recoveries. The least desirable results were usually observed under conditions which caused prolonged speed limit reductions and thus lower freeway speeds than would have been observed without VSLS. This suggests that the tested VSLS control algorithm was able to provide large safety benefits with no significant travel time penalty, but only for a limited range of traffic conditions. It is suspected that by modifying the parameters within the current algorithm (e.g. occupancy threshold,

volume threshold, response zone requirements, etc.), the VSLS may be able to operate effectively over a wider range of traffic conditions and provide more consistent safety and travel time benefits. The next chapter introduces a number of modifications made to the VSLS control algorithm and the general changes in safety and travel time impacts associated with each modification.

6. VSLS CONTROL ALGORITHM SENSITIVITY ANALYSIS

The variable speed limit control algorithm presented and evaluated in the previous chapter was developed only as a preliminary design for practical application, and no attempt has been made to optimize the algorithm parameter values. Rather, the parameter values were selected on the basis of engineering judgment as described in Section 4.5.2. Consequently, it was unknown prior to analysis whether these were the parameter values that would produce the most favourable results. The results of the analysis revealed that the original algorithm does have the potential to operate favourably during some conditions, but produces inconsistent and undesirable results during the near-peak and off-peak scenarios. It was suspected that changes to the original algorithm could result in improvements to the overall VSLS impact results. Therefore, the last stage of this study was to perform a preliminary sensitivity analysis on modifications to the parameter values within the algorithm. The objective of this analysis was not to identify an optimal algorithm but to identify any patterns in the changes to safety and travel times impacts following different modifications to the parameter values. It was found that by making logical modifications to the parameter values, improvements in the VSLS impacts were possible. This chapter presents the modifications made to the parameters values and the resulting VSLS impacts, including a brief discussion for each modification.

6.1 Modifications of Parameter Values

The sensitivity analysis investigated the resulting impacts of modifications to the following parameter values:

- Occupancy threshold for triggering a speed limit reduction;
- Occupancy threshold for allowing reduced speeds limits to increase;
- Volume threshold for triggering a speed limit reduction; and
- Number of VSLS included in response to a speed limit reduction.

Five modifications were tested, each varying one or more of the above parameter values (Table 6-1) to analyse the sensitivity to both individual and combined modifications. Cells that are shaded indicate the parameter that was modified.

Table 6-1: Modifications of Parameter Values for Sensitivity Analysis

Case	Speed Limit Reduction			Speed Limit Increase
	Occupancy Threshold	Volume Threshold	# of Responding VLS*	Occupancy Threshold
Original	15%	1600	80-60-60-60; 80-80-80	15%
Modification 1	20%	1600	80-60-60-60; 80-80-80	20%
Modification 2	20%	1600	80-60-60-60; 80-80-80	15%
Modification 3	15%	1800	80-60-60-60; 80-80-80	15%
Modification 4	15%	1600	80-60; 80-80	15%
Modification 5	20%	1800	80-60; 80-80	15%

*First row in cell indicates the VLS response to a speed limit reduction from 100 km/h to 60 km/h speed limit reduction, whereas the second row indicates the VLS response to a speed limit reduction from 100 km/h to 80 km/h. Signs are listed in sequence from upstream to downstream.

For each of the modifications listed in Table 6-1, ten simulations were performed using the same simulation volumes and seeding values as the original analysis. The overall results for VLS activity, safety and travel time impacts for each modification were compiled in the same manner as the original analysis and are presented in Table 6-2 and Table 6-3. More detailed results and discussions on each modification are provided in the following sections.

Table 6-2: VLS activity resulting from parameter modifications

Case	Proportion of Time Speed Limit is Displayed								
	Peak			Near Peak			Off Peak		
	100 km/h	80 km/h	60 km/h	100 km/h	80 km/h	60 km/h	100 km/h	80 km/h	60 km/h
Original	5%	7%	88%	15%	17%	68%	92%	6%	2%
Modification 1	4%	15%	81%	17%	21%	62%	95%	4%	1%
Modification 2	7%	10%	83%	23%	23%	54%	95%	4%	1%
Modification 3	5%	9%	86%	19%	18%	63%	94%	5%	1%
Modification 4	15%	16%	69%	45%	20%	35%	95%	4%	1%
Modification 5	21%	16%	63%	52%	16%	32%	98%	2%	0%

Table 6-3: Overall network safety and travel time impacts resulting from parameter modifications

Case	Relative Safety Impact			Relative Travel Time Impact		
	Peak	Near-Peak	Off-peak	Peak	Near-Peak	Off-peak
Original	39%	27%	-5%	11%	23%	1%
Modification 1	35%	6%	-4%	9%	25%	1%
Modification 2	41%	20%	-6%	5%	15%	1%
Modification 3	41%	23%	-4%	4%	22%	1%
Modification 4	31%	7%	-4%	6%	23%	1%
Modification 5	39%	19%	-1%	1%	13%	0%

*Positive travel time impacts indicate an increase in travel time per vehicle.

6.1.1 Modification 1

Modification 1 relaxed the occupancy threshold values for triggering a speed limit reduction and for permitting reduced speed limits to increase. The threshold values for both of these parameters were increased from 15% to 20%. The objectives of these modifications were to:

- raise the minimum level of congestion to which VSLs respond, thus reducing the overall degree of VSL response; and
- allow reduced speed limits to increment at a higher level of congestion for a more rapid speed limit rebound.

It was suspected that a reduced VSL response combined with a more rapid rebound would reduce the overall impact on travel times; however, the simulation and analysis results indicate that this was not achieved. Although the percent time that the 60 km/h speed limit was displayed reduced slightly for all three scenarios, the travel times for the peak scenario only slightly decreased and the travel times for the near-peak scenario actually increased. Also, these impacts were associated with a reduction in safety improvements for both the peak and near-peak scenarios.

To investigate these impacts in more detail, traffic data were examined for the near-peak scenario. Inspection of the traffic conditions resulting from both the original algorithm and from Modification 1 revealed that, on average, traffic was more congested upon implementing the modifications. Figure 6-1 shows the average proportions of 20-second station occupancy occurring during the simulation period. Note that the proportion of occupancy values less than 20% decreases after the modification whereas the proportion of occupancy values greater than 20% increases.

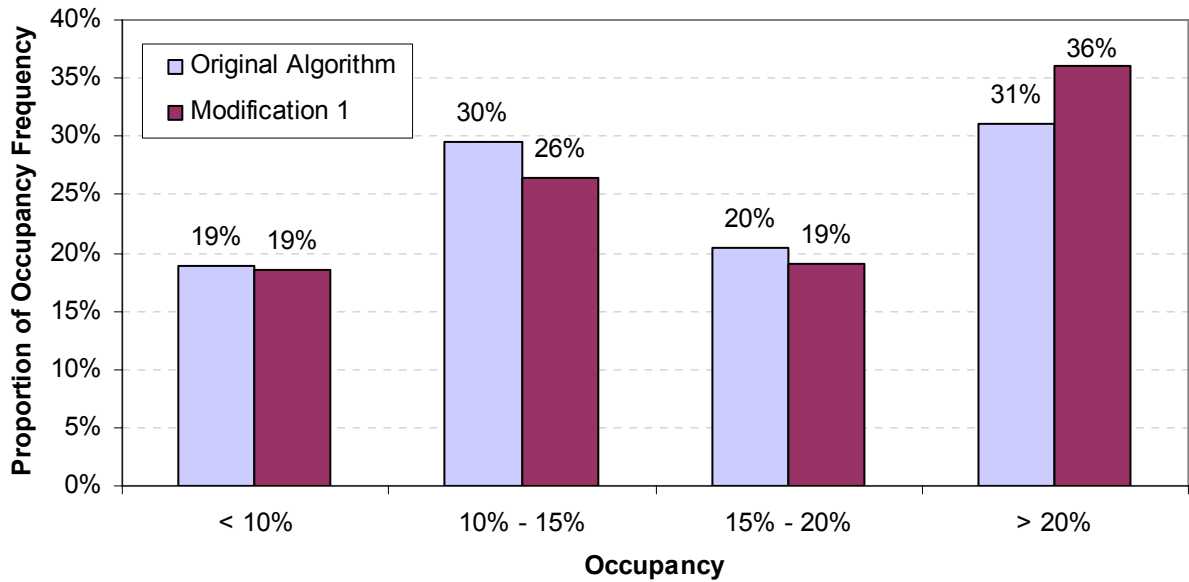


Figure 6-1: Modification 1, Near-Peak Scenario – Average proportions of occupancy levels

Upon observing this increased congestion, the proportions of conditions triggering VSLs responses were also investigated for both control cases. Recall from Figure 4-11 that the four conditions that prompt a speed limit reduction are:

- Condition 2b → [volume < 1600 vphpl; occupancy > 15%⁸; 60 < average speed < 80];
- Condition 2c → [volume < 1600 vphpl; occupancy > 15%; average speed ≤ 60];
- Condition 3b → [volume > 1600 vphpl; any occupancy; 60 < average speed < 80]; and
- Condition 3c → [volume > 1600 vphpl; any occupancy; average speed ≤ 60].

The average frequency of trigger conditions over the simulation runs are shown in Figure 6-2. Conditions 2b and 3b, which trigger an 80 km/h speed limit, were reduced using this modification. In fact, nearly none of the 80 km/h speed limit responses were triggered by occupancy values greater than 20% (i.e. trigger condition 2b). This makes sense, considering that for higher densities (occupancies), traffic speed is likely to decrease below 60 km/h. Note also that the frequencies of trigger conditions 2c and 3c (both triggering a 60 km/h speed limit) increase after the parameter modifications. This agrees with the results of increased congestion as shown in Figure 6-2.

⁸ For Modification 1, Conditions 2b and 2c require an occupancy > 20%.

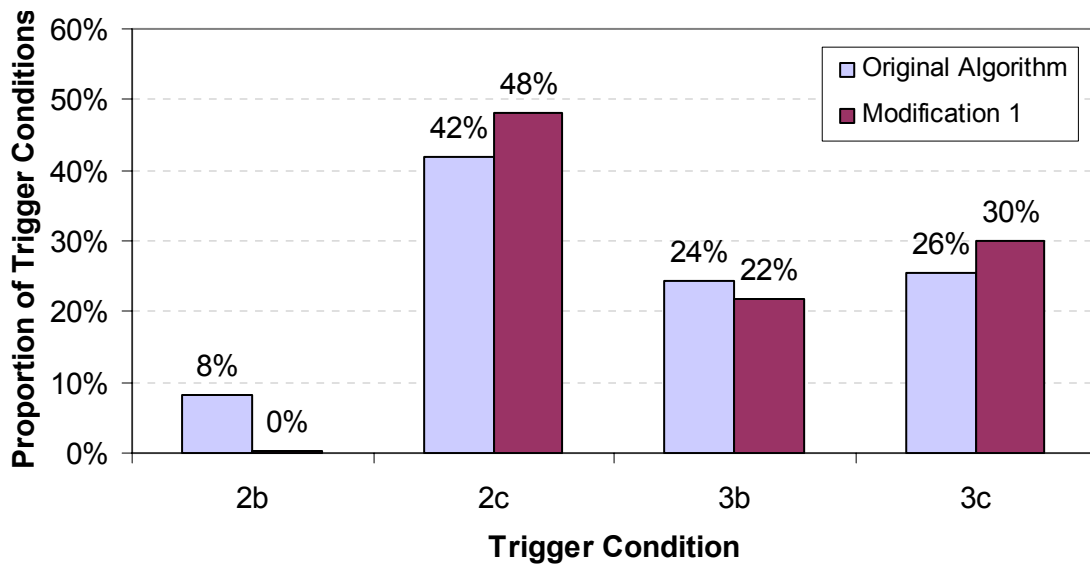


Figure 6-2: Modification 1, Near-Peak Scenario – Average proportions of trigger conditions

It is interesting to compare results in Figure 6-2 with the percent time the reduced speed limits are displayed (Table 6-2). Table 6-2 shows that the percent time the 80 km/h speed limit is displayed increases after the modifications, even though it is triggered less frequently. Conversely, the percent time that the 60 km/h speed limit is displayed decreases, while it is triggered more frequently. These comparisons suggest that, although triggered more frequently after the modifications, the 60 km/h speed limit is not being displayed for as many consecutive intervals as in the original case. Instead, the relaxed occupancy threshold results in more speed limit increases back to 80 km/h. The higher frequency of speed increments combined with the higher frequency of 60 km/h speed limit responses indicates more fluctuation in the variable speed limit displays. It is suspected this is the cause of the increased congestion (Figure 6-1) and consequently an increase in overall traffic turbulence and a reduction in safety. The safety impact results for the near-peak scenario indicate that the average crash potential increases for all stations. Examination of the crash precursor distributions for the stations experiencing the largest increase in crash potential (Stations 90 and 100) reveals that the frequencies of high level *CVS*, *Q*, and *COVV* increase upon the implementation of these modifications.

The resulting impacts of Modification 1 were less desirable than those for the original algorithm. Examination of the data revealed that permitting reduced speed limits to increment upon occupancies of 20% is suspected to increase speed limit fluctuations and increased

turbulence. A premature increase in reduced speed limits may be causing vehicles to increase their speeds only to encounter more congestion downstream. To confirm the impact of this modification, the threshold for incrementing speed limits was returned to 15% in Modification 2, while the occupancy threshold for triggering a speed limit reduction remained at 20%.

6.1.2 Modification 2

Due to the results of Modification 1, the occupancy threshold for incrementing speed limits was returned to 15%, but the occupancy threshold for triggering a speed limit reduction remained at 20%. The results of this modification agreed with the expected objectives much more than the results for Modification 1. The relaxed occupancy threshold reduced the VSLs activity and significant improvements resulted in the travel time impact for both the peak and near-peak scenarios. This was achieved without a significant adverse impact on safety. Although the near-peak safety benefit was reduced, the net result remained positive. Examination of the traffic data and trigger conditions also provide more positive results than those for Modification 1. As shown in Figure 6-3 and Figure 6-4 for the peak and near-peak scenarios, respectively, the frequencies of heavy congestion (occupancy > 20%) were reduced slightly in each scenario after implementing Modification 2.

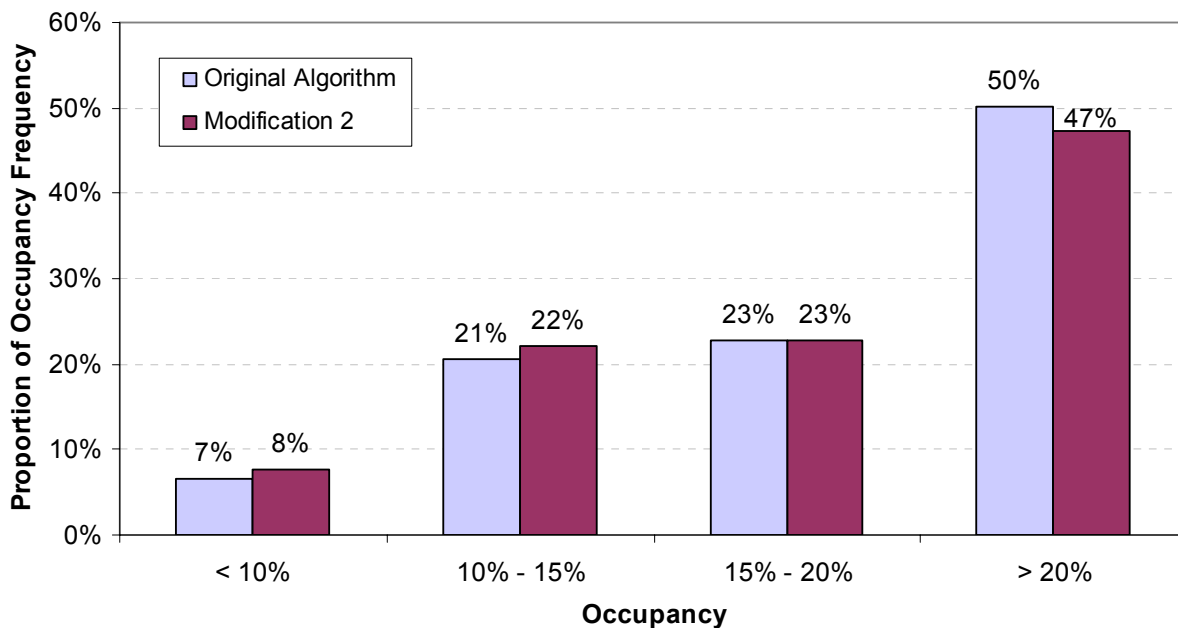


Figure 6-3: Modification 2, Peak Scenario – Comparison of percent time congested

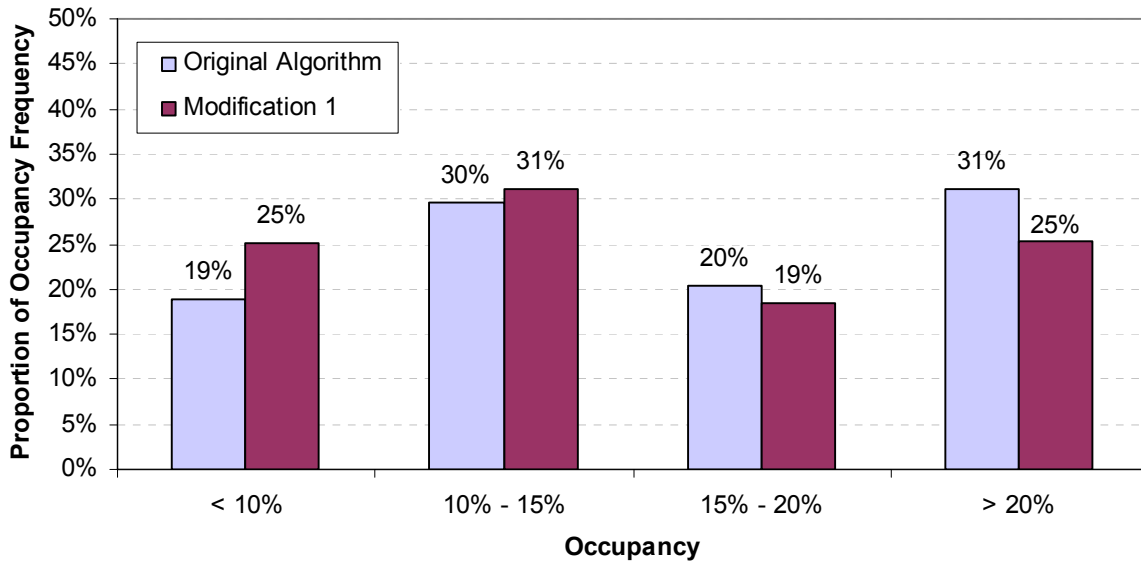


Figure 6-4: Modification 2, Near-Peak Scenario – Comparison of percent time congested

It appears that for the near-peak scenario, a trade-off exists between the impacts of safety and travel time. While reducing the VSLs activity results in a smaller increase in travel time, it is suspected that this decrease in activity is associated with a decrease in the safety benefit. For example, Station 90 experienced the largest negative impact to safety as a result of Modification 2. Investigation of the VSLs activity logs shows that Station 90 also experienced the largest reduction in the percent time the 60 km/h speed limit is displayed – from 43% in the original case to 20% in this modification case.

Overall, Modification 2 produced very positive results. In comparison to the original algorithm, by relaxing the occupancy threshold for speed limit reductions from 15% to 20%, variable speed limit signs responded less frequently, congestion was slightly reduced and substantial reductions in the impacts to travel time were achieved without significant impacts to the safety benefit. These results indicate the poor results from Modification 1 were caused by the increase to the occupancy threshold for a speed limit increment. Therefore it is recommended that 15% is an appropriate threshold for allowing reduced speed limits to increment.

6.1.3 Modification 3

Modification 3 tested the sensitivity of the VSLS impact to relaxing the volume threshold for triggering a speed limit reduction (the thresholds for occupancy were returned to their initial values). The threshold value for volume was increased from 1600 to 1800 vphpl. Recall that the original threshold of 1600 vphpl was selected because it represented a level of service C as stated in the Highway Capacity Manual (HCM, 2000). However, traffic volumes during the peak and near-peak frequently exceed this volume, and therefore a higher threshold may be appropriate. As such, the objective of this modification was similar to that of Modifications 1 and 2 – to reduce the level of responsiveness of the VSLS, particularly for the near-peak scenario, thus reducing the degree of travel time impact.

The results in Table 6-2 and Table 6-3 indicate very little change in any measure between the original case and this modification. The lack of change was found to be a result of the structure of the control algorithm. Although the frequencies of trigger conditions 3b and 3c (when volume threshold is exceeded) were significantly reduced (as much as 50% for the near-peak scenario) the frequencies of trigger conditions 2b and 2c increased. This suggests that traffic volumes between 1600 and 1800 vphpl are associated with occupancies greater than 15% and triggered an occupancy-related response, whereas previously these conditions triggered a volume-related VSLS response. In other words, the VSLS response for this modification is quite similar to that for the original algorithm. Examination of the loop detector data revealed that the majority of these “new” occupancy-related responses could be eliminated if the higher volume threshold is combined with a higher occupancy threshold.

6.1.4 Modification 4

For this modification, both the occupancy and volume threshold values were left unchanged from the original algorithm, but the number of signs responding to a trigger condition was reduced. The response zones for the original algorithm included up to three variable speed limit signs, which may be excessive. Such a long response zone may reduce traffic speeds as far as 2 km upstream from local congestion when it may not be necessary to do so. It was found that under the original algorithm, in the peak and near-peak scenarios, the response zone requirements contributed to VSLS speed reductions cascading upstream. Therefore, the

objective of this modification was to test the resulting impacts to safety and travel times upon shortening the VSLS response zones as follows:

- For a condition triggering a 60 km/h speed limit reduction, only two signs respond – one displaying 60 km/h and the next upstream sign displaying 80 km/h; and
- For a condition triggering an 80 km/h speed limit reduction, two signs respond, both displaying 80 km/h.

This modification resulted in a modest reduction in travel time impact for the peak scenario, but had no positive impact on the travel time for the near-peak scenario. This is somewhat surprising considering the significant reduction in VSLS activity and it is unclear as to why the travel time impact was not reduced. Examination of the traffic conditions for the near peak scenario with and without VSLS revealed that the level of congestion in the network remained largely unchanged. It is possible the limiting factors for traffic throughput were the trigger zones, which responded to the same conditions in this modification as in the original algorithm.

6.1.5 Modification 5

The final modification was a combination of Modifications 2, 3, and 4. The objective of this modification was to reduce the VSLS response through relaxing both the volume and occupancy thresholds and to reduce the number of responding signs to limit the impact on traffic upstream of congestion. The impact results of this modification exhibited the most improvement from the original results. For the peak scenario, the travel time impact was nearly erased without impacting the net decrease in crash potential of 39%. The near peak scenario also experienced positive results, with a reduction in travel time penalty from 23% to 13%, while maintaining a 19% relative safety benefit. Furthermore, the negative safety impact for the off-peak scenario was improved from a 5% increase in crash potential to a 1% increase in crash potential. This improvement was primarily due to the limited response of the VSLS during the off-peak period under the modified algorithm. The results of the VSLS impact analysis for the peak and near-peak scenarios under this algorithm are presented in more detail in the following sections.

6.1.5.1 Peak Scenario

The modified algorithm was successful in achieving a strong relative safety benefit while not contributing to an increase in the average travel time per vehicle. The average coverage of the VLS displayed speed limits reduced significantly from the original case. Figure 6-5 shows the mapping of VLS activity during a simulation run under the modified algorithm.

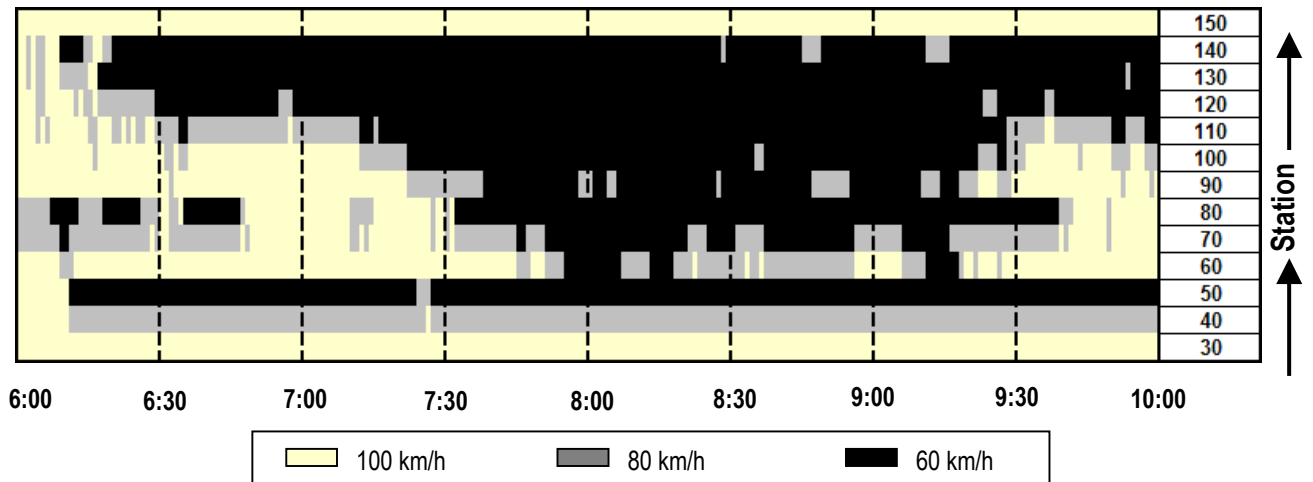


Figure 6-5: Modification 5, Peak Scenario – Mapping of VLS displayed speed limits

With the exception of Stations 40 and 50, the response of the VLS resembles the shape of the shockwave for non-VLS conditions as evident in the contour mapping of non-VLS freeway speeds (Figure 4-8). Therefore the response seems to match the existing conditions much more closely than the original algorithm. Also, the average traffic speed over the simulation period was 29.6 km/h for this modified algorithm, whereas the average traffic speed under the original algorithm was 26.6 km/h. Also, the cascading effect noted in the original analysis is not as evident for this modified algorithm. This combined with the reduction in VLS response may account for the majority of the travel time improvement.

Little change in crash potential was measured following the introduction of the modification. The average network relative safety benefit remained unchanged at 39% while the relative safety benefits for each station also showed little change (Figure 6-6). This indicates that the degree of VLS response under the original algorithm may be unnecessary for achieving significant safety benefits.

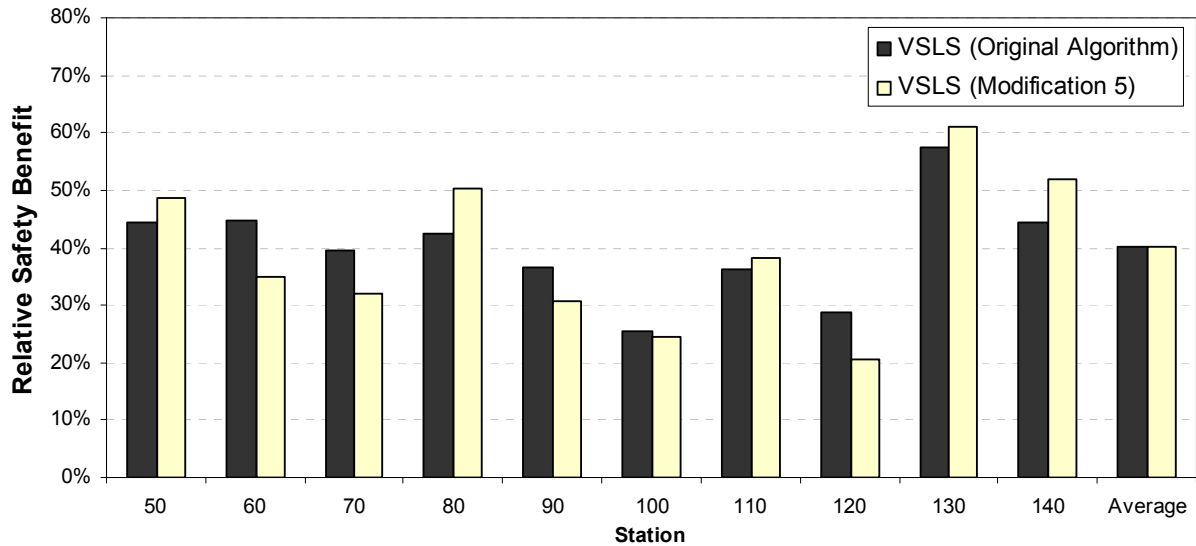


Figure 6-6: Modification 5, Peak Scenario – Station Relative Safety Benefits for the Original and Modified Algorithms

6.1.5.2 Near-Peak Scenario

The modified algorithm was successful in reducing the travel time impact for the near-peak scenario while maintaining a strong safety benefit. The VLS activity in Figure 6-7 shows a much more dynamic response to concentrated areas of congestion than the activity in the original case (Figure 5-12). The consistent VLS response at the upstream end of the network supports the concern raised in Section 5.2.2 that an abnormal degree of turbulence occurs in the vicinity of Station 40. Therefore the response at Station 40 and 50 should be disregarded.

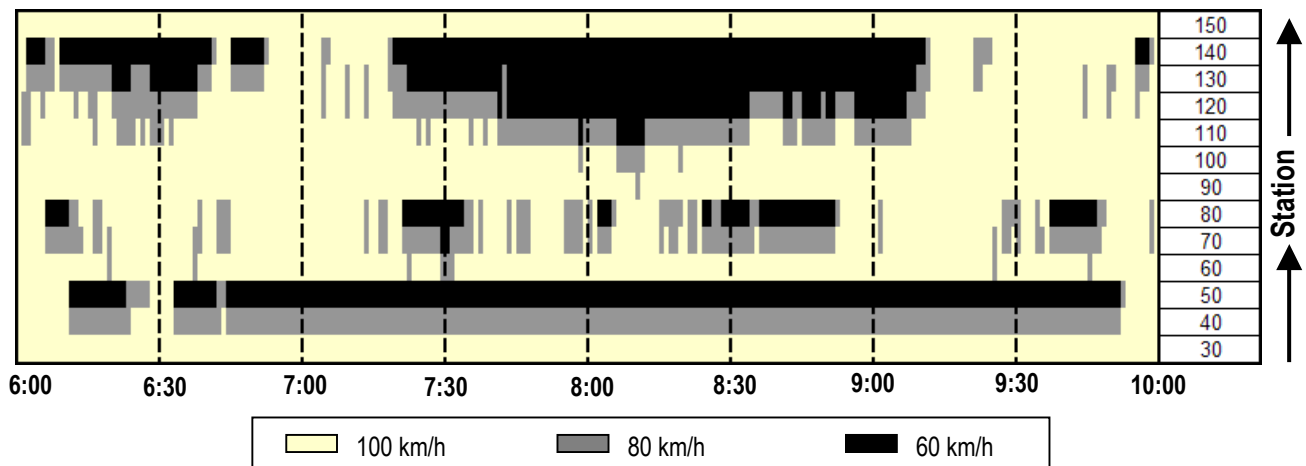


Figure 6-7: Modification 5, Near-Peak Scenario – Mapping of VLS displayed speed limits

In addition to the reduced VSLS response, the average network traffic speed increased from 52.5 km/h to 56.0 km/h, and the overall network congestion was also reduced between the original and modified algorithms (Figure 6-8). These factors contributed to the overall improvement in travel time.



Figure 6-8: Modification 5, Near Peak Scenario – Comparison of percent time congested

It is unclear without further analysis whether the reduction in safety benefit is due to the nature of the new structure of the modified algorithm or whether the reduction in safety benefit is simply a result of less VSLS response. The evidence presented in Section 6.1.2 suggests that such a reduction in VSLS activity is likely to influence the degree of safety impact.

Examination of the safety results revealed that a strong linear relationship ($R^2 = 0.82$) still existed between the congestion present in the non-VSLS case and resulting safety impact from VSLS implementation (Figure 6-9). As evident for the original algorithm, the regression equation, constant, and slope are all significant at the 95% level of confidence.

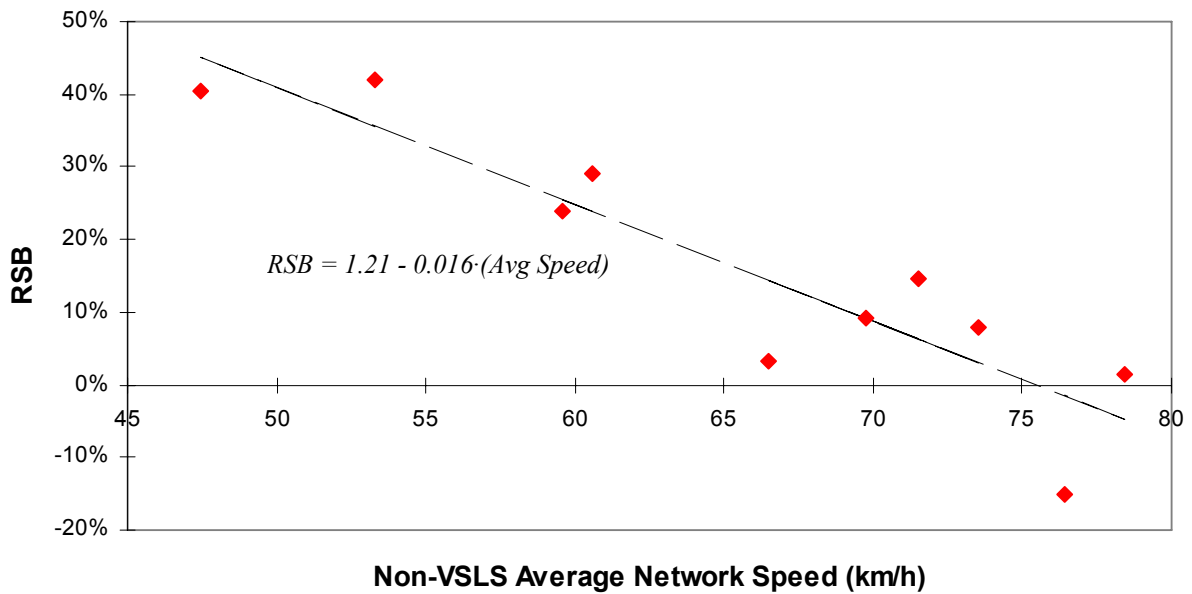


Figure 6-9: Modification 5, Near-Peak Scenario –Correlation of VLS safety impact to traffic congestion

As before, higher safety benefits resulted for simulation runs producing more congested conditions. Note also that the intercepts and slopes in both this regression equation and the equation derived for the original algorithm are quite similar. Further analysis may find that this relationship is general trend among various VLS control strategies.

6.2 Summary of Chapter

This chapter explored the sensitivity of VLS impacts to modifications of the control algorithm parameters. Five modifications were analysed, altering the threshold values for occupancy and volume and the number of VLS included in the response of a speed limit reduction. Of the five modifications, only one produced positive results for all three traffic scenarios. This modification increased the occupancy threshold to 20%, increased the volume threshold to 1800 vphpl, and reduced the response zone requirements from three signs to one sign. The primary benefits from this modification were a reduction in the travel time penalty for each scenario without an adverse impact to the net safety impacts.

This sensitivity analysis provided evidence that significant improvements in VLS performance are possible by modifying the parameters within the control strategy. This analysis was only a preliminary investigation, but it offered encouraging results and some

initial insight into the relationship between the choice of control strategy parameter values and the resulting impacts.

7. CONCLUSIONS AND RECOMMENDATIONS

7.1 Conclusions

The primary objective of this thesis was to provide a framework for evaluating candidate VSL control strategies on an actual freeway segment in Canada, using a microsimulation model combined with a categorical crash model. The study estimated the relative safety and traffic performance impacts of implementing VSL control on three scenarios of traffic congestion on a modelled segment of the Queen Elizabeth Way (QEW) freeway near Toronto, Canada. The major findings of this study are presented in the following sections.

7.1.1 Validation of Crash Potential Model

The safety impacts in this study were quantified using a categorical crash potential model developed by Lee et al. (2003). Their crash model was calibrated from crash data on the Gardiner Expressway in Toronto and it was uncertain if their model structure and calibration parameters were transferable to another freeway section. Therefore, the first stage of this study was to calibrate the crash model from crash data on the study segment of the QEW. A model was successfully fit with statistical significance using log-linear regression; however, the number of statistically significant models from which to select the best model was much more limited than in Lee et al. It was found that the disparity between “pre-crash” conditions and non-crash conditions was not as prominent for the QEW segment as the segment of the Gardiner Expressway. The cause of this difference is unclear. The difference could be an indication that the traffic conditions on the Gardiner Expressway exhibit much less turbulence than those on the QEW or that many more “near misses” occur on the QEW. One other explanation could be that the 12 days of non-crash data collected on the QEW provided a more robust cross section of data than the data from two summer weekdays used by Lee et al. to calibrate their model on the Gardiner Expressway. Regardless, the difference in non-crash precursor distributions and the resulting difference in crash model parameters raise concerns about the reliability in transferring a single calibrated crash potential model from one highway section to another. Other findings from the calibration of the crash potential model are as follows:

- Using an individual categorization structure for each crash precursor was more successful in producing a statistically significant model fit than applying the same structure to all precursors. For example, combining 4 categories of *Q*, 4 categories of *CVS*, and 3 categories of *COVV* was more successful than applying 3 categories to all three precursors.
- The results of the log-linear analysis agree with the trends identified by Lee et al., such as:
 - High level precursors contribute more to crash potential than low level precursors (i.e. higher turbulence is more likely to lead to a crash situation than low turbulence);
 - Merging and diverging road geometry contributes more to crash potential than straight sections;
 - Peak period conditions contribute more to crash potential than off-peak period conditions; and
 - Crash frequency increases as exposure increases.

7.1.2 Framework for Quantifying VSLs Impacts

The analysis framework developed in this study proved to be a useful, robust, and objective tool for evaluating the safety and traffic performance impacts of various VSLs strategies. The evaluation methodology required several major tasks, each of which produced interesting findings.

First, a microsimulation model representing a segment of the QEW was successfully calibrated using 10 days of morning peak traffic data; however, the values of crash precursors calculated from simulated conditions required adjusting to resemble those from field conditions. It was found that the simulated conditions exhibited much more turbulence than the observed conditions with a high degree of speed variation and lane changing activity.

Second, the Application Programming Interface (API) module within PARAMICS was an effective tool for operating a dynamic VSLs system and extracting VSLs activity and traffic response information. A practical VSLs control algorithm was coded into PARAMICS

by processing real-time loop detector data and updating the speed limit signs on 20-second intervals. Individual VSLS were programmed to communicate with upstream and downstream VSLS so that the control strategy would operate effectively over the span of the study network.

Third, relative safety and travel time impacts were quantified for three scenarios of traffic congestion following the implementation of the VSLS system. In addition to the quantification of these benefits, the simulation model reported a significant amount of information useful for tracking and depicting the activity of the VSLS system. The analysis of the original VSLS control algorithm provided no clear indication that the implementation of a VSLS system would positively impact safety and travel efficiency measures for all traffic scenarios; however, this analysis did provide evidence that suggests the following:

1. Traffic scenarios experiencing higher levels of congestion are more likely to benefit from a VSLS system in terms of higher positive relative safety benefits and less negative travel time impact than traffic scenarios with less congestion. These benefits appear to occur, at least in part, as a result of the reduction in the frequency and severity of shockwaves in the congested traffic (i.e. damping of the stop and go oscillations);
2. The most congested locations or locations which trigger speed limit decrements are more likely to experience positive relative safety benefits with less impact to travel time;
3. For less congested conditions, stations upstream of VSLS response zones are more likely to experience negative relative safety benefits;
4. A relationship appears to exist between the relative safety and travel time impact and the degree of congestion already present on the network; and
5. Vehicles making longer trips are more likely to experience negative travel time impacts under the current VSLS control algorithm than vehicles making shorter trips.

The most desirable results (both positive safety and positive travel time impacts) were usually observed for moderately congested scenarios during which the VSLS response exhibited frequent speed limit decrements and frequent recoveries. The least desirable results were usually observed under conditions that caused prolonged speed limit reductions and thus lower freeway speeds than would have been observed without VSLS. This suggests that the tested VSLS control algorithm was able to provide large safety benefits with no significant travel time penalty, but only for a limited range of traffic conditions. As such, the control algorithm did not appear to be sufficiently robust to operate effectively over a wide range of traffic conditions.

Fourth, further analyses were performed on modifying the parameters within the VSLS control algorithm and the resulting impacts were quantified. Although this was only a preliminary analysis, considerable improvements to the original VSLS strategy were identified. It was found that certain modifications were successful in substantially reducing the travel time penalty while maintaining significant safety benefits for the peak scenario. Unfortunately, a strategy was not identified that could provide consistent and positive impacts for both safety and travel time under all degrees of congestion, but this analysis provided evidence that significant improvements are attainable. It is anticipated that further modifications to the algorithm can result in a VSLS that is able to operate over a wide range of traffic conditions and provide more consistent safety and travel time benefits. It is concluded that the evaluation framework employed in this study would be an effective tool for performing such an optimization of the algorithm structure and its parameters.

7.1.3 Comparison of VSLS Impacts to those from Previous Studies

The primary results of this study indicate that, under the tested algorithms, VSLS were capable of providing strong safety benefits, particularly for conditions of high congestion, but were not successful in improving travel time or increasing traffic throughput from the non-VSLS case. These results agree with the majority of the results obtained in previous VSLS impact studies.

The safety benefits measured for the VSLS systems employed for congestion management in the UK (UK Highways Agency, 2004) and The Netherlands (Van den Hoogen

and Smulders, 1994) included a reduction in collisions (UK), more uniform headways, and reduction in speed differential between lanes (the Netherlands). These agree with the impacts of reduced crash potential and reduced turbulence identified in this study. In terms of traffic performance, the empirical systems did not provide evidence of positive impacts on capacity, throughput or travel time. It is also interesting to note that the system on the M25 in the UK experienced a reduction in travel time for congested conditions but an increase in travel time for less congested conditions. These results were repeatedly identified in this study for the near-peak scenario that exhibited a high variation in levels of congestion.

The macroscopic modelling studies of VSL systems to date have produced results that indicate VSL systems are capable of dampening congestion shockwaves and improving network travel time. These results were not evident in the current study. The most likely reason is that the macroscopic models used hypothetical traffic situations and optimization techniques when implementing the VSL control. Therefore, the transferability of these results to simulated field conditions and practical control algorithms is questionable and a direct comparison is not plausible.

Finally, comparison of the results from this study with those from previous microsimulation analysis raises some interesting points. First Lee et al. (2003) found that the application of VSL is successful in reducing crash potential by approximately 25%, particularly for locations of high turbulence. Lee et al. also determined a reduction in crash potential was frequently associated with an increase in travel time. Although Lee et al.'s VSL deployment was more limited than in the current study, the results are quite similar. In contrast, Abdel-Aty et al. found that crash potential could be significantly reduced by VSL for targeted locations during periods of low congestion and travel time could be slightly improved. Also, Abdel-Aty et al. found that VSL were ineffective for periods of high congestion. These results do not agree with the results of this study or the results of Lee et al. This could be a result of the different crash model used by Abdel-Aty et al. to quantify the relative safety impact. One interesting similarity was the "crash migration" observed by Abdel-Aty et al., where crash potential increased upstream of an VSL area. This result was observed in this study for off-peak scenario, during which negative safety impacts occurred upstream of the VSL response zone.

7.2 Limitations of Study

Each aspect of this study, including the crash potential model, the simulation modelling, and the network structure, carried assumptions and limitations that must be considered when evaluating the results of the VSLs impact analysis and identifying issues for further research. This section identifies these limitations and their potential influence on the results.

7.2.1 Crash Potential Model

7.2.1.1 *The Nature of a Categorical Model*

First, since the model is categorical, values for each crash precursor fall under one of a predetermined number of category levels. Each level has a different contribution towards the total crash potential (Figure 7-1). Therefore, the magnitudes of the precursor values within the levels are not used directly in the calculation of crash potential.

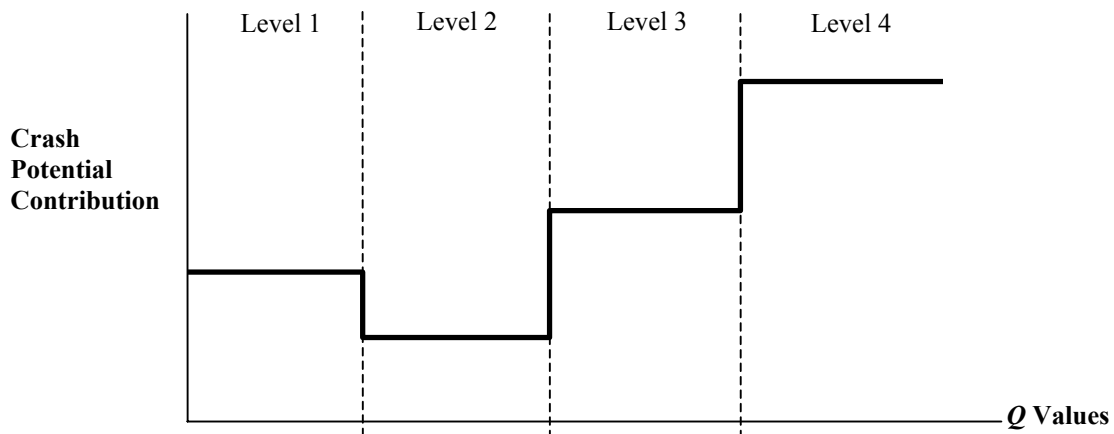


Figure 7-1: Precursor Level Contribution to Crash Potential

This can pose concerns for comparative analysis, particularly for the high category, which does not have an upper boundary. For example, consider a comparison of two crash precursor distributions which exhibit similar frequencies for high-level (Level 4) Q values (Figure 7-2). Closer inspection of the data reveals that Distribution A has many more Q values in the upper tier of that level (Figure 7-3). Although more severe Q values are observed within Level 4 of Distribution A, there is no change in the Level 4 crash potential contribution between A and B.

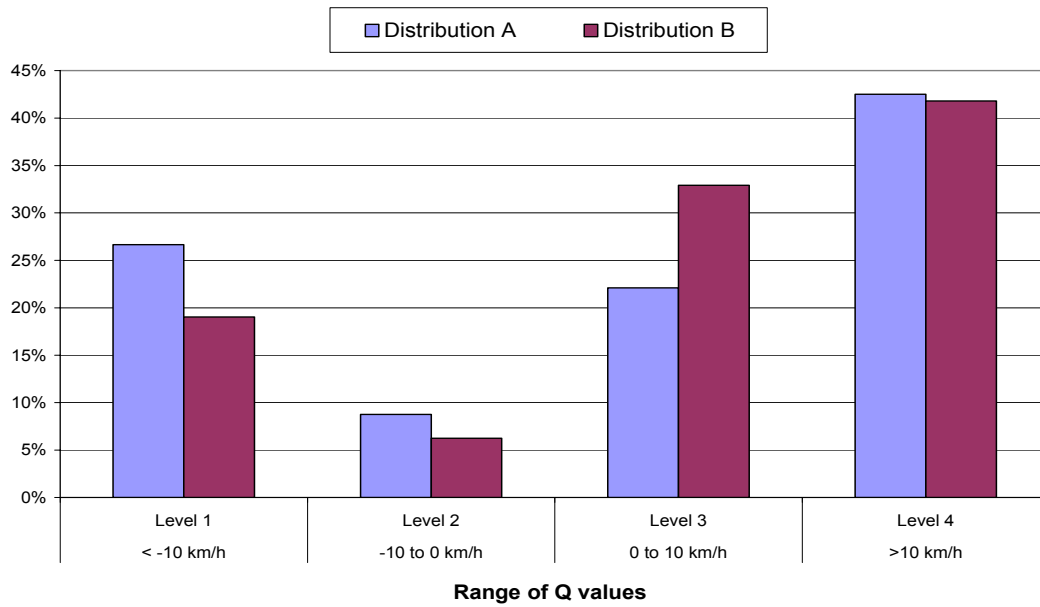


Figure 7-2: Precursor Q Distributions A and B

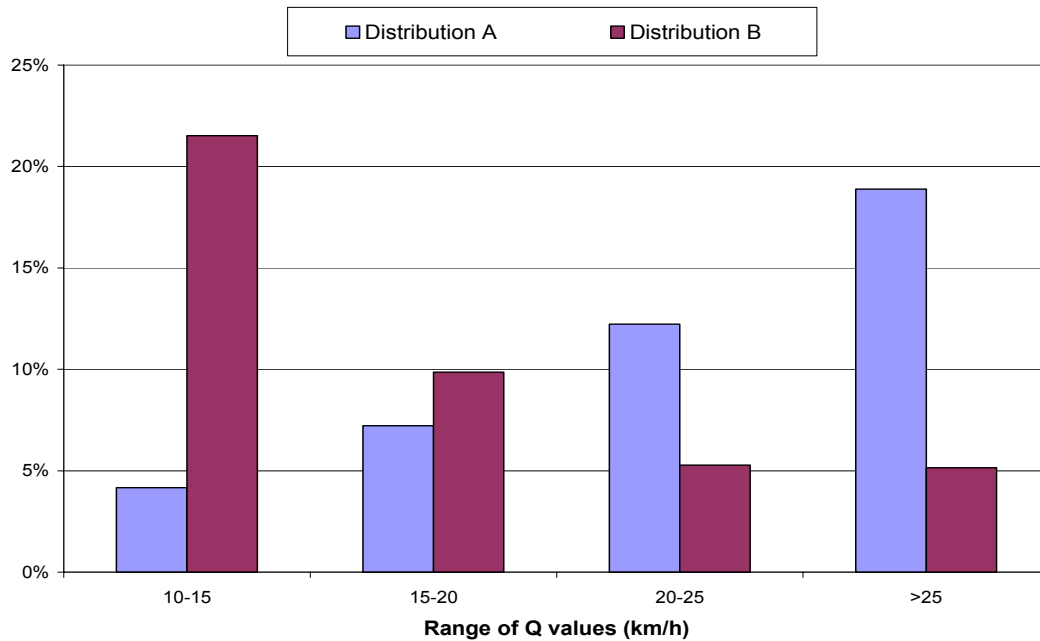


Figure 7-3: Q Distributions within Level 4

Also, since the crash potential is calculated at every station, if moderate speed differentials (10-15 km/h) exist between successive stations (i.e. VSLs transition zone) crash

potential may increase at every station; however, if at just one location a severe speed differential (>25 km/h) exists, then only that location's crash potential changes. This may seem counterintuitive considering that a gradual transition in speed involving several speed limit changes is suspected to be safer than a single speed decrement.

Overall, these issues could have an impact on the VSLs safety impact analysis, but it is uncertain whether the net change in crash potential is underestimated or overestimated. To mitigate this issue, the crash potential model would need to have many more categories, but without a much larger database of crashes for calibration, it is not possible to fit parameters to the model with a high level of confidence.

7.2.1.2 Selection of Real Crash Data

The second limitation of the crash potential model pertains to the selection of real crash data used to calibrate the model. The crashes were selected on the basis that they must be associated with a clear drop in freeway speed so that the period of influence can be identified with high accuracy. Although nearly 300 crashes were included in the database, many others were omitted because the crash occurred during low speed conditions from which the time of crash could not be confirmed. As a result, the crash model was calibrated from crashes occurring predominantly during high-speed conditions. The transferability of the crash potential model parameters from one flow regime to another is unknown. In this study, especially during the peak conditions, the low speed regime occurred frequently. Since drivers have more time to react in low speed conditions, it is possible that the crash potential changes would be overestimated.

7.2.1.3 Roadway Section for Crash Model vs. Simulated Roadway Section

In addition to these limitations, the crash potential model used to evaluate the VSLs safety impact was calibrated for a section of roadway different from the one modelled. Since both road sections were located on the same freeway and separated by a relatively short distance, it was assumed they would service the same commuters and operate under similar conditions. If for some reason, driver behaviour is different for the QEW Burlington section than the QEW Mississauga section, then the relative safety benefits may not be directly transferable.

7.2.1.4 The Role of Exposure in Real-Time Applications

The contribution of exposure to the calibration of the crash potential model was clear as it formed a relationship between the occurrence of different traffic conditions and the corresponding crash frequency. When applied over several years worth of data, the values of exposure are quite large; however, when applied over a short time period (i.e. a morning peak period), the values of exposure are very small in comparison, and became irrelevant in the calculation of crash potential. Also, it is unclear how exposure contributes to a real-time crash prediction model (e.g. on intervals of 20-seconds).

7.2.2 Simulation Modelling

7.2.2.1 Simulation Calibration Parameters

A level of uncertainty always exists when performing simulation modelling. The goal in validating a model is to recreate the most accurate representation of reality as possible within the resource constraints of the project. In the calibration process, several parameters governing driver behaviour and vehicle kinematics were adjusted to provide a satisfactory model. The simulation is most sensitive to the global parameters of mean target headway and driver reaction time. Default values of 1 second are provided for both of these parameters. To model a smooth, prolonged shockwave, these parameter values were slightly increased from their default to 1.2 seconds and 1.1 seconds respectively. Many parameter values were tested, but these provided what seemed to be the most realistic representation of the study network. Other driver behaviour parameters include aggressiveness (set to default) and awareness (shifted toward high familiarity). Also, since PARAMICS default values are calibrated for UK conditions, parameters for vehicle kinematics were adjusted slightly to reflect the larger and heavier North American vehicles.

Although these parameters provided a model that represented reality, their sensitivity to the introduction of VSLs is unknown. For example, in reality upon VSLs activation, driver aggression may change, or the headways might decrease if drivers rely on the system to smooth out shockwaves. Modelling changes in driver behaviour would not only greatly complicate the process, but the changes in driver behaviour are unknown and therefore cannot

be modelled. Nevertheless, this could have significant influence on VSLs impacts and should be considered in further evaluation.

7.2.2.2 *Vehicle Movement Algorithms*

Another issue to consider when using simulation modelling is that vehicle behaviour is governed by algorithms, particularly for car following and lane changing. Based on randomly assigned characteristics when it enters the network, a vehicle will set its speeds and make lane changes when certain conditions are satisfied. For example, in queue conditions, if a vehicle is not meeting its target speed and its patience threshold is exceeded, it will attempt to make a lane change. This differs from reality where drivers have the experience to decide when lane changes may be unnecessary (especially in congested commuting situations where constant lane changing can be of little benefit). Also, simulated vehicles may be much more reactive to speed changes, for both decelerating and accelerating conditions. Considering both of these issues, the simulation may exaggerate the turbulence that exists within the traffic stream.

Even after adjusting the crash precursor values for the simulation model, the increased turbulence in the simulated network could result in higher crash potential values than in the field. Therefore the opportunity to smooth out speed variability with VSLs may not be as pronounced in the field as is evident from the simulation results.

7.2.2.3 *Driver Compliance*

In the simulation model driver compliance rules were selected to remain at the default settings— that is, the speed limit obedience of the vehicle fleet would follow a Normal distribution centred slightly above the posted speed. This means that even with a reduced speed limit of 60 km/h, more aggressive drivers would still choose to travel at 70 km/h. This seems realistic for most roadways, but depending on the speed control policy of a field VSLs system, the simulated compliance rules may or may not be accurate. For example, if a low-tolerance automated enforcement system is to be implemented along with VSLs, the driver compliance would likely follow a tighter distribution about the speed limit.

The issue of automatic enforcement in the simulation model was not included within the scope of this study. Different jurisdictions have different philosophies on enforcement.

For example, variable speed limits are automatically enforced in the UK by way of speed cameras, while sections of the VSL systems in the Netherlands are not enforced. Transportation managers in the Netherlands argue that drivers understand the benefits of complying with VSL and therefore enforcement is not required. In a jurisdiction like North America, however, where VSL are uncommon, it is likely that field systems would include some method of automatic enforcement to ensure motorist compliance with the variable speed limits.

The impacts of automatic enforcement are not assessed in this study, but are regarded as a critical component of a full VSL evaluation. The primary reasons automatic enforcement was not applied or evaluated in this study are as follows:

- Automatic enforcement alone would have significant impacts to traffic flow – If automatic enforcement were to be implemented full time over a freeway section, it would certainly have significant impacts on traffic flow regardless of the VSL activity. Consider an off-peak period when a VSL system is inactive and the speed limit is 100 km/h. Without automatic enforcement, the 85th percentile speed is likely to be 115 km/h or greater. With automatic enforcement, the mean speed would be reduced and the speed distribution tightened. This would likely have safety impacts as well as increases to travel time. This study desired to evaluate the impacts of VSL, which would be difficult to isolate if a combined evaluation with automatic enforcement was performed; and
- Uncertainty in the distribution of vehicle speeds under automatic enforcement – PARAMICS requires speed distributions to be specified for compliance. The approach in this study was to maintain the default compliance, which is basically the compliance calibrated from field conditions under traditional enforcement (i.e. casual police patrol). If automatic enforcement were to be included, the distribution of vehicle speeds could only be assumed, and may be not accurate.

It is recommended that a sensitivity analysis be performed by varying compliance specifications within the model (mean speed and speed distribution). Simulating different

scenarios of tighter enforcement, and comparing the results to those from this study, would provide a further understanding to the additional safety and performance impacts resulting from automatic enforcement policies.

7.2.3 Study Network

The selected freeway segment exhibits an arrangement of traffic volumes that may have influenced the VSLs impact analysis. Of the four interchanges included in the study section, the most downstream one (Burloak Drive) added very high volumes to the mainline in comparison to the others. The congestion at this location caused frequent VSLs decrements often followed by the aforementioned “domino” effect where a wave of VSLs speed decrements cascades upstream. As a result, speed limit reductions were triggered for upstream sections even though no congestion was evident in those locations for the non-VSLs case. This caused increased travel times for many vehicles. If the VSLs system was positioned such that a single point of high congestion was not at the most downstream point, then travel times may not be impacted as negatively.

7.3 Recommendations

Based on the conclusions and limitations identified for this study, the following recommendations have been formed for future work:

7.3.1 Crash Potential Model

- 1) It is recommended that efforts be made to overcome the limitations of including weather as an explanatory variable for crash potential. Weather was omitted as an external control factor due to the limitations discussed in Section 3.3.3.3; however, it is suspected that some relationship exists between weather and/or roadway conditions and crash occurrence;
- 2) It is recommended that efforts be made to modify the calibration methodology to include crash data from more types of flow regimes than just high-speed conditions. Including crashes during regimes of lower speed would increase the reliability of applying the crash potential model to slower, more congested conditions. This

would require a new method of confirming crash time as it is difficult to visually identify a crash during turbulent conditions of low speeds;

- 3) It is recommended that efforts be made to overcome the limitations of a categorical model identified in the previous section. It is recommended that a larger dataset of crashes be used in any future work to increase the number of cells in the contingency table and thus the practical number of categories for each precursor; and
- 4) It is recommended that efforts be made to investigate the role of exposure in real-time crash potential models. The exact contribution of exposure was unclear both in this study and in the work of Lee et al. when the crash potential model was applied on real-time simulation data. Therefore it would be instructive to revisit this aspect of the crash model development and understand what role, if any, exposure can play.

7.3.2 VSLs Evaluation Framework

- 1) In response to the study limitations identified in Section 7.2.2, it is recommended that efforts be made to test the sensitivity of the VSLs impacts to changes to the elements within the simulation framework. The major elements include:
 - a) Selection of simulation parameter values both in calibrating the simulation model and in accounting for changes in driver behaviour upon implementation of VSLs;
 - b) Changes in driver compliance in the context of automatic enforcement policies; and
 - c) The composition of the Origin-Destination matrix (e.g. applying evenly distributed volumes rather than volumes concentrated at the downstream end).
- 2) Further analysis should be performed on evaluating modifications to the VSLs control algorithm. It is not only important to identify successful and comprehensive VSLs control strategies, but also to develop a further understanding of the relationship between the structure of a VSLs control strategy and the resulting safety and traffic performance impacts.

8. REFERENCES

1. Abdel-Aty, M., N. Uddin, A. Pande, M. Abdalla and L. Hsia. (2004) Predicting Freeway Crashes Based on Loop Detector Data Using Matched Case-Control Logistic Regression. *Journal of the Transportation Research Board No. 1897*, TRB, National Research Council, Washington, D.C., pp. 88-95.
2. Abdel-Aty M. and J. Dilmore. (2005) Evaluation of Variable Speed Limits for Real-Time Freeway Safety Improvement. *Accident Analysis and Prevention* 38, pp. 335-345.
3. Abdel-Aty, M., J. Dilmore, and L. Hsia. (2006) Applying Variable Speed Limits and the Potential for Crash Migration. Proceedings of the 85th Annual Meeting of the *Transportation Research Board*, Washington D.C.
4. Alessandri, A., A. Di Febbraro, and A. Ferrara. (1999) Nonlinear Optimization for Freeway Control Using Variable-Speed Signalling. *IEEE Transactions on Vehicular Technology*, Vol. 48, No. 6, pp. 2042-2051.
5. Ben-Akiva, M., H. N. Koutsopoulos, R. Mishalani, and Q. Yang. (1997) Simulation laboratory for evaluating dynamic traffic management systems, *ASCE Journal of Transportation Engineering* 123(4), pp. 283-289.
6. Bourrel, E. and J. B. Lesort. (2003) Mixing Microscopic and Macroscopic Representations of Traffic Flow: Hybrid Model Based on Lighthill-Whitman-Richards Theory. *Transportation Research Record No. 1852*, TRB, National Research Council, Washington, D.C., pp. 193-200.
7. Breton, P., A. Hegyi, B. De Schutter, and J. Hellendoorn. (2002) Shock Wave Elimination/Reduction by Optimal Coordination of Variable Speed Limits. Proceedings of the 5th IEEE International Conference on Intelligent Transportation Systems (ITSC'02), Singapore, pp. 225-230.
8. Dowling, R., A. Skabardonis, and V. Alexiadis. (2004) Traffic Analysis Toolbox Volume III: Guidelines for Applying Traffic Microsimulation Software. Report No. FHWA-HRT-04-040, Federal Highway Administration, U.S. Department of Transportation, Washington, D.C.
9. FHWA (1995). FHWA Study Tour for Speed Management and Enforcement Technology. Summary Report prepared for the Federal Highway Administration, U.S. Department of Transportation, Washington, D.C.
10. FHWA (2006). FHWA Safety, Speed Management Workshop. Federal Highways Administration, U.S. Department of Transportation, Washington, D.C.
http://safety.fhwa.dot.gov/speed_manage/workshops/maspeedworkshop.htm. Updated: January 10, 2006.

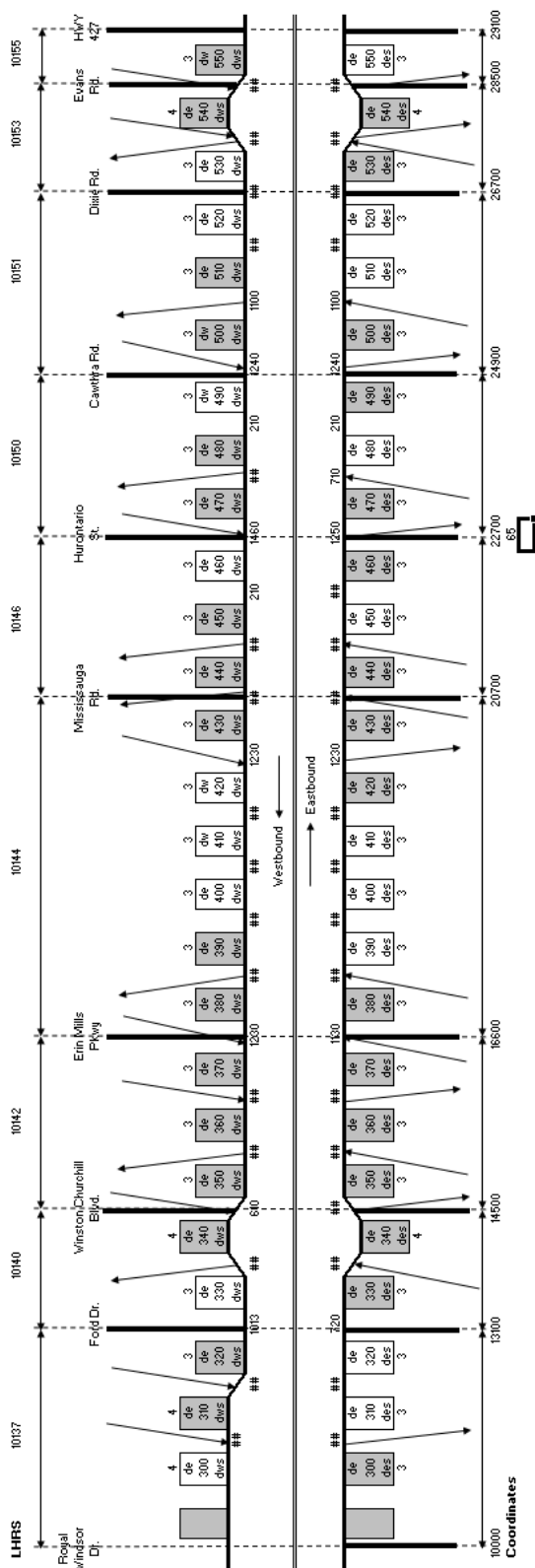
11. Fu, L., J. Henderson, and B. Hellinga. (2003) Inventory of Intelligent Transportation Systems (ITS) in Canada. A report prepared for ITS Canada.
12. Garber, N.J. and A.A. Ehrhart. (2000) Effect of Speed, Flow, and Geometric Characteristics on Crash Frequency for Two-lane Highways. *Transportation Research Record No. 1717*, TRB, National Research Council, Washington, D.C., pp. 76-83.
13. Garber, N. J. and Gadiraju, R. (1989) Factors affecting speed variance and its influence on accidents. In *Transportation Research Record No. 1213*, TRB, National Research Council, Washington, D.C., pp. 64-71.
14. Gardes, Y., D. May, J. Dahlgren, and A. Skabardonis. (2002) Freeway Calibration and Application of the PARAMICS Model. Presented at the *81st Annual Meeting of Transportation Research Board*, Washington, D.C.
15. Golob, T. F. and W. W. Recker. (2004) A Method for Relating Type of Crash to Traffic Flow Characteristics on Urban Freeways. *Transportation Research A 38*, pp. 53-80.
16. Hegyi, A., B. De Schutter, and J. Hellendoorn. (2003) Optimal coordination of variable speed limits to suppress shock waves. *Transportation Research Record No. 1852*, TRB, National Research Council, Washington, D.C., pp.167–174.
17. Hegyi, A., B. De Schutter, and J. Hellendoorn. (2005) Optimal Coordination of Variable Speed Limits to Suppress Shock Waves. *IEEE Transactions on Intelligent Transportation Systems, Vol. 6, No. 1*, pp. 102-112.
18. Hirst, W. M., L. J. Mountain, and M. J. Maher. (2005) Are speed enforcement cameras more effective than other speed management measures? An evaluation of the relationship between speed and accident reduction. *Accident Analysis and Prevention 37*, pp. 731-741.
19. Highway Capacity Manual. Federal Highway Administration, United States Department of Transportation, 2000.
20. Hogema, J. H. and A.R.A. van der Horst. (1994) Evaluation of the A16 Fog-Signaling System with Respect to Driving Behavior. TNO Human Factors Research Institute, Soesterberg, the Netherlands, November 1994.
21. IBI Group. (2005) Variable speed limit system feasibility and preliminary design study. Task 1: Best practices review. Draft report submitted to the Ontario Ministry of Transportation.
22. Lee, C., F. Saccomanno, and B. Hellinga. (2002) Analysis of Crash Precursors on Instrumented Freeways. In *Transportation Research Record No. 1784*, TRB, National Research Council, Washington, D.C., pp. 1-8.
23. Lee, C., B. Hellinga, and F. Saccomanno. (2003b) Real-time crash prediction model for application to crash prevention in freeway traffic. In *Transportation Research Record 1840*, TRB, National Research Council, Washington, D.C., pp. 67-77.

24. Lee, C., B. Hellinga and F. Saccomanno. (2004) Assessing Safety Benefits of Variable Speed Limits. *Transportation Research Record 1897*, TRB, National Research Council, Washington, D.C., 2004, pp. 183-190.
25. Lee, C. (2004) Proactive Vehicle Crash Prevention on Instrumented Freeways Using Real-Time Traffic Control. A doctoral thesis submitted to the University of Waterloo, Waterloo, Ontario.
26. Lee, D., X. Yang, and P. Chandrasekar. (2001) Parameter Calibration for PARAMICS using Genetic Algorithm. Presented at the *80th Annual Meeting of Transportation Research Board*, Washington, D.C.
27. Liu, G. X. and A. Popoff. (1997) Provincial-wide Travel Speed and Traffic Safety Study in Saskatchewan. In *Transportation Research Record No. 1595*, TRB, National Research Council, Washington, D.C., pp. 8-13.
28. *Manual on Uniform Traffic Control Devices*. (2003). Federal Highway Administration, U.S. Department of Transportation.
29. May, A. D. (1990) *Traffic Flow Fundamentals*. Prentice Hall Inc.
30. Oh, C., J. Oh, S. Ritchie and M. Change. (2001) Real-Time Estimation of Freeway Accident Likelihood. Presented at the *80th Annual Meeting of Transportation Research Board*, Washington, D.C.
31. Park, B. and S. Yadlapati. (2004) Development and Testing of Variable Speed Limit Control Logics for Work Zones Using Simulation. Report. Research Report No. UVACTS-13-0-43, Centre for Transportation Studies, University of Virginia.
32. Parviainen, J., D. Sims, I. Nassereddine, L. Sabounghi, R. Zavergiu, and A. Waltho. (1997) Benefit-Cost Assessment of Intelligent Transportation Systems (ITS) Implementation in Canada. Summary Report, Prepared for the Transportation Development Centre Safety and Security Group, Transport Canada, Montreal, Quebec.
33. Pilli-Sihvola, Y. (1996) Weather controlled traffic signs. Proceedings of the *IXth PIARC International Winter Road Congress, Vol. 1*, Vienna.
34. Quadstone Limited (2004). PARAMICS Modeller Version 5.1 Reference Manual, Edinburgh, UK.
35. Rämä, P. (1999) Effects of weather-controlled variable speed limits and warning signs on driver behavior. In *Transportation Research Record No. 1689*, TRB, National Research Council, Washington, D.C., pp. 53-59.
36. Robinson, M. (2000) Examples of Variable speed Limit Applications. Presented at the Speed Management Workshop at the *79th Annual Meeting of Transportation Research Board*, Washington, D.C.

37. Shi, H. and A. Ziliaskopoulos. (2002) Traffic Flow Control Using Variable Speed Limits. Department of Civil Engineering, Northwestern University, Evanston, Illinois.
38. Smulders, S. A. (1990) Control of Freeway Traffic Flow by Variable Speed Signs. *Transportation Research Record B 24*, No. 2, pp. 111-132.
39. Smulders, S. (1992) Control by Variable Speed Signs – The Dutch Experiment. Proceedings of the 6th *International Conference on Road Traffic Monitoring and Control*, pp 99-103.
40. SPSS Inc. (2004) SPSS for Windows Release 13.0. Chicago, Illinois.
41. Taylor, M. C., D. A. Lynam, and A. Baruya. (2000) The Effects of Drivers' Speed on the Frequency of Road Accidents. *Transportation Research Laboratory Report, No. 421*. Transport Research Laboratory, Crowthorne, Berkshire.
42. Torday, A. and M. Bierlaire. (2001) PAPABILES: Simulation Based Evaluation of the Impact of Telematics in the Lausanne Area: A Pilot Study. Proceedings of the *1st Swiss Transport Research Conference*, Ascona, Switzerland.
43. Transportation Research Board. (1998) Managing Speed: Review of Current Practice for Setting and Enforcing Speed Limits. Special Report 254, National Research Council, Washington, D.C.
44. UK Highways Agency. (2004) M25 Controlled Motorways: Summary Report. Issue 1.
45. Ulfarsson, G. F., V. .N. Shankar, and P. Vu. (2005) The effect of Variable Message and Speed Limit Signs on Mean Speeds and Speed Deviations. *International Journal of Vehicle Information and Communication Systems*, Vol.1, Nos. 1/2, pp. 69-87.
46. Van de Hoogen, E. and S. Smulders. (1994) Control by variable speed signs: Results of the Dutch experiment. Conference Publication 391, Road Traffic Monitoring and Control, April 26-28, IEE, pp. 145-149.

APPENDIX A

Schematic of QEW Section used to calibrate Crash Potential Model



APPENDIX B

Crash Database Used in Crash Model Calibration

Note:

1. Reported time is the time of crash reported by the operator in the FTMS incident logs.
2. Estimated time is the time that the shockwave spills back over the loop detector station upstream of the crash location. This time was estimated through visual inspection of the freeway speed profiles from upstream and downstream loop detector data.
3. Weather condition is based on hourly aggregated weather data recorded at the Toronto Lester Pearson Airport weather station (Environment Canada, 2005).
4. Road Geometry is indicated by either M/D for a merging or diverging roadway section or S for a straight roadway section.
5. Crash precursors, *COVV*, *CVS*, and *Q* are calculated for each crash using loop detector data.

#	Date	Upstream Detector	Reported Time	Verified Time	Weather	Time Period	Road Geometry	COVV	Q	CVS
1	05/01/1998	QEWDE0550DWS	17:07:43	17:07:00	Clear	Peak	M/D	0.593	27.0	0.195
2	09/01/1998	QEWDE0530DWS	17:18:37	17:12:00	Clear	Peak	S	1.264	8.5	0.235
3	09/01/1998	QEWDE0490DES	17:30:23	17:19:40	Clear	Peak	M/D	6.583	0.7	0.074
4	12/01/1998	QEWDE0510DWS	18:01:54	17:52:00	Clear	Peak	M/D	2.944	38.4	0.121
5	15/01/1998	QEWDE0360DES	11:41:20	11:40:40	Snow	Off-Peak	M/D	1.861	7.2	0.237
6	15/01/1998	QEWDE0490DWS	11:53:11	11:43:20	snow	Off-Peak	S	1.435	-0.8	0.185
7	15/01/1998	QEWDE0530DWS	13:01:44	12:56:40	snow	Off-Peak	S	1.306	21.7	0.170
8	19/01/1998	QEWDE0510DWS	16:16:32	16:11:00	snow	Peak	M/D	1.694	39.2	0.126
9	19/01/1998	QEWDE0520DES	16:30:05	16:22:40	snow	Peak	S	1.653	8.2	0.059
10	19/01/1998	QEWDE0450DES	17:32:53	17:32:20	snow	Peak	S	1.000	22.1	0.069
11	20/01/1998	QEWDE0500DWS	15:52:14	15:49:20	Clear	Off-Peak	M/D	4.991	-5.3	0.244
12	23/01/1998	QEWDE0460DWS	13:17:42	13:14:40	Clear	Off-Peak	S	3.000	10.9	0.068
13	26/01/1998	QEWDE0310DES	16:56:18	16:51:20	snow	Peak	S	0.694	1.3	0.093
14	10/02/1998	QEWDE0510DWS	06:28:00	6:13:40	Clear	Peak	M/D	0.833	-6.6	0.180
15	11/02/1998	QEWDE0440DES	07:32:46	7:32:40	Clear	Peak	M/D	2.250	-1.3	0.255
16	11/02/1998	QEWDE0440DWS	07:41:33	7:20:00	Clear	Peak	M/D	1.815	-13.2	0.137
17	12/02/1998	QEWDE0450DES	09:07:41	9:03:00	Rain	Peak	S	0.963	-14.5	0.466
18	12/02/1998	QEWDE0470DWS	14:46:45	14:46:40	Clear	Off-Peak	M/D	2.667	1.0	0.084
19	12/02/1998	QEWDE0450DES	17:32:24	17:22:40	Clear	Peak	S	6.528	0.6	0.071
20	13/02/1998	QEWDE0480DES	07:53:27	7:39:40	Snow	Peak	S	1.935	13.1	0.298
21	16/02/1998	QEWDE0480DES	09:38:40	9:24:20	Clear	Peak	S	2.963	8.4	0.325
22	20/02/1998	QEWDE0470DWS	17:41:34	17:18:20	Clear	Peak	M/D	1.167	6.0	0.108
23	25/02/1998	QEWDE0540DES	16:02:24	15:47:40	Clear	Off-Peak	M/D	2.667	-9.8	0.080
24	02/03/1998	QEWDE0520DWS	17:21:11	17:19:20	Rain	Peak	S	4.278	5.5	0.066
25	13/03/1998	QEWDE0490DWS	06:46:53	6:34:00	Clear	Peak	S	0.681	-9.4	0.092
26	16/03/1998	QEWDE0310DES	14:33:13	14:25:20	Clear	Off-Peak	S	1.833	-0.5	0.313
27	20/03/1998	QEWDE0510DES	10:46:14	10:26:00	Clear	Off-Peak	S	0.639	18.6	0.180
28	30/03/1998	QEWDE0480DES	09:09:31	9:00:40	Clear	Peak	S	4.667	24.5	0.187
29	31/03/1998	QEWDE0530DWS	16:27:41	16:16:20	Clear	Peak	S	1.593	-7.4	0.106
30	01/04/1998	QEWDE0460DES	17:58:40	17:54:20	Clear	Peak	M/D	3.769	41.5	0.169
31	02/04/1998	QEWDE0530DWS	12:51:54	12:44:40	Clear	Off-Peak	S	2.375	6.9	0.096
32	06/04/1998	QEWDE0480DES	06:16:33	6:05:20	Clear	Peak	S	2.213	-7.3	0.041

#	Date	Upstream Detector	Reported Time	Verified Time	Weather	Time Period	Road Geometry	COVV	Q	CVS
33	15/04/1998	QEWDE0460DWS	18:19:50	18:06:00	Clear	Peak	S	2.056	20.9	0.320
34	17/04/1998	QEWDE0470DES	09:27:37	9:24:00	Clear	Peak	M/D	4.370	5.4	0.205
35	17/04/1998	QEWDE0510DWS	18:29:27	18:25:00	Clear	Peak	M/D	4.417	23.8	0.168
36	17/04/1998	QEWDE0460DES	19:15:18	19:13:00	Clear	Off-Peak	M/D	2.125	2.1	0.343
37	22/04/1998	QEWDE0460DES	11:28:07	11:16:00	Clear	Off-Peak	M/D	2.782	-20.5	0.282
38	23/04/1998	QEWDE0470DES	07:17:47	7:06:20	Clear	Peak	M/D	1.981	7.2	0.146
39	29/04/1998	QEWDE0540DWS	14:50:19	14:43:00	Clear	Off-Peak	M/D	1.806	39.2	0.565
40	05/06/1998	QEWDE0350DWS	16:11:53	16:11:00	Clear	Peak	M/D	6.083	12.3	0.274
41	10/06/1998	QEWDE0530DES	15:41:58	15:39:40	Clear	Off-Peak	M/D	1.833	12.3	0.054
42	11/06/1998	QEWDE0460DES	09:03:18	8:58:20	Rain	Peak	M/D	2.690	3.5	0.225
43	11/06/1998	QEWDE0470DWS	19:05:22	18:53:20	Clear	Peak	M/D	1.556	7.2	0.110
44	16/06/1998	QEWDE0540DWS	17:47:32	17:45:40	Clear	Peak	M/D	1.111	-10.1	0.269
45	16/06/1998	QEWDE0490DES	17:55:07	17:53:40	Clear	Peak	M/D	2.694	-1.7	0.267
46	23/06/1998	QEWDE0520DWS	12:10:21	12:02:40	Clear	Off-Peak	S	2.236	4.0	0.067
47	24/06/1998	QEWDE0460DWS	10:01:22	9:55:00	Clear	Peak	S	1.222	19.5	0.046
48	29/06/1998	QEWDE0500DES	16:36:06	16:29:20	Clear	Peak	M/D	1.472	-0.4	0.108
49	01/07/1998	QEWDE0340DWS	12:12:56	12:12:40	Clear	Off-Peak	M/D	4.009	85.2	0.623
50	07/07/1998	QEWDE0470DWS	16:36:13	16:32:20	Clear	Peak	M/D	2.556	1.0	0.182
51	15/07/1998	QEWDE0500DWS	07:56:43	7:50:00	Clear	Peak	M/D	2.556	9.1	0.085
52	17/07/1998	QEWDE0470DWS	18:46:13	18:43:00	Clear	Peak	M/D	1.806	36.9	0.093
53	21/07/1998	QEWDE0500DES	08:32:50	8:32:00	Clear	Peak	M/D	1.157	-12.3	0.097
54	22/07/1998	QEWDE0450DES	06:22:33	6:21:00	Clear	Peak	S	0.991	26.6	0.081
55	23/07/1998	QEWDE0450DES	16:39:42	16:36:40	Clear	Peak	S	2.130	-0.5	0.070
56	29/07/1998	QEWDE0470DWS	19:16:27	19:07:00	Clear	Off-Peak	M/D	3.102	71.2	0.086
57	31/07/1998	QEWDE0470DWS	17:41:30	17:35:00	Clear	Peak	M/D	2.208	47.6	0.085
58	05/08/1998	QEWDE0360DES	10:33:11	10:24:00	Clear	Off-Peak	M/D	1.056	-5.9	0.117
59	06/08/1998	QEWDE0470DES	06:26:02	6:17:20	Clear	Peak	M/D	4.713	1.4	0.129
60	10/08/1998	QEWDE0540DWS	17:28:31	17:23:20	Rain	Peak	M/D	4.241	-35.5	0.312
61	12/08/1998	QEWDE0350DES	18:40:03	18:40:00	Clear	Peak	M/D	5.870	13.6	0.141
62	14/08/1998	QEWDE0460DES	07:19:53	7:16:00	Clear	Peak	M/D	5.944	46.4	0.160
63	14/08/1998	QEWDE0540DWS	15:42:58	15:32:20	Clear	Off-Peak	M/D	1.833	22.4	0.245
64	26/08/1998	QEWDE0460DWS	08:46:01	8:34:20	Clear	Peak	S	2.042	14.8	0.068
65	01/09/1998	QEWDE0510DWS	18:28:52	18:24:20	Clear	Peak	M/D	3.333	33.0	0.102
66	02/09/1998	QEWDE0460DWS	19:04:42	19:03:00	Clear	Off-Peak	S	2.491	56.0	0.074
67	08/09/1998	QEWDE0470DES	16:38:08	16:37:40	Clear	Peak	M/D	6.111	1.6	0.059
68	14/09/1998	QEWDE0460DES	09:37:25	9:30:40	Clear	Peak	M/D	2.667	-16.9	0.363
69	18/09/1998	QEWDE0510DWS	17:15:25	17:10:00	Clear	Peak	M/D	1.583	-4.5	0.342
70	23/09/1998	QEWDE0500DES	10:28:10	10:19:00	Clear	Off-Peak	M/D	1.866	27.6	0.196
71	23/09/1998	QEWDE0470DWS	16:16:08	16:12:20	Clear	Peak	M/D	3.056	46.0	0.230
72	23/09/1998	QEWDE0410DES	16:53:24	16:50:00	Clear	Peak	S	4.731	3.4	0.052
73	23/09/1998	QEWDE0460DES	17:27:58	17:27:40	Clear	Peak	M/D	1.833	-36.0	0.202
74	23/09/1998	QEWDE0460DES	18:53:12	18:52:00	Clear	Peak	M/D	0.870	-5.3	0.470
75	28/09/1998	QEWDE0460DWS	16:36:07	16:32:20	Clear	Peak	S	3.444	13.2	0.173
76	29/09/1998	QEWDE0510DWS	19:34:10	19:26:20	Clear	Off-Peak	M/D	1.167	-5.1	0.293
77	01/10/1998	QEWDE0380DWS	15:53:11	15:31:40	Clear	Off-Peak	M/D	1.944	-1.9	0.092
78	06/10/1998	QEWDE0470DWS	12:41:17	12:41:20	Clear	Off-Peak	M/D	2.278	-22.6	0.131
79	06/10/1998	QEWDE0460DES	17:33:27	17:33:00	Clear	Peak	M/D	3.056	32.0	0.099

#	Date	Upstream Detector	Reported Time	Verified Time	Weather	Time Period	Road Geometry	COVV	Q	CVS
80	09/10/1998	QEWDE0450DWS	16:00:01	15:57:20	Clear	Off-Peak	M/D	0.750	8.1	0.098
81	21/10/1998	QEWDE0520DES	09:10:27	9:04:00	Clear	Peak	S	9.731	16.9	0.114
82	23/10/1998	QEWDE0430DES	17:23:51	17:23:00	Clear	Peak	M/D	3.861	14.2	0.331
83	23/10/1998	QEWDE0470DES	18:49:48	18:49:40	Clear	Peak	M/D	2.310	-2.7	0.272
84	03/11/1998	QEWDE0500DWS	07:35:58	7:21:20	Clear	Peak	M/D	1.097	14.9	0.109
85	06/11/1998	QEWDE0460DES	07:29:19	7:23:00	Clear	Peak	M/D	0.648	-66.1	0.550
86	09/11/1998	QEWDE0360DES	16:51:29	16:50:00	Rain	Peak	M/D	1.593	-5.0	0.057
87	09/11/1998	QEWDE0350DES	17:01:13	17:00:00	Clear	Peak	M/D	0.583	87.0	0.070
88	17/11/1998	QEWDE0460DES	17:33:47	17:31:00	Clear	Peak	M/D	1.648	-11.8	0.263
89	26/11/1998	QEWDE0490DWS	17:43:05	17:38:20	Clear	Peak	S	2.093	-5.8	0.147
90	27/11/1998	QEWDE0500DES	10:31:58	10:27:40	Clear	Off-Peak	M/D	3.806	17.4	0.417
91	27/11/1998	QEWDE0440DES	12:10:00	12:05:20	Clear	Off-Peak	M/D	2.921	-2.1	0.064
92	30/11/1998	QEWDE0540DWS	16:18:17	16:04:20	Clear	Peak	M/D	1.319	37.3	0.246
93	08/12/1998	QEWDE0410DWS	07:53:16	7:48:20	Clear	Peak	S	6.375	-1.2	0.070
94	10/12/1998	QEWDE0350DES	17:23:11	17:15:20	Clear	Peak	M/D	1.847	7.7	0.211
95	14/12/1998	QEWDE0440DES	08:55:26	8:52:40	Clear	Peak	M/D	1.167	-5.1	0.285
96	14/12/1998	QEWDE0450DWS	16:33:17	16:28:40	Clear	Peak	M/D	1.722	20.9	0.185
97	16/12/1998	QEWDE0540DES	16:09:24	16:04:00	Clear	Peak	M/D	3.537	7.2	0.069
98	22/12/1998	QEWDE0510DES	18:24:21	18:20:40	Clear	Peak	S	3.819	4.6	0.090
99	23/12/1998	QEWDE0490DES	08:04:28	7:57:40	Clear	Peak	M/D	2.222	10.0	0.066
100	08/01/1999	QEWDE0490DES	07:21:18	7:19:00	Clear	Peak	M/D	0.954	-36.1	0.606
101	11/01/1999	QEWDE0520DWS	16:19:06	16:12:40	Clear	Peak	S	1.398	2.8	0.101
102	13/01/1999	QEWDE0540DES	12:45:18	12:37:40	Clear	Off-Peak	M/D	2.750	-12.8	0.084
103	20/01/1999	QEWDE0480DES	17:15:36	17:13:20	Clear	Peak	M/D	3.954	7.0	0.086
104	21/01/1999	QEWDE0510DES	10:55:57	10:53:00	Clear	Off-Peak	S	2.528	10.1	0.174
105	25/01/1999	QEWDE0530DES	16:37:03	16:29:40	Clear	Peak	M/D	1.602	-10.3	0.087
106	26/01/1999	QEWDE0300DES	15:49:48	15:48:00	Clear	Off-Peak	M/D	1.167	-21.2	0.072
107	28/01/1999	QEWDE0380DWS	08:16:47	8:07:00	Snow	Peak	M/D	1.792	9.7	0.111
108	03/02/1999	QEWDE0520DWS	15:04:48	15:03:00	Clear	Off-Peak	S	1.486	11.5	0.057
109	04/02/1999	QEWDE0450DES	09:59:18	9:57:00	Snow	Peak	S	1.667	-4.1	0.066
110	09/02/1999	QEWDE0480DES	15:46:18	15:43:20	Clear	Off-Peak	S	3.259	8.9	0.052
111	09/02/1999	QEWDE0490DES	18:27:20	18:14:40	Clear	Peak	M/D	1.727	16.7	0.061
112	10/02/1999	QEWDE0490DES	10:04:07	10:02:40	Clear	Off-Peak	M/D	1.764	26.3	0.181
113	11/02/1999	QEWDE0470DES	09:35:47	9:34:20	Clear	Peak	M/D	3.125	42.2	0.222
114	19/02/1999	QEWDE0460DES	18:26:04	18:22:20	Clear	Peak	M/D	2.463	36.9	0.056
115	26/02/1999	QEWDE0520DWS	15:33:40	15:30:40	Clear	Off-Peak	S	4.352	13.0	0.072
116	26/02/1999	QEWDE0470DWS	15:35:28	15:27:00	Clear	Off-Peak	M/D	2.347	-0.4	0.158
117	08/03/1999	QEWDE0550DWS	09:24:27	9:18:00	Clear	Peak	M/D	1.194	-9.7	0.072
118	26/03/1999	QEWDE0450DES	09:05:56	9:02:00	Clear	Peak	S	1.880	8.2	0.304
119	26/03/1999	QEWDE0500DES	17:27:07	17:25:40	Clear	Peak	M/D	5.944	53.0	0.112
120	26/03/1999	QEWDE0460DES	18:54:05	18:50:40	Clear	Peak	M/D	0.917	17.7	0.220
121	30/03/1999	QEWDE0360DWS	08:56:55	8:41:00	Clear	Peak	M/D	2.472	4.8	0.089
122	02/04/1999	QEWDE0540DWS	16:49:27	16:45:20	Clear	Peak	M/D	6.648	20.8	0.070
123	06/04/1999	QEWDE0450DES	09:42:35	9:33:00	Clear	Peak	S	3.486	20.8	0.239
124	09/04/1999	QEWDE0520DWS	08:41:45	8:35:40	Clear	Peak	S	4.056	10.7	0.045
125	12/04/1999	QEWDE0340DWS	06:48:01	6:25:00	Clear	Peak	M/D	3.167	-8.5	0.180
126	29/04/1999	QEWDE0470DES	09:41:36	9:36:20	Clear	Peak	M/D	1.375	28.3	0.140

#	Date	Upstream Detector	Reported Time	Verified Time	Weather	Time Period	Road Geometry	COVV	Q	CVS
127	30/04/1999	QEWDE0460DES	09:22:08	9:18:40	Clear	Peak	M/D	1.935	82.5	0.118
128	07/05/1999	QEWDE0450DES	17:39:12	17:38:00	Clear	Peak	S	1.569	16.1	0.114
129	27/05/1999	QEWDE0460DES	11:53:43	11:47:40	Clear	Off-Peak	M/D	1.361	-7.9	0.057
130	27/05/1999	QEWDE0540DES	12:51:27	12:44:40	Clear	Off-Peak	M/D	4.204	8.2	0.057
131	31/05/1999	QEWDE0500DWS	09:03:27	8:48:20	Clear	Peak	M/D	1.477	29.7	0.058
132	01/06/1999	QEWDE0400DES	15:45:01	15:41:20	Clear	Off-Peak	S	1.681	-7.4	0.090
133	07/06/1999	QEWDE0450DES	06:45:27	6:44:20	Clear	Peak	S	1.556	13.5	0.302
134	08/06/1999	QEWDE0530DWS	10:25:17	10:17:00	Clear	Off-Peak	S	2.028	-1.7	0.106
135	16/06/1999	QEWDE0370DES	15:14:50	15:13:20	Clear	Off-Peak	M/D	1.722	13.3	0.146
136	21/06/1999	QEWDE0440DES	06:51:27	6:50:20	Clear	Peak	M/D	2.764	-10.9	0.156
137	21/06/1999	QEWDE0490DWS	13:54:05	13:51:40	Clear	Off-Peak	S	5.306	-23.9	0.092
138	23/06/1999	QEWDE0400DES	09:13:34	8:58:00	Clear	Peak	S	1.750	21.7	0.378
139	24/06/1999	QEWDE0450DES	18:22:46	18:18:00	Clear	Peak	M/D	10.315	33.6	0.240
140	29/06/1999	QEWDE0530DES	12:16:00	12:07:20	Clear	Off-Peak	S	6.620	6.5	0.050
141	30/06/1999	QEWDE0470DWS	08:59:13	8:52:40	Clear	Peak	M/D	1.653	-9.0	0.292
142	30/06/1999	QEWDE0440DES	09:13:08	9:07:00	Clear	Peak	M/D	2.111	-31.0	0.349
143	05/07/1999	QEWDE0410DWS	11:02:09	10:54:40	Clear	Off-Peak	S	3.208	6.5	0.066
144	06/07/1999	QEWDE0540DWS	19:51:27	19:44:20	Clear	Off-Peak	M/D	4.319	11.0	0.080
145	14/07/1999	QEWDE0500DES	16:36:08	16:34:40	Clear	Peak	M/D	2.083	3.1	0.104
146	16/07/1999	QEWDE0480DES	08:09:07	8:06:40	Clear	Peak	S	3.361	20.6	0.229
147	20/07/1999	QEWDE0490DWS	12:20:42	12:13:20	Clear	Off-Peak	S	3.278	-30.5	0.098
148	26/07/1999	QEWDE0530DWS	17:43:39	17:38:20	Clear	Peak	S	1.042	12.0	0.212
149	27/07/1999	QEWDE0450DES	06:18:24	6:14:20	Clear	Peak	S	2.926	3.9	0.069
150	17/08/1999	QEWDE0480DWS	07:05:21	7:02:00	Clear	Peak	M/D	1.097	-5.6	0.111
151	26/08/1999	QEWDE0540DWS	16:33:02	16:21:00	Clear	Peak	M/D	1.167	5.4	0.305
152	03/09/1999	QEWDE0360DWS	14:41:44	14:35:40	Clear	Off-Peak	M/D	4.806	-0.7	0.114
153	15/09/1999	QEWDE0460DES	18:01:31	17:58:40	Clear	Peak	M/D	4.852	52.4	0.234
154	17/09/1999	QEWDE0540DWS	16:56:36	16:53:00	Clear	Peak	M/D	3.222	51.4	0.213
155	28/09/1999	QEWDE0450DES	06:20:07	6:18:40	Clear	Peak	S	1.111	30.5	0.074
156	30/09/1999	QEWDE0460DWS	07:41:44	7:41:40	Clear	Peak	S	2.778	7.0	0.063
157	30/09/1999	QEWDE0470DWS	07:54:08	7:44:00	Clear	Peak	M/D	4.597	-12.0	0.213
158	01/10/1999	QEWDE0530DES	06:50:54	6:44:40	Clear	Peak	M/D	2.778	48.7	0.092
159	08/10/1999	QEWDE0480DES	18:32:31	18:29:00	Clear	Peak	S	1.458	7.1	0.262
160	13/10/1999	QEWDE0450DES	09:48:29	9:32:00	Clear	Peak	S	2.699	-7.0	0.122
161	15/10/1999	QEWDE0460DES	06:17:38	6:08:40	Clear	Peak	M/D	4.083	13.8	0.050
162	18/10/1999	QEWDE0450DWS	15:48:47	15:45:00	Rain	Off-Peak	M/D	5.218	-5.4	0.061
163	26/10/1999	QEWDE0450DES	09:41:53	9:37:40	Clear	Peak	S	4.403	33.1	0.132
164	29/10/1999	QEWDE0500DES	16:34:27	16:32:20	Clear	Peak	M/D	1.167	25.8	0.113
165	02/11/1999	QEWDE0480DES	09:15:02	9:09:40	Clear	Peak	S	0.769	-2.8	0.297
166	08/11/1999	QEWDE0510DES	07:06:34	6:51:20	Clear	Peak	S	1.148	-7.7	0.112
167	10/11/1999	QEWDE0540DWS	16:14:25	16:05:20	Clear	Peak	M/D	0.500	5.8	0.176
168	17/11/1999	QEWDE0520DWS	17:34:55	17:29:20	Clear	Peak	S	2.819	-3.3	0.178
169	19/11/1999	QEWDE0490DES	10:31:07	10:25:00	Rain	Off-Peak	M/D	4.000	28.3	0.262
170	29/11/1999	QEWDE0540DWS	16:38:17	16:32:40	Clear	Peak	M/D	2.083	-23.2	0.284
171	02/12/1999	QEWDE0490DES	17:14:49	17:09:00	Rain	Peak	M/D	3.319	1.3	0.066
172	03/12/1999	QEWDE0420DES	06:30:07	6:28:00	Clear	Peak	M/D	1.944	41.0	0.045
173	03/12/1999	QEWDE0490DES	17:18:11	17:13:00	Clear	Peak	M/D	2.870	26.2	0.100

#	Date	Upstream Detector	Reported Time	Verified Time	Weather	Time Period	Road Geometry	COVV	Q	CVS
174	03/12/1999	QEWDE0500DWS	17:34:47	17:20:20	Clear	Peak	M/D	1.125	17.0	0.217
175	08/12/1999	QEWDE0480DES	06:56:32	6:44:00	Clear	Peak	S	1.194	5.4	0.267
176	08/12/1999	QEWDE0510DWS	18:13:46	18:10:40	Clear	Peak	M/D	1.444	-9.3	0.247
177	10/12/1999	QEWDE0460DES	18:58:08	18:55:00	Clear	Peak	M/D	0.708	-22.4	0.171
178	16/12/1999	QEWDE0470DES	17:31:26	17:24:40	Clear	Peak	M/D	5.088	-1.8	0.125
179	23/12/1999	QEWDE0520DWS	16:46:37	16:28:40	Clear	Peak	S	1.306	0.2	0.137
180	02/01/2000	QEWDE0480DES	16:01:00	15:47:40	Clear	Off-Peak	S	2.569	9.0	0.053
181	07/01/2000	QEWDE0470DES	09:44:00	9:37:40	Clear	Peak	M/D	6.500	18.5	0.179
182	13/01/2000	QEWDE0470DES	18:35:00	18:33:00	Clear	Peak	M/D	5.917	0.6	0.089
183	14/01/2000	QEWDE0540DWS	06:51:00	6:39:20	Clear	Peak	M/D	1.407	12.2	0.101
184	18/01/2000	QEWDE0460DWS	17:27:00	17:23:00	Rain	Peak	S	1.898	18.9	0.060
185	19/01/2000	QEWDE0470DWS	19:17:00	19:14:00	Snow	Off-Peak	M/D	7.361	0.8	0.195
186	20/01/2000	QEWDE0510DWS	18:49:00	18:46:20	Clear	Peak	M/D	2.986	9.9	0.155
187	21/01/2000	QEWDE0420DES	06:44:00	6:40:40	Clear	Peak	M/D	2.833	43.5	0.052
188	24/01/2000	QEWDE0440DES	11:25:00	11:23:40	Snow	Off-Peak	M/D	3.306	-9.6	0.124
189	27/01/2000	QEWDE0460DES	10:03:00	10:02:40	Clear	Off-Peak	M/D	1.426	35.9	0.056
190	28/01/2000	QEWDE0510DES	11:20:00	11:15:00	Clear	Off-Peak	S	1.144	7.8	0.040
191	01/02/2000	QEWDE0530DWS	14:41:00	14:37:20	Clear	Off-Peak	S	9.972	4.1	0.102
192	04/02/2000	QEWDE0480DES	18:42:00	18:38:40	Clear	Peak	S	3.824	4.8	0.069
193	09/02/2000	QEWDE0490DES	17:50:00	17:47:20	Clear	Peak	M/D	1.120	31.1	0.153
194	10/02/2000	QEWDE0380DES	17:06:00	16:51:00	Clear	Peak	M/D	1.639	18.0	0.126
195	14/02/2000	QEWDE0530DWS	11:38:00	11:31:20	Clear	Off-Peak	S	2.000	10.2	0.156
196	22/02/2000	QEWDE0480DES	16:33:00	16:29:00	Clear	Peak	S	0.991	9.3	0.054
197	25/02/2000	QEWDE0450DES	18:40:00	18:39:20	Clear	Peak	S	3.537	28.0	0.175
198	28/02/2000	QEWDE0470DES	10:13:00	10:11:40	Snow	Off-Peak	M/D	1.944	1.0	0.058
199	03/03/2000	QEWDE0540DWS	10:53:00	10:46:00	Snow	Off-Peak	M/D	2.139	10.0	0.076
200	16/03/2000	QEWDE0460DES	09:11:00	9:07:40	Clear	Peak	M/D	2.417	14.2	0.143
201	23/03/2000	QEWDE0450DES	10:01:00	10:00:40	Clear	Off-Peak	S	2.222	41.3	0.179
202	31/03/2000	QEWDE0540DWS	17:04:00	16:57:20	Clear	Peak	M/D	3.829	-13.4	0.246
203	06/04/2000	QEWDE0520DWS	15:34:00	15:29:40	Clear	Off-Peak	S	2.917	-2.1	0.139
204	19/04/2000	QEWDE0480DWS	17:42:00	17:35:20	Clear	Peak	M/D	3.426	-10.6	0.049
205	03/05/2000	QEWDE0520DWS	19:14:00	19:05:40	Clear	Off-Peak	S	3.537	-1.1	0.115
206	05/05/2000	QEWDE0510DWS	17:00:00	16:53:00	Clear	Peak	M/D	1.565	24.9	0.124
207	19/05/2000	QEWDE0510DES	09:40:00	9:37:20	Clear	Peak	S	3.565	9.0	0.133
208	19/05/2000	QEWDE0480DES	16:51:00	16:44:40	Clear	Peak	S	8.556	17.1	0.096
209	26/05/2000	QEWDE0490DWS	08:56:00	8:44:20	Clear	Peak	S	1.991	-24.9	0.066
210	30/05/2000	QEWDE0510DWS	17:18:00	17:03:00	Clear	Peak	M/D	14.625	7.1	0.137
211	12/06/2000	QEWDE0470DWS	15:13:00	15:10:40	Rain	Off-Peak	M/D	4.167	-4.5	0.126
212	23/06/2000	QEWDE0540DWS	12:36:00	12:34:00	Clear	Off-Peak	M/D	4.917	7.9	0.089
213	18/07/2000	QEWDE0480DES	07:55:00	7:48:00	Clear	Peak	S	1.111	12.3	0.247
214	21/07/2000	QEWDE0460DES	07:18:00	7:09:20	Clear	Peak	M/D	6.843	54.2	0.408
215	09/08/2000	QEWDE0480DES	06:28:00	6:26:00	Clear	Peak	S	3.417	53.3	0.057
216	10/08/2000	QEWDE0450DES	17:49:00	17:47:20	Clear	Peak	S	4.528	47.0	0.089
217	23/08/2000	QEWDE0400DES	06:35:00	6:34:00	Clear	Peak	S	1.028	-8.8	0.427
218	23/08/2000	QEWDE0440DES	11:20:00	11:09:40	Clear	Off-Peak	M/D	1.681	-2.6	0.048
219	23/08/2000	QEWDE0520DWS	16:13:00	16:10:40	Clear	Peak	S	2.356	8.9	0.052
220	24/08/2000	QEWDE0460DES	06:14:00	6:11:00	Clear	Peak	M/D	4.731	-1.3	0.061

#	Date	Upstream Detector	Reported Time	Verified Time	Weather	Time Period	Road Geometry	COVV	Q	CVS
221	25/08/2000	QEWDE0450DES	16:17:00	16:16:00	Rain	Peak	S	1.815	11.0	0.380
222	05/09/2000	QEWDE0450DWS	12:33:00	12:28:20	Clear	Off-Peak	M/D	2.824	6.9	0.136
223	06/09/2000	QEWDE0520DES	16:57:00	16:45:40	Clear	Peak	S	0.500	2.2	0.052
224	08/09/2000	QEWDE0410DES	12:47:00	12:42:00	Clear	Off-Peak	S	1.139	-5.7	0.078
225	15/09/2000	QEWDE0380DES	08:50:00	8:42:40	Clear	Peak	M/D	4.000	47.0	0.155
226	20/09/2000	QEWDE0340DES	13:43:00	13:34:20	Clear	Off-Peak	M/D	2.472	-21.5	0.088
227	22/11/2000	QEWDE0530DWS	11:13:00	11:12:00	Clear	Off-Peak	S	1.398	15.8	0.144
228	23/11/2000	QEWDE0470DWS	08:26:00	8:16:20	Clear	Peak	M/D	3.778	76.9	0.191
229	24/11/2000	QEWDE0470DES	06:14:00	6:08:20	Clear	Peak	M/D	5.162	1.2	0.097
230	30/11/2000	QEWDE0420DWS	18:23:00	18:18:20	Clear	Peak	S	1.333	-2.3	0.066
231	12/12/2000	QEWDE0450DES	10:07:00	10:00:40	Clear	Off-Peak	S	2.417	1.4	0.111
232	14/12/2000	QEWDE0540DES	10:37:00	10:36:00	Clear	Off-Peak	M/D	1.204	-36.1	0.062
233	18/12/2000	QEWDE0410DES	06:42:00	6:38:40	Snow	Peak	S	1.963	24.3	0.113
234	20/12/2000	QEWDE0410DES	09:59:00	9:55:40	Clear	Peak	S	2.176	18.5	0.358
235	20/12/2000	QEWDE0440DES	12:51:00	12:44:20	Clear	Off-Peak	M/D	5.889	12.9	0.118
236	20/12/2000	QEWDE0540DWS	18:33:00	18:25:20	Clear	Peak	M/D	0.991	-15.5	0.285
237	21/12/2000	QEWDE0450DWS	06:46:00	6:46:00	Snow	Peak	M/D	1.157	-9.6	0.229
238	21/12/2000	QEWDE0320DES	09:57:00	9:45:20	Snow	Peak	S	2.333	40.7	0.178
239	27/12/2000	QEWDE0390DES	19:12:00	19:06:40	Clear	Off-Peak	S	1.370	-13.1	0.142
240	29/12/2000	QEWDE0440DES	12:47:00	12:42:40	Clear	Off-Peak	M/D	2.431	15.2	0.255
241	04/01/2001	QEWDE0480DES	14:56:48	14:45:00	Clear	Off-Peak	S	4.389	-0.5	0.048
242	12/01/2001	QEWDE0480DES	06:17:42	6:09:00	Clear	Peak	S	4.500	7.2	0.063
243	25/01/2001	QEWDE0460DWS	19:20:47	19:19:00	Snow	Off-Peak	S	1.667	16.0	0.100
244	25/01/2001	QEWDE0450DWS	19:24:34	19:17:20	Snow	Off-Peak	M/D	2.009	8.4	0.073
245	02/02/2001	QEWDE0510DES	09:09:27	9:07:20	Snow	Peak	S	1.667	-29.7	0.199
246	07/02/2001	QEWDE0490DES	15:25:11	15:20:40	Clear	Off-Peak	M/D	1.500	17.0	0.055
247	08/02/2001	QEWDE0340DWS	08:24:51	8:01:00	Snow	Peak	M/D	1.315	7.0	0.100
248	22/02/2001	QEWDE0440DES	09:31:47	9:29:20	Clear	Peak	M/D	2.125	-15.1	0.450
249	08/03/2001	QEWDE0320DES	11:32:07	11:29:20	Clear	Off-Peak	S	3.671	50.6	0.147
250	23/03/2001	QEWDE0450DES	18:53:47	18:50:40	Clear	Peak	S	1.898	9.2	0.325
251	30/03/2001	QEWDE0410DES	18:18:27	18:14:00	Clear	Peak	S	2.222	31.8	0.051
252	09/04/2001	QEWDE0490DES	17:49:47	17:43:20	Clear	Peak	M/D	3.005	34.3	0.138
253	22/05/2001	QEWDE0500DES	09:33:15	9:22:00	Clear	Peak	M/D	0.583	6.8	0.109
254	25/05/2001	QEWDE0490DES	10:01:41	9:46:40	Clear	Peak	M/D	1.722	33.2	0.178
255	06/06/2001	QEWDE0450DES	06:33:53	6:21:20	Clear	Peak	S	7.370	27.8	0.063
256	11/06/2001	QEWDE0470DES	07:24:46	7:16:20	Rain	Peak	M/D	0.611	-7.5	0.419
257	20/06/2001	QEWDE0530DWS	18:38:27	18:36:00	Clear	Peak	S	0.833	5.3	0.234
258	04/07/2001	QEWDE0450DWS	10:40:48	10:32:40	Clear	Off-Peak	M/D	3.287	1.5	0.110
259	12/07/2001	QEWDE0420DES	09:57:59	9:43:00	Clear	Peak	M/D	0.972	4.1	0.084
260	19/07/2001	QEWDE0510DWS	19:21:34	19:12:00	Clear	Off-Peak	M/D	3.903	-14.7	0.170
261	14/08/2001	QEWDE0450DES	08:30:59	8:26:00	Clear	Peak	S	5.296	37.3	0.159
262	28/08/2001	QEWDE0540DWS	18:26:00	18:22:40	Clear	Peak	M/D	1.625	2.4	0.485
263	12/09/2001	QEWDE0420DWS	09:05:31	8:47:20	Clear	Peak	S	1.944	-4.1	0.069
264	29/11/2001	QEWDE0530DES	05:59:35	5:38:40	Rain	Off-Peak	M/D	2.935	11.9	0.064
265	06/12/2001	QEWDE0380DES	08:28:59	8:13:00	Clear	Peak	M/D	1.065	0.8	0.571
266	06/12/2001	QEWDE0540DWS	17:31:14	17:17:00	Clear	Peak	M/D	1.870	-10.3	0.412
267	10/12/2001	QEWDE0460DES	06:35:24	6:21:40	Clear	Peak	M/D	1.088	17.1	0.050

#	Date	Upstream Detector	Reported Time	Verified Time	Weather	Time Period	Road Geometry	COVV	Q	CVS
268	13/12/2001	QEWDE0450DWS	19:21:32	19:12:00	Clear	Off-Peak	M/D	3.833	-0.8	0.224
269	01/07/2002	QEWDE0540DES	14:20:27	14:13:00	Clear	Off-Peak	M/D	3.176	82.7	0.059
270	03/07/2002	QEWDE0330DES	11:42:50	11:34:20	Clear	Off-Peak	M/D	4.963	-13.4	0.111
271	09/07/2002	QEWDE0510DWS	17:36:43	17:25:20	Clear	Peak	M/D	1.713	26.7	0.116
272	11/07/2002	QEWDE0400DES	06:27:48	6:16:20	Clear	Peak	S	1.222	40.2	0.091
273	23/07/2002	QEWDE0530DES	11:49:27	11:45:40	Clear	Off-Peak	M/D	4.806	3.4	0.059
274	09/08/2002	QEWDE0540DWS	15:13:47	15:09:40	Clear	Off-Peak	M/D	2.356	27.8	0.099
275	09/08/2002	QEWDE0450DES	17:31:27	17:24:00	Clear	Peak	S	4.176	36.3	0.097
276	09/08/2002	QEWDE0470DES	18:54:59	18:51:20	Clear	Peak	M/D	1.407	69.4	0.424
277	28/08/2002	QEWDE0460DES	08:37:54	8:20:00	Clear	Peak	M/D	2.019	29.2	0.462
278	29/08/2002	QEWDE0490DES	10:38:07	10:34:20	Clear	Off-Peak	M/D	4.278	40.8	0.074
279	03/09/2002	QEWDE0460DES	17:31:33	17:23:00	Clear	Peak	M/D	4.542	29.1	0.058
280	19/09/2002	QEWDE0550DWS	08:58:21	8:41:20	Clear	Peak	M/D	1.806	43.2	0.384
281	19/09/2002	QEWDE0390DWS	14:28:47	14:27:20	Clear	Off-Peak	M/D	1.889	-9.4	0.139
282	01/10/2002	QEWDE0520DWS	17:00:40	16:51:40	Clear	Peak	S	1.722	5.2	0.217
283	02/10/2002	QEWDE0360DES	08:37:17	8:21:20	Clear	Peak	M/D	3.528	75.3	0.096
284	10/10/2002	QEWDE0450DES	16:44:19	16:25:40	Clear	Peak	S	10.361	3.1	0.099
285	11/10/2002	QEWDE0540DWS	19:26:16	19:10:20	Clear	Off-Peak	M/D	1.153	-4.0	0.315
286	15/10/2002	QEWDE0480DES	14:51:07	14:40:40	Clear	Off-Peak	S	4.389	7.1	0.061
287	18/10/2002	QEWDE0440DES	16:26:47	16:24:40	Clear	Peak	M/D	1.792	31.7	0.123
288	05/11/2002	QEWDE0480DES	18:14:07	18:12:40	Clear	Peak	S	6.639	8.4	0.145
289	27/11/2002	QEWDE0470DWS	08:19:46	8:12:20	Clear	Peak	M/D	2.583	10.5	0.145
290	29/11/2002	QEWDE0470DWS	07:26:46	7:16:00	Snow	Peak	M/D	4.389	35.0	0.175
291	04/12/2002	QEWDE0380DES	09:48:16	9:38:00	Clear	Peak	M/D	3.750	1.6	0.476
292	10/12/2002	QEWDE0370DES	07:55:14	7:41:40	Clear	Peak	M/D	1.194	52.2	0.231
293	17/12/2002	QEWDE0470DES	11:33:47	11:31:20	Clear	Off-Peak	M/D	1.889	8.8	0.058
294	19/12/2002	QEWDE0530DES	07:47:05	7:44:20	Rain	Peak	M/D	1.736	-11.4	0.067
295	01/02/03	QEWDE0480DES	07:59:20	7:33:00	Clear	Peak	S	3.079	-1.0	0.046
296	01/10/03	QEWDE0500DES	07:59:20	9:34:00	Clear	Peak	M/D	1.167	14.7	0.098
297	01/10/03	QEWDE0520DWS	07:59:20	11:55:00	Snow	Off-Peak	S	1.417	16.3	0.065
298	01/14/03	QEWDE0460DES	07:59:20	17:15:40	Snow	Peak	M/D	5.333	17.8	0.071
299	01/15/03	QEWDE0530DWS	07:59:20	15:48:00	Clear	Off-Peak	S	0.870	18.6	0.113

APPENDIX C

Crash Potential Model Contingency Table (SPSS, 2004)

Note:

1. Geometry is categorized as: Straight Section = 0, Merge/Diverge Section = 1.
2. Time is categorized as: Off-Peak period = 0, Peak Period = 1
3. COVV is categorized with 3 categories from low (1) to high (3).
4. CVS and Q are categorized with 4 categories from low (1) to high (4).

Geometry	Time	COVV	Q	CVS	Observed		Expected		Residual	Standardized Residual	Adjusted Residual	Deviance		
					Count	%	Count	%						
0	0	1	1	1	0	0.0%	0.03	0.0%	-0.035	-0.187	-0.187	-0.187		
				2	0	0.0%	0.02	0.0%	-0.015	-0.124	-0.124	-0.124		
				3	0	0.0%	0.02	0.0%	-0.020	-0.140	-0.140	-0.140		
				4	1	0.3%	0.83	0.3%	0.170	0.187	0.191	0.181		
			2	1	0	0.0%	0.01	0.0%	-0.015	-0.121	-0.122	-0.121		
				2	1	0.3%	1.03	0.3%	-0.033	-0.033	-0.034	-0.033		
				3	0	0.0%	0.01	0.0%	-0.008	-0.091	-0.091	-0.091		
				4	1	0.3%	1.08	0.4%	-0.080	-0.077	-0.079	-0.078		
			3	1	1	0.3%	0.55	0.2%	0.455	0.616	0.627	0.551		
				2	0	0.0%	0.01	0.0%	-0.008	-0.090	-0.090	-0.090		
				3	0	0.0%	0.01	0.0%	-0.010	-0.102	-0.102	-0.102		
				4	0	0.0%	0.05	0.0%	-0.046	-0.215	-0.216	-0.215		
			4	1	1	0.3%	0.80	0.3%	0.202	0.226	0.231	0.217		
				2	1	0.3%	1.08	0.4%	-0.083	-0.080	-0.082	-0.081		
				3	1	0.3%	1.38	0.5%	-0.376	-0.321	-0.330	-0.337		
				4	3	1.0%	1.99	0.7%	1.010	0.716	0.745	0.665		
		2	1	1	1	0	0.0%	0.05	0.0%	-0.053	-0.230	-0.231	-0.230	
					2	0	0.0%	0.02	0.0%	-0.023	-0.153	-0.153	-0.153	
					3	1	0.3%	0.87	0.3%	0.130	0.139	0.143	0.136	
					4	0	0.0%	0.13	0.0%	-0.132	-0.363	-0.367	-0.363	
				2	1	0	0.0%	0.02	0.0%	-0.022	-0.149	-0.150	-0.149	
					2	0	0.0%	0.01	0.0%	-0.010	-0.099	-0.099	-0.099	
					3	2	0.7%	1.99	0.7%	0.010	0.007	0.008	0.007	
					4	2	0.7%	1.64	0.5%	0.362	0.283	0.292	0.273	
				3	1	0	0.0%	0.03	0.0%	-0.028	-0.168	-0.168	-0.168	
					2	2	0.7%	1.97	0.7%	0.030	0.021	0.022	0.021	
					3	2	0.7%	2.50	0.8%	-0.503	-0.318	-0.338	-0.330	
					4	0	0.0%	0.07	0.0%	-0.070	-0.265	-0.267	-0.265	
			4	1	2	0.7%	1.21	0.4%	0.790	0.718	0.738	0.656		
				2	2	0.7%	1.64	0.5%	0.358	0.279	0.289	0.270		
				3	1	0.3%	2.09	0.7%	-1.086	-0.752	-0.781	-0.838		
				4	3	1.0%	3.02	1.0%	-0.017	-0.010	-0.010	-0.010		
			3	1	1	1	0	0.0%	0.13	0.0%	-0.128	-0.358	-0.360	-0.358
						2	0	0.0%	0.06	0.0%	-0.056	-0.237	-0.238	-0.237

			3	1	0.3%	0.39	0.1%	0.612	0.982	0.994	0.818	
			4	0	0.0%	0.32	0.1%	-0.320	-0.565	-0.572	-0.565	
		2	1	1	0.3%	0.29	0.1%	0.707	1.306	1.318	1.020	
			2	0	0.0%	0.02	0.0%	-0.024	-0.154	-0.155	-0.154	
			3	1	0.3%	0.38	0.1%	0.619	1.002	1.013	0.831	
			4	0	0.0%	0.13	0.0%	-0.135	-0.367	-0.370	-0.367	
		3	1	2	0.7%	0.37	0.1%	1.631	2.687	2.718	1.871	
			2	0	0.0%	0.03	0.0%	-0.030	-0.173	-0.174	-0.173	
			3	1	0.3%	0.48	0.2%	0.520	0.751	0.761	0.655	
			4	0	0.0%	0.17	0.1%	-0.170	-0.412	-0.416	-0.412	
		4	1	0	0.0%	0.31	0.1%	-0.307	-0.554	-0.560	-0.554	
			2	1	0.3%	0.73	0.2%	0.267	0.312	0.318	0.296	
			3	0	0.0%	0.17	0.1%	-0.172	-0.414	-0.419	-0.414	
			4	1	0.3%	2.37	0.8%	-1.365	-0.888	-0.927	-1.004	
1	1	1	1	1	0	0.0%	0.12	0.0%	-0.122	-0.350	-0.352	-0.350
			2	0	0.0%	0.05	0.0%	-0.054	-0.232	-0.233	-0.232	
			3	1	0.3%	0.97	0.3%	0.026	0.026	0.027	0.026	
			4	1	0.3%	1.79	0.6%	-0.794	-0.593	-0.618	-0.647	
		2	1	0	0.0%	0.05	0.0%	-0.052	-0.227	-0.228	-0.227	
			2	1	0.3%	1.22	0.4%	-0.221	-0.200	-0.207	-0.206	
			3	1	0.3%	1.55	0.5%	-0.551	-0.442	-0.459	-0.474	
			4	2	0.7%	1.83	0.6%	0.166	0.122	0.127	0.121	
		3	1	1	0.3%	0.93	0.3%	0.075	0.078	0.080	0.077	
			2	0	0.0%	0.03	0.0%	-0.029	-0.169	-0.170	-0.169	
			3	3	1.0%	1.95	0.7%	1.049	0.751	0.782	0.695	
			4	4	1.3%	2.31	0.8%	1.692	1.114	1.164	1.008	
		4	1	2	0.7%	1.73	0.6%	0.275	0.209	0.217	0.204	
			2	3	1.0%	1.84	0.6%	1.161	0.856	0.888	0.784	
			3	1	0.3%	2.34	0.8%	-1.336	-0.874	-0.911	-0.988	
			4	2	0.7%	4.30	1.4%	-2.302	-1.110	-1.180	-1.241	
	2	1	1	1	0	0.0%	0.19	0.1%	-0.186	-0.431	-0.435	-0.431
			2	1	0.3%	1.16	0.4%	-0.162	-0.151	-0.155	-0.154	
			3	0	0.0%	0.10	0.0%	-0.104	-0.322	-0.325	-0.322	
			4	1	0.3%	2.72	0.9%	-1.719	-1.043	-1.105	-1.199	
		2	1	2	0.7%	1.11	0.4%	0.885	0.838	0.864	0.753	
			2	3	1.0%	1.85	0.6%	1.149	0.845	0.886	0.775	
			3	2	0.7%	2.35	0.8%	-0.351	-0.229	-0.242	-0.235	
			4	2	0.7%	2.78	0.9%	-0.780	-0.468	-0.494	-0.493	
		3	1	1	0.3%	1.40	0.5%	-0.403	-0.340	-0.352	-0.359	
			2	2	0.7%	2.33	0.8%	-0.328	-0.215	-0.226	-0.220	
			3	0	0.0%	0.06	0.0%	-0.055	-0.235	-0.237	-0.235	
			4	3	1.0%	3.50	1.2%	-0.498	-0.266	-0.283	-0.273	
		4	1	4	1.3%	2.62	0.9%	1.385	0.856	0.902	0.794	
			2	1	0.3%	2.79	0.9%	-1.788	-1.071	-1.124	-1.235	
			3	2	0.7%	3.54	1.2%	-1.542	-0.819	-0.869	-0.893	
			4	9	3.0%	6.52	2.2%	2.479	0.971	1.053	0.917	
	3	1	1	1	0	0.0%	0.45	0.2%	-0.449	-0.670	-0.680	-0.670
			2	0	0.0%	0.20	0.1%	-0.197	-0.444	-0.448	-0.444	

			3	0	0.0%	0.25	0.1%	-0.251	-0.501	-0.506	-0.501
			4	0	0.0%	1.12	0.4%	-1.120	-1.058	-1.086	-1.058
		2	1	0	0.0%	0.19	0.1%	-0.189	-0.435	-0.439	-0.435
			2	1	0.3%	0.61	0.2%	0.389	0.498	0.508	0.456
			3	0	0.0%	0.11	0.0%	-0.106	-0.325	-0.328	-0.325
			4	0	0.0%	0.47	0.2%	-0.472	-0.687	-0.701	-0.687
		3	1	1	0.3%	0.90	0.3%	0.101	0.106	0.109	0.104
			2	4	1.3%	0.77	0.3%	3.232	3.688	3.763	2.596
			3	2	0.7%	0.98	0.3%	1.024	1.037	1.062	0.907
			4	1	0.3%	2.24	0.7%	-1.242	-0.830	-0.866	-0.932
		4	1	1	0.3%	2.61	0.9%	-1.610	-0.997	-1.060	-1.141
			2	1	0.3%	1.79	0.6%	-0.787	-0.589	-0.611	-0.643
			3	6	2.0%	2.27	0.8%	3.730	2.475	2.583	2.050
			4	5	1.7%	6.51	2.2%	-1.508	-0.591	-0.656	-0.617
1	0	1	1	1	0.3%	0.52	0.2%	0.483	0.672	0.684	0.595
			2	1	0.3%	0.67	0.2%	0.330	0.402	0.411	0.375
			3	0	0.0%	0.03	0.0%	-0.033	-0.182	-0.183	-0.182
			4	0	0.0%	0.15	0.0%	-0.148	-0.385	-0.389	-0.385
		2	1	1	0.3%	0.64	0.2%	0.357	0.445	0.454	0.411
			2	0	0.0%	0.01	0.0%	-0.011	-0.105	-0.105	-0.105
			3	1	0.3%	1.82	0.6%	-0.821	-0.608	-0.638	-0.665
			4	2	0.7%	1.60	0.5%	0.396	0.313	0.325	0.301
		3	1	0	0.0%	0.03	0.0%	-0.031	-0.177	-0.178	-0.177
			2	0	0.0%	0.01	0.0%	-0.014	-0.118	-0.118	-0.118
			3	1	0.3%	2.29	0.8%	-1.290	-0.853	-0.903	-0.961
			4	0	0.0%	0.08	0.0%	-0.079	-0.280	-0.283	-0.280
		4	1	1	0.3%	1.24	0.4%	-0.239	-0.215	-0.222	-0.222
			2	0	0.0%	0.06	0.0%	-0.063	-0.250	-0.252	-0.250
			3	0	0.0%	0.08	0.0%	-0.080	-0.282	-0.285	-0.282
			4	0	0.0%	0.36	0.1%	-0.355	-0.596	-0.611	-0.596
		2	1	1	0.3%	0.97	0.3%	0.025	0.026	0.026	0.025
			2	1	0.3%	2.17	0.7%	-1.172	-0.795	-0.845	-0.890
			3	1	0.3%	2.76	0.9%	-1.760	-1.059	-1.128	-1.220
			4	1	0.3%	2.43	0.8%	-1.431	-0.918	-0.960	-1.042
		3	1	2	0.7%	1.23	0.4%	0.774	0.699	0.720	0.640
			2	2	0.7%	2.73	0.9%	-0.733	-0.443	-0.473	-0.466
			3	2	0.7%	3.47	1.2%	-1.472	-0.790	-0.847	-0.859
			4	2	0.7%	3.06	1.0%	-1.058	-0.605	-0.638	-0.646
		4	1	3	1.0%	1.88	0.6%	1.122	0.818	0.852	0.752
			2	3	1.0%	2.44	0.8%	0.563	0.361	0.378	0.348
			3	1	0.3%	3.10	1.0%	-2.096	-1.191	-1.253	-1.390
			4	6	2.0%	4.68	1.6%	1.316	0.608	0.651	0.582
		3	1	1	0	0.0%	0.22	0.1%	-0.218	-0.467	-0.467
			2	0	0.0%	0.10	0.0%	-0.096	-0.309	-0.311	-0.309

			3	1	0.3%	0.62	0.2%	0.384	0.489	0.497	0.448	
			4	1	0.3%	1.60	0.5%	-0.602	-0.476	-0.495	-0.511	
		2	1	1	0.3%	0.47	0.2%	0.535	0.784	0.795	0.679	
			2	0	0.0%	0.04	0.0%	-0.040	-0.201	-0.202	-0.201	
			3	2	0.7%	0.59	0.2%	1.415	1.849	1.880	1.444	
			4	2	0.7%	1.16	0.4%	0.840	0.779	0.801	0.706	
		3	1	2	0.7%	0.59	0.2%	1.415	1.849	1.880	1.444	
			2	0	0.0%	0.05	0.0%	-0.051	-0.225	-0.227	-0.225	
			3	1	0.3%	0.74	0.2%	0.264	0.307	0.313	0.291	
			4	1	0.3%	1.46	0.5%	-0.460	-0.381	-0.393	-0.404	
		4	1	0	0.0%	0.52	0.2%	-0.522	-0.723	-0.734	-0.723	
			2	2	0.7%	1.16	0.4%	0.837	0.776	0.797	0.703	
			3	1	0.3%	1.48	0.5%	-0.478	-0.393	-0.405	-0.418	
			4	3	1.0%	3.84	1.3%	-0.841	-0.429	-0.457	-0.447	
1	1	1	1	1	0	0.0%	0.21	0.1%	-0.208	-0.456	-0.461	-0.456
			2	1	0.3%	1.17	0.4%	-0.172	-0.159	-0.164	-0.163	
			3	1	0.3%	1.49	0.5%	-0.489	-0.400	-0.415	-0.426	
			4	7	2.3%	2.84	0.9%	4.160	2.469	2.619	2.076	
		2	1	0	0.0%	0.09	0.0%	-0.088	-0.296	-0.299	-0.296	
			2	0	0.0%	0.04	0.0%	-0.039	-0.196	-0.198	-0.196	
			3	2	0.7%	2.25	0.8%	-0.247	-0.165	-0.173	-0.168	
			4	4	1.3%	2.80	0.9%	1.198	0.716	0.757	0.672	
		3	1	0	0.0%	0.11	0.0%	-0.110	-0.332	-0.336	-0.332	
			2	1	0.3%	2.23	0.7%	-1.225	-0.821	-0.865	-0.922	
			3	3	1.0%	2.83	0.9%	0.173	0.103	0.109	0.102	
			4	3	1.0%	3.53	1.2%	-0.525	-0.280	-0.298	-0.287	
		4	1	2	0.7%	2.73	0.9%	-0.731	-0.442	-0.469	-0.464	
			2	1	0.3%	2.81	0.9%	-1.810	-1.080	-1.143	-1.246	
			3	4	1.3%	3.57	1.2%	0.431	0.228	0.242	0.224	
			4	8	2.7%	6.81	2.3%	1.191	0.456	0.502	0.444	
	2	1	1	1	0.3%	1.73	0.6%	-0.726	-0.553	-0.580	-0.600	
			2	2	0.7%	1.78	0.6%	0.224	0.168	0.176	0.165	
			3	1	0.3%	2.26	0.8%	-1.256	-0.836	-0.880	-0.941	
			4	8	2.7%	4.30	1.4%	3.696	1.781	1.928	1.589	
		2	1	1	0.3%	1.70	0.6%	-0.703	-0.539	-0.564	-0.584	
			2	0	0.0%	0.06	0.0%	-0.058	-0.242	-0.244	-0.242	
			3	0	0.0%	0.07	0.0%	-0.074	-0.273	-0.276	-0.273	
			4	6	2.0%	4.25	1.4%	1.752	0.850	0.920	0.800	
		3	1	0	0.0%	0.17	0.1%	-0.167	-0.409	-0.415	-0.409	
			2	2	0.7%	3.37	1.1%	-1.373	-0.747	-0.797	-0.809	
			3	2	0.7%	4.28	1.4%	-2.285	-1.104	-1.186	-1.234	
			4	5	1.7%	5.34	1.8%	-0.344	-0.149	-0.161	-0.150	
		4	1	4	1.3%	4.14	1.4%	-0.139	-0.068	-0.074	-0.069	
			2	3	1.0%	4.26	1.4%	-1.259	-0.610	-0.656	-0.644	
			3	14	4.7%	5.41	1.8%	8.589	3.693	4.020	3.073	
			4	10	3.3%	10.32	3.5%	-0.322	-0.100	-0.113	-0.101	
	3	1	1	0	0.0%	0.76	0.3%	-0.763	-0.873	-0.893	-0.873	
			2	0	0.0%	0.34	0.1%	-0.335	-0.579	-0.587	-0.579	

			3	0	0.0%	0.43	0.1%	-0.426	-0.653	-0.664	-0.653
			4	3	1.0%	4.45	1.5%	-1.451	-0.688	-0.769	-0.731
		2	1	1	0.3%	1.15	0.4%	-0.151	-0.141	-0.146	-0.144
			2	0	0.0%	0.14	0.0%	-0.141	-0.376	-0.380	-0.376
			3	1	0.3%	1.22	0.4%	-0.217	-0.197	-0.203	-0.203
			4	0	0.0%	0.80	0.3%	-0.802	-0.896	-0.924	-0.896
		3	1	1	0.3%	1.45	0.5%	-0.449	-0.373	-0.386	-0.395
			2	4	1.3%	1.21	0.4%	2.795	2.546	2.623	2.002
			3	3	1.0%	1.53	0.5%	1.469	1.187	1.228	1.048
			4	2	0.7%	3.61	1.2%	-1.612	-0.848	-0.901	-0.927
		4	1	2	0.7%	4.28	1.4%	-2.280	-1.102	-1.216	-1.232
			2	2	0.7%	2.88	1.0%	-0.879	-0.518	-0.548	-0.548
			3	2	0.7%	3.66	1.2%	-1.658	-0.867	-0.922	-0.949
			4	13	4.3%	10.67	3.6%	2.327	0.712	0.836	0.689

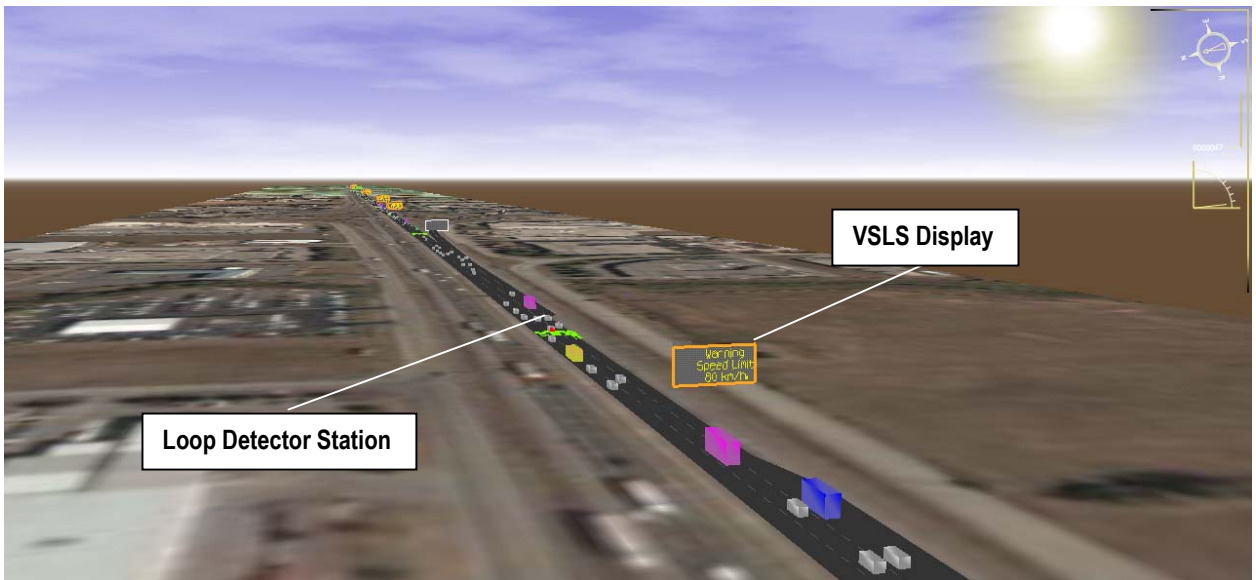
APPENDIX D

Images from PARAMICS

PARAMICS Screen Shot: Walker's Line Interchange



PARAMICS Screenshot: 3D Rendering of Network Mainline



APPENDIX E

Program Code for VLS Control in PARAMICS

```
/* -----
 * Paramics Programmer API (paramics-support@quadstone.com)
 * ----- */
/* VLS Control Algorithm
 * -----

/* include our function definitions explicit to this example */
#include "plugin_p.h"

#define SPEED_80 1
#define SPEED_60 2
#define SPEED_50 3
#define SPEED_NORM 4

const char *g_ParamFile = "api_example7";
static char **g_LinkLookup = NULL;
static char **g_BeaconLinks = NULL;
static char **g_LoopLinks = NULL;
static int nLinks = 0;
static int nLoops = 0;
static int nBeacons = 0;
static int nPeriods = 0;
static int Duration = 0;
static float *g_Speed = NULL;
static float *g_StationSpeed = NULL;
static float *g_StationFlow = NULL;
static float *g_StationCount = NULL;
static float *g_StationOccupancy = NULL;
static float *g_SpeedLimit = NULL;
static float *VolThresh = NULL;
static float SumSpeeds[20][5];
static float *StationCount = NULL;
static int *Release = NULL;
static float g_SumSpeed[20][999];
static float g_VehCount[20][999];
static float LaneCountOld[20][5];
static float *g_LaneCount = NULL;
static float *g_LaneSpeed = NULL;
static float *g_LaneOccupancy = NULL;
static float SumSpeedsOld[20][5];
static float *g_CountbySpeed = NULL;
static float g_StimulateTime = 0.0;
static float *g_BaseSpeeds = NULL;
static int *BeaconName = NULL;
static int TriggerStation[20];
static Bool *SpeedDown;

FILE* fp;
FILE* fpb;
FILE* fpdata;

/* -----
 * call qpx_NET_postOpen once when the full network has been read into modeller
 * ----- */
void qpx_NET_postOpen(void)
{
    int i;
    char *link_ref;

    fp = fopen("VSLSPrint.out","w");
    fprintf(fp, "%15s %15s %15s %15s %15s %15s\n", "Station", "Time", "Ave Speed", "Volume", "Occupancy",
        "Speed Limit");

    fpb = fopen("ResultantSpeed.out", "w");
    fprintf(fpb, "%15s %15s %15s %15s %15s\n", "Station", "Time", "Release", "Speed Limit", "Trigger");

    fpdata = fopen("LoopData.out", "w");
    fprintf(fpdata, "%15s %15s %10s %10s %10s %10s %10s %10s %10s %10s\n", "Station", "Time", "Vol3", "Vol2",
        "Vol1", "Speed3", "Speed2", "Speed1", "Occ3", "Occ2", "Occ1");
}
```



```

qps_GUI_printf("\nParams Programmer API: Using VMS and Detectors\n");

nLinks = qpg_NET_links();
nLoops = qpg_NET_detectors();
nBeacons = qpg_NET_beacons();
    Duration = qpg_CFG_duration();
    nPeriods = Duration/20;

/* now allocate memory for all dynamic objects in our plugin */
pp_allocate_memory();
if (nLoops != nBeacons)
{
    /* warning as each VMS beacon should ideally only have one loop
    * associated with it */
    qps_GUI_printf("\nWARNING: Number of Beacons and Loops found in network \n"
        " do not match, this may cause problems !\n");
}
/* now collect information about the Detectors/VMS objects in our network */
pp_check_beacons();
pp_check_loops();

/* at this point we know the location of each beacon and each loop in our
* network. Now we must initialize the speed limits and trigger conditions*/
for (i = 0; i < nBeacons; i++)
{
    g_SpeedLimit[i] = 100;
    SpeedDown[i] = FALSE;
    TriggerStation[i] = 0;

    BeaconName[i] = qpg_BCI_name(i+1);
    qps_GUI_printf("\n Speed on Link %d, %s, is %3.0f\n", i, g_LoopLinks[i], g_SpeedLimit[i]);
    qps_GUI_printf("\n Beacon name: %s (Beacon %d) on Link %s\n", BeaconName[i], i, g_LoopLinks[i]);
}

/* -----
* Called once for every time step - The main body of our plugin.
* ----- */
void qpx_NET_timeStep(void)
{
int i;
int n;
int j;
int k;
int t;
int s;
LINK* linkP;
LINK* linkC;
char* link_ref_name;
char* link_name;
int loop_count;
int loop_lanes;
int loop_index;
int LaneCount;
int LaneCountNew;
float LaneSpeed;
float CountbySpeed;
float SumSpeedsNew;
float LaneSpeeds;
float SumLaneSpeeds;
float AvgLaneSpeed;
float LaneOccupancy;
float SumOccupancy;
float OccupancybyCount;

/* as the timestep is usually > 1 we should check that we are in
* a whole second first */
if ((qpg_CFG_simulationTime() - (float)floor((double)qpg_CFG_simulationTime())) > 0.0)
return;

/* we are in a whole second so query each of the detectors associated
* with the VMS beacons */
for (i = 0; i < nLoops; i++)
{
/* link data */
link_ref_name = g_LoopLinks[i];
linkP = qpg_NET_link(link_ref_name);

loop_lanes = 0;

/* the number of detectors on the link associated with the current

```

```

* beacon */

loop_count = qpg_LNK_detectors(linkP);

for (k = 0; k < loop_count; k++)
{
    /* get the network index of the loop(s) associated with
    * the the current VMS beacon on the current link */
    loop_index = qpg_LNK_detectorIndexByIndex(linkP, k+1);
    /* the number of lanes the current detector covers */
    loop_lanes += qpg_LNK_lanes(linkP);
}

if ((int)qpg_CFG_simulationTime() % 10 == 0) /* Extract 20-second average data */
{
    s = (int)((qpg_CFG_simulationTime() - 21540)/10);

    if (s > 1)
    {
        if ((int)qpg_CFG_simulationTime() % 20 == 0) /* Extract 20-second average data */
        {
            /* No. of 20-sec. time intervals starting at 6:00:00 (=6*3600) */
            t = (int)((qpg_CFG_simulationTime() - 21540)/20);

            if (t > 0)
            {
                g_CountbySpeed[i] = 0.0;
                g_StationCount[i] = 0.0;
                SumOccupancy = 0.0;

                for (j = 0; j < loop_lanes; j++)
                {
                    /*Collect traffic count on each lane at each 20 second interval*/
                    LaneCountNew = qpg_DTI_count(loop_index, j+1, 0);
                    LaneCount = LaneCountNew - LaneCountOld[i][j];
                    g_LaneCount[j] = LaneCount;
                    LaneSpeed = qpg_DTI_speed(loop_index, j+1, APILOOP_SMOOTHED);
                    g_LaneSpeed[j] = LaneSpeed*3.6;
                    LaneOccupancy = qpg_DTI_occupancy(loop_index, j+1, APILOOP_SMOOTHED);
                    g_LaneOccupancy[j] = LaneOccupancy*LaneCount/20;

                    SumOccupancy += LaneOccupancy;
                    CountybySpeed = LaneSpeed*LaneCount*3.6;

                    g_CountbySpeed[i] += CountybySpeed;
                    g_StationCount[i] += LaneCount;

                    LaneCountOld[i][j] = LaneCountNew;
                }

                g_StationSpeed[i] = g_CountbySpeed[i]/g_StationCount[i];
                g_StationFlow[i] = g_StationCount[i]*180;
                g_StationOccupancy[i] = ((SumOccupancy/loop_lanes)*(g_StationCount[i]/loop_lanes))/20;
                VolThresh[i] = loop_lanes*1600;

                qps_GUI_printf("\n Speeds at Detector %d: %3.0f%4.0f%3.1f on %s at %s.\n", i,
                    _StationSpeed[i], g_StationFlow[i], g_StationOccupancy[i], link_ref_name,
                    pg_UTL_integerToTimeString((int)qpg_CFG_simulationTime()));

                if (t > 2)
                {
                    fprintf(fp, "\nStation %7d %15s %15.0f %15.0f %15.2f %15.0f\n", (i+1),
                        pg_UTL_integerToTimeString((int)qpg_CFG_simulationTime()),
                        _StationSpeed[i], g_StationFlow[i], g_StationOccupancy[i], g_SpeedLimit[i]);

                    fprintf(fpdata, "\nStation %7d %15s %10.0f %10.0f %10.0f %10.1f %10.1f %10.1f %10.2f %10.2f\n",
                        i+1, qpg_UTL_integerToTimeString((int)qpg_CFG_simulationTime()), g_LaneCount[2], g_LaneCount[1], g_LaneCount[0],
                        _LaneSpeed[2], g_LaneSpeed[1], g_LaneSpeed[0], g_LaneOccupancy[2], g_LaneOccupancy[1], g_LaneOccupancy[0]);
                }
            }
        }
    }
}

if (s > 5)
{
    if (i >= 0) && (i < 12)
    {
        if ((g_StationOccupancy[i] <= 0.15) && (SpeedDown[i]))
        {

```

```

if ((int)qpg_CFG_simulationTime() % 20 == 0)
{
Release[i] += 1;
link_name = g_LoopLinks[i];
qps_GUI_printf("\n Speed Release3 = %d at Beacon %d on Link %s at %s.\n", Release[i],
i, link_name, qpg_UTL_integerToTimeString((int)qpg_CFG_simulationTime()));

if(Release[i] > 2)
{
if(g_SpeedLimit[i] < 80)
{
link_name = g_LoopLinks[i];
linkC = qpg_NET_link(link_name);
pp_adjust_speed(linkC, SPEED_80, i+1);
qps_GUI_printf("\n Speed Increased to 80 km/h at Beacon %d on Link %s at %s.\n",
i, link_name, qpg_UTL_integerToTimeString((int)qpg_CFG_simulationTime()));

g_SpeedLimit[i] = 80;
Release[i] = 0;
}
else if(g_SpeedLimit[i+1] > 60)
{
link_name = g_LoopLinks[i];
linkC = qpg_NET_link(link_name);
pp_adjust_speed(linkC, SPEED_NORM, i+1);
qps_GUI_printf("\n Speed Returned to 100 km/h at Beacon %d on Link %s at %s.\n",
i, link_name, qpg_UTL_integerToTimeString((int)qpg_CFG_simulationTime()));

g_SpeedLimit[i] = 100;
SpeedDown[i] = FALSE;
Release[i] = 0;
}
}
}
}
if((g_StationFlow[i] < VolThresh[i])&&(g_StationOccupancy[i] > 0.20))
{
n = i;

if(g_StationSpeed[n] <= 60)
{
if(n > 3)
{
TriggerStation[n] = 1;
/* Assign Speed to third upstream beacon*/
if(g_SpeedLimit[n-3] > 60)
{
link_name = g_LoopLinks[n-3];
linkC = qpg_NET_link(link_name);
pp_adjust_speed(linkC, SPEED_80, n-2);
qps_GUI_printf("\n Speed Reduced to 80 km/h at Beacon %d on Link %s at %s.\n",
n-3, link_name, qpg_UTL_integerToTimeString((int)qpg_CFG_simulationTime()));

if(g_SpeedLimit[n-3] > 80)
Release[n-3] = 0;

g_SpeedLimit[n-3] = 80;
SpeedDown[n-3] = TRUE;
}

/* Assign Speed to second upstream beacon*/
if((g_SpeedLimit[n-2] < 100)&&(g_SpeedLimit[n] < 100))
{
link_name = g_LoopLinks[n-2];
linkC = qpg_NET_link(link_name);
pp_adjust_speed(linkC, SPEED_60, n-1);
qps_GUI_printf("\n Speed Reduced to 60 km/h at Beacon %d on Link %s at %s.\n",
n-2, link_name, qpg_UTL_integerToTimeString((int)qpg_CFG_simulationTime()));

if(g_SpeedLimit[n-2] > 60)
Release[n-2] = 0;

g_SpeedLimit[n-2] = 60;
SpeedDown[n-2] = TRUE;
}
}
else
{
link_name = g_LoopLinks[n-2];
linkC = qpg_NET_link(link_name);
pp_adjust_speed(linkC, SPEED_80, n-1);
}
}
}

```

```

qps_GUI_printf("\n Speed Reduced to 80 km/h at Beacon %d on Link %s at %s.\n",
n-2, link_name, qpg_UTL_integerToTimeString((int)qpg_CFG_simulationTime()));

if(g_SpeedLimit[n-2] > 80)
    Release[n-2] = 0;

    g_SpeedLimit[n-2] = 80;
    SpeedDown[n-2] = TRUE;
}

/*Assign Speed to first upstream beacon*/
if((g_SpeedLimit[n-1] < 100)&&(g_SpeedLimit[n] < 100))
{
link_name = g_LoopLinks[n-1];
linkC = qpg_NET_link(link_name);
pp_adjust_speed(linkC, SPEED_60, n);
qps_GUI_printf("\n Speed Reduced to 60 km/h at Beacon %d on Link %s at %s.\n",
n-1, link_name, qpg_UTL_integerToTimeString((int)qpg_CFG_simulationTime()));

if(g_SpeedLimit[n-1] > 60)
    Release[n-1] = 0;

    g_SpeedLimit[n-1] = 60;
    SpeedDown[n-1] = TRUE;
}
else
{
link_name = g_LoopLinks[n-1];
linkC = qpg_NET_link(link_name);
pp_adjust_speed(linkC, SPEED_80, n);
qps_GUI_printf("\n Speed Reduced to 80 km/h at Beacon %d on Link %s at %s.\n",
n-1, link_name, qpg_UTL_integerToTimeString((int)qpg_CFG_simulationTime()));

if(g_SpeedLimit[n-1] > 80)
    Release[n-1] = 0;

    g_SpeedLimit[n-1] = 80;
    SpeedDown[n-1] = TRUE;
}

/*Assign Speed to current beacon*/
if(g_SpeedLimit[n] < 100)
{
link_name = g_LoopLinks[n];
linkC = qpg_NET_link(link_name);
pp_adjust_speed(linkC, SPEED_60, n+1);
qps_GUI_printf("\n Speed Reduced to 60 km/h at Beacon %d on Link %s at %s.\n",
n, link_name, qpg_UTL_integerToTimeString((int)qpg_CFG_simulationTime()));

if(g_SpeedLimit[n] > 60)
{
Release[n] = 0;
Release[n-1] = 0;
Release[n-2] = 0;
Release[n-3] = 0;
}
g_SpeedLimit[n] = 60;
SpeedDown[n] = TRUE;
}
else
{
link_name = g_LoopLinks[n];
linkC = qpg_NET_link(link_name);
pp_adjust_speed(linkC, SPEED_80, n+1);
qps_GUI_printf("\n Speed Reduced to 80 km/h at Beacon %d on Link %s at %s.\n",
n, link_name, qpg_UTL_integerToTimeString((int)qpg_CFG_simulationTime()));

if(g_SpeedLimit[n] > 80)
{
Release[n] = 0;
Release[n-1] = 0;
Release[n-2] = 0;
Release[n-3] = 0;
}
g_SpeedLimit[n] = 80;
SpeedDown[n] = TRUE;
}
}
}
}
else if((g_StationSpeed[n] > 60)&&(g_StationSpeed[n] <= 80))
{

```

```

if(n > 3)
{
TriggerStation[n] = 2;
/*Assign Speed to current beacon*/
if(g_SpeedLimit[n] > 60)
{
link_name = g_LoopLinks[n];
linkC = qpg_NET_link(link_name);
pp_adjust_speed(linkC, SPEED_80, n+1);
qps_GUI_printf("\n Speed Reduced to 80 km/h at Beacon %d on Link %s at %s.\n",
n, link_name, qpg_UTL_integerToTimeString((int)qpg_CFG_simulationTime()));

if(g_SpeedLimit[n] > 80)
{
Release[n] = 0;
Release[n-1] = 0;
Release[n-2] = 0;
}

g_SpeedLimit[n] = 80;
SpeedDown[n] = TRUE;

/*Assign Speed to first upstream beacon*/
if(g_SpeedLimit[n-1] > 60)
{
link_name = g_LoopLinks[n-1];
linkC = qpg_NET_link(link_name);
pp_adjust_speed(linkC, SPEED_80, n);
qps_GUI_printf("\n Speed Reduced to 80 km/h at Beacon %d on Link %s at %s.\n",
n-1, link_name, qpg_UTL_integerToTimeString((int)qpg_CFG_simulationTime()));

if(g_SpeedLimit[n-1] > 80)
Release[n-1] = 0;

g_SpeedLimit[n-1] = 80;
SpeedDown[n-1] = TRUE;
}
/*Assign Speed to second upstream beacon*/
if(g_SpeedLimit[n-2] > 60)
{
link_name = g_LoopLinks[n-2];
linkC = qpg_NET_link(link_name);
pp_adjust_speed(linkC, SPEED_80, n-1);
qps_GUI_printf("\n Speed Reduced to 80 km/h at Beacon %d on Link %s at %s.\n",
n-2, link_name, qpg_UTL_integerToTimeString((int)qpg_CFG_simulationTime()));

if(g_SpeedLimit[n-2] > 80)
Release[n-2] = 0;

g_SpeedLimit[n-2] = 80;
SpeedDown[n-2] = TRUE;
}
}
}

else if(g_StationFlow[i] > VolThresh[i])
{
n = i;

if(g_StationSpeed[n] <= 60)
{
if(n > 3)
{
TriggerStation[n] = 3;
/*Assign Speed to third upstream beacon*/
if(g_SpeedLimit[n-3] > 60)
{
link_name = g_LoopLinks[n-3];
linkC = qpg_NET_link(link_name);
pp_adjust_speed(linkC, SPEED_80, n-2);
qps_GUI_printf("\n Speed Reduced to 80 km/h at Beacon %d on Link %s at %s.\n",
n-3, link_name, qpg_UTL_integerToTimeString((int)qpg_CFG_simulationTime()));

if(g_SpeedLimit[n-3] > 80)
Release[n-3] = 0;

g_SpeedLimit[n-3] = 80;
SpeedDown[n-3] = TRUE;
}
}
}
}
}

```

```

}

/* Assign Speed to second upstream beacon*/
if ((g_SpeedLimit[n-2] < 100)&&(g_SpeedLimit[n] < 100))
{
link_name = g_LoopLinks[n-2];
linkC = qpg_NET_link(link_name);
pp_adjust_speed(linkC, SPEED_60, n-1);
qps_GUI_printf("\n Speed Reduced to 60 km/h at Beacon %d on Link %s at %s.\n",
n-2, link_name, qpg_UTL_integerToTimeString((int)qpg_CFG_simulationTime()));

if(g_SpeedLimit[n-2] > 60)
Release[n-2] = 0;

g_SpeedLimit[n-2] = 60;
SpeedDown[n-2] = TRUE;
}
else
{
link_name = g_LoopLinks[n-2];
linkC = qpg_NET_link(link_name);
pp_adjust_speed(linkC, SPEED_80, n-1);
qps_GUI_printf("\n Speed Reduced to 80 km/h at Beacon %d on Link %s at %s.\n",
n-2, link_name, qpg_UTL_integerToTimeString((int)qpg_CFG_simulationTime()));

if(g_SpeedLimit[n-2] > 80)
Release[n-2] = 0;

g_SpeedLimit[n-2] = 80;
SpeedDown[n-2] = TRUE;
}

/* Assign Speed to first upstream beacon*/
if ((g_SpeedLimit[n-1] < 100)&&(g_SpeedLimit[n] < 100))
{
link_name = g_LoopLinks[n-1];
linkC = qpg_NET_link(link_name);
pp_adjust_speed(linkC, SPEED_60, n);
qps_GUI_printf("\n Speed Reduced to 60 km/h at Beacon %d on Link %s at %s.\n",
n-1, link_name, qpg_UTL_integerToTimeString((int)qpg_CFG_simulationTime()));

if(g_SpeedLimit[n-1] > 60)
Release[n-1] = 0;

g_SpeedLimit[n-1] = 60;
SpeedDown[n-1] = TRUE;
}
else
{
link_name = g_LoopLinks[n-1];
linkC = qpg_NET_link(link_name);
pp_adjust_speed(linkC, SPEED_80, n);
qps_GUI_printf("\n Speed Reduced to 80 km/h at Beacon %d on Link %s at %s.\n",
n-1, link_name, qpg_UTL_integerToTimeString((int)qpg_CFG_simulationTime()));

if(g_SpeedLimit[n-1] > 80)
Release[n-1] = 0;

g_SpeedLimit[n-1] = 80;
SpeedDown[n-1] = TRUE;
}

/* Assign Speed to current beacon*/
if(g_SpeedLimit[n] < 100)
{
link_name = g_LoopLinks[n];
linkC = qpg_NET_link(link_name);
pp_adjust_speed(linkC, SPEED_60, n+1);
qps_GUI_printf("\n Speed Reduced to 60 km/h at Beacon %d on Link %s at %s.\n",
n, link_name, qpg_UTL_integerToTimeString((int)qpg_CFG_simulationTime()));

if(g_SpeedLimit[n] > 60)
{
Release[n] = 0;
Release[n-1] = 0;
Release[n-2] = 0;
Release[n-3] = 0;
}

g_SpeedLimit[n] = 60;

```



```

}
}

if ((int)qpg_CFG_simulationTime() % 20 == 0)
{
    fprintf(fpb, "\\Station %7d %15s %15d %15.0f %10d\\n", (i+1),
            qpg_UTL_integerToTimeString((int)qpg_CFG_simulationTime()),
            Release[i], g_SpeedLimit[i], TriggerStation[i]);
}

TriggerStation[i] = 0;

if ((int)qpg_CFG_simulationTime() == 36000)
{
    fprintf(fp, "\\Station %7d %15s\\n", (i+1),
            qpg_UTL_integerToTimeString((int)qpg_CFG_simulationTime()));
    fprintf(fpb, "\\Station %7d %15s\\n", (i+1),
            qpg_UTL_integerToTimeString((int)qpg_CFG_simulationTime()));
    fprintf(fpdata, "\\Station %7d %15s\\n", (i+1),
            qpg_UTL_integerToTimeString((int)qpg_CFG_simulationTime()));
}
}
}
}
}
}
fclose (fp);
fclose (fpb);
fclose (fpdata);

/* -----
* Allocate memory for all dynamic objects
* ----- */
void pp_allocate_memory(void)
{
    /* for each object clear old memory, and allocate new */

    if (g_BaseSpeeds != NULL) free(g_BaseSpeeds);
        g_BaseSpeeds = calloc(sizeof(float), nLinks);

    if (g_Speed != NULL) free(g_Speed);
        g_Speed = calloc(sizeof(float), nLinks);

    if (g_LaneCount != NULL) free(g_LaneCount);
        g_LaneCount = calloc(sizeof(float), nLinks);

    if (g_LaneSpeed != NULL) free(g_LaneSpeed);
        g_LaneSpeed = calloc(sizeof(float), nLinks);

    if (g_LaneOccupancy != NULL) free(g_LaneOccupancy);
        g_LaneOccupancy = calloc(sizeof(float), nLinks);

    if (SpeedDown != NULL) free(SpeedDown);
        SpeedDown = calloc(sizeof(Bool), nLinks);

    if (g_StationSpeed != NULL) free(g_StationSpeed);
        g_StationSpeed = calloc(sizeof(float), nLinks);

    if (g_CountbySpeed != NULL) free(g_CountbySpeed);
        g_CountbySpeed = calloc(sizeof(float), nLinks);

    if (g_StationCount != NULL) free(g_StationCount);
        g_StationCount = calloc(sizeof(float), nLinks);

    if (g_StationOccupancy != NULL) free(g_StationOccupancy);
        g_StationOccupancy = calloc(sizeof(float), nLinks);

    if (g_SpeedLimit != NULL) free(g_SpeedLimit);
        g_SpeedLimit = calloc(sizeof(float), nLinks);

    if (g_StationFlow != NULL) free(g_StationFlow);
        g_StationFlow = calloc(sizeof(float), nLinks);

    if (VolThresh != NULL) free(VolThresh);
        VolThresh = calloc(sizeof(float), nLinks);

    if (g_SpeedLimit != NULL) free(g_SpeedLimit);
        g_SpeedLimit = calloc(sizeof(int), nLinks);
}

```



```

if (g_LinkLookup != NULL) free(g_LinkLookup);
    g_LinkLookup = calloc(sizeof(char), nLinks);

if (g_BeaconLinks != NULL) free(g_BeaconLinks);
    g_BeaconLinks = calloc(sizeof(char), nLinks);

if (g_LoopLinks != NULL) free(g_LoopLinks);
    g_LoopLinks = calloc(sizeof(char), nLinks);

    if (BeaconName != NULL) free(BeaconName);
        BeaconName = calloc(sizeof(int), nLinks);
}

/* -----
* Collect the initial links speeds throughout the network and build a
* lookup table of Link index No/Names
* ----- */
void pp_collect_initial_speeds(void)
{
    int i;

    qps_GUI_printf("\nCollecting data about existing link speed limits.\n");

    for (i = 0; i < nLinks; i++)
    {
        g_BaseSpeeds[i] = qpg_LNK_speedlimit(qpg_NET_linkByIndex(i+1));
        g_LinkLookup[i] = qpg_LNK_name(qpg_NET_linkByIndex(i+1));
    }
}

/* -----
* Collect information on beacons in our network
* ----- */
void pp_check_beacons(void)
{
    int i;
    int j;
    LINK* linkP = NULL;

    /* tell the user about the VMS signs we found in our network */
    if (nBeacons <= 0)
    {
        /* no VMS beacons in our network ? */
        qps_GUI_printf("\nWARNING: No VMS beacons found in current network.\n");
        return;
    }
    else
    {
        /* report and store data */
        qps_GUI_printf("\n%d Beacons found in current network.\n", nBeacons);

        for (i = 0; i < nLinks; i++)
        {
            linkP = qpg_NET_linkByIndex(i+1);
            if (qpg_LNK_beacons(linkP) > 0)
            {
                /* this link has a beacon(s) */
                qps_GUI_printf("\n :Link %s has %d beacons(s)\n",
                    qpg_LNK_name(linkP), qpg_LNK_beacons(linkP));
                /* report the details of each beacon */
                for (j = 0; j < qpg_LNK_beacons(linkP); j++)
                {
                    qps_GUI_printf(" :Beacon %d (%s)\n", (j+1),
                        qpg_BCI_name(qpg_LNK_beaconIndexByIndex(linkP, j+1)));

                    /* store the link name associated with each beacon index */
                    g_BeaconLinks[(qpg_LNK_beaconIndexByIndex(linkP, j+1) - 1)] = qpg_LNK_name(linkP);
                }
            }
            linkP = NULL;
        }
    }
}

/* -----
* Collect information on loops in our network
* ----- */
void pp_check_loops(void)
{

```

```

int i = 0;
int j = 0;
    int s = 0;
LINK* linkP;
char *name;

/* tell the user about the loop detectors we found in our network */
if (nLoops <= 0)
{
    /* no detectors found in our network ? */
    qps_GUI_printf("\nWARNING: No loop detectors found in current network.\n");
    return;
}
else
{
    /* report and store data */
    qps_GUI_printf("\n%d Loop Detectors found in current network.\n", nLoops);

    for (i = 0; i < nLinks; i++)
    {
        linkP = qpg_NET_linkByIndex(i+1);
        if (qpg_LNK_detectors(linkP) > 0)
        {
            /* this link has a detector(s) */
            qps_GUI_printf("\n  .Link %s (%d) has %d detector(s)\n",
                qpg_LNK_name(linkP), i, qpg_LNK_detectors(linkP));
            /* report the details of each detector */
            for (j = 0; j < qpg_LNK_detectors(linkP); j++)
            {
                qps_GUI_printf("  .Detector %d (%s)\n", (j+1) ,
                    qpg_DTI_name(qpg_LNK_detectorIndexByIndex(linkP, j+1)));

                name = qpg_DTI_name(qpg_LNK_detectorIndexByIndex(linkP, j+1));
                g_LoopLinks[s] = qpg_LNK_name(linkP);
                qps_GUI_printf(" Linkname(%d): %s\n", s, g_LoopLinks[s]);
                s++;
            }
            linkP = NULL;
        }
    }
}

/* -----
* Match at least one loop on the same link as a beacon
* ----- */
Bool pp_beacon_loop_match(char *linkC)
{
    int i = 0;
    Bool found = FALSE;

    while(i < nLoops && !found)
    {
        if (g_LoopLinks[i] == linkC)
        {
            found = TRUE;
        }
        i++;
    }
    return found;
}

/* -----
* Apply the required speed restriction / adjustments
* Note: this function can be used with the SPEED_NORM flag to remove
* any currently imposed speed restrictions.
* ----- */
void pp_adjust_speed(LINK* linkC, int flagS, int indexB)
{
    /* hex color ID for VMS signs */
    int hex_red = 0x000001ff;
    int hex_amber = 0x001aa6ff;
    int hex_green = 0x0035dd6b;

    float dist = 0.0;
    LINK* linkP;
    /*Accomodate for screw up in program*/
    if(indexB == 8)
        indexB = 13;
}

```

```

        else if (indexB > 8)
            indexB = indexB - 1;

switch (flagS)
{
    case SPEED_80:
        /* reduce link speeds to 80kph */
        qps_BCI_colour(indexB, hex_amber);
        qps_BCI_message(indexB, "    Warning  \n"
                           "    Speed Limit \n"
                           "    80 km/h.  ");

        /* apply speed restriction */
        qps_LNK_speedlimit(linkC, (float)80);

        break;

    case SPEED_60:
        /* reduce link speeds to 60kph */
        qps_BCI_colour(indexB, hex_red);
        qps_BCI_message(indexB, "    Warning  \n"
                           "    Reduce Speed to \n"
                           "    60 km/h.  ");

        /* apply speed restriction */
        qps_LNK_speedlimit(linkC, (float)60);

        break;

    case SPEED_50:
        /* reduce link speeds to 50kph */
        qps_BCI_colour(indexB, hex_red);
        qps_BCI_message(indexB, "    Warning  \n"
                           "    Reduce Speed to \n"
                           "    50 km/h.  ");

        /* apply speed restriction */
        qps_LNK_speedlimit(linkC, (float)50);

        break;

    case SPEED_NORM:
        /* restore link speeds to original */
        qps_BCI_colour(indexB, hex_green);
        qps_BCI_message(indexB, "    \n"
                           "    Drive Safely \n"
                           "    100 km/h  ");

        /* restore original speeds */
        qps_LNK_speedlimit(linkC, (float)100);

        break;

    default: /* do nothing */

        break;
}
}

/* -----
 * Given a pointer to a link in the current network, this function returns
 * the network wide index (1-N) for that link.
 * ----- */
int pp_link_id_lookup(LINK* linkC)
{
    char* link_ref_name = qpg_LNK_name(linkC);
    int i;

    for (i = 0; i < nLinks; i++)
        if (g_LinkLookup[i] == link_ref_name) return i+1;

    return -1;
}

```